UNIVERSITY OF CALIFORNIA
SANTA CRUZ

HYBRID CLOCK SYNCHRONIZATION IN NETWORKED CONTROL SYSTEMS

A dissertation submitted in partial satisfaction of the
requirements for the degree of

DOCTOR OF PHILOSOPHY

in

COMPUTER ENGINEERING

by

Marcello Guarro

December 2021

The dissertation of Marcello Guarro
is approved:

Professor Ricardo G. Sanfelice, Chair

Professor Alvaro Cardenas

Professor Abhishek Halder

Peter Biehl
Vice Provost and Dean of Graduate Studies

Table of Contents

List of Figures

Abstract

Hybrid Clock Synchronization
in
Networked Control Systems

by

Marcello Guarro
DOCTOR OF PHILOSOPHY in Computer Engineering

University of California, Santa Cruz

Professor Ricardo G. Sanfelice, Chair

Clock synchronization over networks is a nontrivial problem that has long been an important topic in the fields of computer science and engineering as it pertains to digital networks and distributed systems. Recently, clock synchronization has received much attention in the study of networked control theory due to the importance of consensus on time in distributed control and estimation settings.This dissertation addresses the need for new clock synchronization schemes with the presentation of several hybrid based approach to clock synchronization problem.

To motivate this work, the problem of a hybrid observer, with a clock synchronization scheme, that receives information sporadically over a network is presented. Through an attractivity result on the convergence properties of the observer system, sufficient conditions on the convergence properties of the accompanying clock synchronization scheme demonstrate the need for clock synchronization algorithms with performance guarantees.

In one of the solutions to the problem, a distributed hybrid algorithm that synchronizes the time and rate of a set of clocks connected over a network is presented. Clock measurements of the nodes are given at aperiodic time instants and the controller at each node uses these measurements to achieve synchronization. Due to the continuous and impulsive nature of the clocks and the network, a hybrid system model to effectively capture the dynamics of the system and proposed hybrid algorithm is introduced. Moreover, the hybrid algorithm allows each agent to estimate the skew of its internal clock in order to

allow for synchronization to a common timer rate. Sufficient conditions guaranteeing synchronization of the timers, exponentially fast are provided. Numerical results illustrate the synchronization property induced by the proposed algorithm as well as robustness to communication noise.

Next, an innovative hybrid systems approach to the sender-receiver synchronization of timers is presented. Via the hybrid systems framework, the traditional sender-receiver algorithm for clock synchronization is united with an online, adaptive strategy to achieve synchronization of the clock rates to exponentially synchronize a pair of clocks connected over a network. Following the conventions of the algorithm, clock measurements of the nodes are given at periodic time instants, and each node uses these measurements to achieve synchronization. For this purpose, a hybrid system model of a network with continuous and impulsive dynamics that captures the sender-receiver algorithm as a state-feedback controller to synchronize the network clocks is introduced. Moreover, sufficient design conditions that ensure attractivity of the synchronization set are provided with numerical examples to validate the theoretical results.

Finally, a general approach and framework to modeling clock synchronization protocols using hybrid systems is presented. Using the general framework, several existing algorithms from the literature are modeled. The models are then simulated numerically to demonstrate the feasibility of the proposed modeling framework.

Dedicated to my wife,

Amanda J. Andrade,

parents,

Clorinda Donato and Sergio Guarro

and daughter,

Emilia Guarro

Acknowledgments

I would like to express my thanks and gratitude to Professor Ricardo G. Sanfelice for believing in me and my strengths toward the pursuit of my degree and contributions to this field. Your direction and guidance throughout the years has transformed the way I view and approach engineering problems.

Thank you to my wife, Amanda J. Andrade for embarking on this long academic journey with me. Your unconditional love, support, and guidance throughout the years has helped enable this journey and I am forever grateful.

Thank you to my parents, Clorinda Donato and Sergio Guarro, and my siblings Adriana Guarro Romero and Gianluca Guarro, for the love and support all of these years.

Chapter 1

Introduction

Clock synchronization has long been a topic of great importance to the field of computer science and engineering due to the temporal demands of applications operating over networks in a distributed computing setting. In recent years, the topic has received much attention from the controls and cyber-physical systems community due to the increased use of networks in sensing and control applications that operate on evolving dynamical systems. Some of these applications include, but are certainly not limited to, distributed estimation via remote sensing, multi-agent robotics, industrial automation, and non-collocated control.

In particular, distributed control applications, such as robotic swarms, automated manufacturing, and distributed optimization rely on precise time synchronization among distributed agents for their operation; see [1]. For example, in the case of distributed control and estimation over networks, the uncertainties of packet-based network communication requires precision timestamping of sensor and actuator messages in order to synchronize the information to the evolution of the dynamical system being controlled or estimated. Such a scenario is impossible without the existence of a common timescale among the non-collocated agents in the system. In fact, the lack of a shared timescale among the networked agents can result in performance degradation that can destabilize the system; see [2]. Moreover, one cannot always assume that consensus on time is a given, especially when the network associated to the distributed system is subject to perturbations such as noise, delay, or jitter. Hence, it is essential that these networked systems utilize clock synchronization schemes that establish and maintain a common timescale for their algorithms.

The union of communication networks in control and sensing applications has given way to the interdisciplinary study of Networked Control Systems (NCS) that seeks

to address the problems that lie at the intersection of control and network theory, see [3]. One of the main set of challenges that arises in the study of NCSs, are those that relate to the sample and delay based nature of the exchanged data. To transmit information about a continuous time system over a discrete network, information collected by sensors are first digitally sampled and quantized, the digital measurement is then encoded into a data packet, then the packet is placed in a buffer before being broadcast to the network. When the measurement packet is received by a separate node on the network, such as an observer or controller, the packet must then be arbitrated and decoded. This process of measurement sampling, transmission, arbitration, and decoding introduces a measurable delay that, if left unaccounted for, can adversely affect system performance in a control system setting, see [3]. Moreover, depending on the networking protocol, the length of the delay can be either deterministic or time-varying.

One solution to address the issue of delay is to include the delay information via message timestamping as noted in [3] and [4]. For the information on delays to properly be utilized, consensus on a common timescale must exist among the distributed agents in the networked control system. To ensure consensus on a common timescale, the system is coupled with a clock synchronization subsystem that periodically synchronizes the clocks to ensure their relative error is within an acceptable tolerance that is sufficient for desired system performance. However, the design of such a clock synchronization subsystem in the context of networked control is nontrivial as it is faced with many of the same communication constraints faced by networked control systems. These issues and constraints include but are not limited to: delays, sporadic communication events, and network traffic, see [5] and [6]. Moreover, if the rate by which the clocks converge in a networked control system setting is insufficient, adverse effects on the system performance may occur.

Motivated by these challenges, this work presents new solutions to the clock synchronization problem based on hybrid system designs that seeks to close the performance gaps that exist with in the current state of the art. To illustrate the motivation, we present two examples which are introduced in Section 1.1 and Section 1.2. The first example demonstrates how a nondeterministic delay adversely affects a networked control system by examining the behavior of a networked observer system that is subjected to delayed measurements from a linear time-invariant plant. We will then present a sketch of our proposed solution to address the delayed measurements that requires the use of a clock synchronization scheme. The second example prevents on overview of the clock synchro-

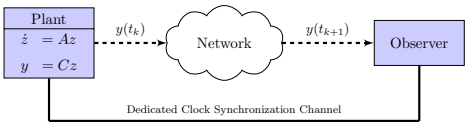

Figure 1.1: Block diagram of the system.

nization problem and some of the noted challenges. In Section 1.3 we present examples on the existing state of the art in clock synchronization and note their associated shortcomings that further motivates the research of new hybrid-based solutions.

1.1 Motivational example: state estimation via networked observer

Consider a continuous-time linear system, given by

$$\begin{aligned} \dot{z} &= Az \\ y &= Mz \end{aligned} \tag{1.1}$$

where $z \in \mathbb{R}^n$ is the system state and $y \in \mathbb{R}^R$ is the measured output. The matrices A and M are constant and of appropriate dimensions. Now, consider a network-connected observer designed to generate estimates $\hat{z}$ of the system state z utilizing measurements y sampled and broadcast at random times t_k, $k \in \mathcal{I}_R \setminus \{0\}$, where

$$\mathcal{I}_R := \{2i + 1 : i \in \mathbb{N}\}$$

Moreover, the network experiences varying transmission delays: the sampled measurements $y(t_k)$ are available only at random times t_k, $k \in \mathcal{I}_d \setminus \{0\}$, where

$$\mathcal{I}_d := \{2i : i \in \mathbb{N}\}$$

See Figure 1.1 for a block diagram representation of the system.

The measurement sampling and arrival events are described by a strictly increasing unbounded sequence of instants $\{t_k\}_{k=0}^{\infty}$ where

$$\begin{aligned} 0 \leq t_1 &\leq T_2^N \\ T_1^N \leq t_k - t_{k-2} &\leq T_2^N \quad \forall k \in \mathcal{I}_R \setminus \{0\} \\ 0 \leq t_k - t_{k-1} &\leq T^d \quad \forall k \in \mathcal{I}_d \setminus \{0\} \end{aligned} \tag{1.2}$$

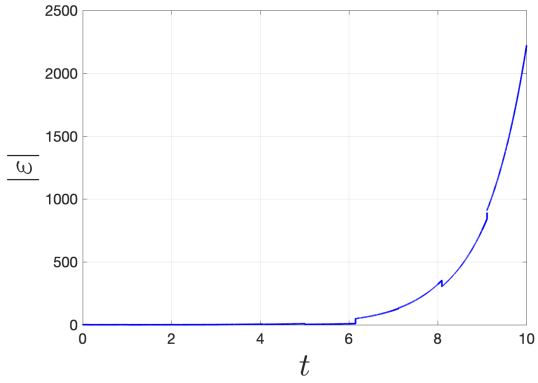

Figure 1.2: The evolution of the estimation error with respect to time. The vertical dashes represent the jumps of $\hat{z}$ according to $\hat{z}^+$.

with $t_0 = 0$. The scalars T_1^N and T_2^N define the minimum and maximum allowable transfer interval (MATI), respectively, while T^d is an upper bound on the transmission delay and are such that $T_2^N \geq T_1^N \geq T^d > 0$.

Then, the goal is to generate an estimate of the state $\hat{z} \in \mathbb{R}^n$, using the measured output from the plant in an impulsive-type Luenberger observer. The algorithm presented by Ferrante et. al in [7] is a viable solution for the scenario where the measurement output is aperiodic and instantaneously available. However, it is not robust to small delays when the when the plant state grows unbounded.

To show this, consider the impulsive observer,

$$\begin{cases} \dot{\hat{z}}{=}A\hat{z} & \forall t \notin \{t_k\}_0^{+\infty} \\ \hat{z}(t_k^+){=}\begin{cases} \hat{z}(t_k){+}L(y(t_{k-1}){-}M\hat{z}(t_k)) & \forall t{=}t_k, k \in \mathcal{I}_d \setminus \{0\} \\ \hat{z}(t_k) & \forall t{=}t_k, k \in \mathcal{I}_R \setminus \{0\} \end{cases} \end{cases} \tag{1.3}$$

where $L \in \mathbb{R}^{m \times n}$ is a gain matrix designed according to the algorithm in [7] such that the estimation error $\varepsilon := z - \hat{z}$ converges to zero.

Now, consider the scalar example from [7] given by the following system data: $A = 1$, $M = 1$ with chosen constants $T_1 = T_2 = 1$ and $L = 1 - e^{-1}$ designed such that the conditions outlined in [7] are satisfied. Then, let $T^d = 0.2$. Simulating the observer in (1.3), Figure 1.2 shows that the norm of the estimate error $\varepsilon = z - \hat{z}$ for the given data diverges due to the small delay introduced on the measurements.

Now suppose the measurements $y(t_k)$ are accompanied by a timestamp $\ell_t(t_k)$.

Then, consider the observer from (1.3) modified such that only instantaneous measurement arrivals are used and those that have incurred a delay during transmission are ignored by the observer

$$\begin{cases} \dot{\hat{z}} = A\hat{z} & \forall t \notin \{t_k\}_0^\infty \\ \hat{z}(t_k^+) = \begin{cases} \hat{z}'(t_k^+) & \forall k \in \mathcal{I}_d \\ \hat{z}(t_k) & \forall k \in \mathcal{I}_R \end{cases} \end{cases} \tag{1.4}$$

where

$$\hat{z}'(t_k^+) = \begin{cases} \hat{z}(t_k) + L(y(t_{k-1}) - M\hat{z}(t_k)) & \text{if } \ell_t(t_{k-1}) = t_k \\ \hat{z}(t_k) & \text{if } \ell_t(t_{k-1}) \neq t_k \end{cases}$$

Note that for this observer scheme, a local clock at the observer synchronized with the plant clock is necessary for the algorithm to identify the delayed measurements. Even then, this observer does not reconstruct the state for all scenarios.

In fact, consider the same system data as above, namely $A = 1$, $M = 1$, $L = 1 - e^{-1}$ with constants $T_1 = T_2 = 1$. Then, let $T^d = 0.2$. Simulating the observer in (1.4), at times $t \in \{t_k\}_{k=0}^\infty$ the estimate is corrected and the error decreases, but when the measurements are delayed, then the estimate provided by the observer does not converge. Figure 1.3 shows the behavior of the norm of the estimate error $\varepsilon = z - \hat{z}$ under such a scenario.

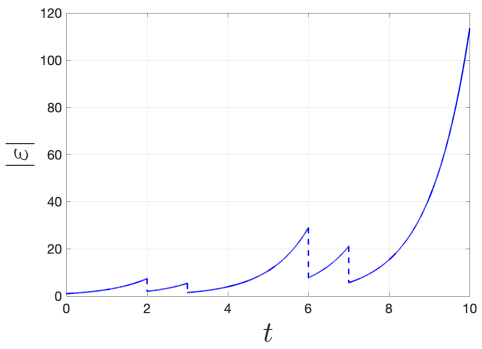

Figure 1.3: The evolution of the estimation error with respect to real time with the observer law that rejects delayed measurements. The vertical dashes represent the resets of $\hat{z}$ according to $\hat{z}^+$ in (1.4).

The issues outlined in the aforementioned examples motivate a hybrid observer design, with a clock synchronization scheme, that properly uses the information received even under the scenario of measurement delays.

As demonstrated by the preceding examples, the prime challenges to solve this problem are given as follows:

1. *Aperiodic measurement broadcast events at unknown times:* the event times at which plant measurements are sampled and broadcast to the network for the observer are not known a priori. In addition, the time elapsed between each broadcast event time instant is variable within a minimum and maximum allowable transfer interval.

2. *Variable transmission delays:* the network is treated as a non-ideal communication medium hence, it is subject to latency delays that are also assumed to be variable. Similar to the aperiodicity of the broadcast event times, the time-elapsed between between measurement broadcast and arrival is not fixed nor is it known a priori.

3. *De-Synchronized network clocks:* due to the variability in the broadcast and arrival times of measurements, consensus between networked agents on the system time frame is necessary to maintain the temporal ordering of measurement sampling events. However, imperfections in the dynamics and initialization of the clocks for each agent can lead to de-synchronization and thus a lack of consensus on event ordering.

In Chapter 3, we present our proposed solution through a formulation and analysis of the system model using the hybrid framework in [8]. Our proposed solution considers a modification to the impulsive observer in (1.3) that utilizes information on the incurred measurement delay. Similar to the impulsive observer in (1.4), the output measurements from the plant are timestamped then, by assuming the existence of synchronized clocks at the plant and observer, the observer compares the measurement timestamp to its own clock to retrieve the information on the incurred delay. Upon arrival of the measurement and timestamp at the observer, the current state estimate is back propagated via state transition matrix by the delay amount, the Luenberger observer law is applied using the back propagated estimate and measurement then, the new estimate is forward propagated to the current time.

We present the viability of our proposed solution through a series of results: We first show feasibility by presenting results for the ideal case where there is no incurred delay in the transmission of the measurements and we assume the observer clocks are synchronized. We then provide results with the incurred delay under the assumption that the clocks at the plant and observer are synchronized. Our third result relaxes the assumption

on the synchronized clocks by providing an attractivity analysis for the case where the clocks synchronize in finite time.

Our system formulation and, in particular, the attractivity analysis with the clocks that are not initially synchronized, demonstrates the need for clock synchronization scheme in a networked control system setting.

1.2 Introduction to the clock synchronization problem

In the previous example we highlighted the need for a clock synchronization scheme as it applies to a networked control system setting. In this section, we outline the motivation for a hybrid systems approach to clock synchronization. For many networked control system settings, each agent in the system is fitted with its own internal hardware clock and an instance of a software clock based on the dynamics of the hardware clock. Ideally, the ith agent in the system would have a clock $\tau_i \in \mathbb{R}_{\geq 0}$ such that $\tau_i(t) = t$ where t is the global or real time. However, many hardware clocks utilize quartz-crystal or MEMS oscillators that are susceptible to manufacturing imperfections and environmental factors and affect the oscillator frequency, see [5] and [9]. Due to the observed variability in oscillator frequency, one generally considers the continuous-time dynamics of the ith hardware clock node given by

$$\dot{\tau}_i = a_i \tag{1.5}$$

where $a_i \in \mathbb{R}$ defines the clock's drift or skew due to an imperfect oscillator. Solving the differential equation gives the following relationship to the ideal clock or real-time reference t

$$\tau_i(t) = a_i t + \tau_i(0) \tag{1.6}$$

where the initial condition $\tau_i(0)$ gives the offset from t. For a network of n agents, the notion of clock synchronization can be defined as the state of the networked system such that $\tau_i = \tau_j$ for all $i, j \in \{1, 2, \ldots, n\}$, $i \neq j$.

In an ideal setting with no delay and identical clock skews, synchronization between two nodes A and B can be achieved by the following algorithm: Node A send its time to Node B. Node B calculates its offset relative to A. Node B applies the offset correction to its clock. For the case of non-identical clock skews, a pair of measurements from Node A would allow Node B to calculate its relative skew $\frac{a_A}{a_B}$ and apply a correction accordingly.

In a realistic setting, however, network communication between nodes are often subjected to a variety of delays. Without loss of generality, these delays can be divided into two types: *propagation* time and *residence* time. Propagation time represents the actual time elapsed during message transmission between two nodes when the message is in the network channel. The residence time defines the time elapsed between message reception and egress of its response message, it captures all of the hardware-related delays such as *send* time, *access* time, *transmission* time, *reception* time and *receive* time, see [5] and [10] for more details. Moreover, depending on the system setting, these observed delays can either be deterministic or stochastic in nature and are the key challenge in networked clock synchronization. In light of this challenge, the goal of clock synchronization is to achieve synchronization while removing or mitigating the effects of delay.

1.3 Current state of the art in clock synchronization

Many of the existing clock synchronization protocols rely on message based exchanges of timestamps to synchronize the clocks to a common or shared reference. The reference based or centralized nature of these protocols requires that a common reference or a set of references be established first in order to achieve synchronization. Therefore, many of the existing message-based protocols implement a two-stage algorithm: the first stage establishes the node hierarchy based on clock accuracy while the second phase synchronizes the clocks. In the following examples, we will assume the network hierarchy is given as an analysis of the algorithms that establish the node hierarchy is beyond the scope of this proposal. For the clock synchronization phase, there exist three types of commonly used message based approaches: *two-way* message synchronization (or sender-receiver message synchronization), *one-way* message synchronization, and *receiver-receiver* synchronization.

1.3.1 Sender-Receiver message synchronization

The sender-receiver (or two-way) based synchronization algorithm is the most common of the message exchange synchronization protocols due to its utilization in the Network Time Protocol (NTP) in [11], the Precision Time Protocol (PTP) in [12] , and the Timing-sync Protocol for Sensor Networks (TPSN) in [10].

The core algorithm upon which these protocols are based relies on the existence of a known reference that is either injected to the system or provided by an elected agent in

the distributed system; synchronization is then achieved through a series of chronologically ordered and time stamped two-way message exchanges between each synchronizing node and the designated reference. With sufficient information from the exchanged messages and underlying assumptions on the clocks and communication delays, the relative differences in the clock rates and offset can be estimated and applied as a correction to the clock of the synchronizing node, see [13]. However, while the difference in the output can be determined and implemented online, the relative clock rate is estimated through offline filtering techniques (see [11]) or least-squares estimation (see [5]). Moreover, these algorithms are often not robust to changing network topology and asymmetry in transmission times, thus many protocols (such as NTP, PTP, and TPSN) often stipulate the following assumptions:

a) the existence of an established hierarchical structure such that each node has a designated reference;

b) fixed and symmetric transmission and residence times;

c) synchronized clock skews, i.e., $a_i = a_j$. [1]

Each of the aforementioned protocols, however, utilize different strategies in regards to the availability of the algorithm and the layer of implementation. For instance, the Network Time Protocol is an "always-on" implementation that runs entirely as a system process in the software layer. This level of implementation subjects the protocol to frequent computational delays due to the execution of system processes that have higher priority. These delays contribute to timing inaccuracy that renders NTP unfit for networked control systems with fast sampling periods, see [14].

Improving upon NTP to address its concerns and meet the demands of time-sensitive distributed system, the Precision Time Protocol utilizes a hybrid implementation of software and hardware to improve the synchronization accuracy. The protocol utilizes timestamping of the exchanged messages at the hardware layer to minimize the computational delays associated with software timestamps on the exchanged messages.

The Timing-sync Protocol for Sensor Networks seeks to address the scalability issues posed by the NTP and PTP protocols by allowing the algorithm to work on an in-

[1] Protocols such as TPSN assume that the clock offset between any two nodes does not change during synchronization which would imply that the clock skews are identical, see [10]. NTP assumes the existence of closed-loop controllers at each clock to give a common skew such that errors due to resolution and skew are minimized, see [11] and [6]. PTP assumes that the relative skews between two nodes is known or can be estimated, see [12].

termittent schedule. The intermittent strategy enable its use in low-energy sensor networks with limited computational capacity at the cost of synchronization accuracy.

The mechanics of the algorithm are given as follows: consider a designated reference agent R and a synchronizing agent S, with the following dynamics

$$\begin{aligned} \dot{\tau}_R &= a_R \\ \dot{\tau}_S &= a_S \end{aligned} \tag{1.7}$$

where $a_R = a_S$. At some time instances t_k, $k \in \mathbb{N}$ the nodes broadcast a message with embedded timestamp

$$T_k^i := \tau_i(t_k) = a_i(t_k) + \tau_i(0) \tag{1.8}$$

Assuming the sequence of time instants $\{t_k\}_{k=1}^{\infty}$ is strictly increasing and unbounded, the two-way message synchronization algorithm is given as follows:

1. - At time t_1, Node R sends a message with an embedded timestamp

   $$T_1^R = a_R(t_1) + \tau_R(0)$$

   to node S.

2. - At time t_2, Node S receives the message and records the arrival time

   $$T_2^S = a_S(t_2) + \tau_S(0)$$

3. - At time t_3, Node S responds to node R with embedded timestamp

   $$T_3^S = a_S(t_3) + \tau_S(0)$$

   indicating the time of transmission.

4. - At time t_4, Node R receives the message from node S and records the arrival time

   $$T_4^R = a_R(t_4) + \tau_R(0)$$

5. - At time t_5, Node R responds to node S with the timestamp T_4^R embedded.

6. - At time t_6, Node S has collected timestamps T_1^R, T_2^S, T_3^S, and T_4^R.

Then at time t_6, the relative offset $\theta := \tau_R(0) - \tau_S(0)$ is calculated as follows:

$$\begin{aligned}\frac{1}{2}\big((T_4^R - T_3^S) - (T_2^S - T_1^R)\big) &= \frac{1}{2}\Big(\big((a_R(t_4) + \tau_R(0)) - (a_S(t_3) + \tau_S(0))\big) \\ &\quad - \big((a_S(t_2) + \tau_S(0)) - (a_R(t_1) + \tau_R(0))\big)\Big) \\ &= \frac{1}{2}\Big(\big(a_R(t_4) - a_S(t_3) + \theta\big) - \big(a_S(t_2) - a_R(t_1) - \theta\big)\Big)\end{aligned}$$

Since the skews are assumed to be synchronized, let $a_S = a_R$ and suppose $a_R = 1$, then

$$\begin{aligned}\frac{1}{2}\big((T_4^R - T_3^S) - (T_2^S - T_1^R)\big) &= \frac{1}{2}\Big(\big(a_R(t_4 - t_3) + \theta\big) - \big(a_R(t_2 - t_1) - \theta\big)\Big) \\ &= \frac{1}{2}\Big(\big((t_4 - t_3) + \theta\big) - \big((t_2 - t_1) - \theta\big)\Big)\end{aligned} \tag{1.9}$$

Now, since the propagation and residence times are assumed to be fixed and symmetric, let d be some positive constant, then

$$t_2 - t_1 = t_4 - t_3 = t_6 - t_5 = d$$

Making the appropriate substitutions in (1.9),

$$\begin{aligned}\frac{1}{2}\big((T_4^R - T_3^S) - (T_2^S - T_1^R)\big) &= \frac{1}{2}\Big(\big(d + \theta\big) - \big(d - \theta\big)\Big) \\ &= \frac{1}{2}\big(\theta + \theta\big) \\ &= \theta\end{aligned}$$

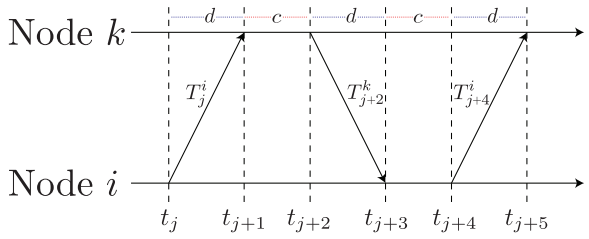

Figure 1.4: Diagram to illustrate the message exchange between the reference and synchronizing nodes for the synchronization algorithm. R refers to the time frame of the reference node while S refers to the time frame of the synchronizing node.

As noted, the success of two-way message based algorithms hinges on the given assumptions which aren't always necessarily guaranteed in every distributed system. In particular, it is not always the case that the propagation times will remain fixed and symmetric especially in a wireless network with dynamic topology. Moreover, a dynamic topology poses

issues to the established hierarchical structure and would thus require the re-execution of network discovery algorithms to reestablish hierarchical topology. The conjunction of a dynamic topology and the execution of algorithms to establish the network hierarchy algorithms can introduce additional delay to the clock synchronization.

1.3.2 One-way message synchronization

One-way message synchronization is the approach used by the Flooding Time Synchronization Protocol (FTSP) [15]. This approach assumes the existence of a reference node to which all of the nodes in the network must synchronize. The reference node periodically broadcasts timestamps, each node records its time of arrival and stores the pair of timestamps. Each receiving node performs a least-squares minimization using the stored timestamp pairs to calculate the relative clock skew and offset. To demonstrate how the least-squares minimization is formulated, consider the same two nodes R and S with dynamics as in (6.1) and timestamps as in (5.2). For a strictly increasing and unbounded sequence of time instants $\{t_k\}_{k=1}^{\infty}$, a sample of the protocol execution is given as follows

1. At time t_1, the reference node R broadcasts timestamp

$$T_1^R = a_R(t_1) + \tau_R(0)$$

2. At time t_2 Node S receives T_1^R and records its time of arrival

$$T_2^S = a_S(t_2) + \tau_S(0)$$

Now, if one assumes that the propagation time is fixed, then let $d = t_2 - t_1$ for some positive constant d. By rearranging T_1^R, one has

$$t_1 = \frac{1}{a_R}(T_1^R - \tau_R(0)) \tag{1.10}$$

substituting the expression for t_1 into the equation for the propagation time, $d = t_2 - t_1$, t_2 can be expressed as follows

$$t_2 = \frac{1}{a_R}\big(T_1^R - \tau_R(0)\big) + d \tag{1.11}$$

then making the appropriate substitutions into T_2^S, one has

$$\begin{aligned} T_2^S &= a_S(t_2) + \tau_S(0) \\ &= a_S\Big(\frac{1}{a_R}(T_1^R - \tau_R(0)) + d\Big) + \tau_S(0) \\ &= \frac{a_S}{a_R}\Big(T_1^R - \tau_R(0) + a_R d\Big) + \tau_S(0) \\ &= \frac{a_S}{a_R}T_1^R - \frac{a_S}{a_R}\tau_R(0) + a_R d + \tau_S(0) \\ &= \frac{a_S}{a_R}T_1^R + a_R d + \tau_S(0) - \frac{a_S}{a_R}\tau_R(0) \end{aligned} \tag{1.12}$$

By letting $\theta = \tau_R(0) - \tau_S(0)$ be the initial relative offset and then rearranging the expression such that $\tau_S(0) = \tau_R(0) - \theta$ it can then be substituted in (1.12) to give

$$\begin{aligned} T_2^S &= \frac{a_S}{a_R}T_1^R + a_R d + \tau_R(0) - \theta - \frac{a_S}{a_R}\tau_R(0) \\ &= \frac{a_S}{a_R}T_1^R + a_R d - \theta + \big(1 - \frac{a_S}{a_R}\big)\tau_R(0) \end{aligned}$$

Then for any subsequent timestamp pair $\{T_{k+1}^S, T_k^R\}$, T_{k+1}^S can be expressed as follows

$$T_{k+1}^S = f^{SM}T_k^R + a_R d - \theta + \epsilon$$

where $f^{SM} := \frac{a_S}{a_R}$ and $\epsilon := \big(1 - f^{SM}\big)\tau_R(0)$. The idea is to then estimate the relative clock skew f^{SM} and offset θ via linear regression once a sufficient number of measurement pairs has been collected.

Note that in the estimation, the offset cannot be differentiated from the skewed propagation delay $a_R d$ contributing an error to the offset estimation. This does not pose an issue if the propagation delay is assumed to be small or negligible as assumed in [10]. However, if the propagation delay is variable and non-Gaussian then the least-squares estimation will not be able to give an accurate estimation. Moreover, if the reference node become compromised or lost, the system must re-elect a new reference node to serve as the system reference contributing additional delay to the synchronization.

1.3.3 Receiver-receiver synchronization

Receiver-receiver based synchronization is the scheme proposed by the authors of [16]. Similar to the one-way messaging scheme, there exists a master node that broadcasts a 'ping' message to the network. Though, instead of synchronizing to the master node, the

receivers synchronize to a common time scale by exchanging timestamps of their ping receipt time observations with neighboring receivers. Consider three nodes R, S_1, and S_2 with dynamics as in 6.1 and timestamps as in 5.2. Then for a strictly increasing and unbounded sequence of time instants $\{t_k\}_{k=1}^{\infty}$, the protocol operates as follows

1. At time t_1, the master node R broadcasts a ping

$$T_1^R = a_R(t_1) + \tau_R(0)$$

2. At time t_2, Node S_1 receives the ping and records its time of arrival

$$T_2^{S_1} = a_{S_1}(t_2) + \tau_{S_1}(0)$$

3. At time t_3, Node S_2 receives the ping and records its time of arrival

$$T_3^{S_2} = a_{S_2}(t_3) + \tau_{S_2}(0)$$

4. At time t_4, Node S_1 broadcasts its arrival timestamp $T_2^{S_1}$
5. At time t_5, Node S_2 broadcasts its arrival timestamp $T_3^{S_2}$
6. At time t_6, Node S_2 receives timestamp $T_2^{S_1}$
7. At time t_7, Node S_1 receives timestamp $T_3^{S_2}$

Following the receipt of each timestamp from a neighboring node, nodes S_1 and S_2 perform corrections to their respective clocks using the timestamp pair $\{T_2^{S_1}, T_3^{S_2}\}$. Let d_{ij} denote the propagation time between any two nodes i and j and assume it is a fixed positive constant. Then, by observing $d_{RS_1} = t_2 - t_1$, $d_{RS_2} = t_3 - t_1$, and that T_1^R gives the transmit time of the ping in the time reference frame of the master node, then by using the relation

$$t_1 = \frac{1}{a_R}(T_1^R - \tau_R(0))$$

to give

$$t_2 = \frac{1}{a_R}\big(T_1^R - \tau_R(0)\big) + d_{RS_1}$$
$$t_3 = \frac{1}{a_R}\big(T_1^R - \tau_R(0)\big) + d_{RS_2}$$

the timestamps $T_2^{S_1}$ and $T_3^{S_2}$ can be expressed as follows

$$\begin{aligned} T_2^{S_1} &= \frac{a_{S_1}}{a_R} T_1^R + a_R d_{RS_1} + \tau_{S_1}(0) - \frac{a_{S_1}}{a_R}\tau_R(0) \\ T_3^{S_2} &= \frac{a_{S_2}}{a_R} T_1^R + a_R d_{RS_2} + \tau_{S_2}(0) - \frac{a_{S_2}}{a_R}\tau_R(0) \end{aligned} \tag{1.13}$$

If the clock skews of S_1 and S_2 are synchronized, i.e., $a_R = a_S$, then taking the difference in the timestamps gives

$$\begin{aligned} T_3^{S_2} - T_2^{S_1} &= \big(\frac{a_{S_1}}{a_R} T_1^R + a_R d_{RS_1} + \tau_{S_1}(0) - \frac{a_{S_1}}{a_R}\tau_R(0)\big) \\ &\qquad - \big(\frac{a_{S_2}}{a_R} T_1^R + a_R d_{RS_2} + \tau_{S_2}(0) - \frac{a_{S_2}}{a_R}\tau_R(0)\big) \\ &= a_R d_{RS_1} + \tau_{S_1}(0) - a_R d_{RS_2} - \tau_{S_2}(0) \\ &= a_R d_{RS_1} - a_R d_{RS_2} + \tau_{S_1}(0) - \tau_{S_2}(0) \\ &= a_R (d_{RS_1} - d_{RS_2}) + \tau_{S_1}(0) - \tau_{S_2}(0) \end{aligned} \tag{1.14}$$

Now, if the propagation delay is assumed to be identical $d_{RS_1} = d_{RS_2}$ or effectively zero $d_{RS_1} = d_{RS_2} = 0$, as is assumed in the RBS protocol (see [16]), then

$$T_3^{S_2} - T_2^{S_1} = \tau_{S_1}(0) - \tau_{S_2}(0) \tag{1.15}$$

yielding the clock offset of nodes S_1 and S_2.

If the clock skews are not initially synchronized, observe that a second set of timestamps will allow each node to its relative skew. Suppose the master node broadcasts a second ping T_7^R at time t_7 arriving at nodes S_1 and S_2 at times t_8 and t_9, respectively. Following the exchange of timestamps $T_8^{S_1}$ and $T_9^{S_2}$, the relative skew rate between nodes S_1 and S_2 is calculated as follows

$$\begin{aligned} \frac{T_8^{S_1} - T_2^{S_1}}{T_9^{S_2} - T_3^{S_2}} &= \frac{\big(\frac{a_{S_1}}{a_R} T_7^R + a_R d_{RS_1} + \tau_{S_1}(0) - \frac{a_{S_1}}{a_R}\tau_R(0)\big) - \big(\frac{a_{S_1}}{a_R} T_1^R + a_R d_{RS_1} + \tau_{S_1}(0) - \frac{a_{S_1}}{a_R}\tau_R(0)\big)}{\big(\frac{a_{S_2}}{a_R} T_7^R + a_R d_{RS_2} + \tau_{S_2}(0) - \frac{a_{S_2}}{a_R}\tau_R(0)\big) - \big(\frac{a_{S_2}}{a_R} T_1^R + a_R d_{RS_2} + \tau_{S_2}(0) - \frac{a_{S_2}}{a_R}\tau_R(0)\big)} \\ &= \frac{\frac{a_{S_1}}{a_R}(T_7^R - T_1^R)}{\frac{a_{S_2}}{a_R}(T_7^R - T_1^R)} \\ &= \frac{a_{S_1}}{a_{S_2}} \end{aligned} \tag{1.16}$$

Alternatively, if a timestamp rather than a ping is sent by the master node, then both the skew and offset can be estimated by performing a least-squares linear regression. Assume the propagation delay is identical $d_{RS_1} = d_{RS_2}$ or effectively zero $d_{RS_1} = d_{RS_2} = 0$,

assume further that the master node is an ideal clock with skew $a_R = 1$ and offset $\tau_R(0) = 0$, then equation (1.18) gives

$$\begin{aligned} T_3^{S_2} - T_2^{S_1} &= \big(\frac{a_{S_1}}{a_R} T_1^R + a_R d_{RS_1} + \tau_{S_1}(0) - \frac{a_{S_1}}{a_R}\tau_R(0)\big) - \big(\frac{a_{S_2}}{a_R} T_1^R + a_R d_{RS_2} + \tau_{S_2}(0) - \frac{a_{S_2}}{a_R}\tau_R(0)\big) \\ &= (a_{S_1} - a_{S_2}) T_1^R + \big(\tau_{S_1}(0) - \tau_{S_2}(0)\big) \end{aligned} \tag{1.17}$$

This can be generically extended to any subsequent timestamp triplet $\{T_{k+2}^{S_2}, T_{k+1}^{S_1}, T_k^R\}$ as follows

$$T_{k+2}^{S_2} - T_{k+1}^{S_1} = (a_{S_1} - a_{S_2}) T_k^R + \big(\tau_{S_1}(0) - \tau_{S_2}(0)\big) \tag{1.18}$$

Once a sufficient quantity of timestamp triplets the least-squares regression can be performed to give the skew and offset.

Similarly to the other two message based algorithms, receiver-receiver synchronization requires assumptions on the propagation delay in order to achieve synchronization that may not necessarily exist in every scenario. It is also not robust to any losses or compromises to the master node and also requires a re-election of a master node resulting in additional synchronization delays.

1.3.4 Issues with current state of the art algorithms and protocols

In the original works presented on the respective message based synchronization schemes, the authors would provide analytical and experimental results to verify the validity of their algorithms but would omit any analysis on their rate of convergence and robustness. The survey paper [6] provides some high level analysis of current algorithms citing qualitative advantages and disadvantages of the various message based schemes but fails to provide any formal analytical results. The work in [13] gives results on the feasibility of synchronization for these message based algorithms under various assumptions but does not provide any details on convergence or robustness.

Additionally, we have outlined the following challenges associated with clock synchronization:

1. *Stochastic and deterministic delays:* As discussed in Section 1.2, communication over digital networks introduces a variety of delay sources that have both deterministic and stochastic origins. The accumulation of these delays poses the greatest challenge to synchronization since they are difficult to measure or estimate.

2. *Variable clock skews:* Many of the existing algorithms assume the clock skew over the synchronization period is relatively static. Realistically, clock skews have time-varying characteristics due to the environmental susceptibilities of the hardware oscillators such as swings in temperature and the corrosion of parts.

3. *Network Traffic / Sporadic broadcasts:* Since clock synchronization protocols are often a subsystem to larger systems communicating over the same network, it is often subject to network traffic leading to asynchronous broadcasts of timestamps and increasing the issue of delay.

4. *Centralization:* As has been observed in each of the message based synchronization examples, each synchronization scheme uses a centralized algorithm. The centralized nature of each algorithm adds additional complexity to the protocol design and poses challenges in synchronization with a dynamic network topology.

5. *Scalability:* Most protocols are often designed with scalability in mind however, in some instances different performance parameters can degrade as the size of the network increases. For instance, in the case of two-way message synchronization, synchronization can only occur between a sender-receiver pair of nodes at any give time, thus for a network of n nodes with a single reference and $n-1$ nodes, system-wide synchronization will increase by a factor of $n-1$. Moreover, it can contribute significant traffic overhead to the network. Receiver-receiver based synchronization for instance requires $O(n^2)$ message exchanges in order to achieve synchronization, see [6].

Chapter 2

Preliminaries

2.1 Notation

In this proposal the following notation and definitions will be used. $\mathbb{N}$ denotes the set of natural numbers, i.e., $\mathbb{N} = \{0, 1, 2, ..\}$. $\mathbb{N}_{>0}$ denotes the set of natural numbers not including 0, i.e., $\mathbb{N}_{>0} = \{1, 2, ..\}$. $\mathbb{R}$ denotes the set of real numbers. $\mathbb{R}_{\geq 0}$ denotes the set of non-negative real numbers, i.e., $\mathbb{R}_{\geq 0} = [0, \infty)$. $\mathbb{R}^n$ denotes n-dimensional Euclidean space. Given topological spaces A and B, $F : A \rightrightarrows B$ denotes a set-valued map from A to B. For a matrix $A \in \mathbb{R}^{n \times m}$, A^{T} denotes the transpose of A. For a matrix $A \in \mathbb{R}^{n \times m}$, A^* denotes the conjugate transpose of A. Given a vector $x \in \mathbb{R}^n$, $|x|$ denotes the Euclidean norm. Given two vectors $x \in \mathbb{R}^n$ and $y \in \mathbb{R}^R$, $(x, y) = [x^{\mathsf{T}} \ y^{\mathsf{T}}]^{\mathsf{T}}$. Given a matrix $A \in \mathbb{R}^n$, $\lambda_{\max}(A)$ denotes the largest eigenvalue of A and $\lambda_{\min}(A)$ denotes the smallest eigenvalue of A. Given a matrix $A \in \mathbb{R}^n$, $|A| := \max\{\sqrt{|\lambda|} : \lambda \in \text{eig}(A^{\mathsf{T}}A)\}$. For two symmetric matrices $A \in \mathbb{R}^n$ and $B \in \mathbb{R}^n$, $A \succ B$ means that $A - B$ is positive definite, conversely $A \prec B$ means that $A - B$ is negative definite. Given a closed set $A \subset \mathbb{R}^n$ and closed set $B \subset A$, the projection of A onto B is denoted by $\Pi_B(A)$. Given a function $f : \mathbb{R}^n \to \mathbb{R}^R$, the range of f is given by $\text{rge } f := \{y \mid \exists\, x \text{ with } y \in f(x)\}$. A vector of N ones is denoted $\mathbf{1}_N$. The matrix I_n is used to denote the identity matrix of size $n \times n$.

2.2 Preliminaries on Hybrid Systems

In this chapter we introduce some preliminaries on hybrid systems and the framework by which we model them. In addition, we provide some introductory preliminaries on

graph theory that will be used in later chapters.

A hybrid system $\mathcal{H}$ in $\mathbb{R}^n$ is composed by the following *data*:

- a set $C \subset \mathbb{R}^n$, called the flow set;
- a set-valued mapping $F : \mathbb{R}^n \rightrightarrows \mathbb{R}^n$ with $C \subset \text{dom } F$, called the flow map;
- a set $D \subset \mathbb{R}^n$, called the jump set;
- a set-valued mapping $G : \mathbb{R}^n \rightrightarrows \mathbb{R}^n$ with $D \subset \text{dom } G$, called the jump map;

Then, a hybrid system $\mathcal{H} := (C, f, D, G)$ is written in its compact form is given by

$$\mathcal{H} : \begin{cases} x \in C & \dot{x} \ = f(x) \\ x \in D & x^+ \in G(x) \end{cases} \tag{2.1}$$

where x is the system state. Solutions to hybrid systems are denoted by ϕ and are parameterized by (t, j), where $t \in \mathbb{R}_{\geq 0}$ defines ordinary time and $j \in \mathbb{N}$ is a counter that defines the number of jumps. A solution ϕ is defined by a *hybrid arc* on its domain dom ϕ with *hybrid time domain* structure [4]. The domain dom ϕ is a hybrid time domain if dom $\phi \subset \mathbb{R}_{\geq 0} \times \mathbb{N}$ and for each $(T, J) \in$ dom ϕ, dom $\phi \cap ([0, T] \times \{0, 1, ..., J\})$ is of the form $\bigcup_{j=0}^{J}([t_j, t_{j+1}] \times \{j\})$, with $0 = t_0 \leq t_1 \leq t_2 \leq t_{J+1}$. A function $\phi : \text{dom } \phi \to \mathbb{R}^n$ is a *hybrid arc* if dom ϕ is a hybrid time domain and if for each $j \in \mathbb{N}$, the function $t \mapsto \phi(t, j)$ is locally absolutely continuous on the interval $I^j = \{t : (t, j) \in \text{dom } \phi\}$. A solution ϕ satisfies the system dynamics; see [4, Definition 2.6] for more details. A solution ϕ is said to be *maximal* if it cannot be extended by flow or a jump, and *complete* if its domain is unbounded. The set of all maximal solutions to a hybrid system $\mathcal{H}$ is denoted by $\mathcal{S}_{\mathcal{H}}$ and the set of all maximal solutions to $\mathcal{H}$ with initial condition belonging to a set A is denoted by $\mathcal{S}_{\mathcal{H}}(A)$. A hybrid system is *well-posed* if it satisfies the hybrid basic conditions in [4, Assumption 6.5].

Definition 2.2.1. *Given a hybrid system $\mathcal{H}$ defined on $\mathbb{R}^n$, the closed set $\mathcal{A} \subset \mathbb{R}^n$ is said to be*

- *stable for $\mathcal{H}$ if for every $\epsilon > 0$ there exists $\delta > 0$ such that every maximal solution ϕ to $\mathcal{H}$ with $|\phi(0,0)|_{\mathcal{A}} \leq \delta$ satisfies $|\phi(t,j)|_{\mathcal{A}} \leq \epsilon$ for all $(t, j) \in$ dom ϕ;*
- *attractive for $\mathcal{H}$ if there exists $\mu > 0$ such that every maximal solution ϕ to $\mathcal{H}$ with $|\phi(0,0)|_{\mathcal{A}} \leq \mu$ is complete and satisfies $\lim_{t+j\to\infty} |\phi(t,j)|_{\mathcal{A}} = 0$;*

- *asymptotically stable for $\mathcal{H}$ if both stable and attractive for $\mathcal{H}$.*
- *globally exponentially stable (GES) for $\mathcal{H}$ if there exists positive scalars $\kappa, \alpha > 0$ such that every solution ϕ to $\mathcal{H}$ is such that every maximal solution ϕ to $\mathcal{H}$ is complete and satisfies $|\phi(t,j)|_{\mathcal{A}} \leq \kappa e^{-\alpha(t+j)} |\phi(0,0)|_{\mathcal{A}}$ for each $(t,j) \in$ dom ϕ.*

Moreover, when inputs are present for a given linear time invariant system, one has similar notions as long as every static solution for every input satisfies the properties in Definition 2.2.1. For details on hybrid systems, see [8].

2.3 Preliminaries on Graph Theory

Let $\mathcal{G} = (\mathcal{V}, \mathcal{E}, A)$ be a weighted directed graph (digraph) where $\mathcal{V} = \{v_1, v_2, \ldots, v_n\}$ represents the set of n nodes, $\mathcal{E} \subset \mathcal{V} \times \mathcal{V}$ the set of edges, and $A \in \{0,1\}^{n \times n}$ represents the adjacency matrix. An edge of $\mathcal{G}$ is denoted by $e_{ij} = (v_i, v_j)$. The elements of A are denoted by a_{ij} where $a_{ij} = 1$ if $e_{ij} \in \mathcal{E}$ and $a_{ij} = 0$ otherwise. The in-degree and out-degree of a node v_i are defined by $d^{in}(v_i) = \sum_{k=1}^{n} a_{ki}$ and $d^{out}(v_i) = \sum_{k=1}^{n} a_{ik}$, respectively. The largest and smallest in-degree of a digraph is given by $\bar{d} = \max_{i \in \mathcal{V}} d^{in}(v_i)$ and $\underline{d} = \min_{i \in \mathcal{V}} d^{in}(v_i)$. The in-degree matrix is a diagonal matrix denoted $\mathcal{D}$ with elements given by

$$d_{ij} = \begin{cases} d^{in}(i) & \text{if } i = j \\ 0 & \text{if } i \neq j \end{cases} \qquad \forall v_i \in \mathcal{V}$$

The Laplacian matrix of a digraph $\mathcal{G}$, denoted by $\mathcal{L}$, is defined as $\mathcal{L} = \mathcal{D} - A$ and has the property that $\mathcal{L}\mathbf{1}_n = 0$. The set of nodes corresponding to the neighbors that share an edge with node v_i is denoted by $\mathcal{N}(v_i) := \{k \in \mathcal{V} \ : \ e_{ki} \in \mathcal{E} \ \}$. In the context of networks $\mathcal{N}(v_i)$, this represents the set of nodes for which an agent v_i can communicate with.

Lemma 2.3.1. *((Olfati-Saber and Murray, 2004, Theorem 6),(Fax and Murray, 2004, Propositions 1, 3, and 4)) For an undirected graph, $\mathcal{L}$ is symmetric and positive semidefinite and each eigenvalue of $\mathcal{L}$ is real. For a directed graph, zero is a simple eigenvalue of $\mathcal{L}$ if the directed graph is strongly connected.*

Lemma 2.3.2. *(Godsil and Royle (2013)) Consider an $n \times n$ symmetric matrix $A = \{a_{ik}\}$ satisfying $\sum_{i=1}^{n} a_{ik} = 0$ for each $k \in \{1, 2, \ldots, n\}$. The following statements hold:*

- *There exists an orthogonal matrix U such that $U^\top AU = \begin{bmatrix} 0 & 0 \\ 0 & \star \end{bmatrix}$ where $\star$ represents any nonsingular matrix with appropriate dimensions and 0 represents any zero matrix with appropriate dimensions.*

- *The matrix A has a zero eigenvalue with eigenvector $\mathbf{1}_n \in \mathbb{R}^n$.*

Definition 2.3.3. *A weighted digraph is said to be*

- *balanced* if the in-degree matrix and out-degree matrix for every node is equal, i.e., $d^{in}(v_i) = d^{out}(v_i)$ for each $v_i \in \mathcal{V}$.

- *complete* if every pair of distinct nodes is connected by a unique edge, i.e., $a_{ik} = 1$ for each $i, k \in \mathcal{V}, i \neq k$.

- *strongly connected* if and only if for any two distinct nodes there exists a path of directed edges that connects them.

Chapter 3

A Hybrid Observer for Linear Systems under Delayed Sporadic Measurements

In this chapter, we present a hybrid observer for state estimation over a network that motivates our work on algorithms for clock synchronization. To construct the problem, we assume a networked plant and observer whereby the network provides delayed measurements of the output of the plant at time instants that are not necessarily periodic. The measurements are accompanied by timestamps provided by a clock that synchronizes with the clock of the observer in finite time. The proposed observer, along with the plant and communication network, are modeled by a hybrid dynamical system that has two timers, a logic variable, and two memory states to capture the mechanisms involved in the events associated with sampling and arrival of information, as well as the logic in the estimation algorithm. The hybrid model also includes a generic clock synchronization scheme to cope with a mismatch between the clocks at the plant and the observer. Convergence properties of the estimation error of the system are shown analytically and supported by numerical examples.

3.1 Problem Statement

Problem 3.1.1. *Given the linear time invariant system (1.1) and positive constants* $0 < T^d \leq T_1^N \leq T_2^N$*, design a hybrid algorithm including the hybrid observer in (3.1) such that the resulting closed-loop system* $\mathcal{H}$ *is such that* $\hat{z}(t,j) - z(t,j)$ *converges to zero as* $t+j \to \infty$*.*

To solve this problem, we propose the following hybrid strategy for reconstructing the state z:

- Measurements y broadcast at times t_k, $k \in \mathcal{I}_d$, are accompanied by a time-stamp $\ell_t(t_k) = t_k$.
- When the subsequent measurements arrive at times t_k, $k \in \mathcal{I}_m$, the current state estimate $\hat{z}(t_k)$ is backward propagated to $\hat{z}(t_{k-1})$ via

$$\hat{z}(t_{k-1}) = e^{-A\delta_k}\hat{z}(t_k)$$

  where $\delta_k := t_k - \ell_t(t_{k-1})$ is the incurred delay.

- With the estimate $\hat{z}(t_k)$ retrieved, the reset law in (1.3) is applied, namely,

$$\begin{aligned}\hat{z}^* &= \hat{z}(t_{k-1}) + L\big(y(t_{k-1}) - M\hat{z}(t_{k-1})\big)\\ &= e^{-A\delta_k}\hat{z}(t_k) + L\big(y(t_{k-1}) - Me^{-A\delta_k}\hat{z}(t_k)\big)\end{aligned}$$

  where $\hat{z}^*$ is the value of the estimate obtained after the reset law is applied.

- The reset estimate $\hat{z}^*(t_{k-1}^+)$ is then forward propagated to t_k

$$\hat{z}^*(t_k) = e^{A\delta_k}\hat{z}^*$$

Combining the above steps into a model, the proposed hybrid observer law can be summarized as follows:

$$\begin{cases}\dot{\hat{z}} = A\hat{z} & \forall t \notin \{t_k\}_0^\infty\\ \hat{z}(t_k^+) = \begin{cases}\hat{z}(t_k) + e^{A\delta_k}L\big(y(t_{k-1}) - Me^{-A\delta_k}\hat{z}(t_k)\big) & \forall t{=}t_k, k \in \mathcal{I}_d\\ \hat{z}(t_k) & \forall t{=}t_k, k \in \mathcal{I}_m\end{cases}\end{cases} \tag{3.1}$$

Excluding the measurement output y, the proposed strategy relies on the accessibility to information on the delay interval δ_k however, such information requires that both plant and

observer have consensus on the global time. Therefore, in addition to the presented strategy for state estimation, the proposed system incorporates a clock synchronization scheme to ensure consensus on the global time and maintain accessibility to the information on δ_k.

The design of this hybrid algorithm requires finding a proper choice of the matrix L. To find such an L, we consider the LMI condition presented in [7] for which an algorithm is given to solve. The hybrid algorithm proposed in this thesis also includes provisions for a clock synchronization algorithm the clocks determining time for both the plant and the observer.

Next, we define the hybrid model that provides the framework and solution to Problem 3.1.1. The model is constructed such that the observer defined in (3.1) is recast with the dynamics of the network as a hybrid system with a set-valued jump map. Moreover, provisions are included to facilitate the inclusion of a clock synchronization strategy to ensure proper function of the hybrid observer. To build such a model, we treated the observer and clock synchronization strategy as individual but interconnected subsystems. Figure 3.1 describes such a system where, $\mathcal{H}_a$ is the plant-observer subsystem and $\mathcal{H}_b$ is the clock synchronization subsystem. With the chosen design of $\mathcal{H}$, the system can be viewed as the interconnection of two hybrid subsystems.

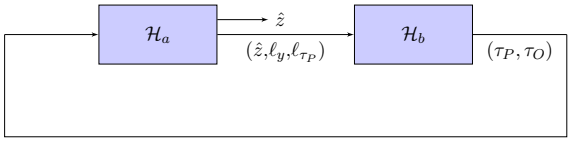

Figure 3.1: Diagram of the observer $\mathcal{H}_a$ and clock synchronization $\mathcal{H}_b$ subsystems and their interconnection.

To model the aperiodic measurement sampling of the plant, a timer variable τ_N is used. Between measurement sampling events the timer flows with dynamics given by $\dot{\tau}_N = -1$ and when $\tau_N = 0$, the state τ_N is reset to a value in the interval $[T_1^N, T_2^N]$. The transmission delay is modeled by an additional timer τ_δ with dynamics $\dot{\tau}_\delta = -q$. Here $q \in \{0, 1\}$ is a discrete variable used to control the dynamics of τ_δ such that the timer is active only following measurement broadcast events. More precisely, $q = 1$ denotes an active measurement in the network and $q = 0$ denotes the absence of such a measurement in the network. Thus, when $\tau_N = 0$, τ_δ is reset to a point in the interval $[0, T^d]$ and q is reset to 1. When $\tau_\delta = 0$, indicating measurement arrival, τ_δ is reset to -1 and q is reset

to 0. Having the timers τ_N and τ_δ defined in this way, with the addition of q, enforces the constraints defined in (1.2) for broadcast and arrival events.

Additionally, we let ℓ_y and ℓ_{τ_P} represent memory states that define the plant measurement data and associated timestamp, respectively. The states τ_P and τ_O represent the global clocks for the respective plant and observer. The state μ represents the state variables for a clock synchronization algorithm.

Then, we define the state vector of the interconnection of the plant and the observer system $\mathcal{H}$ as $x := (x_a, x_b) \in \mathcal{X}_a \times \mathcal{X}_b =: \mathcal{X}$ where $x_a := (z, \hat{z}, \tau_N, \tau_\delta, q, \ell_y, \ell_{\tau_P}) \in \mathcal{X}_a$, $x_b := (\tau_P, \tau_O, \mu) \in \mathcal{X}_b$ with $\mathcal{X}_a := \mathbb{R}^n \times \mathbb{R}^n \times [0, T_2^N] \times \big(\{-1\} \cup [0, T^d]\big) \times \{0, 1\} \times \mathbb{R}^m \times \mathbb{R}_{\geq 0}$ and $\mathcal{X}_b := \mathbb{R}_{\geq 0} \times \mathbb{R}_{\geq 0} \times \mathcal{M}$. The closed set $\mathcal{M}$ defines possible values of μ. The flow map is given by

$$F(x) := \begin{bmatrix} F_a(x_a) \\ F_b(x_b, \hat{z}, \ell_y, \ell_{\tau_P}) \end{bmatrix} \quad \forall x \in C$$

where

$$F_a(x_a) := \big(Az, A\hat{z}, -1, -q, 0, 0, 0\big)$$

and

$$F_b(x_b, \hat{z}, \ell_y, \ell_{\tau_P}) := \big(1, 1, F_s(x_b, \hat{z}, \ell_y, \ell_{\tau_P})\big)$$

with F_s governing the continuous dynamics of μ. The flow set C is defined as $C := C_a \cap C_b$ where $C_a := C_{a_1} \cup C_{a_2}$ and

$$C_{a_1} := \{x \in \mathcal{X} : q = 0, \tau_\delta = -1\}$$
$$C_{a_2} := \{x \in \mathcal{X} : q = 1, \tau_\delta \in [0, T^d]\}$$

and C_b is the flow set defined by the clock synchronization algorithm. The jump map is given by

$$G(x) := \begin{bmatrix} G_a(x_a, \tau_P, \tau_O) \\ G_b(\hat{z}, \ell_y, \ell_{\tau_P}, x_b) \end{bmatrix} \quad \forall x \in D$$

where G_a is defined as

$$G_a(x_a, \tau_P, \tau_O) := \begin{cases} G_1(x_a, \tau_P) & \text{if } x \in D_{a_1} \setminus D_b \\ G_2(x_a, \tau_O) & \text{if } x \in D_{a_2} \setminus D_b \\ x_a & \text{if } x \in D_b \backslash (D_{a_1} \cup D_{a_2}) \\ \{x_a, G_1(x_a, \tau_P)\} & \text{if } x \in D_{a_1} \cap D_b \\ \{x_a, G_2(x_a, \tau_O)\} & \text{if } x \in D_{a_2} \cap D_b \end{cases}$$

for each $x \in D$

$$G_1(x_a, \tau_P) = \begin{bmatrix} z \\ \hat{z} \\ [T_1^N, T_2^N] \\ [0, T^d] \\ 1 \\ Mz \\ \tau_P \end{bmatrix} \qquad \forall (x_a, \tau_P) : x \in D_{a_1}$$

$$G_2(x_a, \tau_O) = \begin{bmatrix} z \\ \hat{z} + e^{A(\tau_O - \ell_{\tau_P})} L\big(\ell_y - M e^{-A(\tau_O - \ell_{\tau_P})} \hat{z}\big) \\ \tau_N \\ -1 \\ 0 \\ \ell_y \\ \ell_{\tau_P} \end{bmatrix} \qquad \forall (x_a, \tau_O) : x \in D_{a_2}$$

where

$$D_{a_1} := \{x \in \mathcal{X} : \tau_N = 0, q = 0\}$$
$$D_{a_2} := \{x \in \mathcal{X} : \tau_\delta = 0, q = 1\}$$

In the definitions above, G_b and D_b, respectively, define the jump map and jump set for the clock synchronization algorithm. The resulting jump set is

$$D := D_a \cup D_b$$

where

$$D_a := D_{a_1} \cup D_{a_2}$$

The hybrid system data above now define $\mathcal{H}$ as follows

$$\mathcal{H} = (C, F, D, G) \tag{3.2}$$

Separating the clock synchronization from the system, one has a subsystem that is comprised only of the plant, observer, and network dynamics, denoted by

$$\mathcal{H}_a = (C_a, F_a, D_a, G_a) \tag{3.3}$$

Conversely, the hybrid subsystem denoted by

$$\mathcal{H}_b = (C_b, F_b, D_b, G_b) \tag{3.4}$$

models the clock dynamics and synchronization algorithm.

For several of the results that follow, we consider the hybrid system $\mathcal{H}_a$ with $D_b = \emptyset$. Observe that $\mathcal{H}_a$ with $D_b = \emptyset$ has data

$$\Big(C_a, F_a, D_a\big|_{D_b=\emptyset}, G_a\big|_{D_b=\emptyset}\Big) = \left(C_a, F_a, D_{a_1} \cup D_{a_2}, \begin{cases} G_1(x_a, \tau_P) & \text{if } x \in D_{a_1} \\ G_2(x_a, \tau_O) & \text{if } x \in D_{a_2} \end{cases}\right)$$

Definition 3.1.1. *A solution $\phi \in \mathcal{S}_{\mathcal{H}_a}$ is a nominal maximal solution if it belongs to the subset of maximal solutions defined by*

$$\mathcal{S}^{\text{nom}}_{\mathcal{H}_a} := \big\{\phi \in \mathcal{S}_{\mathcal{H}_a} : \text{rge } \phi_{\tau_\delta} \subset \{0, -1\}\big\} \tag{3.5}$$

where ϕ_{τ_δ} is the τ_δ component of ϕ. Additionally, we say that a solution $\phi \in \mathcal{S}_{\mathcal{H}_a}$ is a delay maximal solution if it belongs to the subset of maximal solutions defined by $\mathcal{S}^{\delta}_{\mathcal{H}_a} := \mathcal{S}_{\mathcal{H}_a} \setminus \mathcal{S}^{\text{nom}}_{\mathcal{H}_a}$.

Qualitatively, one can interpret solutions belonging to $\mathcal{S}^{\text{nom}}_{\mathcal{H}_a}$ as a representation of the scenario where the measurements are free of transmission delays. For a given $\phi \in \mathcal{S}_{\mathcal{H}_a}$, when the timer τ_N expires (i.e., $\tau_N = 0$) the state jumps according to G_1. As a consequence of (3.5), the τ_δ component of the respective ϕ_{τ_δ} solution is mapped to zero following the construction of G_1. Then, nominal maximal solutions jump from D_{a_1} to D_{a_2}, resulting in a subsequent jump with no flow between the two jumps.

Remark 3.1.2. *Definition 3.1.1 applies to both $\mathcal{H}_a$ and $\mathcal{H}$. Thus, we let $\mathcal{S}^{\text{nom}}_{\mathcal{H}}$ denote the set of nominal maximal solutions to $\mathcal{H}$ and $\mathcal{S}^{\delta}_{\mathcal{H}} = \mathcal{S}_{\mathcal{H}} \setminus \mathcal{S}^{\text{nom}}_{\mathcal{H}}$ denote the set of delay solutions to $\mathcal{H}$.*

With the hybrid system defined, the next two results establish existence of solutions to $\mathcal{H}_a$ and that every maximal solution to $\mathcal{H}_a$ is complete.

Lemma 3.1.3. *The hybrid system $\mathcal{H}_a$ with $D_b = \emptyset$ satisfies the hybrid basic conditions in [8, Assumption 6.5].*

Lemma 3.1.4. *The data (C_a, F_a, D_a, G_a) of $\mathcal{H}_a$ with $D_b = \emptyset$ and inputs (τ_P, τ_O) is such that*

1. *$G_a(x_a, \tau_P, \tau_O) \subset C_a \cup D_a$ for all $(x_a, \tau_P, \tau_O) : x \in D_a$*
2. *$F_a(x_a) \subset T_{C_a}(x_a)$ for all $(x_a, \tau_P, \tau_O) : x \in C_a \setminus D_a$*

Lemma 3.1.5. *For every initial condition $\xi \in C_a \cup D_a$ there exists, at least, a nontrivial solution ϕ to the hybrid system $\mathcal{H}_a$ with $D_b = \emptyset$ and inputs (τ_P, τ_O) such that $\{t : (t, j) \in \text{dom } (\tau_P, \tau_O)\}$ is unbounded, and in particular, every maximal solution to $\mathcal{H}_a$ with $D_b = \emptyset$ and such an input is complete.*

Remark 3.1.6. *For the closed-loop hybrid system $\mathcal{H}$, the completeness of maximal solutions to the interconnection between $\mathcal{H}_a$ and $\mathcal{H}_b$ depend on the hybrid system data that defines $\mathcal{H}_b$. See [8, Proposition 2.10] and [8, Proposition 6.10] for details.*

In this section, results guaranteeing convergence of the estimation error $\varepsilon := z - \hat{z}$ to zero with the proposed algorithm are given. First, attractivity is shown for nominal solutions through a comparison to the exponentially converging trajectories guaranteed by the observer in [7]. Next, a Lyapunov-like approach is used to show convergence of delay maximal solutions to a set of interest by comparing the observer trajectories of a delay maximal solution against those of a corresponding nominal maximal solution. Finally, we present a result on the convergence of the estimation error to zero for the case where the plant and observer clocks are mismatched but synchronize in finite time due to the inclusion of a clock synchronization algorithm such as the one in Example 3.5.2.

3.2 Asymptotic attractivity for nominal solutions

In this section we show that the nominal maximal solutions to $\mathcal{H}_a$ are such that the estimation error converges to zero. We prove this claim by showing that for a given

set of parameters and initial conditions, the trajectories of the component $\hat{z}$ for $\mathcal{H}_a$ with synchronized clocks inputs are equivalent to those for the hybrid model presented in [7]. To this end, let us consider the hybrid system in [7] written in plant-observer coordinates, $x_r := (z, \hat{z}, \tau_N) \in \mathbb{R}^{2n} \times \mathbb{R}_{\geq 0}$

$$F_r(x_r) := \begin{bmatrix} Az \\ A\hat{z} \\ -1 \end{bmatrix} \qquad \forall x_r \in C_r$$

$$G_r(x_r) := \begin{bmatrix} z \\ \hat{z} + LM(z - \hat{z}) \\ [T_1^N, T_2^N] \end{bmatrix} \qquad \forall x_r \in D_r$$

$$C_r := \{(z, \hat{z}, \tau) \in \mathbb{R}^n \times \mathbb{R}^n \times \mathbb{R}_{\geq 0} : \tau_N \in [0, T_2^N]\}$$
$$D_r := \{(z, \hat{z}, \tau) \in \mathbb{R}^n \times \mathbb{R}^n \times \mathbb{R}_{\geq 0} : \tau_N = 0\}$$

We denote this system as $\mathcal{H}_r$, which has the compact form

$$\mathcal{H}_r \begin{cases} \dot{x}_r = F_r(x_r) & x_r \in C_r \\ x_r^+ \in G_r(x_r) & x_r \in D_r \end{cases} \tag{3.6}$$

The hybrid time domain for solutions ϕ^r to $\mathcal{H}_r$ is given by

$$\text{dom } \phi^r = \bigcup_{j \in \mathbb{N}} \Big([t_j, t_{j+1}] \times \{j\} \Big) \tag{3.7}$$

where

$$T_1^N \leq t_{j+1} - t_j \leq T_2^N \quad \forall j \in \{k \geq 1 : k \in \mathbb{N}\}$$
$$0 \leq t_1 \leq T_2^N$$

Following [7], if matrices L and $P = P^\mathsf{T} \succ 0$ are such that

$$(\mathbf{I} - LM)^\mathsf{T} e^{A^\mathsf{T} v} P e^{Av} (\mathbf{I} - LM) - P \prec 0 \quad \forall v \in [T_1^N, T_2^N] \tag{3.8}$$

holds for given $T_2^N \geq T_1^N \geq 0$, then the system $\mathcal{H}_r$ has the set

$$\mathcal{A}_r := \big\{ (z, \hat{z}, \tau_N) \in \mathbb{R}^n \times \mathbb{R}^n \times [0, T_2^N] : z = \hat{z} \big\} \tag{3.9}$$

globally exponentially stable. Prior to comparing the trajectories of $\mathcal{H}_r$ and $\mathcal{H}_a$, note that $\mathcal{H}_r$ resembles system $\mathcal{H}_a$ with synchronized clock inputs τ_P and τ_O for the case where

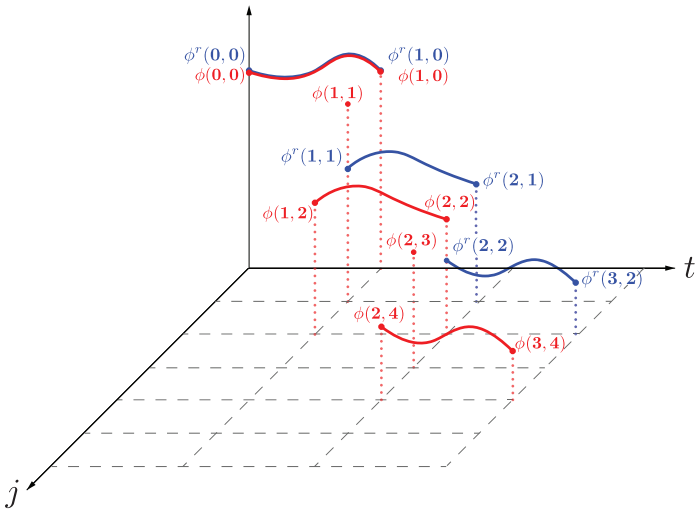

Figure 3.2: Plot of ϕ^r and ϕ solution trajectories.

$T^d = 0$. However, the hybrid time domain of a solution ϕ^{nom} to $\mathcal{H}_a$ observes an additional jump in between periods of flow as demonstrated in Figure 3.2.

Observe that x_r is a strict subvector of x_a. Thus, for a given initial condition $\phi^r(0,0)$ for $\mathcal{H}_r$, we can consider the following initial condition for $\mathcal{H}_a$:

$$\phi(0,0) = \big(\phi_r(0,0), \phi_{\tau_\delta}(0,0), \phi_q(0,0), \phi_{\ell_y}(0,0), \phi_{\ell_{\tau_P}}(0,0)\big)$$

Moreover, for given matrices A, M, and L of appropriate dimensions, constants $0 < T_1^N \leq T_2^N$, one can pick solutions ϕ^r and ϕ belonging to $\mathcal{H}_r$ and $\mathcal{H}_a$, respectively, such that the solutions observe the same $\tau_N = 0$ triggered jump times, i.e., $\phi_{\tau_N}(t, s_\phi(j)) = \phi^r_{\tau_N}(t,j)$ for all $(t,j) \in \operatorname{dom} \phi^r$.

Using the observed relationships between the two systems, in the result that follows, we claim attractivity for nominal solutions by showing that $\phi_z \equiv \phi^r_z$ and $\phi_{\hat{z}} \equiv \phi^r_{\hat{z}}$. The proof of the result is segmented into two cases; the first addresses attractivity for solutions to $\mathcal{H}_a$ with initial condition $\phi(0,0) \in C_{a_1} \cup D_{a_1}$ or $\phi(0,0) \in \{x \in C_{a_2} \cup D_{a_2} : \ell_y = Mz, \ell_{\tau_P} = \tau_P\}$, the second address attractivity for solutions with initial condition $\phi(0,0) \in \{x \in C_{a_2} \cup D_{a_2} : \ell_y \neq Mz, \ell_{\tau_P} \neq \tau_P\}$. A separate proof for the second case is necessary to address the scenario of incorrectly initialized memory states that could lead to an "incorrect" observer law update when a jump according to G_2 is triggered. To this end, we define sets $\mathcal{W}_1 := C_{a_1} \cup D_{a_1}$ and $\mathcal{W}_2 := \{x \in C_{a_2} \cup D_{a_2} : \ell_y = Mz, \ell_{\tau_P} = \tau_P(0,0)\}$. Then solutions ϕ to $\mathcal{H}_a$ with $\phi(0,0) \in \mathcal{W}_1 \cup \mathcal{W}_2$ we refer to as *conventional* solutions and

for solutions with $\phi(0,0) \in (C_a \cup D_a) \setminus (\mathcal{W}_1 \cup \mathcal{W}_2)$ we refer to as *non-conventional*.

Proposition 3.2.1. *Given hybrid systems $\mathcal{H}_r$ in (3.6) and $\mathcal{H}_a$ in (3.3) with $D_b = \emptyset$ and input pair $\tau_P \equiv \tau_O$ such that $\{t : (t,j) \in dom\ (\tau_P, \tau_O)\}$ is unbounded, suppose that there exist $P = P^\top \succ 0$ such that T_2^N, T_1^N, L, and M satisfy condition (3.8). Then, for $T^d = 0$, each solution ϕ to $\mathcal{H}_a$ with $D_b = \emptyset$ and input pair $\tau_P \equiv \tau_O$ is such that*

$$\lim_{t+j\to\infty} |\phi(t,j)|_{\mathcal{A}_a} = 0$$

where

$$\mathcal{A}_a := \mathcal{A}_r \times \big(\{-1\} \cup [0, T^d]\big) \times \{0,1\} \times \mathbb{R}^m \times \mathbb{R}_{\geq 0} \tag{3.10}$$

Proof. Pick solutions ϕ^r and ϕ with initial conditions $\phi^r(0,0) \in C_r \cup D_r$ and $\phi(0,0) \in \{(\phi^r(0,0), \tau_\delta, q, \ell_y, \ell_{\tau_P}) \in C_a \cup D_a : \ell_y = Mz\}$ such that

$$\phi_{\tau_N}(t,j) = \phi^r_{\tau_N}(t, r_\phi(j)) \qquad\qquad \forall (t,j) \in \text{dom } \phi$$

where $r_{\phi^r}(j) := 2j$ is a parameterization function that maps a solution ϕ^r to $\mathcal{H}_r$ onto the hybrid time domain of ϕ to $\mathcal{H}_a$.

• Proof of Conventional Case

Following ϕ^r from $\phi^r(0,0)$, if $\phi^r(t,j) \in C_r$ it flows according to F_r. If $\phi^r(t,j) \in D_r$, a jump according to G_r is triggered. In particular, the trajectory for $\phi^r_{\hat{z}}$ after jumps is given by

$$\phi^r_{\hat{z}}(t_j, j) = \phi^r_{\hat{z}}(t_j, j\text{-}1) + LM\big(\phi^r_z(t_j, j\text{-}1) - \phi^r_{\hat{z}}(t_j, j\text{-}1)\big) \tag{3.11}$$

at each $(t_j, j-1)$, $(t_j, j) \in \text{dom } \phi^r$.

For the solution ϕ with $\phi(0,0) \in \mathcal{W}_1 \cup \mathcal{W}_2$, if $\phi(t,j) \in C_a$ it flows according to F_a. If $\phi \in D_{a_1}$, a reset according to G_1 is triggered. The trajectory for $\phi_{\hat{z}}$ after jumps according to G_1 is given by,

$$\phi_{\hat{z}}(t_j, j) = \phi_{\hat{z}}(t_j, j-1) \tag{3.12}$$

at each $(t_j, j-1)$, $(t_j, j) \in \text{dom } \phi$ for all $j \in \{2k : k \in \mathbb{N}_{>0}\}$ when $\phi(0,0) \in \mathcal{W}_1$ and for all $j \in \{2k+1 : k \in \mathbb{N}_{>0}\}$ when $\phi(0,0) \in \mathcal{W}_2$. If or when $\phi \in D_{a_2}$, $\phi(t_j, j)$ maps according to

G_2 with $\phi_{\hat{z}}$ after jumps given by

$$\begin{aligned}\phi_{\hat{z}}(t_j, j) = \phi_{\hat{z}}(t_j, j\text{-}1) \\ + e^{A(\tau_O(t_j,j-1)-\phi_{\ell_{\tau_P}}(t_j,j-1))} L\Big(\phi_{\ell_y}(t_j, j\text{-}1) \\ - Me^{-A(\tau_O(t_j,j-1)-\phi_{\ell_{\tau_P}}(t_j,j-1))}\phi_{\hat{z}}(t_j, j\text{-}1)\Big)\end{aligned} \tag{3.13}$$

at each $(t_j, j-1)$, $(t_j, j) \in \text{dom } \phi$ for all $j \in \{2k+1 : k \in \mathbb{N}_{>0}\}$ when $\phi(0,0) \in \mathcal{W}_1$ and for all $j \in \{2k : k \in \mathbb{N}_{>0}\}$ when $\phi(0,0) \in \mathcal{W}_2$.

Now, since $T^d = 0$ and $\phi_{\ell_{\tau_P}}(0,0) = \tau_O(0,0)$, the delay term $\tau_O(t,j) - \phi_{\ell_{\tau_P}}(t,j)$ in the expression for the update law in (3.13) is zero at each jump according to G_2 or for all $(t_j, j) \in \{(t,j) \in \text{dom } \phi : t = t_j, j \in \mathcal{I}_m\}$. Furthermore, $\phi_{\ell_y}(0,0) = M\phi_z(0,0)$, thus $\phi_{\ell_y}(t_j, j) = M\phi_z(t,j)$ at each reset according to G_2 or for all $(t_j, j) \in \{(t,j) \in \text{dom } \phi : t = t_j, j \in \mathcal{I}_m\}$. Then, (3.13) can be expressed as

$$\phi_{\hat{z}}\big(t_j, j\big) = \phi_{\hat{z}}(t_j, j\text{-}1) + LM\big(\phi_z(t_j, j\text{-}1) - \phi_{\hat{z}}(t_j, j\text{-}1)\big)$$

Noting the equivalence to the expression in (3.11), we can express $\phi_{\hat{z}}$ along jumps as a function of $\phi^r_{\hat{z}}$ as follows:

$$\phi_{\hat{z}}(t_j, j) = \begin{cases} \phi^r_{\hat{z}}(t_j, r_\phi(j\text{-}1)) & \forall j \in \mathcal{I}_d \\ \phi^r_{\hat{z}}(t_j, r_\phi(j)) & \forall j \in \mathcal{I}_m \end{cases}$$

Now, given identical flow dynamics in z, $\hat{z}$, and τ_N, one then has

$$\phi(t,j) = \big(\phi^r(t, r_\phi(j)), \phi_{\tau_\delta}(t,j), \phi_q(t,j), \phi_{\ell_y}(t,j), \phi_{\ell_{\tau_P}}(t,j)\big)$$

thus since solutions to $\mathcal{H}_r$ converge exponentially to $\mathcal{A}_r$ by [7, Theorem 1], it follows that

$$\lim_{t+j\to\infty} |\phi^r(t,j)|_{\mathcal{A}_r} = 0$$

moreover, given that $\mathcal{A}_r \subset \mathcal{A}_a$ it can be concluded that

$$\lim_{t+j\to\infty} |\phi(t,j)|_{\mathcal{A}_a} = 0$$

• Proof of Non-conventional Case

For solutions with initial conditions $\phi(0,0) \in (C_a \cup D_a) \setminus (\mathcal{W}_1 \cup \mathcal{W}_2)$, namely those with $\phi_{\ell_y}(0,0) \neq M\phi_z(0,0)$ and $\phi_{\ell_{\tau_P}}(0,0) \neq \tau_P(0,0)$, after a period of time $T^* \geq t + j$ the

solution converges towards $\mathcal{A}_a$. Consider a solution ϕ with initial condition $\phi(0,0) \in \{x \in C_{a_2} \cup D_{a_2} : \ell_y \neq Mz, \ell_{\tau_P} \neq \tau_P(0,0)\}$. Since $T^d = 0$, $\phi(0,0) \in D_{a_2}$ and the solution jumps according to G_2. In particular, at $(t_1, 1)$,

$$\begin{aligned}\phi_{\hat{z}}(t_1,1) = \phi_{\hat{z}}(0,0) + e^{A(\tau_O(0,0)-\phi_{\ell_{\tau_P}}(0,0))} L\big(\phi_{\ell_y}(0,0) \\ - Me^{-A(\tau_O(0,0)-\phi_{\ell_{\tau_P}}(0,0))}\phi_{\hat{z}}(0,0)\big)\end{aligned}$$

with $\phi_{\ell_y}(0,0) \neq M\phi_z(0,0)$ and $\phi_{\ell_{\tau_P}}(0,0) \neq \tau_P(0,0)$, $\phi(t_1,1)$ may diverge away from $\mathcal{A}_a$. The solution then flows in the interval $[t_1, t_2] \times \{1\}$ until $\phi(t_2,1) \in D_{a_1}$, when the solution jumps according to G_1. In particular, at $(t_2,2)$, $\phi_{\ell_y}(t_2,2) = M\phi_z(t_2,1)$ and $\phi_{\ell_{\tau_P}}(t_2,2) = \tau_P(t_2,1)$ which means $\phi(t_2,2) \in \mathcal{W}_1 \cup \mathcal{W}_2$. Thus, we can show that for some $(t,j) \in \operatorname{dom}\phi$ such that $t + j \geq T^*$, $\phi(t,j) \in \mathcal{W}_1 \cup \mathcal{W}_2$. Moreover, following the proof for the conventional case, the solution converges to $\mathcal{A}_a$. □

3.3 Attractivity for delay solutions with synchronized clocks

With attractivity established for the nominal case, we now present attractivity to $\mathcal{A}_a$ for the delay case. Consider the Lyapunov function candidate from [7] defined for every $x_a \in \mathcal{X}_a$ as

$$V(x_a) = \varepsilon^{\mathsf{T}} e^{A^{\mathsf{T}}\tau_N} P e^{A\tau_N}\varepsilon \tag{3.14}$$

where $\varepsilon = z - \hat{z}$ and $P = P^{\mathsf{T}} \succ 0$. Then, given $\phi^\delta(0,0) \in C_a \cup D_a$, it can be shown that delay solutions $\phi^\delta \in \mathcal{S}^\delta_{\mathcal{H}_a}$ converge to the set $\mathcal{A}_a$, exponentially. Moreover, it can be shown that the Lyapunov function evaluated along a delay solution ϕ^δ for a given initial condition is bounded by the Lyapunov function evaluated along its nominal counterpart ϕ^{nom} and a bounded perturbation. To facilitate the analysis in the result that follows, let $\phi^{\text{nom}}_\varepsilon = \phi^{\text{nom}}_z - \phi^{\text{nom}}_{\hat{z}}$ and $\phi^\delta_\varepsilon = \phi^\delta_z - \phi^\delta_{\hat{z}}$ denote the trajectories of the state error for the respective nominal (ϕ^{nom}) and delay (ϕ^δ) solutions.

To assist with the analysis between the two solution types, given a solution to $\mathcal{H}_a$, we define a reparameterization function s_ϕ, given as follows:

- If $\phi(0,0) \in C_{a_1} \cup D_{a_1}$

$$s_\phi(j) := \begin{cases} j & \forall j \in \mathcal{I}_d \\ j+1 & \forall j \in \mathcal{I}_m \end{cases}$$

- If $\phi(0,0) \in C_{a_2} \cup D_{a_2}$

$$s_\phi(j) := \begin{cases} j & \forall j \in \mathcal{I}_m \\ j+1 & \forall j \in \mathcal{I}_d \end{cases}$$

The function s_ϕ allows to compare solutions ϕ^{nom} to $\mathcal{H}_a$ and ϕ^δ to $\mathcal{H}_a$.

Theorem 3.3.1. *Given the hybrid system $\mathcal{H}_a$ in (3.3) with $D_b = \emptyset$ and input pair $\tau_P \equiv \tau_O$ such that $\{t : (t,j) \in \text{dom } (\tau_P, \tau_O\}$ is unbounded, suppose that there exist $P = P^\top \succ 0$ such that T_2^N, T_1^N, L, and M satisfy condition (3.8). Then, for each $T^d \in [0, T_1^N]$, each solution ϕ to $\mathcal{H}_a$ with $D_b = \emptyset$ and input pair $\tau_P \equiv \tau_O$ is such that*

$$\lim_{t+j\to\infty} |\phi(t,j)|_{\mathcal{A}_a} = 0$$

Furthermore, there exist positive constants α and β such that each $\phi^\delta \in \mathcal{S}^\delta_{\mathcal{H}_a}$ with $D_b = \emptyset$ and input pair $\tau_P \equiv \tau_O$ satisfies

$$\begin{aligned} \alpha|\phi^\delta(t,j)|_{\mathcal{A}_a} \leq V\big(\phi^\delta(t,j)\big) \leq V\big(\phi^{\text{nom}}(t, s_\phi(j))\big) \\ + \beta \phi_\varepsilon^{\text{nom}}(t,j)^\mathsf{T} \phi_\varepsilon^{\text{nom}}(t,j) \end{aligned} \tag{3.15}$$

for each $(t,j) \in \text{dom } \phi^\delta$, where ϕ^{nom} is a nominal maximal solution for the same initial condition to ϕ^δ and $\phi_\varepsilon^{\text{nom}} = \phi_z^{\text{nom}} - \phi_{\hat{z}}^{\text{nom}}$.

Proof. Given matrices A, L, and M of appropriate dimensions and positive scalars $T^d \leq T_1^N \leq T_2^N$. Pick a solution ϕ^δ with initial condition $\phi^\delta(0,0) \in \{x_a \in C_a \cup D_a : \ell_y = Mz\}$ and its nominal counterpart ϕ^{nom} for the same initial condition and identical τ_N trajectories, i.e., $\phi^{\text{nom}}_{\tau_N}(t,j) = \phi^\delta_{\tau_N}(t,j)$ for all (t,j) dom ϕ^δ. Consider the Lyapunov function candidate (4.36). Then, let

$$\begin{aligned} V^{\text{nom}}(t, s_\phi(j)) &:= V(\phi^{\text{nom}}(t, s_\phi(j))) \quad \forall (t,j) \in \text{ dom } \phi^\delta \\ V^\delta(t,j) &:= V(\phi^\delta(t,j)) \qquad\qquad\qquad\quad \forall (t,j) \in \text{ dom } \phi^\delta \end{aligned}$$

Noting the relationship between ϕ^{nom} and ϕ^δ, let $V^\delta(t,j)$ be expressed as a perturbation of $V^{\text{nom}}(t, s_\phi(j))$, i.e.

$$V^\delta(t,j) = V(\phi^{\text{nom}}(t, s_\phi(j))) + \rho(t,j) \quad \forall (t,j) \in \text{ dom } \phi^\delta$$

Since $\phi^{\text{nom}}(t,j) = \phi^{\delta}(t,j)$ for all $(t,j) \in \mathcal{T}_1$ when the initial condition is in $C_{a_1} \cup D_{a_1}$. The quantity $\rho(t,j)$ is given by,

$$\rho(t,j) = \begin{cases} V(\phi^{\delta}(t,j)) - V(\phi^{\text{nom}}(t, s_{\phi}(j))) & \forall (t,j) \in \mathcal{T}_2 \\ 0 & \forall (t,j) \in \mathcal{T}_1 \end{cases}$$

Observe that for each $x_a \in C_a$, $\langle \nabla V(x_a), F_a(x_a) \rangle = 0$, therefore ρ remains constant during flows and can be expressed by its value at jumps as follows:

$$\rho(t,j) = \begin{cases} V(\phi^{\delta}(t_j,j)) - V(\phi^{\text{nom}}(t_{s_{\phi}(j)}, s_{\phi}(j))) & \forall (t,j) \in \mathcal{T}_2 \\ 0 & \forall (t,j) \in \mathcal{T}_1 \end{cases}$$

Before expanding ρ, note that the reparameterization of ϕ^{nom} onto the domain of ϕ^{δ} via $s_{\phi}(j)$ following each $(t_{j+1}, j) \in \mathcal{T}_1$, gives the nominal solution mapped according to G_2. In particular, one has

$$\begin{aligned} \phi_{\varepsilon}^{\text{nom}}(t_{s_{\phi}(j)}, s_{\phi}(j)) &= \phi_{z}^{\text{nom}}(t_{s_{\phi}(j)}, s_{\phi}(j\text{-}1)) \\ &\quad - \Big(\phi_{\hat{z}}^{\text{nom}}(t_{s_{\phi}(j)}, s_{\phi}(j\text{-}1)) + LM \Big(\phi_{z}^{\text{nom}}(t_{s_{\phi}(j)}, s_{\phi}(j\text{-}1)) \\ &\qquad - \phi_{\hat{z}}^{\text{nom}}(t_{s_{\phi}(j)}, s_{\phi}(j\text{-}1)) \Big) \Big) \\ &\qquad = (I - LM) \phi_{\varepsilon}^{\text{nom}}(t_{s_{\phi}(j)}, s_{\phi}(j\text{-}1)) \end{aligned}$$

at each $(t_j, s_{\phi}(j-1)), (t_j, s_{\phi}(j)) \in \text{dom } \phi^{\delta}$. For the same jump index j, that is, following each $(t_{j+1}, j) \in \mathcal{T}_1$, the delay solution $\phi_{\varepsilon}^{\delta}$ is given by

$$\phi_{\varepsilon}^{\delta}(t_j, j) = \phi_{z}^{\delta}(t_j, j\text{-}1) - \phi_{\hat{z}}^{\delta}(t_j, j\text{-}1)$$

at each $(t_j, j-1), (t_j, j) \in \text{dom } \phi^{\delta}$ for all $j \in \mathcal{I}_m$. Then, substituting the expressions into ρ leads to

$$\begin{aligned} \rho(t,j) &= V\big(\phi^{\delta}(t_j,j)\big) - V\big(\phi^{\text{nom}}(t_j,j)\big) \\ &= \phi_{\varepsilon}^{\delta}(t_j, j\text{-}1)^{\mathsf{T}} Q(t_j, j\text{-}1) \phi_{\varepsilon}^{\delta}(t_j, j\text{-}1) \text{-} \phi_{\varepsilon}^{\text{nom}}(t_{s_{\phi}(j)}, s_{\phi}(j\text{-}1))^{\mathsf{T}} \\ &\quad \times (I\text{-}LM)^{\mathsf{T}} Q(t_j, s_{\phi}(j\text{-}1)) (I\text{-}LM) \phi_{\varepsilon}^{\text{nom}}(t_{s_{\phi}(j)}, s_{\phi}(j\text{-}1)) \end{aligned}$$

where $Q(t,j) := e^{A^{\mathsf{T}} \tau_N(t,j)} P e^{A \tau_N(t,j)}$. Then, since $\phi^{\text{nom}}(t,j) = \phi^{\delta}(t,j)$ for all $(t,j) \in \mathcal{T}_1$, we make the appropriate substitutions to get

$$\begin{aligned} \rho(t,j) &= \phi_{\varepsilon}^{\text{nom}}(t_{s_{\phi}(j)}, s_{\phi}(j\text{-}1))^{\mathsf{T}} \Big(Q(t_j, j-1) \\ &\quad \text{-}(I\text{-}LM)^{\mathsf{T}} Q(t_{s_{\phi}(j)}, s_{\phi}(j\text{-}1)) (I\text{-}LM) \Big) \phi_{\varepsilon}^{\text{nom}}(t_{s_{\phi}(j)}, s_{\phi}(j\text{-}1)) \end{aligned}$$

Thus allowing ρ to be bounded as follows

$$|\rho(t,j)| \leq \beta \phi_{\varepsilon}^{\text{nom}}(t_{s_\phi(j)}, s_\phi(j\text{-}1))^{\mathsf{T}} \phi_{\varepsilon}^{\text{nom}}(t_{s_\phi(j)}, s_\phi(j\text{-}1)) \tag{3.16}$$

where

$$\beta := \max_{\tau_N \in [0, T_2^N]} \lambda_{\max}\big(e^{A^{\mathsf{T}}\tau_N} P e^{A\tau_N}\big) |I\text{-}(I\text{-}LM)^{\mathsf{T}}(I\text{-}LM)|$$

which exists due to continuity of the matrix exponential. Then, one has

$$V^{\delta}(t,j) = \begin{cases} V\big(\phi^{\text{nom}}(t, s_\phi(j))\big) + \rho(t,j) & \forall (t,j) \in \mathcal{T}_2 \\ V\big(\phi^{\text{nom}}(t, s_\phi(j))\big) & \forall (t,j) \in \mathcal{T}_1 \end{cases}$$

In particular, one has

$$\alpha |\phi^{\delta}(t,j)|_{\mathcal{A}_a} \leq V\big(\phi^{\delta}(t,j)\big) \leq V\big(\phi^{\text{nom}}(t, s_\phi(j))\big) + \rho(t,j) \tag{3.17}$$

where

$$\alpha := \min_{v \in [0, T_2]} \lambda_{min}\big(e^{A^{\mathsf{T}}\tau_N} P e^{A\tau_N}\big)$$

Now, since $\rho(t,j)$ decays to zero in the limit due to (3.16) and $\phi^{\text{nom}}(t, s_\phi(j))$ converges to the set $\mathcal{A}_a^{\text{nom}}$ via Proposition 3.2.1, then by the relations in (3.17) solutions ϕ^{δ} also converge to the set $\mathcal{A}_a$.

For the case of ϕ^{δ} solutions with initial condition $\phi^{\delta}(0,0) \in C_{a_2} \cup D_{a_2}$, the result follows from similar steps with $V^{\delta}(t,j)$ and $\rho(t,j)$ given by

$$V^{\delta}(t,j) = \begin{cases} V\big(\phi^{\text{nom}}(t, s_\phi(j))\big) + \rho(t,j) & \forall (t,j) \in \mathcal{T}_1 \\ V\big(\phi(t, s_\phi(j))\big) & \forall (t,j) \in \mathcal{T}_2 \end{cases}$$

where

$$\rho(t,j) = \begin{cases} V(\phi^{\delta}(t,j)) - V(\phi^{\text{nom}}(t, s_\phi(j))) & \forall (t,j) \in \mathcal{T}_1 \\ 0 & \forall (t,j) \in \mathcal{T}_2 \end{cases}$$

□

Figure 3.3 illustrates the evolution of the function V along the trajectories for the two solution types. From the same initial condition, both solutions flow together. Then the solutions separate with the nominal solution (blue) decreasing upon measurement retrieval and the delayed solution (red) diverging due to the measurement delay. After some hybrid time, the delayed solution retrieves the delayed measurement and converges with the nominal solution. Example 3.5.2 illustrates Theorem 3.3.1 in Section 3.5.

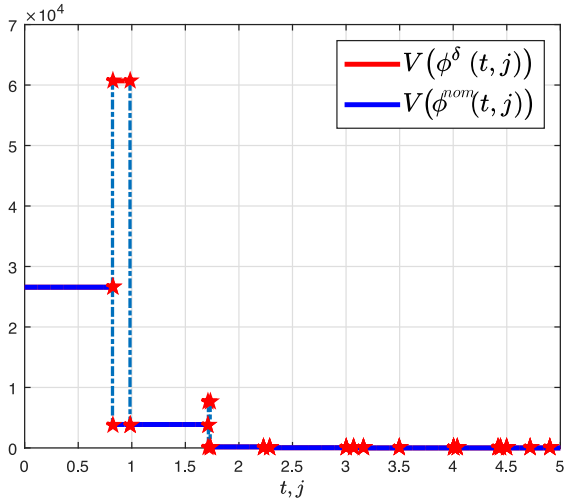

Figure 3.3: Plot of the Lyapunov trajectories of ϕ^r and ϕ.

3.4 Attractivity for delay solutions with clocks that synchronize in finite time.

In this section, we present our results for the case where the clock inputs τ_P and τ_O to $\mathcal{H}_a$ are not necessarily the same initially, but eventually synchronize in finite time (see Remark 3.4.4). The first result establishes attractivity to $\mathcal{A}_a$ for $\mathcal{H}_a$ with $D_b = \emptyset$ and input pair (τ_P, τ_O) satisfying conditions such that solutions to $\mathcal{H}_a$ are complete and the input pair synchronize in finite time. In the result that follows, we show attractivity to a set of interest for the full hybrid system $\mathcal{H}$ with conditions on the clock synchronization subsystem $\mathcal{H}_b$ such that the solutions to $\mathcal{H}$ are complete and the clock inputs to the subsystem $\mathcal{H}_a$ synchronize in finite time.

For the following results we will distinguish between solutions to $\mathcal{H}_a$ and solutions to $\mathcal{H}$ by denoting $\phi_a \in \mathcal{S}_{\mathcal{H}_a}$ and $\phi \in \mathcal{S}_{\mathcal{H}}$.

Proposition 3.4.1. *Given the hybrid system $\mathcal{H}_a$ in (3.3), suppose that there exist $P = P^\top \succ 0$ such that T_2^N, T_1^N, L, and M satisfy condition (3.8). Then, for each $T^d \in [0, T_1^N]$ and each input pair (τ_P, τ_O) to $\mathcal{H}_a$ satisfying*

B1) $\{t : (t, j) \in dom\ (\tau_P, \tau_O)\}$ is unbounded, and

B2) there exists $T^* \geq 0$ such that

$$\tau_P(t,j) = \tau_O(t,j)$$

for all $t + j \geq T^*$

each solution ϕ_a to $\mathcal{H}_a$ with input pair (τ_P, τ_O) and $D_b = \emptyset$ is such that

1. *$\{t : (t,j) \in dom\ \phi_a\}$ is unbounded, and*
2. *$\lim_{t+j\to\infty} |\phi_a(t,j)|_{\mathcal{A}_a} = 0$.*

Proof. To prove item 1), we will disprove the impossibility of a maximal solution to $\mathcal{H}_a$ with input pair (τ_P, τ_O) and $D_b = \emptyset$ to flow for arbitrarily large t. To this end, suppose there exists such a solution with input pair (τ_P, τ_O) satisfying B1). Then, $\{t : (t,j) \in \text{dom } \phi_a\}$ is bounded. The existence of such a solution implies that either

a) ϕ_a is not Zeno and died after finite time t, this further implies that either

a.1) G_a (with $D_b = \emptyset$ mapped the solution ϕ_a to a point outside of $C_a \cup D_a$; or

a.2) the solution ϕ_a died at a point in $C_a \setminus D_a$, at which F_a points outward of C_a;

or

b) ϕ_a is Zeno with $t \nearrow t_Z \notin \{t : (t,j) \in \text{dom } \phi_a\}$ as $j \to \infty$

Case a.1) does not happen due to (τ_P, τ_O) satisfying B1) and, by Lemma 3.1.4 item 1), G_a cannot map points in D_a outside of $C_a \cup D_a$ with $D_b = \emptyset$. Moreover, a.2) does not happen since (τ_P, τ_O) satisfies B1) and, by Lemma 3.1.4 item 2), $F_a(x_a) \subset T_{C_a}(x)$ for each x_a such that $x \in C_a \setminus D_a$. Case b) does not happen since (τ_P, τ_O) satisfies B1) and after any reset of ϕ_a via $\phi_a(t_j, j) = G_2(\phi_a(t_j, j\text{–}1), \tau_P)$ then for the same t_j there exists t_{j+1} such that $0 < T_1^N \leq t_{j+1} - t_j \leq T_2^N - T^d$. Therefore, it must be the case that the solution ϕ_a to $\mathcal{H}_a$ with input pair (τ_P, τ_O) satisfying B1) is such that $\{t : (t,j) \in \text{dom } \phi_a\}$ is unbounded. This contradicts our assumption that $\{t : (t,j) \in \text{dom } \phi_a\}$ is bounded and concludes the proof of item 1).

To prove item 2), pick a maximal solution $\phi_a \in \mathcal{S}_{\mathcal{H}_a}$ with input pair (τ_P, τ_O) satisfying B1) and B2) with $D_b = \emptyset$. By item 1), $\{t : (t,j) \in \text{dom } \phi_a\}$ is unbounded. Moreover, by Lemma 3.1.4, $\phi_a(t,j) \in C_a \cup D_a$ for all $(t,j) \in \text{dom } \phi_a$. Now observe, for $t + j \geq T^*$, the conditions in Theorem 3.3.1 are satisfied since condition (3.8) is satisfied and the inputs (τ_P, τ_O) satisfy B2). Therefore, by Theorem 3.3.1, item 2) holds. □

Theorem 3.4.2. *Given the hybrid system $\mathcal{H}$ in 3.2, suppose that there exist $P = P^\top \succ 0$ such that T_2^N, T_1^N, L, and M satisfy condition (3.8). Suppose further that the subsystem $\mathcal{H}_b$ in (3.4) is such that*

1. *every maximal solution ϕ to $\mathcal{H}$ is complete, and*
2. *condition B2) in Proposition 3.4.1 holds;*

Then, for each $T^d \in [0, T_1^N]$, each maximal solution ϕ to $\mathcal{H}$ is such that

$$\lim_{t+j\to\infty} |\phi(t,j)|_{\mathcal{A}} = 0$$

where $\mathcal{A} := \mathcal{A}_a \times \mathbb{R}_{\geq 0} \times \mathbb{R}_{\geq 0} \times \mathcal{M}$.

Proof. Pick a maximal solution ϕ to $\mathcal{H}$. By Lemma 3.1.4, $\phi_{x_a}(t,j) \in C_a \cup D_a$ for all $(t,j) \in \text{dom } \phi$ since ϕ does not escape in finite time. For $t + j \geq T^*$, the conditions in Proposition 3.4.1 for the hybrid subsystem $\mathcal{H}_a$ are satisfied since (3.8) is satisfied and $\mathcal{H}_b$ renders $\phi_{\tau_P}(t,j) = \phi_{\tau_O}(t,j)$ for all $t+j \geq T^*$. Then by Proposition 3.4.1, $\lim_{t+j\to\infty} |\phi(t,j)|_{\mathcal{A}} = 0$. □

Remark 3.4.3. *Observe that this result builds on the design of the nominal system $\mathcal{H}_a$ for synchronized clock inputs by interconnecting it with $\mathcal{H}_b$ representing a finite time clock synchronization algorithm (see Remark 3.4.4) that satisfies the conditions in Theorem 3.4.2. We note that the authors of [17] provide LMI conditions that renders a similar observer-based networked system with variable delays, stable for a bounded clock synchronization error. However, as the authors note in their results, the design of the observer and controller gains to satisfy the associated LMI conditions are not straightforward. We remind the reader that our approach uses a tractable LMI condition (3.8) (see algorithm in [7]) and a finite time clock synchronization algorithm for which several solutions exist.*

Remark 3.4.4. *Concerning the existence of finite time clock synchronizations implementable in $\mathcal{H}$, we point the reader to the IEEE 1588 precision time protocol design for networked control system in [12] and firefly-based algorithms as given in [18] both of which guarantee synchronization in finite time.*

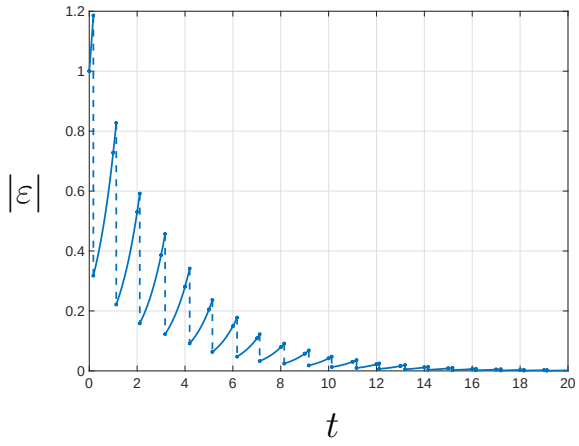

Figure 3.4: The evolution of the estimation error with respect to hybrid time. The vertical dashes represent the resets of $\hat{z}$ according to $\hat{z}^+$ in (3.1).

3.5 Examples

Example 3.5.1. *Recall the system data from the motivation example in Section 5.1,* $A = 1$, $M = 1$, $L = 1 - e^{-1}$ *with constants* $T_1^N = T_2^N = 1$. *Then, let* $T^d = 0.2$. *Simulating the system* $\mathcal{H}_a$ *with synchronized clock inputs* τ_P *and* τ_O, *the estimate converges even in the presence of measurements delays as shown in Figure 3.4. Recall that this was not the case in the example presented in the introduction.* [1]

Example 3.5.2. *Consider an oscillatory autonomous system given by* $A = \begin{bmatrix} 0 & 1 \\ -1 & 0 \end{bmatrix}$ *and matrix* $M = \begin{bmatrix} 1 & 0 \end{bmatrix}$ *with timer bounds* $T^d = T_1^N = 0.2$, $T_2^N = 1$. *Using the design algorithm outlined in [7] for the given parameters, the gain matrix is given by* $L = \begin{bmatrix} 1.0097 & 0.6015 \end{bmatrix}^\mathsf{T}$.

Starting with the case of synchronized clocks, i.e. $\phi(0,0) \in C_1 \cup D_1$ *such that* $\phi_{\tau_P}(0,0) = \phi_{\tau_O}(0,0)$, *Figure 3.5 depicts the error in each state component for* ϕ^{nom} *and* ϕ^δ *and shows the norm of the error for the two solutions, in addition the bound in (5.45) is plotted to demonstrate the asymptotic attractivity of* ϕ^δ.

Observe that the two trajectories flow together from the initial condition, at the first jump the error on the estimate for ϕ^{nom} *decreases due to the measurement arrival at*

[1] Code at github.com/HybridSystemsLab/HybridObsScalarPlant

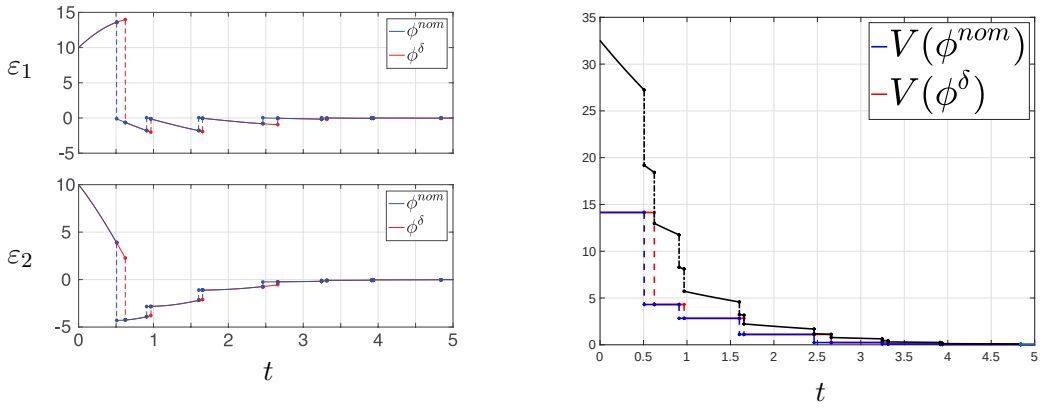

Figure 3.5: Plot of the error on the state components (left) and of $V(x)$ evaluated along the trajectories of ϕ^{nom} and ϕ^{δ} (right) for synchronized clocks from Example 3.5.2. Furthermore, a plot of the bound from (5.45) plotted in black.

broadcast while ϕ^{δ} continues flowing. At the next jump the error for ϕ^{δ} decreases due to the arrival of the delay measurement and then resumes flowing with ϕ^{nom}.

For the case where the clock nodes are not synchronized i.e. $\phi(0,0) \in C_1 \cup D_1$ such that $\phi_{\tau_P}(0,0) \neq \phi_{\tau_O}(0,0)$, consider a simulation of the full system $\mathcal{H}$ where $\mathcal{H}_b$ is a model representation of the IEEE 1588 protocol, see [19] for details on the model. Figure 3.6 presents the error norm trajectories and displays the error in the components for both ϕ^{nom} and ϕ^{δ}.

In both figures, the trajectories flow together from the initial condition, at the first jump the estimation error for ϕ^{nom} decreases while ϕ^{δ} continues flowing. In the sequence of jumps that follow, the error on the estimate of ϕ^{nom} converges to zero. The error on the estimate of ϕ^{δ} however, increases until the clocks are synchronized as marked by the dashed line denoted 'sync'. In the jumps that follow from the synchronization point, the error estimate of ϕ^{δ} converges toward zero.

Example 3.5.3. *To demonstrate the flexibility of the system to account for a scenario of drifting clocks, consider the same system from the previous example but with a drifting observer clock i.e. $\dot{\tau}_O = 1 + \gamma$ where $\gamma = 0.001$. In Figure 3.7, the error norm of the two trajectories for the simulation is given. Note the periodic synchronization of the plant and observer clocks prevents the drift in the observer clock from adversely affecting the norm of*

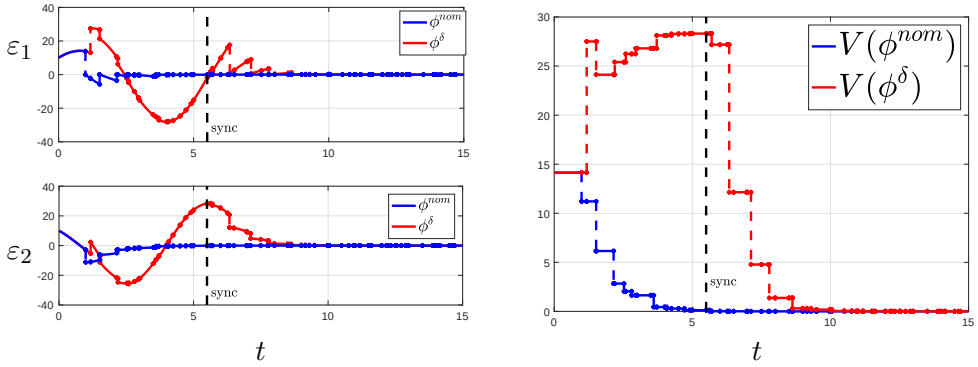

Figure 3.6: Plot of the error on the state components (left) and of $V(x)$ evaluated along the trajectories of ϕ^{nom} and ϕ^{δ} (right) for the case of initially mismatched clocks τ_P and τ_O.

the error on the estimate for the delay solution.[2]

3.6 Summary

In this chapter, we modeled an NCS with aperiodic sampling and network delays in a state estimation setting, using the hybrid systems framework in [8]. We proposed a modified state estimation algorithm for such a setting and a method to include a clock synchronization scheme. Results were given to show the model's equivalence to an NCS with aperiodic sampling and no network delay. Results were also provided regarding its asymptotic attractivity to a set of interest in the presence of network delays and initially mismatched clocks that eventually synchronize. Numerical results validating the theoretical findings were also given.

[2]Code at github.com/HybridSystemsLab/HybridObsPlanarPlant

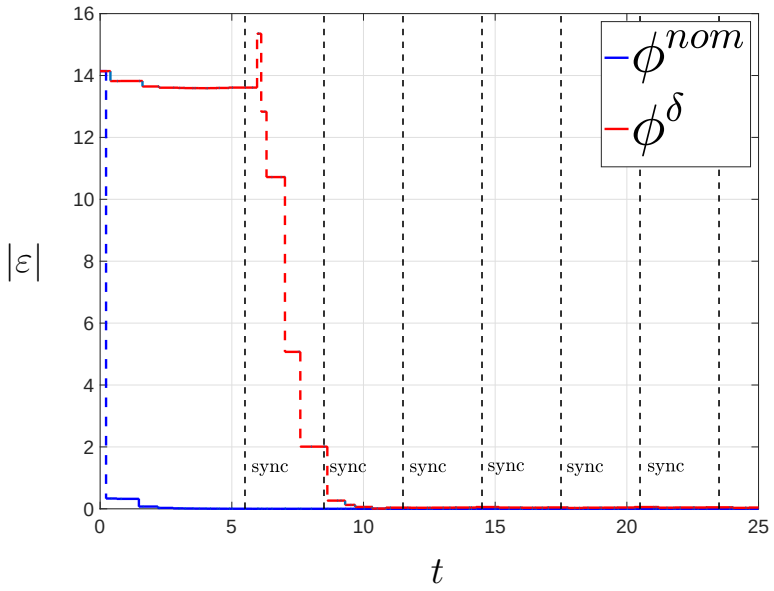

Figure 3.7: Plot of he error norm for ϕ^{nom} and ϕ^{δ} with drifting τ_O clock.

Chapter 4

HyNTP: A Hybrid Consensus Algorithm for Clock Synchronization

This chapter presents *HyNTP*, a distributed hybrid algorithm that synchronizes the time and rate of a set of clocks connected over a network. Clock measurements of the nodes are given at aperiodic time instants and the controller at each node uses these measurements to achieve synchronization. Due to the continuous and impulsive nature of the clocks and the network, a hybrid system model to effectively capture the dynamics of the system and the proposed hybrid algorithm is introduced. Moreover, the hybrid algorithm allows each agent to estimate the skew of its internal clock in order to allow for synchronization to a common timer rate. We provide sufficient conditions guaranteeing synchronization of the timers, exponentially fast. Numerical results illustrate the synchronization property induced by the proposed algorithm as well as its performance against comparable algorithms from the literature.

4.1 Problem Statement

Consider a group of n sensor nodes connected over a network represented by a digraph $\mathcal{G} = (\mathcal{V}, \mathcal{E}, A)$. Two clocks are attached to each node i of $\mathcal{G}$: an (uncontrollable)

internal clock $\tau_i^* \in \mathbb{R}_{\geq 0}$ whose dynamics are given by

$$\dot{\tau}_i^* = a_i \tag{4.1}$$

and an adjustable clock $\tilde{\tau}_i \in \mathbb{R}_{\geq 0}$ with dynamics

$$\dot{\tilde{\tau}}_i = a_i + u_i \tag{4.2}$$

where $u_i \in \mathbb{R}$ is a control input. In both of these models, the (unknown) constant a_i represents the unknown drift of the internal clock. At times t_j for $j \in \mathbb{N}_{>0}$ (we assume $t_0 = 0$), node i receives measurements $\tilde{\tau}_k$ from its neighbors, namely, for each $k \in \mathcal{N}(i)$. The resulting sequence of time instants $\{t_j\}_{j=1}^{\infty}$ is assumed to be strictly increasing and unbounded. Moreover, for such a sequence, the time elapsed between each time instant when the clock measurements are exchanged satisfies

$$\begin{aligned} T_1 \leq t_{j+1} - t_j \leq T_2 \quad \forall j \in \mathbb{N}_{>0} \\ 0 \leq t_1 \leq T_2 \end{aligned} \tag{4.3}$$

where $0 < T_1 \leq T_2$, with T_1 defining a minimum time between consecutive measurements and T_2 defines the maximum allowable transfer interval (MATI).

Remark 4.1.1. *The models for the clocks are based on the hardware and software relationship of the real-time system that implements them. That is, the internal clock τ_i^* is treated as a type of hardware oscillator while the adjustable clock $\tilde{\tau}_i$ is treated as a virtual clock, implemented in software (as part of the proposed algorithm), that evolves according to the dynamics of the hardware oscillator. Any virtual clock implemented in node i inherits the drift parameter a_i of the internal clock, which cannot be controlled. More importantly, this drift parameter is not known due to the fact that universal time information is not available to any node. The input u_i is unconstrained as allowed by hardware platforms.*

Under such a setup, our goal is to design a distributed hybrid controller that, without knowledge of the drift parameter and of the communication times in advance, assigns the input u_i to drive each clock $\tilde{\tau}_i$ to synchronization with every other clock $\tilde{\tau}_k$, with $\tilde{\tau}_k$ evolving at a common prespecified constant rate of change $\sigma^* > 0$ for each $k \in \mathcal{V}$. This problem is formally stated as follows:

Problem 4.1.1. *Given a network of n agents with dynamics as in (6.3) and (4.2) represented by a directed graph $\mathcal{G}$ and $\sigma^* > 0$, design a distributed hybrid controller that achieves*

the following two properties when information between agents is exchanged at times t_j satisfying (6.5):

i) Global clock synchronization: for each initial condition, the components $\tilde{\tau}_1, \tilde{\tau}_2, \ldots, \tilde{\tau}_n$ of each complete solution to the system satisfy

$$\lim_{t\to\infty} |\tilde{\tau}_i(t) - \tilde{\tau}_k(t)| = 0 \quad \forall i, k \in \mathcal{V}, i \neq k$$

ii) Common clock rate: for each initial condition, the components $\tilde{\tau}_1, \tilde{\tau}_2, \ldots, \tilde{\tau}_n$ of each complete solution to the system satisfy

$$\lim_{t\to\infty} |\dot{\tilde{\tau}}_i(t) - \sigma^*| = 0 \quad \forall i \in \mathcal{V}$$

4.2 Distributed Hybrid Controller for Time Synchronization

We define the hybrid model that provides the framework and a solution to Problem 6.0.1. First, since we are interested in the ability of the rate of each clock to synchronize to a constant rate σ^*, we propose the following change of coordinates: for each $i \in \mathcal{V}$, define $e_i := \tilde{\tau}_i - r$, where $r \in \mathbb{R}_{\geq 0}$ is an auxiliary variable such that $\dot{r} = \sigma^*$. The state r is only used for analysis. Then, the dynamics for e_i are given by

$$\dot{e}_i = \dot{\tilde{\tau}}_i - \sigma^* \qquad \forall i \in \mathcal{V} \tag{4.4}$$

By making the appropriate substitutions, one has

$$\dot{e}_i = a_i + u_i - \sigma^* \qquad \forall i \in \mathcal{V} \tag{4.5}$$

To model the network dynamics for aperiodic communication events at t_j's satisfying (6.5), we consider a timer variable τ with hybrid dynamics

$$\dot{\tau} = -1 \quad \tau \in [0, T_2], \quad \tau^+ \in [T_1, T_2] \quad \tau = 0 \tag{4.6}$$

This model is such that when $\tau = 0$, a communication event is triggered, and τ is reset to a point in the interval $[T_1, T_2]$ in order to preserve the bounds given in (6.5); see [20].

Remark 4.2.1. *Observe that the timer τ solely models the communication events between the nodes. Moreover, the nodes are independent of any information on the timer state thus, we do not assume any synchronization between the clock states of the nodes $\tilde{\tau}_i$ and τ.*

The proposed hybrid algorithm assigns a value to u_i so as to solve Problem 6.0.1, which in the e_i coordinates requires e_i to converge to zero for each $i \in \mathcal{V}$. In fact, the algorithm implements two feedback laws: a distributed feedback law and a local feedback law. The distributed feedback law utilizes a control variable $\eta_i \in \mathbb{R}$ that is impulsively updated at communication event times using both local and exchanged measurement information $\tilde{\tau}_k$. Specifically, it takes the form

$$\eta_i^+ = \sum_{k \in \mathcal{N}(i)} K_i^k(\tilde{\tau}_i, \tilde{\tau}_k)$$

where $K_i^k(\tilde{\tau}_i, \tilde{\tau}_k) := -\gamma_i(e_i - e_k)$ with $\gamma_i > 0$. Between communication event times, η_i evolves continuously. The local feedback strategy utilizes a continuous-time linear adaptive estimator with states $\hat{\tau}_i \in \mathbb{R}$ and $\hat{a}_i \in \mathbb{R}$ to estimate the drift a_i of the internal clock. The estimate of the drift is then injected as feedback to compensate for the effect of a_i on the evolution of $\tilde{\tau}_i$. Furthermore, the local feedback strategy injects σ^* to attain the desired clock rate for $\tilde{\tau}_i$.

Inspired by the protocol in [21, Protocol 4.1], the dynamics of the i-th hybrid controller are given by

$$\left.\begin{aligned} \dot{u}_i &= h_i\eta_i - \mu_i(\hat{\tau}_i - \tau_i^*),\ \dot{\eta}_i = h_i\eta_i \\ \dot{\hat{a}}_i &= -\mu_i(\hat{\tau}_i - \tau_i^*),\ \dot{\hat{\tau}}_i = \hat{a}_i - (\hat{\tau}_i - \tau_i^*) \end{aligned}\right\} \ \tau \in [0, T_2]$$
$$\left.\begin{aligned} u_i^+ &= -\gamma_i \sum_{k \in \mathcal{N}(i)} (\tilde{\tau}_i - \tilde{\tau}_k) - \hat{a}_i + \sigma^*,\ \hat{a}_i^+ = \hat{a}_i \\ \eta_i^+ &= -\gamma_i \sum_{k \in \mathcal{N}(i)} (\tilde{\tau}_i - \tilde{\tau}_k),\ \hat{\tau}_i^+ = \hat{\tau}_i \end{aligned}\right\} \ \tau = 0 \tag{4.7}$$

where $h_i \in \mathbb{R}$, $\gamma_i > 0$ are controller parameters for the distributed hybrid consensus controller and $\mu_i > 0$ is a parameter for the local parameter estimator. The state η is included in the model to facilitate a model reduction used in the results that follow. Note that u_i is treated (with some abuse of notation) as an auxiliary state of the controller. This state is kept constant in between events and is reset to the new value of $\eta_i - \hat{a}_i + \sigma^*$ at jumps. Observe that the distributed controller only uses local and communicated information from the neighboring nodes at communication event times t_j, which, as explained above (6.3), are times at which τ is zero.

With the timer variable and hybrid controller defined in (4.7), we construct the hybrid closed-loop system $\mathcal{H}$ obtained from the interconnection between the distributed

hybrid controller and the local adaptive estimator given in error coordinates. The state of the closed-loop system is

$$x = (e, u, \eta, \tau^*, \hat{a}, \hat{\tau}, \tau) \in \mathbb{R}^n \times \mathbb{R}^n \times \mathbb{R}^n \times \mathbb{R}^n_{\geq 0} \times \mathbb{R}^n \times \mathbb{R}^n_{\geq 0} \times [0, T_2] =: \mathcal{X} \tag{4.8}$$

where $e = (e_1, e_2, \ldots, e_n)$, $u = (u_1, u_2, \ldots u_n)$, $\eta = (\eta_1, \eta_2, \ldots, \eta_n)$, $\tau^* = (\tau_1^*, \tau_2^*, \ldots, \tau_N^*)$, $\hat{\tau} = (\hat{\tau}_1, \hat{\tau}_2, \ldots, \hat{\tau}_N)$, $a = (a_1, a_2, \ldots, a_N)$, and $\hat{a} = (\hat{a}_1, \hat{a}_2, \ldots, \hat{a}_n)$. The dynamics and data (C, f, D, G) of $\mathcal{H}$ are given by

$$\begin{bmatrix} \dot{e} \\ \dot{u} \\ \dot{\eta} \\ \dot{\tau}^* \\ \dot{\hat{a}} \\ \dot{\hat{\tau}} \\ \dot{\tau} \end{bmatrix} = \begin{bmatrix} a + u - \sigma^* \mathbf{1}_n \\ h\eta - \mu(\hat{\tau} - \tau^*) \\ h\eta \\ a \\ -\mu(\hat{\tau} - \tau^*) \\ \hat{a} - (\hat{\tau} - \tau^*) \\ -1 \end{bmatrix} =: f(x) \; x \in C, \quad \begin{bmatrix} e^+ \\ u^+ \\ \eta^+ \\ \tau^{*+} \\ \hat{a}^+ \\ \hat{\tau}^+ \\ \tau^+ \end{bmatrix} = \begin{bmatrix} e \\ -\gamma \mathcal{L} e - \hat{a} + \sigma^* \mathbf{1}_n \\ -\gamma \mathcal{L} e \\ \tau^* \\ \hat{a} \\ \hat{\tau} \\ [T_1, T_2] \end{bmatrix} =: G(x) \;\; x \in D \tag{4.9}$$

where $C := \mathcal{X}$ and $D := \{x \in \mathcal{X} : \tau = 0\}$. Note that $\mathcal{X} \subset \mathbb{R}^m$ where $m = 7n$.

With the hybrid system $\mathcal{H}$ defined, the next two results establish existence of solutions to $\mathcal{H}$ and that every maximal solution to $\mathcal{H}$ is complete. In particular, we show that, through the satisfaction of some basic conditions on the hybrid system data, which is shown first, the system $\mathcal{H}$ is well-posed and that each maximal solution to the system is defined for arbitrarily large $t + j$. The next two lemmas hold for any choice of parameters T_1, T_2, σ^*, h, γ, μ, and strongly connected digraph $\mathcal{G}$.

Lemma 4.2.2. *The hybrid system $\mathcal{H}$ satisfies the following conditions, defined in [4, Assumption 6.5] as the hybrid basic conditions.*

(A1) C and D are closed subsets of $\mathbb{R}^m$.

(A2) $f : \mathcal{X} \to \mathcal{X}$ is continuous and locally bounded relative to C and $C \subset$ dom f;

(A3) $G : \mathbb{R}^m \rightrightarrows \mathbb{R}^m$ is outer semicontinuous and locally bounded relative to D, and $D \subset$ dom G.

See the appendix for proof.

Lemma 4.2.3. *For every $\xi \in C \cup D (= \mathcal{X})$, every maximal solution ϕ to $\mathcal{H}$ with $\phi(0,0) = \xi$ is complete.*

See the appendix for proof.

With the hybrid closed-loop system $\mathcal{H}$ in (4.9), the set to asymptotically stabilize so as to solve Problem 6.0.1 is

$$\mathcal{A} := \{x \in \mathcal{X} : e_i = e_k, \eta_i = 0, \hat{a}_i = a_i, \hat{\tau}_i = \tau_i^*, u_i = \eta_i - \hat{a}_i + \sigma^* \; \forall i, k \in \mathcal{V}\} \tag{4.10}$$

Note that $e_i = e_k$ and $\eta_i = 0$ for all $i, k \in \mathcal{V}$ imply synchronization of the clocks, meanwhile $\hat{a}_i = a_i$ and $\tau_i^* = \hat{\tau}_i$ for all $i, k \in \mathcal{V}$ ensure no error in the estimation of the clock skew and that the internal and estimated clocks are synchronized, respectively. The inclusion of $u_i = -\hat{a}_i + \sigma^*$ in $\mathcal{A}$ ensures that, for each $i \in \mathcal{V}$, e_i remains constant (at zero) so that e_i does not leave the set $\mathcal{A}$. This property is captured in the following result using the notion of forward invariance of a set.

Remark 4.2.4. *Given that each maximal solution ϕ to $\mathcal{H}$ is complete, with the state variable τ acting as a timer for $\mathcal{H}$, for every initial condition $\phi(0,0) \in C \cup D$ we can characterize the domain of each solution ϕ to $\mathcal{H}$ as follows:*

$$\text{dom } \phi = \bigcup_{j \in \mathbb{N}} [t_j, t_{j+1}] \times \{j\} \tag{4.11}$$

with $t_0 = 0$ and $t_{j+1} - t_j$ as in (6.5). Furthermore, the structure of the above hybrid time domain implies that for each $(t, j) \in$ dom ϕ we have

$$t \leq T_2(j+1) \tag{4.12}$$

Lemma 4.2.5. *Given a strongly connected digraph $\mathcal{G}$, the set $\mathcal{A}$ in (4.10) is forward invariant for the hybrid system $\mathcal{H}$, i.e., each maximal solution ϕ to $\mathcal{H}$ with $\phi(0,0) \in \mathcal{A}$ is complete and satisfies $\phi(t, j) \in \mathcal{A}$ for each $(t, j) \in$ dom ϕ (see [?, Chapter 10]).*

See the appendix for proof.

With the definitions of the closed-loop system $\mathcal{H}$ in (4.9) and the set of interest $\mathcal{A}$ in (4.10) to asymptotically stabilize in order to solve Problem 6.0.1, we introduce our main result showing global exponential stability of $\mathcal{A}$ to $\mathcal{H}$. This result is established through an analysis of an auxiliary system $\widetilde{\mathcal{H}}_\varepsilon$ presented in (4.27) and its global exponential stability for the auxiliary set $\tilde{\mathcal{A}}_\varepsilon$ in (4.29), the details of which can be found in Section 4.3.4.

Theorem 4.2.6. *Given a strongly connected digraph $\mathcal{G}$, if the parameters $T_2 \geq T_1 > 0$, $\mu > 0$, $h \in \mathbb{R}$, and $\gamma > 0$, the positive definite matrices P_1, P_2, and P_3 are such that*

$$P_2 A_{f_3} + A_{f_3}^\top P_2 \prec 0 \tag{4.13}$$

$$P_3 A_{f_4} + A_{f_4}^\top P_3 \prec 0 \tag{4.14}$$

$$A_{g_2}^\top \exp(A_{f_2}^\top \nu) P_1 \exp(A_{f_2}\nu) A_{g_2} - P_1 \prec 0 \quad \forall \nu \in [T_1, T_2] \tag{4.15}$$

$$\left| \exp\left(\frac{\bar{\kappa}_1}{\alpha_2} T_2\right)\left(1 - \frac{\bar{\kappa}_2}{\alpha_2}\right)\right| < 1 \tag{4.16}$$

hold, where A_{f_2}, A_{g_2} are given in (4.28) and

$$\begin{aligned}
&\bar{\kappa}_1 = \max\left\{\frac{\kappa_1}{2\epsilon}, \frac{\kappa_1 \epsilon}{2} - \beta_2\right\}, \quad \bar{\kappa}_2 = \min\{1, \kappa_2\} \\
&\kappa_1 = 2 \max_{\nu \in [0, T_2]} \left| \exp(A_{f_2}^\top \nu) P_1 \exp(A_{f_2}\nu)\right| \\
&\kappa_2 \in \Big(0, - \min_{\nu \in [T_1, T_2]} \left\{\lambda_{min}(A_{g_2}^\top \exp(A_{f_2}^\top \nu) P_1 \exp(A_{f_2}\nu) A_{g_2} - P_1)\right\}\Big) \\
&\alpha_2 = \max_{\nu \in [0, T_2]} \Big\{ \exp(2h\nu), \lambda_{max}\big(\exp(A_{f_2}^\top \nu) P_1 \exp(A_{f_2}\nu)\big), \\
&\qquad\qquad \lambda_{max}(P_2), \lambda_{max}(P_3)\Big\}
\end{aligned} \tag{4.17}$$

with $\epsilon > 0$, and $\beta_1 > 0$ and $\beta_2 > 0$ such that, in light of (4.13), $P_2 A_{f_3} + A_{f_3}^\top P_2 \leq -\beta_1 I_2$, and $P_3 A_{f_4} + A_{f_4}^\top P_3 \leq -\beta_2 I_{2(n-1)}$ then, the set $\mathcal{A}$ in (4.10) is globally exponentially stable for the hybrid system $\mathcal{H}$ in (4.9).

To validate our theoretical stability result in Theorem 4.2.6, consider five agents with dynamics as in (6.3) and (4.2) over a strongly connected digraph with the following adjacency matrix

$$\mathcal{G}_A = \begin{pmatrix} 0 & 1 & 1 & 0 & 1 \\ 1 & 0 & 1 & 0 & 0 \\ 1 & 0 & 0 & 1 & 0 \\ 0 & 0 & 1 & 0 & 1 \\ 1 & 0 & 1 & 1 & 0 \end{pmatrix}$$

Given $T_1 = 0.01$, $T_2 = 0.1$, and $\sigma^* = 1$, then it can be found that the parameters $h = -1.3$, $\mu = 3$, $\gamma = 0.125$, suitable matrices P_1, P_2, P_3 (see [22] for details), and $\epsilon = 1.607$ satisfy conditions (4.15) and (4.16) in Theorem 4.2.6 with $\bar{\kappa}_1 = 9.78$, $\kappa_1 = 31.44$, $\bar{\kappa}_2 = 1$, and $\alpha_2 = 18.923$. Figure 4.1 shows the trajectories of $e_i - e_k$, ε_{a_i} for components $i \in \{1, 2, 3, 4, 5\}$ of a solution ϕ for the case where $\sigma = \sigma^*$ with initial conditions $\phi_e(0, 0) = (1, -1, 2, -2, 0)$, $\phi_\eta(0, 0) = (0, -3, 1, -4, -1)$, and clock rates a_i in the range $(0.85, 1.15)$. The bottom plot

$$
\begin{aligned}
P_1 &= \begin{bmatrix}
33.61 & 0 & 0 & 0 & 4.20 & 0 & 0 & 0 \\
0 & 28.61 & 0 & 0 & 0 & 5.73 & 0 & 0 \\
0 & 0 & 25.35 & 0 & 0 & 0 & 4.75 & 0 \\
0 & 0 & 0 & 28.61 & 0 & 0 & 0 & 5.73 \\
4.20 & 0 & 0 & 0 & 7.02 & 0 & 0 & 0 \\
0 & 5.73 & 0 & 0 & 0 & 11.13 & 0 & 0 \\
0 & 0 & 4.75 & 0 & 0 & 0 & 14.96 & 0 \\
0 & 0 & 0 & 5.73 & 0 & 0 & 0 & 11.13
\end{bmatrix} \\
P_2 &= \begin{bmatrix}
5.26 & -2.24 \\
-2.24 & 7.54
\end{bmatrix} \\
P_3 &= \begin{bmatrix}
6.47 & 0 & 0 & 0 & -2.36 & 0 & 0 & 0 \\
0 & 6.47 & 0 & 0 & 0 & -2.36 & 0 & 0 \\
0 & 0 & 6.47 & 0 & 0 & 0 & -2.36 & 0 \\
0 & 0 & 0 & 6.47 & 0 & 0 & 0 & -2.36 \\
-2.35 & 0 & 0 & 0 & 7.90 & 0 & 0 & 0 \\
0 & -2.35 & 0 & 0 & 0 & 7.90 & 0 & 0 \\
0 & 0 & -2.35 & 0 & 0 & 0 & 7.90 & 0 \\
0 & 0 & 0 & -2.35 & 0 & 0 & 0 & 7.90
\end{bmatrix}
\end{aligned}
\tag{4.18}
$$

in Figure 4.1 depicts the Lyapunov trajectory V evaluated along the solution ϕ with the upper bound given in (4.50) projected onto the regular time domain. Observe that the exponential bound provided in (4.50) jumps along the solution, validating our theoretical results on the exponential stability of the system.[1]

[1] Code at github.com/HybridSystemsLab/HybridClockSync

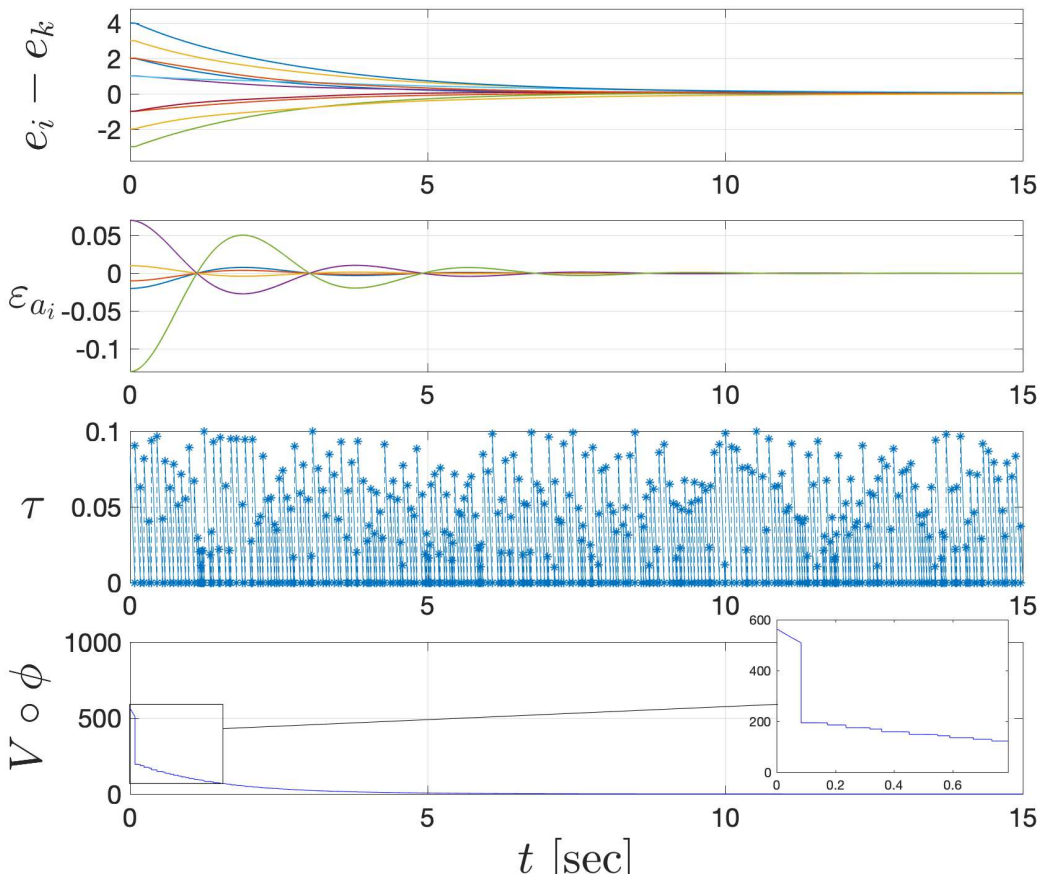

Figure 4.1: The trajectories of the solution ϕ for state component errors $e_i - e_k$, ε_{a_i}, and τ. Plot of V evaluated along the solution ϕ projected onto the regular time domain. (bottom)

4.3 Key Properties of the Nominal Closed-Loop System

4.3.1 Reduced Model – First Pass

In this section, we recast the hybrid system $\mathcal{H}$ into a reduced model obtained by setting $u = \eta - \hat{a} + \sigma^* \mathbf{1}_n$. This reduced model enables assessing asymptotic stability of $\mathcal{A}$. It is given in error coordinates for the parameter estimation of the internal clock rate and also the error of the internal clock state. We let $\varepsilon_a = a - \hat{a}$ denote the estimation error of the internal clock rate and $\varepsilon_\tau = \hat{\tau} - \tau^*$ represent the estimation error of the internal clock state. The state of the reduced model is given by $x_\varepsilon := (e, \eta, \varepsilon_a, \varepsilon_\tau, \tau) \in \mathbb{R}^n \times \mathbb{R}^n \times \mathbb{R}^n \times \mathbb{R}^n \times [0, T_2] =: \mathcal{X}_\varepsilon$ with dynamics defined by the data

$$f_\varepsilon(x_\varepsilon) := \begin{bmatrix} \eta + \varepsilon_a \\ h\eta \\ \mu\varepsilon_\tau \\ -\varepsilon_\tau - \varepsilon_a \\ -1 \end{bmatrix} \ \forall x_\varepsilon \in C_\varepsilon, \quad G_\varepsilon(x_\varepsilon) := \begin{bmatrix} e \\ -\gamma \mathcal{L} e \\ \varepsilon_a \\ \varepsilon_\tau \\ [T_1, T_2] \end{bmatrix} \ \forall x_\varepsilon \in D_\varepsilon \tag{4.19}$$

where $C_\varepsilon := \mathcal{X}_\varepsilon$ and $D_\varepsilon := \{x_\varepsilon \in \mathcal{X}_\varepsilon : \tau = 0\}$. This system is denoted $\mathcal{H}_\varepsilon = (C_\varepsilon, f_\varepsilon, D_\varepsilon, G_\varepsilon)$. Note that the construction $u = \eta - \hat{a} + \sigma^* \mathbf{1}_n$, which holds along all solutions after the first jump, leads to $\dot{e} = \eta + \varepsilon_a$.

To relate the properties of the reduced model to those of the hybrid system $\mathcal{H}$, we establish a result showing an equivalency between the solutions of $\mathcal{H}$ in (4.9) and $\mathcal{H}_\varepsilon$ defined above. The result shows that after the first jump, each solution ϕ to $\mathcal{H}$ is equivalent to a solution ϕ^ε to $\mathcal{H}_\varepsilon$ when the trajectories of the timer variable τ for both solutions are equal. To facilitate such a result, we define the function $M : \mathcal{X} \to \mathcal{X}_\varepsilon$ given by

$$M(x) := (e, \eta, a - \hat{a}, \hat{\tau} - \tau^*, \tau) \tag{4.20}$$

where $x = (e, u, \eta, \tau^*, \hat{a}, \hat{\tau}, \tau)$, as defined in (4.8), and the function $\widetilde{M} : \mathcal{X}_\varepsilon \times \mathbb{R}^n_{\geq 0} \times \mathbb{R}^n_{\geq 0} \to \mathcal{X}$

given by

$$\widetilde{M}(x_\varepsilon, \hat{\tau}, \tau^*) := \begin{bmatrix} e \\ \eta - (a - \varepsilon_a) + \sigma^* \mathbf{1}_n \\ \eta \\ \hat{\tau} - \varepsilon_\tau \\ a - \varepsilon_a \\ \varepsilon_\tau + \tau^* \\ \tau \end{bmatrix} \tag{4.21}$$

Lemma 4.3.1. *Let $T_2 \geq T_1 > 0$, digraph $\mathcal{G}$, and hybrid systems $\mathcal{H}$ and $\mathcal{H}_\varepsilon$ be given as in (4.9) and (4.19), respectively. For each $\phi \in \mathcal{S}_\mathcal{H}$ and each[2] $\phi^\varepsilon \in \mathcal{S}_{\mathcal{H}_\varepsilon}$ such that $\phi(0,0) = \widetilde{M}\big(\phi^\varepsilon(0,0), \phi_{\hat{\tau}}(0,0), \phi_{\tau^*}(0,0)\big)$ and timer components $\phi_\tau(t,j) = \phi^\varepsilon_\tau(t,j)$ for all $(t,j) \in \operatorname{dom} \phi$, it follows that dom ϕ = dom ϕ^ε and*

$$\phi(t,j) = \widetilde{M}\big(\phi^\varepsilon(t,j), \phi_{\hat{\tau}}(t,j), \phi_{\tau^*}(t,j)\big) \qquad \forall (t,j) \in \operatorname{dom}\, \phi \tag{4.22}$$

See the appendix for proof.

With the reduced model $\mathcal{H}_\varepsilon$ in place, we consider the following set to asymptotically stabilize for $\mathcal{H}_\varepsilon$:

$$\mathcal{A}_\varepsilon := \{x_\varepsilon \in \mathcal{X}_\varepsilon : e_i = e_k, \eta_i = 0 \; \forall i,k \in \mathcal{V}, \varepsilon_a = 0, \varepsilon_\tau = 0\} \tag{4.23}$$

This set is equivalent to $\mathcal{A}$ in the sense that the point-to-set distance metrics $|x|_\mathcal{A}$ and $|x|_{\mathcal{A}_\varepsilon}$ are equivalent when the map $\widetilde{M}$ is applied, as demonstrated in the results that follow.

Lemma 4.3.2. *Given sets $\mathcal{A}$ and $\mathcal{A}_\varepsilon$ as in (4.10) and (4.23), respectively, for each $x = (e, u, \eta, \tau^*, \hat{a}, \hat{\tau}, \tau)$, x_ε, $\hat{\tau}$, and τ^* such that $x \in \mathcal{X}$, $(x_\varepsilon, \hat{\tau}, \tau^*) \in \mathcal{X}$, and $u = \eta - \hat{a} + \sigma^* \mathbf{1}_n$ then*

$$|x|_\mathcal{A} = |x_\varepsilon|_{\mathcal{A}_\varepsilon} \tag{4.24}$$

and

$$|\widetilde{M}(x_\varepsilon, \hat{\tau}, \tau^*)|_\mathcal{A} = |x|_\mathcal{A} \tag{4.25}$$

[2]Note that for a given solution $\phi^\varepsilon(t,j)$ to $\mathcal{H}_\varepsilon$, the solution components are given by

$$\phi^\varepsilon(t,j) = \big(\phi^\varepsilon_e(t,j), \phi^\varepsilon_\eta(t,j), \phi^\varepsilon_{\varepsilon_a}(t,j), \phi^\varepsilon_{\varepsilon_\tau}(t,j), \phi^\varepsilon_\tau(t,j)\big)$$

With the stabilization set defined for $\mathcal{H}_\varepsilon$, we have the following result that shows that if the set $\mathcal{A}_\varepsilon$ is globally exponentially stable for $\mathcal{H}_\varepsilon$ then the set $\mathcal{A}$ is also globally exponentially stable for $\mathcal{H}$.

Lemma 4.3.3. *Given $T_2 \geq T_1 > 0$ and a strongly connected digraph $\mathcal{G}$, the set $\mathcal{A}$ in (4.10) is GES for the hybrid system $\mathcal{H}$ if $\mathcal{A}_\varepsilon$ in (4.23) is GES for the hybrid system $\mathcal{H}_\varepsilon$.*

See the appendix for proof.

4.3.2 Reduced Model – Second Pass

Global exponential stability of $\mathcal{A}_\varepsilon$ for $\mathcal{H}_\varepsilon$ is established by performing a Lyapunov analysis on a version of $\mathcal{H}_\varepsilon$ obtained after an appropriate change of coordinates, one where the flow and jump dynamics are linearized. The model is obtained by exploiting an important property of the eigenvalues of the Laplacian matrix for strongly connected digraphs.

To this end, let $\mathcal{G}$ be a strongly connected digraph. By Lemma 2.3.1 and Lemma 2.3.2, one has that zero is a simple eigenvalue of the Laplacian matrix $\mathcal{L}$ with an associated eigenvector $v_1 = \frac{1}{\sqrt{N}}\mathbf{1}_N$. Furthermore, there exists a nonsingular matrix

$$\mathcal{T} = [v_1, \mathcal{T}_1] \tag{4.26}$$

where $\mathcal{T}_1 \in \mathbb{R}^{N\times N-1}$ is a matrix whose columns are the remaining eigenvectors of $\mathcal{L}$, i.e., $[v_2, \ldots, v_N]$, such that $\mathcal{T}^{-1}\mathcal{L}\mathcal{T} = \begin{bmatrix} 0 & 0 \\ 0 & \bar{\mathcal{L}} \end{bmatrix}$, where $\mathcal{L}$ is the graph Laplacian of $\mathcal{G}$ and $\bar{\mathcal{L}}$ is a diagonal matrix with the nonnegative eigenvalues of $\mathcal{L}$ as the diagonal elements given by $(\lambda_2, \lambda_3, \ldots, \lambda_N)$, see [12], [23], and [24] for more details.

To perform the said change of coordinates, we use $\mathcal{T}$ to first perform the following transformations: $\bar{e} = \mathcal{T}^{-1}e$, $\bar{\eta} = \mathcal{T}^{-1}\eta$, $\bar{\varepsilon}_a = \mathcal{T}^{-1}\varepsilon_a$ and $\bar{\varepsilon}_\tau = \mathcal{T}^{-1}\varepsilon_\tau$. Then, we define vectors $\bar{z} = (\bar{z}_1, \bar{z}_2)$ and $\bar{w} = (\bar{w}_1, \bar{w}_2)$, where $\bar{z}_1 := (\bar{e}_1, \bar{\eta}_1)$, $\bar{z}_2 := (\bar{e}_2, \ldots, \bar{e}_N, \bar{\eta}_2, \ldots, \bar{\eta}_N)$, $\bar{w}_1 = (\bar{\varepsilon}_{a_1}, \bar{\varepsilon}_{\tau_1})$, and $\bar{w}_2 = (\bar{\varepsilon}_{a_2}, \ldots, \bar{\varepsilon}_{a_n}, \bar{\varepsilon}_{\tau_2}, \ldots, \bar{\varepsilon}_{\tau_n})$. Finally, we define $\chi_\varepsilon := (\bar{z}_1, \bar{z}_2, \bar{w}_1, \bar{w}_2, \tau) \in \mathbb{R}^2 \times \mathbb{R}^{2(n-1)} \times \mathbb{R}^2 \times \mathbb{R}^{2(n-1)} \times [0, T_2] =: \mathcal{X}_\varepsilon$ as the state of the new version of $\mathcal{H}_\varepsilon$, which is

denoted $\widetilde{\mathcal{H}}_\varepsilon$ and has data given by

$$\widetilde{f}_\varepsilon(\chi_\varepsilon) := \begin{bmatrix} A_{f_1}\bar{z}_1 \\ A_{f_2}\bar{z}_2 \\ A_{f_3}\bar{w}_1 \\ A_{f_4}\bar{w}_2 \\ -1 \end{bmatrix} + \begin{bmatrix} B_{f_1}\bar{w}_1 \\ B_{f_2}\bar{w}_2 \\ 0 \\ 0 \\ 0 \end{bmatrix} \quad \forall \chi_\varepsilon \in \tilde{C}_\varepsilon, \quad \widetilde{G}_\varepsilon(\chi_\varepsilon) := \begin{bmatrix} A_{g_1}\bar{z}_1 \\ A_{g_2}\bar{z}_2 \\ \bar{w}_1 \\ \bar{w}_2 \\ [T_1, T_2] \end{bmatrix} \quad \forall \chi_\varepsilon \in \tilde{D}_\varepsilon \tag{4.27}$$

for each χ_ε in $\widetilde{C}_\varepsilon := \mathcal{X}_\varepsilon$ and in $\widetilde{D}_\varepsilon := \{\chi_\varepsilon \in \mathcal{X}_\varepsilon : \tau = 0\}$, respectively, with

$$\begin{aligned} A_{f_1} &= \begin{bmatrix} 0 & 1 \\ 0 & h \end{bmatrix}, \qquad A_{f_2} = \begin{bmatrix} 0 & I_m \\ 0 & hI_m \end{bmatrix}, \quad A_{f_3} = \begin{bmatrix} 0 & \mu \\ -1 & -1 \end{bmatrix} \\ A_{f_4} &= \begin{bmatrix} 0 & \mu I_m \\ -I_m & -I_m \end{bmatrix}, \quad B_{f_1} = \begin{bmatrix} 1 & 0 \\ 0 & 0 \end{bmatrix}, \qquad B_{f_2} = \begin{bmatrix} I_m & 0 \\ 0 & 0 \end{bmatrix} \\ A_{g_1} &= \begin{bmatrix} 1 & 0 \\ 0 & 0 \end{bmatrix}, \qquad A_{g_2} = \begin{bmatrix} I_m & 0 \\ -\gamma\bar{\mathcal{L}} & 0 \end{bmatrix} \end{aligned} \tag{4.28}$$

and $m = N - 1$. Then, $\widetilde{\mathcal{H}}_\varepsilon = (\widetilde{C}_\varepsilon, \widetilde{f}_\varepsilon, \widetilde{D}_\varepsilon, \widetilde{G}_\varepsilon)$ denotes the new version of $\mathcal{H}_\varepsilon$. The set $\mathcal{A}_\varepsilon$ to stabilize in the new coordinates for this hybrid system is given by

$$\widetilde{\mathcal{A}}_\varepsilon := \{\chi_\varepsilon \in \mathcal{X}_\varepsilon : \bar{z}_1 = (e^*, 0), \bar{z}_2 = 0, \bar{w}_1 = 0, \bar{w}_2 = 0, e^* \in \mathbb{R}\} \tag{4.29}$$

In the following two results, we first demonstrate the relationship between the sets $\tilde{\mathcal{A}}_\varepsilon$ for $\widetilde{\mathcal{H}}_\varepsilon$ and $\mathcal{A}_\varepsilon$ for $\mathcal{H}_\varepsilon$ so as to solve Problem 6.0.1. Then, similar to Lemma 4.3.3, we show that global exponential stability of $\tilde{\mathcal{A}}_\varepsilon$ for $\widetilde{\mathcal{H}}_\varepsilon$ implies global exponential stability of $\mathcal{A}_\varepsilon$ for $\mathcal{H}_\varepsilon$. See the appendix for proofs.

Lemma 4.3.4. *Let $T_2 \geq T_1 > 0$, digraph $\mathcal{G}$, and hybrid systems $\mathcal{H}_\varepsilon$ and $\tilde{\mathcal{H}}_\varepsilon$ be given as in (4.19) and (4.27), respectively. For each solutions $\phi \in \mathcal{S}_{\mathcal{H}_\varepsilon}$ there exists a solution $\tilde{\phi} \in \mathcal{S}_{\tilde{\mathcal{H}}_\varepsilon}$ such that $\phi(t,j) = \Gamma\tilde{\phi}(t,j)$ for each $(t,j) \in$ dom ϕ if and only if for each solutions $\tilde{\phi} \in \mathcal{S}_{\tilde{\mathcal{H}}_\varepsilon}$ there exists a solution $\phi \in \mathcal{S}_{\mathcal{H}_\varepsilon}$ such that $\tilde{\phi}(t,j) = \Gamma^{-1}\phi(t,j)$ for each $(t,j) \in$ dom $\tilde{\phi}$, where $\Gamma = \text{diag}(\mathcal{T}, \mathcal{T}, \mathcal{T}, \mathcal{T}, 1)$.*

See the appendix for proof.

Lemma 4.3.5. *Given $0 < T_1 \leq T_2$ and a strongly connected digraph $\mathcal{G}$, $\xi \in \mathcal{A}_\varepsilon$ if and only if $\chi_\varepsilon := \Gamma^{-1}\xi \in \tilde{\mathcal{A}}_\varepsilon$, where $\Gamma^{-1} = \text{diag}(\mathcal{T}^{-1}, \mathcal{T}^{-1}, \mathcal{T}^{-1}, \mathcal{T}^{-1}, 1)$ and $\mathcal{T}$ is given in (4.26).*

Moreover, for each $x_\varepsilon \in \mathcal{X}_\varepsilon$ and each $\chi_\varepsilon \in \mathcal{X}_\varepsilon$

$$|\chi_\varepsilon|_{\tilde{\mathcal{A}}_\varepsilon} \leq |\Gamma^{-1}||x_\varepsilon|_{\mathcal{A}_\varepsilon} \tag{4.30}$$

and

$$|x_\varepsilon|_{\mathcal{A}_\varepsilon} \leq |\Gamma||\chi_\varepsilon|_{\tilde{\mathcal{A}}_\varepsilon} \tag{4.31}$$

See the appendix for proof.

Lemma 4.3.6. *Given $0 < T_1 \leq T_2$ and a strongly connected digraph $\mathcal{G}$, the set $\tilde{\mathcal{A}}_\varepsilon$ is GES for the hybrid system $\widetilde{\mathcal{H}}_\varepsilon$ if and only if $\mathcal{A}_\varepsilon$ is GES for the hybrid system $\mathcal{H}_\varepsilon$.*

See the appendix for proof.

4.3.3 Parameter Estimator

Exponential stability of the set $\tilde{\mathcal{A}}_\varepsilon$ for $\widetilde{\mathcal{H}}_\varepsilon$ hinges upon the convergence of the estimate $\hat{a}$ to a. We present a result establishing convergence of $\hat{a}$ to a by considering a model reduction of $\widetilde{\mathcal{H}}_\varepsilon$. To this end, consider the state $\chi_{\varepsilon_r} := (\bar{w}_1, \bar{w}_2, \tau) \in \mathbb{R}^2 \times \mathbb{R}^{2(n-1)} \times [0, T_2] =: \mathcal{X}_{\varepsilon_r}$. Its dynamics are given by the system $\widetilde{\mathcal{H}}_{\varepsilon_r} = (\widetilde{C}_{\varepsilon_r}, \widetilde{f}_{\varepsilon_r}, \widetilde{D}_{\varepsilon_r}, \widetilde{G}_{\varepsilon_r})$ with data

$$\tilde{f}_{\varepsilon_r}(\chi_{\varepsilon_r}) := \begin{bmatrix} A_{f_3}\bar{w}_1 \\ A_{f_4}\bar{w}_2 \\ -1 \end{bmatrix} \quad \forall \chi_{\varepsilon_r} \in \tilde{C}_{\varepsilon_r} := \mathcal{X}_{\varepsilon_r},$$

$$\tilde{G}_{\varepsilon_r}(\chi_{\varepsilon_r}) := \begin{bmatrix} \bar{w}_1 \\ \bar{w}_2 \\ [T_1, T_2] \end{bmatrix} \quad \forall \chi_{\varepsilon_r} \in \tilde{D}_{\varepsilon_r} := \{\chi_{\varepsilon_r} \in \mathcal{X}_{\varepsilon_r} : \tau = 0\}$$

For this system, the set to exponentially stabilize is given by

$$\widetilde{\mathcal{A}}_{\varepsilon_r} := \{0\} \times \{0\} \times [0, T_2] \tag{4.32}$$

In the next result, we show global exponential stability of the set $\tilde{\mathcal{A}}_{\varepsilon_r}$ for $\widetilde{\mathcal{H}}_{\varepsilon_r}$ through the satisfaction of matrix inequalities. See the appendix for proof.

Proposition 4.3.7. *If there exists a positive scalar μ and positive definite symmetric matrices P_2, P_3 such that, with A_{f_3} and A_{f_4} as in (4.28),*

$$P_2 A_{f_3} + A_{f_3}^\top P_2 \prec 0 \tag{4.33}$$

$$P_3 A_{f_4} + A_{f_4}^\top P_3 \prec 0 \tag{4.34}$$

hold, then the set $\widetilde{\mathcal{A}}_{\varepsilon_r}$ *is globally exponentially stable for the hybrid system* $\widetilde{\mathcal{H}}_{\varepsilon_r}$*. Furthermore, every solution* $\tilde{\phi}$ *to* $\widetilde{\mathcal{H}}_{\varepsilon_r}$ *satisfies*

$$|\tilde{\phi}(t,j)|_{\widetilde{\mathcal{A}}_{\varepsilon_r}} \leq \sqrt{\frac{\alpha_{\bar{w}_2}}{\alpha_{\bar{w}_1}}} \exp\Big(-\frac{\bar{\gamma}\tilde{\beta}}{2\alpha_{\bar{w}_2}}(t+j)\Big)|\tilde{\phi}(0,0)|_{\widetilde{\mathcal{A}}_{\varepsilon_r}} \tag{4.35}$$

for each $(t,j) \in \operatorname{dom} \tilde{\phi}$*, with* $\alpha_{\bar{w}_1} = \min\{\lambda_{min}(P_2),\ \lambda_{min}(P_3)\}$*,* $\alpha_{\bar{w}_2} = \max\{\lambda_{max}(P_2),\ \lambda_{max}(P_3)\}$*,* $\tilde{\beta} > 0$*, and* $\bar{\gamma} = \min\{1-\gamma, \gamma T_1\}$*.*

See the appendix for proof.

4.3.4 Proof of Theorem 4.2.6

Consider the following Lyapunov function candidate for $\widetilde{\mathcal{H}}_\varepsilon$

$$V(\chi_\varepsilon) := V_1(\chi_\varepsilon) + V_2(\chi_\varepsilon) + V_{\varepsilon_r}(\chi_\varepsilon) \quad \forall \chi_\varepsilon \in \mathcal{X}_\varepsilon \tag{4.36}$$

where

$$\begin{aligned} V_1(\chi_\varepsilon) &= \exp(2h\tau)\bar{\eta}_1^2 \\ V_2(\chi_\varepsilon) &= \bar{z}_2^\top \exp(A_{f_2}^\top \tau) P_1 \exp(A_{f_2}\tau)\bar{z}_2 \\ V_{\varepsilon_r}(\chi_\varepsilon) &= \bar{w}_1^\top P_2 \bar{w}_1 + \bar{w}_2^\top P_3 \bar{w}_2 \end{aligned}$$

Note that there exist two positive scalars α_1, α_2 such that

$$\alpha_1 |\chi_\varepsilon|_{\tilde{\mathcal{A}}_\varepsilon}^2 \leq V(\chi_\varepsilon) \leq \alpha_2 |\chi_\varepsilon|_{\tilde{\mathcal{A}}_\varepsilon}^2 \qquad \forall \chi_\varepsilon \in \tilde{C}_\varepsilon \cup \tilde{D}_\varepsilon \tag{4.37}$$

With P_1 positive definite and noting the nonsingularity of $\exp(A_{f_2}\tau)$ for every τ, we have

$$\alpha_1 = \min_{\nu\in[0,T_2]} \Big\{ \exp(2h\nu), \lambda_{min}\big(\exp(A_{f_2}^\top \nu) P_1 \exp(A_{f_2}\nu)\big), \lambda_{min}(P_2), \lambda_{min}(P_3) \Big\}$$

and α_2 as in (4.17). For each $\chi_\varepsilon \in \tilde{C}_\varepsilon$, one has

$$\begin{aligned} \langle \nabla V(\chi_\varepsilon), \tilde{f}_\varepsilon(\chi_\varepsilon)\rangle = {} & 2\bar{z}_2^\top \big(\exp(A_{f_2}^\top \tau) P_1 \exp(A_{f_2}\tau)\big) B_{f_2} \bar{w}_2 \\ & + \bar{w}_1^\top (P_2 A_{f_3} + A_{f_3}^\top P_2)\bar{w}_1 \\ & + \bar{w}_2^\top (P_3 A_{f_4} + A_{f_4}^\top P_3)\bar{w}_2 \end{aligned} \tag{4.38}$$

Now, by noting (4.13) and (4.14), with $\beta_1 > 0$ and $\beta_2 > 0$ such that $P_2 A_{f_3} + A_{f_3}^\top P_2 \leq -\beta_1 I$, and $P_3 A_{f_4} + A_{f_4}^\top P_3 \leq -\beta_2 I$ then one has

$$\langle \nabla V(\chi_\varepsilon), \tilde{f}_\varepsilon(\chi_\varepsilon) \rangle \leq \kappa_1 |\bar{z}_2||\bar{w}_2| - \beta_1 |\bar{w}_1|^2 - \beta_2 |\bar{w}_2|^2 \tag{4.39}$$

where

$$\kappa_1 = 2 \max_{\nu \in [0, T_2]} \left| \exp(A_{f_2}^\top \nu) P_1 \exp(A_{f_2} \nu) \right| |B_{f_2}|$$

Applying Young's inequality to $\kappa_1 |\bar{z}_2||\bar{w}_2|$, [3] we obtain

$$\begin{aligned} \langle \nabla V(\chi_\varepsilon), \tilde{f}_\varepsilon(\chi_\varepsilon) \rangle &\leq \frac{\kappa_1}{2\epsilon} |\bar{z}_2|^2 + \frac{\kappa_1 \epsilon}{2} |\bar{w}_2|^2 - \beta_1 |\bar{w}_1|^2 - \beta_2 |\bar{w}_2|^2 \\ &\leq \frac{\kappa_1}{2\epsilon} |\bar{z}_2|^2 - \beta_1 |\bar{w}_1|^2 + \Big(\frac{\kappa_1 \epsilon}{2} - \beta_2 \Big) |\bar{w}_2|^2 \end{aligned} \tag{4.40}$$

where $\epsilon > 0$, we then upper bound the inequality by picking the largest coefficient, i.e, $\bar{\kappa}_1 = \max \Big\{ \frac{\kappa_1}{2\epsilon}, \Big(\frac{\kappa_1 \epsilon}{2} - \beta_2 \Big) \Big\}$, leading to

$$\begin{aligned} \langle \nabla V(\chi_\varepsilon), \tilde{f}_\varepsilon(\chi_\varepsilon) \rangle &\leq \bar{\kappa}_1 \big(|\bar{z}_2|^2 + |\bar{w}_1|^2 + |\bar{w}_2|^2 \big) \\ &\leq \bar{\kappa}_1 \big(|\chi_\varepsilon|^2_{\tilde{\mathcal{A}}_\varepsilon} \big) \\ &\leq \bar{\kappa}_1 \Big(\frac{1}{\alpha_2} V(\chi_\varepsilon) \Big) \\ &\leq \frac{\bar{\kappa}_1}{\alpha_2} V(\chi_\varepsilon) \end{aligned} \tag{4.41}$$

Now, for the analysis across jumps, note that for all $\chi_\varepsilon \in \tilde{D}_\varepsilon$, $\tau = 0$. At jumps, τ is mapped to some point $\nu \in [T_1, T_2]$. Then, at jumps, for each $g \in \tilde{G}_\varepsilon$ one has

$$\begin{aligned} V(g) - V(\chi_\varepsilon) &= -\bar{\eta}_1^2 - \bar{z}_2^\top P_1 \bar{z}_2 \\ &\quad + (A_{g_2} \bar{z}_2)^\top \exp(A_{f_2}^\top \nu) P_1 \exp(A_{f_2} \nu) (A_{g_2} \bar{z}_2) \\ &= -\bar{\eta}_1^2 \\ &\quad + \bar{z}_2^\top \big(A_{g_2}^\top \exp(A_{f_2}^\top \nu) P_1 \exp(A_{f_2} \nu) A_{g_2} - P_1 \big) \bar{z}_2 \\ &\leq -|\bar{\eta}_1|^2 - \kappa_2 |\bar{z}_2|^2 \\ &\leq -\bar{\kappa}_2 \big(|\bar{\eta}_1|^2 + |\bar{z}_2|^2 \big) \end{aligned} \tag{4.42}$$

where $\bar{\kappa}_2 = \max\{1, \kappa_2\}$ and, by continuity of condition (4.15), $\kappa_2 > 0$ such that

$$\kappa_2 \in \Big(0, - \min_{v \in [T_1, T_2]} \lambda_{min} (A_{g_2}^\top \exp(A_{f_2}^\top v) P_1 \exp(A_{f_2} v) A_{g_2} - P_1) \Big)$$

[3] In particular, we are utilizing the relation $ab \leq \frac{a^2}{2\epsilon} + \frac{\epsilon b^2}{2}$ where $a, b \in \mathbb{R}$ and $\epsilon > 0$.

for where we have

$$V(g) - V(\chi_\varepsilon) \leq -\bar{\kappa}_2\big(|\bar{\eta}_1|^2 + |\bar{z}_2|^2\big) \tag{4.43}$$

Utilizing the upper bound α_2 from the definition of V in (4.37), for all $\chi_\varepsilon \in \tilde{D}_\varepsilon$, one has

$$V(\chi_\varepsilon) \leq \alpha_2\big(|\bar{\eta}_1|^2 + |\bar{z}_2|^2 + |\bar{w}|^2\big) \tag{4.44}$$

Dividing by α_2 and rearranging terms, one has

$$-(|\bar{\eta}_1|^2 + |\bar{z}_2|^2) \leq -\frac{1}{\alpha_2}V(\chi_\varepsilon) + |\bar{w}|^2 \tag{4.45}$$

Then, by inserting (4.45) into (4.43),

$$\begin{aligned} V(g) - V(\chi_\varepsilon) &\leq -\bar{\kappa}_2\big(|\bar{\eta}_1|^2 + |\bar{z}_2|^2\big) \\ V(g) - V(\chi_\varepsilon) &\leq \bar{\kappa}_2\Big(-\frac{1}{\alpha_2}V(\chi_\varepsilon) + |\bar{w}|^2\Big) \\ V(g) &\leq -\frac{\bar{\kappa}_2}{\alpha_2}V(\chi_\varepsilon) + \bar{\kappa}_2|\bar{w}|^2 + V(\chi_\varepsilon) \\ V(g) &\leq \Big(1 - \frac{\bar{\kappa}_2}{\alpha_2}\Big)V(\chi_\varepsilon) + \bar{\kappa}_2|\bar{w}|^2 \end{aligned} \tag{4.46}$$

Now, by noting that $\langle \nabla V(\chi_\varepsilon), \tilde{f}(\chi_\varepsilon)\rangle \leq \frac{\bar{\kappa}_1}{\alpha_2}V(\chi_\varepsilon)$ and by (4.46), pick a solution $\tilde{\phi}$ to $\widetilde{\mathcal{H}}_\varepsilon$ with initial condition $\tilde{\phi}(0,0) \in \widetilde{C}_\varepsilon \cup \widetilde{D}_\varepsilon$. Let the jumps of $\tilde{\phi}$ occur at times $(t_j, j) \in \{j' : \exists t' : (t', j') \in \text{dom } \phi\}$. For each $(t, j) \in [0, t_1] \times \{0\}$ one has

$$V(t,0) \leq \exp\Big(\frac{\bar{\kappa}_1}{\alpha_2}t_1\Big)V(0,0) \tag{4.47}$$

At $(t_1, 1)$

$$\begin{aligned} V(t_1,1) &\leq \Big(1 - \frac{\bar{\kappa}_2}{\alpha_2}\Big)V(t_1,0) + \bar{\kappa}_2|\bar{w}(t_1,0)|^2 \\ &\leq \Big(1 - \frac{\bar{\kappa}_2}{\alpha_2}\Big)\exp\Big(\frac{\bar{\kappa}_1}{\alpha_2}t_1\Big)V(0,0) + \bar{\kappa}_2|\bar{w}(t_1,0)|^2 \end{aligned}$$

Then, for each $(t, j) \in [t_1, t_2] \times \{1\}$

$$\begin{aligned}
V(t,1) &\leq \exp\Big(\frac{\bar{\kappa}_1}{\alpha_2}(t_2 - t_1)\Big) V(t_1, 1) \\
&\leq \exp\Big(\frac{\bar{\kappa}_1}{\alpha_2}(t_2 - t_1)\Big)\Big[\Big(1 - \frac{\bar{\kappa}_2}{\alpha_2}\Big)\exp\big(\bar{\kappa}_1 t_1\big) V(0,0) \\
&\quad + \bar{\kappa}_2 |\bar{w}(t_1, 0)|^2\Big] \\
&\leq \exp\Big(\frac{\bar{\kappa}_1}{\alpha_2}(t_2 - t_1)\Big)\Big(1 - \frac{\bar{\kappa}_2}{\tilde{\alpha}_1}\Big)\exp\Big(\frac{\bar{\kappa}_1}{\alpha_2} t_1\Big) V(0,0) \\
&\quad + \exp\Big(\frac{\bar{\kappa}}{\alpha_2}(t_2 - t_1)\Big)\bar{\kappa}_2 |\bar{w}(t_1, 0)|^2 \\
&= \exp\Big(\frac{\bar{\kappa}_1}{\alpha_2} t_2\Big)\Big(1 - \frac{\bar{\kappa}_2}{\alpha_2}\Big) V(0,0) \\
&\quad + \exp\big(\frac{\bar{\kappa}_1}{\alpha_2}(t_2 - t_1)\big)\bar{\kappa}_2 |\bar{w}(t_1, 0)|^2
\end{aligned}$$

At $(t_2, 2)$

$$\begin{aligned}
V(t_2,2) &\leq \Big(1 - \frac{\bar{\kappa}_2}{\alpha_2}\Big) V(t_2, 1) + \bar{\kappa}_2 |\bar{w}(t_2, 1)|^2 \\
&\leq \Big(1 - \frac{\bar{\kappa}_2}{\alpha_2}\Big)\exp\Big(\frac{\bar{\kappa}_1}{\alpha_2} t_2\Big)\Big(1 - \frac{\bar{\kappa}_2}{\alpha_2}\Big) V(0,0) \\
&\quad + \exp\Big(\frac{\bar{\kappa}_1}{\alpha_2}(t_2 - t_1)\Big)\bar{\kappa}_2 |\bar{w}(t_1, 0)|^2 + \bar{\kappa}_2 |\bar{w}(t_2, 1)|^2 \\
&\leq \exp\Big(\frac{\bar{\kappa}_1}{\alpha_2} t_2\Big)\Big(1 - \frac{\bar{\kappa}_2}{\alpha_2}\Big)^2 V(0,0) \\
&\quad + \bar{\kappa}_2\Big[\exp\Big(\frac{\bar{\kappa}_1}{\alpha_2}(t_2 - t_1)\Big)|\bar{w}(t_1, 0)|^2 + |\bar{w}(t_2, 1)|^2\Big]
\end{aligned}$$

A general form of the bound is given by

$$\begin{aligned}
V(t,j) \leq \exp\Big(\frac{\bar{\kappa}_1}{\alpha_2} t_j\Big)\Big(1 - \frac{\bar{\kappa}_2}{\tilde{\alpha}_1}\Big)^j V(0,0) \\
+ \bar{\kappa}_2\Big(\sum_{k=1}^{j} \exp\Big(\frac{\bar{\kappa}_1}{\alpha_2}(t_{k+1} - t_k)\Big)|\bar{w}(t_k, k-1)|^2\Big)
\end{aligned} \tag{4.48}$$

Noting that $t_{j+1} - t_j \leq T_2$ and $\frac{\bar{\kappa}_1}{\alpha_2} > 0$, the latter term can be further bounded as

$$\begin{aligned}
\bar{\kappa}_2\Big(\sum_{k=1}^{j} \exp\big(\frac{\bar{\kappa}_1}{\alpha_2}(t_{k+1} - t_k)\big)|\bar{w}(t_k, k-1)|^2\Big) \\
\leq \bar{\kappa}_2 \exp\big(\frac{\bar{\kappa}_1}{\alpha_2} T_2\big) \sup_{(t,j) \in \mathrm{dom}\tilde{\phi}} |\bar{w}(t, j)|^2
\end{aligned}$$

Moreover, since $t_j \leq T_2(j+1)$ and $\frac{\bar{\kappa}_1}{\alpha_2} > 0$, we can also put a stricter bound on the first term in (4.48) as follows:

$$\begin{aligned}
&\exp\Big(\frac{\bar{\kappa}_1}{\alpha_2}\, t_j\Big)\Big(1-\frac{\bar{\kappa}_2}{\alpha_2}\Big)^j V(0,0) \\
&\qquad \leq \exp\Big(\frac{\bar{\kappa}_1}{\alpha_2}\, T_2(j+1)\Big)\Big(1-\frac{\bar{\kappa}_2}{\alpha_2}\Big)^j V(0,0) \\
&\qquad \leq \exp\Big(\frac{\bar{\kappa}_1}{\alpha_2}\, T_2\Big)\Big(\exp\Big(\frac{\bar{\kappa}_1}{\alpha_2}\, T_2\Big)\Big(1-\frac{\bar{\kappa}_2}{\alpha_2}\Big)\Big)^j V(0,0)
\end{aligned}$$

Thus

$$\begin{aligned}
V(t,j) \leq \exp\Big(\frac{\bar{\kappa}_1}{\alpha_2}\, T_2\Big)\Big(\exp\Big(\frac{\bar{\kappa}_1}{\alpha_2}\, T_2\Big)\Big(1-\frac{\bar{\kappa}_2}{\alpha_2}\Big)\Big)^j V(0,0) \\
+ \bar{\kappa}_2 \exp\Big(\frac{\bar{\kappa}_1}{\alpha_2}\, T_2\Big)\sup\nolimits_{(t,j)\in \mathrm{dom}\tilde{\phi}} |\bar{w}(t,j)|^2
\end{aligned} \tag{4.49}$$

Then, from the result of Proposition 4.3.7, we have

$$|\tilde{\phi}_{\bar{w}}(t,j)| \leq \sqrt{\frac{\alpha_{\bar{w}_2}}{\alpha_{\bar{w}_1}}} \exp\Big(-\frac{\tilde{\beta}}{2\alpha_{\bar{w}_2}} t\Big) |\tilde{\phi}_{\bar{w}}(0,0)|_{\tilde{\mathcal{A}}_{\varepsilon r}}$$

with $\alpha_{\bar{w}_1} = \min\{\lambda_{min}(P_2), \lambda_{min}(P_3)\}$ and $\alpha_{\bar{w}_2} = \max\{\lambda_{max}(P_2), \lambda_{max}(P_3)\}$. Now, to improve readability, we have omitted including the use of the notation $V(\tilde{\phi}(t,j))$ when evaluating V along the trajectory for the solution $\tilde{\phi}$ opting instead for the use of the state components of χ_ε directly. In particular, we remind the reader that the notation $\bar{w}(t,j)$ corresponds to the $\bar{w}$ component of a solution, i.e., $\phi_{\bar{w}}(t,j)$. Thus, we have

$$\begin{aligned}
V(t,j) \leq \exp\Big(\frac{\bar{\kappa}_1}{\alpha_2}\, T_2\Big)\Big(\exp\Big(\frac{\bar{\kappa}_1}{\alpha_2}\, T_2\Big)\Big(1-\frac{\bar{\kappa}_2}{\alpha_2}\Big)\Big)^j V(0,0) \\
+ \bar{\kappa}_2 \exp\Big(\frac{\bar{\kappa}_1}{\alpha_2}\, T_2\Big)\frac{\alpha_{\bar{w}_2}}{\alpha_{\bar{w}_1}} \exp\Big(-\frac{\bar{\gamma}\tilde{\beta}}{2\alpha_{\bar{w}_2}}(t+j)\Big)^2 |\phi_{\bar{w}}(0,0)|^2_{\tilde{\mathcal{A}}_{\varepsilon r}} \\
\forall (t,j) \in \mathrm{dom}\ \tilde{\phi}
\end{aligned} \tag{4.50}$$

Now, combining the inequality with (4.37) and noting $V(\phi(0,0)) \leq \alpha_2 |\phi(0,0)|^2_{\tilde{\mathcal{A}}_\varepsilon}$ one has

$$\begin{aligned}
|\phi(t,j)|^2_{\tilde{\mathcal{A}}_\varepsilon} \leq \alpha_1^{-1}\Big(\alpha_2 |\phi(0,0)|^2_{\tilde{\mathcal{A}}_\varepsilon}\Big) \exp\Big(\frac{\bar{\kappa}_1}{\alpha_2}\, T_2\Big)\Big(\exp\Big(\frac{\bar{\kappa}_1}{\alpha_2}\, T_2\Big)\Big(1-\frac{\bar{\kappa}_2}{\alpha_2}\Big)\Big)^j \\
+ \bar{\kappa}_2 \exp\Big(\frac{\bar{\kappa}_1}{\alpha_2}\, T_2\Big)\frac{\alpha_{\bar{w}_2}}{\alpha_{\bar{w}_1}} \exp\Big(\frac{-\bar{\gamma}\tilde{\beta}}{2\alpha_{\bar{w}_2}}(t+j)\Big)^2 |\phi_{\bar{w}}(0,0)|^2_{\tilde{\mathcal{A}}_{\varepsilon r}} \\
\forall (t,j) \in \mathrm{dom}\ \phi
\end{aligned} \tag{4.51}$$

Then, taking the square root on both sides, one has

$$|\phi(t,j)|_{\tilde{\mathcal{A}}_\varepsilon} \leq \sqrt{\frac{\alpha_2}{\alpha_1}}|\phi(0,0)|_{\tilde{\mathcal{A}}_\varepsilon} \exp\Big(\frac{\bar{\kappa}_1}{2\alpha_2}T_2\Big)\Big(\exp\Big(\frac{\bar{\kappa}_1}{2\alpha_2}T_2\Big)\Big(1-\frac{\bar{\kappa}_2}{2\alpha_2}\Big)\Big)^j$$
$$+\sqrt{\bar{\kappa}_2}\exp\Big(\frac{\bar{\kappa}_1}{2\alpha_2}T_2\Big)\sqrt{\frac{\alpha_{\bar{w}_2}}{\alpha_{\bar{w}_1}}\exp\Big(-\frac{\bar{\gamma}\tilde{\beta}}{2\alpha_{\bar{w}_2}}(t+j)\Big)^2|\phi_{\bar{w}}(0,0)|^2_{\tilde{\mathcal{A}}_{\varepsilon r}}} \tag{4.52}$$
$$\forall (t,j) \in \text{dom } \phi$$

By the given conditions, the set $\tilde{\mathcal{A}}_\varepsilon$ is globally exponentially stable and attractive for $\widetilde{\mathcal{H}}_\varepsilon$. Now, by utilizing Lemmas 4.3.4 - 4.3.6, we can establish global exponential stability to the set $\mathcal{A}_\varepsilon$ for $\mathcal{H}_\varepsilon$, in turn we can then make use of Lemmas 4.3.1 - 4.3.3 to then show that the set $\mathcal{A}$ is globally exponentially stable and attractive for $\mathcal{H}$ in (4.9).

4.4 Robustness to Communication Noise, Clock Drift Perturbations, and Error on σ

Under a realistic scenario, it is often the case that the system is subjected to various noise disturbances. Environmental factors can affect the internal clock dynamics and introduce noise to the communication medium in the form of communication delay. In this section we present results on input-to-state stability (ISS) of the system when it is affected by such sources of noise. We will first present an ISS result on the parameter estimation sub-system when it is subjected to noise on the internal clock output, we will then present an ISS result that considers communication noise, last but not least, we will present an ISS result on noise introduced to the desired clock rate reference σ^*. We will henceforth refer to the following notion of ISS for Hybrid Systems in the presentation of these results, defined as follows:

Definition 4.4.1. *(Input-to-state stability) A hybrid system $\mathcal{H}$ with input m is input-to-state stable with respect to a set $\mathcal{A} \subset \mathbb{R}^n$ if there exist $\beta \in \mathcal{KL}$ and $\kappa \in \mathcal{K}$ such that each solution pair (ϕ, m) to $\mathcal{H}$ satisfies $|\phi(t,j)|_{\mathcal{A}} \leq \max\{\beta(|\phi(0,0)|_{\mathcal{A}}, t+j), \kappa(|m|_\infty)\}$ for each $(t,j) \in \text{dom } \phi$.*

4.4.1 Robustness to Communication Noise

We consider the case when the measurements of the timer $\tilde{\tau}_i$ is affected by noise $m_{e_i} \in \mathbb{R}$, $i \in \mathcal{V}$. As a result, the output of each agent is given by $\tilde{\tau}_i + m_{e_i}$. In the presence

of this noise, the update law to η_i^+ in the hybrid controller in (4.7) becomes

$$\begin{aligned}\eta_i^+ &= -\gamma \sum_{k\in\mathcal{N}(i)} (y_i - y_k) \\ &= -\gamma \sum_{k\in\mathcal{N}(i)} (\tilde{\tau}_i - \tilde{\tau}_k) - \gamma \sum_{k\in\mathcal{N}(i)} (m_{e_i} - m_{e_k})\end{aligned}$$

Performing the same change of coordinates, as in the proof of Theorem 4.2.6, we show that $\widetilde{\mathcal{H}}_\varepsilon$ is ISS to communication noise $m_e := (m_{e_1}, m_{e_2}, \ldots, m_{e_n}) \in \mathbb{R}^n$. Recalling the change of coordinates $\bar{e} = \mathcal{T}^{-1}e$ and $\bar{\eta} = \mathcal{T}^{-1}\eta$, let $\bar{m}_e = \mathcal{T}^{-1}m_e$. The update law $\bar{\eta}^+$, is given by $\bar{\eta}^+ = (0, -\gamma\bar{\mathcal{L}}\bar{e} - \gamma\bar{\mathcal{L}}\bar{m}_e)$ with $\bar{\eta}_1$ unaffected by the communication noise.

Using the update law for $\bar{\eta}$ under the effect of $\bar{m}_e$, we define the perturbed hybrid system $\widetilde{\mathcal{H}}_m$ with state vector $\chi_m := (\bar{z}_1, \bar{z}_2, \bar{w}_1, \bar{w}_2, \tau) \in \mathcal{X}_\varepsilon$, where, again $\bar{z}_1 = (\bar{e}_1, \bar{\eta}_1)$, $\bar{z}_2 = (\bar{e}_2, \ldots, \bar{e}_N, \bar{\eta}_2, \ldots, \bar{\eta}_N)$, $\bar{w}_1 = (\bar{\varepsilon}_{a_1}, \bar{\varepsilon}_{\tau_1})$, and $\bar{w}_2 = (\bar{\varepsilon}_{a_2}, \ldots, \bar{\varepsilon}_{a_n}, \bar{\varepsilon}_{\tau_2}, \ldots, \bar{\varepsilon}_{\tau_n})$. Moreover, let $\bar{m}_{\bar{z}_2} = (0, \bar{m}_e)$. The data $(\tilde{C}_m, \tilde{f}_m, \tilde{D}_m, \tilde{G}_m)$ for the new system $\widetilde{\mathcal{H}}_m$ is given by

$$\widetilde{f}_m(\chi_m) := \widetilde{f}_\varepsilon(\chi_m) \qquad \forall \chi_m \in \widetilde{C}_m$$

$$\widetilde{G}_m(\chi_m, \bar{m}_\varepsilon) := \widetilde{G}_\varepsilon(\chi_m) - \begin{bmatrix} 0 \\ B_g\bar{m}_{\bar{z}_2} \\ 0 \\ 0 \\ 0 \end{bmatrix} \quad \forall \chi_m \in \widetilde{D}_m$$

where $\widetilde{C}_m := \mathcal{X}_\varepsilon$, $\widetilde{D}_m := \{\chi_m \in \mathcal{X}_m : \tau = 0\}$, and $B_g = \begin{bmatrix} 0 & \gamma\bar{\mathcal{L}} \end{bmatrix}^\top$.

Theorem 4.4.2. *Given a strongly connected digraph $\mathcal{G}$, if the parameters $T_2 \geq T_1 > 0$, $\mu > 0$, $h \in \mathbb{R}$, $\gamma > 0$, and positive definite symmetric matrices P_1, P_2, and P_3 are such that (4.15) and (4.16) hold, the hybrid system $\widetilde{\mathcal{H}}_m$ with input $\bar{m}_e$ is ISS with respect to $\widetilde{\mathcal{A}}_\varepsilon$ in (4.29).*

Proof. Consider the same Lyapunov function candidate $V(\chi_m) = V_1(\chi_m) + V_2(\chi_m) + V_{\varepsilon_r}(\chi_m)$ from the proof of Theorem 4.2.6. During flows, there is no contribution from the perturbation thus the derivative of V is unchanged from the proof of Theorem 4.2.6. Thus, one has

$$\begin{aligned}\langle \nabla V(\chi_m), \tilde{f}(\chi_m) \rangle \leq\ & 2\bar{z}_2^\top \big(\exp A_{f_2}^\top \tau P \exp A_{f_2}\tau \big) B_{f_2}\bar{w}_2 \\ & + \bar{w}_1^\top (P_1 A_{f_3} + A_{f_3}^\top P_1)\bar{w}_1 \\ & + \bar{w}_2^\top (P_2 A_{f_4} + A_{f_4}^\top P_2)\bar{w}_2\end{aligned}$$

then by following the same notions of the proof in Theorem 4.2.6, one has

$$\begin{aligned}\langle \nabla V(\chi_m), \tilde{f}(\chi_m)\rangle &\leq \frac{\kappa_1}{2\epsilon}|\bar{z}_2|^2 - \beta_1|\bar{w}_1|^2 + \Big(\frac{\kappa_1\epsilon}{2} - \beta_2\Big)|\bar{w}_2|^2 \\ &\leq \bar{\kappa}_1\big(|\bar{z}_2|^2 + |\bar{w}_1|^2 + |\bar{w}_2|^2\big) \\ &\leq \bar{\kappa}_1 V(x)\end{aligned}$$

where $\bar{\kappa}_1 = \max\Big\{\frac{\kappa_1}{2\epsilon}, \Big(\frac{\kappa_1\epsilon}{2} - \beta_2\Big)\Big\}$ and $\varepsilon > 0$. At jumps, triggered when $\tau = 0$, one has, for each $\chi_m \in \tilde{D}_m \setminus \tilde{\mathcal{A}}_\varepsilon$ and $g \in \tilde{G}_m(\chi_m)$

$$\begin{aligned}V(g)\text{-}V(\chi_m) \leq & -\bar{\eta}_1^2 + (A_{g_2}\bar{z}_2 - B_g\bar{m}_{\bar{z}_2})^\top Q(A_{g_2}\bar{z}_2 - B_g\bar{m}_{\bar{z}_2}) \\ & - \bar{z}_2^\top P_1\bar{z}_2 \\ \leq & -\bar{\eta}_1^2 + (A_{g_2}\bar{z}_2)^\top \exp A_{f_2}^\top\tau P_1 \exp A_{f_2}\tau(A_{g_2}\bar{z}_2) \\ & -2(B_g\bar{m}_{\bar{z}_2})^\top \exp A_{f_2}^\top\tau P_1 \exp A_{f_2}\tau(A_{g_2}\bar{z}_2) \\ & + (B_g\bar{m}_{\bar{z}_2})^\top \exp A_{f_2}^\top\tau P_1 \exp A_{f_2}\tau(B_g\bar{m}_{\bar{z}_2}) \\ & -\bar{z}_2^\top P_1\bar{z}_2\end{aligned} \tag{4.53}$$

From 4.15 and the proof in Theorem 4.2.6, there exists a scalar κ_2 such that

$$\bar{z}_2^\top(A_{g_2}^\top \exp A_{f_2}^\top vP_1 \exp A_{f_2}vA_{g_2} - P_1)\bar{z}_2 \leq -\kappa_2\bar{z}_2^\top\bar{z}_2$$

leading to

$$\begin{aligned}V(g)\text{-}V(\chi_m) \leq & -\bar{\eta}_1^2 - \kappa_2\bar{z}_2^\top\bar{z}_2 \\ & - 2(B_g\bar{m}_{\bar{z}_2})^\top \exp A_{f_2}^\top\tau P_1 \exp A_{f_2}\tau(A_{g_2}\bar{z}_2) \\ & + (B_g\bar{m}_{\bar{z}_2})^\top \exp A_{f_2}^\top\tau P_1 \exp A_{f_2}\tau(B_g\bar{m}_{\bar{z}_2})\end{aligned} \tag{4.54}$$

Let $Q = \exp A_{f_2}^\top\tau P_1 \exp A_{f_2}\tau$, then applying Young's inequality on the third term such that

$$\begin{aligned}\bar{m}_{\bar{z}_2}^\top B_g^\top QA_{g_2}\bar{z}_2 &\leq \frac{1}{2\epsilon_2}\Big(\bar{m}_{\bar{z}_2}^\top B_g^\top QA_{g_2}\Big)^\top\Big(\bar{m}_{\bar{z}_2}^\top B_g^\top QA_{g_2}\Big) \\ &\quad + \frac{\epsilon_2}{2}\bar{z}_2^\top\bar{z}_2 \\ &\leq \frac{1}{2\epsilon_2}\Big|\big(B_g^\top QA_{g_2}\big)\big(B_g^\top QA_{g_2}\big)^\top\Big|\bar{m}_{\bar{z}_2}^\top\bar{m}_{\bar{z}_2} \\ &\quad + \frac{\epsilon_2}{2}\bar{z}_2^\top\bar{z}_2\end{aligned}$$

where $\epsilon_2 > 0$, we then have

$$\begin{aligned} V(g)\text{-}V(\chi_m) \leq & -\bar{\eta}_1^2 - \kappa_2 \bar{z}_2^\top \bar{z}_2 \\ & -\Big(\frac{1}{2\epsilon_2}|\big(B_g^\top Q A_{g_2}\big)\big(B_g^\top Q A_{g_2}\big)^\top|\bar{m}_{\bar{z}_2}^\top \bar{m}_{\bar{z}_2} \\ & + \frac{\epsilon_2}{2}\bar{z}_2^\top \bar{z}_2\Big) + \bar{m}_{\bar{z}_2} B_g^\top Q B_g \bar{m}_{\bar{z}_2} \\ \leq & -\bar{\eta}_1^2 - \big(\kappa_2 + \frac{\epsilon_2}{2}\big)\bar{z}_2^\top \bar{z}_2 + \big(|B_g^\top Q B_g| \\ & -\frac{1}{2\epsilon_2}|(B_g^\top Q A_{g_2})(B_g^\top Q A_{g_2})^\top|\big)\bar{m}_{\bar{z}_2}^\top \bar{m}_{\bar{z}_2} \end{aligned} \tag{4.55}$$

by noting $|A_{g_2}|, |B_g| \leq \gamma \lambda_{max}(\bar{\mathcal{L}})$ let

$$\kappa_{\bar{m}_2} = \big(\lambda_{max}(\bar{\mathcal{L}})\big)^2 \max_{v\in[0,T_2]}\Big\{\lambda_{max}\big(\exp A_{f_2}^\top v P_1 \exp A_{f_2} v\big)\Big\}$$

then we let $\epsilon_2 = \kappa_2$ and

$$\begin{aligned} V(g) - V(\chi_m) \leq & -\bar{\eta}_1^2 - \big(\kappa_2 + \frac{\kappa_2}{2}\big)\bar{z}_2^\top \bar{z}_2 \\ & + \big(\gamma^2 \kappa_{\bar{m}_2} - \frac{1}{2\kappa_2}\gamma^4 \kappa_{\bar{m}_2}^2\big)\bar{m}_{\bar{z}_2}^\top \bar{m}_{\bar{z}_2} \end{aligned}$$

now let $\tilde{\kappa}_{\bar{m}_2} = \big(\gamma^2 \kappa_{\bar{m}_2} - \frac{1}{2\kappa_2}\gamma^4 \kappa_{\bar{m}_2}^2\big)$ then at jumps one has

$$V(g) - V(\chi_m) \leq -\bar{\kappa}_2(|\bar{\eta}_1|^2 + |\bar{z}_2|^2) + \tilde{\kappa}_{\bar{m}_2}|\bar{m}_{\bar{z}_2}|^2 \tag{4.56}$$

where $\bar{\kappa}_2 = \max\big\{1, \frac{3\kappa_2}{2}\big\}$. Now, recall from (4.45) in the proof of Theorem 4.2.6,

$$-(|\bar{\eta}_1|^2 + |\bar{z}_2|^2) \leq -\frac{1}{\alpha_2}V(\chi_\varepsilon) + |\bar{w}|^2 \tag{4.57}$$

by then plugging (4.45) in to (B.32) one has

$$\begin{aligned} V(g) - V(\chi_m) \leq & \frac{3\kappa_2}{2}\Big(-\frac{1}{\alpha_2}V(\chi_\varepsilon) + |\bar{w}|^2\Big) + \tilde{\kappa}_{\bar{m}_2}|\bar{m}_{\bar{z}_2}|^2 \\ \leq & -\frac{3\kappa_2}{2\alpha_2}V(\chi_\varepsilon) + \frac{3\kappa_2}{2}|\bar{w}|^2 + \tilde{\kappa}_{\bar{m}_2}|\bar{m}_{\bar{z}_2}|^2 \end{aligned}$$

then at jumps one has

$$V(g) \leq \Big(1 - \frac{3\kappa_2}{2\alpha_2}\Big)V(\chi_\varepsilon) + \frac{3\kappa_2}{2}|\bar{w}|^2 + \tilde{\kappa}_{\bar{m}_2}|\bar{m}_{\bar{z}_2}|^2$$

Noting $\langle \nabla V(\chi_\varepsilon), \tilde{f}(\chi_\varepsilon)\rangle \leq \bar{\kappa} V(\chi_\varepsilon)$, one can then pick a solution with initial conditions $\phi(0,0) \in \tilde{C}_m \cup \tilde{D}_m$ and find the trajectory of $V(t,j)$ is bounded as follows

$$\begin{aligned} V(t,j) \leq & \exp\big(\bar{\kappa}\, T_2\big)\Big(\exp\big(\bar{\kappa}\, T_2\big)\Big(1 - \frac{3\kappa_2}{2\alpha_2}\Big)\Big)^j V(0,0) \\ & + \frac{3\kappa_2}{2}\exp\big(\bar{\kappa}\, T_2\big)\sup_{(t,j)\in \mathrm{dom}\phi}|\bar{w}(t,j)|^2 \\ & + \tilde{\kappa}_{\bar{m}_2}\exp\Big(\frac{\kappa}{2\epsilon_2}T_2\Big)\sup_{(t,j)\in \mathrm{dom}\phi}|\bar{m}_{\bar{z}_2}|^2 \end{aligned}$$

□

4.4.2 Robustness to Perturbations on Internal Clock Drift

In this section, we consider a disturbance $m_{\tau_i^*} \in \mathbb{R}$, $i \in \mathcal{V}$ added to the output of the internal clock. Let $y_i^{\tau^*} := \tau_i^* + m_{\tau_i^*}$, $i \in \mathcal{V}$, define the perturbed internal clock output. Then the dynamics of the original estimation system in (4.9) under this disturbance becomes

$$\begin{aligned} &\dot{\hat{\tau}}_i = \hat{a}_i - (\hat{\tau}_i - y_i^{\tau^*}), \quad \dot{\hat{a}}_i = -\mu(\hat{\tau}_i - y_i^{\tau^*}) \quad \tau \in [0, T_2] \\ &\hat{\tau}_i^+ = \hat{\tau}_i, \qquad\qquad \hat{a}_i^+ = \hat{a}_i \qquad\qquad \tau = 0 \end{aligned} \tag{4.58}$$

In error coordinates $\varepsilon_{\hat{a}_i} = a_i - \hat{a}_i$, $\varepsilon_{\tau_i} = \hat{\tau}_i - \tau_i^*$, this leads to

$$\begin{aligned} &\dot{\varepsilon}_{\tau_i} = -\varepsilon_{\tau_i} - \varepsilon_{a_i} + m_{\tau_i^*}, \ \dot{\varepsilon}_{\hat{a}_i} = \mu\varepsilon_{\tau_i} - \mu m_{\tau_i^*} \qquad\qquad \tau \in [0, T_2] \\ &\varepsilon_{\tau_i}^+ = \varepsilon_{\tau_i}, \qquad\qquad \varepsilon_{a_i}^+ = \varepsilon_{a_i} \qquad\qquad \tau = 0 \end{aligned}$$

Similar to the result presented in Proposition 4.3.7, for the estimation sub-system we will consider the same reduction $\widetilde{\mathcal{H}}_{\varepsilon_r}$ that now captures the perturbation. Recall the coordinate transformations $\bar{\varepsilon}_a = \mathcal{T}^{-1}\varepsilon_a$ and $\bar{\varepsilon}_\tau = \mathcal{T}^{-1}\varepsilon_\tau$ for the respective internal clock and parameter estimation errors. Moreover, recall $\bar{w} = (\bar{w}_1, \bar{w}_2)$ where $\bar{w}_1 = (\bar{\varepsilon}_{a_1}, \bar{\varepsilon}_{\tau_1})$ and $\bar{w}_2 = (\bar{\varepsilon}_{a_2}, \ldots, \bar{\varepsilon}_{a_n}, \bar{\varepsilon}_{\tau_2}, \ldots, \bar{\varepsilon}_{\tau_n})$. Let $\bar{m}_{\tau^*} = \mathcal{T}^{-1} m_{\tau^*}$ and $\bar{q} = (\bar{q}_1, \bar{q}_2)$ where $\bar{q}_1 = (\bar{m}_{\tau_1^*}, \bar{m}_{\tau_1^*})$ and $\bar{q}_2 = (\bar{m}_{\tau_2^*}, \ldots, \bar{m}_{\tau_n^*}, \bar{m}_{\tau_2^*}, \ldots, \bar{m}_{\tau_n^*})$. Now, consider the reduced coordinates $\chi_{m_r} := (\bar{w}_1, \bar{w}_2, \tau) \in \mathbb{R}^n \times \mathbb{R}^n \times [0, T_2] =: \mathcal{X}_\varepsilon$. The data of this reduced system is given by $\widetilde{\mathcal{H}}_{m_r} = (\widetilde{C}_\varepsilon, \widetilde{f}_\varepsilon, \widetilde{D}_\varepsilon, \widetilde{G}_\varepsilon)$ where

$$\widetilde{f}_{mr}(\chi_{mr}) := \begin{bmatrix} A_{f_3}\bar{w}_1 \\ A_{f_4}\bar{w}_2 \\ -1 \end{bmatrix} + \begin{bmatrix} B_{m_1}\bar{q}_1 \\ B_{m_2}\bar{q}_2 \\ 0 \end{bmatrix} \quad \forall \chi_{mr} \in \widetilde{C}_{mr}$$

$$\widetilde{G}_{mr}(\chi_{mr}) := \begin{bmatrix} \bar{w}_1 \\ \bar{w}_2 \\ [T_1, T_2] \end{bmatrix} \qquad\qquad \forall \chi_{mr} \in \widetilde{D}_{mr}$$

where $\tilde{C}_{m_r} := \mathcal{X}_\varepsilon$, $\tilde{D}_{m_r} := \{\chi_m \in \mathcal{X}_\varepsilon : \tau = 0\}$, and

$$B_{m_1} = \begin{bmatrix} \mu & 0 \\ 0 & 1 \end{bmatrix}, \ B_{m_2} = \begin{bmatrix} \mu I & 0 \\ 0 & I \end{bmatrix}$$

Theorem 4.4.3. *If there exists a positive scalar μ and positive definite symmetric matrices P_2, P_3 such that (4.13) and (4.14) hold, the hybrid system $\widetilde{\mathcal{H}}_{mr}$ with input $\bar{m}_{\tau^*}$ is ISS with respect to $\widetilde{\mathcal{A}}_{\varepsilon_r}$.*

Proof. Since the matrices A_{f_3} and A_{f_4} are Hurwitz and the states $\bar{w}_1$ and $\bar{w}_2$ do not jump, we can estimation system as a continuous time system and write the solution explicitly for the states $\bar{w}_1$ and $\bar{w}_2$.

$$\begin{aligned}\phi_{\bar{w}_1}(t,j) = &\exp(A_{f_3}(t-0))\phi_{\bar{w}_1}(0,0) \\ &+ \int_0^t \exp(A_{f_3}(t-s))B_{m_1}\bar{q}_1(s)ds\end{aligned} \tag{4.59}$$

and

$$\begin{aligned}\phi_{\bar{w}_2}(t,j) = &\exp(A_{f_4}(t-0))\phi_{\bar{w}_2}(0,0) \\ &+ \int_0^t \exp(A_{f_4}(t-s))B_{m_2}\bar{q}_2(s)ds\end{aligned} \tag{4.60}$$

then by bounding $|\exp(A_{f_3}(t-0))| \leq \rho_1 \exp -\lambda_1(t-0)$ and $|\exp(A_{f_4}(t-0))| \leq \rho_2 \exp -\lambda_2(t-0)$ one has

$$\begin{aligned}|\phi_{\bar{w}_1}(t,j)| &\leq \rho_1 \exp -\lambda_1(t-0)|\phi_{\bar{w}_1}(0,0)| \\ &\quad + \int_0^t \rho_1 \exp -\lambda_1(t-s)|B_{m_1}||\bar{q}_1(s)|ds \\ &\leq \rho_1 \exp -\lambda_1(t-0)|\phi_{\bar{w}_1}(0,0)| + \frac{\rho_1|B_{m_1}|}{\lambda_1}\sup_{0\leq s\leq t}|\bar{q}_2(s)|\end{aligned} \tag{4.61}$$

and

$$\begin{aligned}|\phi_{\bar{w}_2}(t,j)| &\leq \rho_2 \exp -\lambda_2(t-0)|\phi_{\bar{w}_2}(0,0)| \\ &\quad + \int_0^t \rho_2 \exp -\lambda_2(t-s)|B_{m_2}||\bar{q}_2(s)|ds \\ &\leq \rho_2 \exp -\lambda_2(t-0)|\phi_{\bar{w}_2}(0,0)| + \frac{\rho_2|B_{m_2}|}{\lambda_2}\sup_{0\leq s\leq t}|\bar{q}_2(s)|\end{aligned} \tag{4.62}$$

□

4.4.3 Robustness to Error on σ

In this section, we consider a disturbance on σ^* to capture the scenario where σ^* is not precisely known, i.e., $\sigma_i \neq \sigma^*$. Let $\varepsilon_{\sigma_i} = \sigma_i - \sigma^*$ represent the error between the

injected and the ideal clock rate. Treating ε_σ as a perturbation to the system $\mathcal{H}_\varepsilon$, one has

$$\dot{x}_\varepsilon = \begin{bmatrix} \eta + \varepsilon_a \\ h\eta \\ \mu\varepsilon_\tau \\ -\varepsilon_\tau - \varepsilon_a \\ -1 \end{bmatrix} + \begin{bmatrix} \varepsilon_\sigma \\ 0 \\ 0 \\ 0 \\ 0 \end{bmatrix} \qquad \forall x_\varepsilon \in C_\varepsilon$$

$$x_\varepsilon^+ \in \big(e, -\gamma\mathcal{L}e, \varepsilon_a, \varepsilon_\tau, [T_1, T_2]\big) \quad \forall x_\varepsilon \in D_\varepsilon$$

To show how the perturbation affects $\widetilde{\mathcal{H}}_\varepsilon$, let $\bar{\varepsilon}_\sigma = \mathcal{T}^{-1}\varepsilon_\sigma$, then let $\bar{m}_\sigma = (\bar{m}_{\sigma_1}, \bar{m}_{\sigma_2})$ where $\bar{m}_{\sigma_1} = \bar{\varepsilon}_{\sigma_1}$ and $\bar{m}_{\sigma_2} = (\bar{\varepsilon}_{\sigma_2}, \ldots, \bar{\varepsilon}_{\sigma_n})$.

We define this perturbed hybrid system $\widetilde{\mathcal{H}}_{m_\sigma}$ with state vector $\chi_{m_\sigma} := (\bar{z}_1, \bar{z}_2, \bar{w}_1, \bar{w}_2, \tau) \in \mathcal{X}_\varepsilon$. Its dynamics are given by the new system $\widetilde{\mathcal{H}}_{m_\sigma} = (\tilde{C}_{m_\sigma}, \tilde{f}_{m_\sigma}, \tilde{D}_{m_\sigma}, \tilde{G}_{m_\sigma})$ with data $\tilde{f}_{m_\sigma}(\chi_{m_\sigma})$ for each $\chi_{m_\sigma} \in \tilde{C}_{m_\sigma} := \mathcal{X}_\varepsilon$ and $\tilde{G}_{m_\sigma}(\chi_{m_\sigma})$ for each $\chi_{m_\sigma} \in \tilde{D}_{m_\sigma} := \{\chi_{m_\sigma} \in \mathcal{X}_\varepsilon : \tau = 0\}$ where

$$\widetilde{f}_{m_\sigma}(\chi_{m_\sigma}) := \begin{bmatrix} A_{f_1}\bar{z}_1 + B_{f_1}\bar{w}_1 \\ A_{f_2}\bar{z}_2 + B_{f_2}\bar{w}_2 \\ A_{f_3}\bar{w}_1 \\ A_{f_4}\bar{w}_2 \\ -1 \end{bmatrix} + \begin{bmatrix} \bar{m}_{\sigma_1} \\ \bar{m}_{\sigma_2} \\ 0 \\ 0 \\ 0 \end{bmatrix}$$

$$\widetilde{G}_{m_\sigma}(\chi_{m_\sigma}) := \Big[[A_{g_1}\bar{z}_1]^\top, \quad [A_{g_2}^\top\bar{z}_2]^\top, \quad \bar{w}_1^\top, \quad \bar{w}_2^\top, \quad [T_1, T_2]\Big]^\top$$

Theorem 4.4.4. *Given a strongly connected digraph $\mathcal{G}$, if the parameters $T_2 \geq T_1 > 0$, $\mu > 0$, $h \in \mathbb{R}$, $\gamma > 0$, and positive definite symmetric matrices P_1, P_2, and P_3 are such that (4.15) and (4.16) hold, the hybrid system $\widetilde{\mathcal{H}}_{m_\sigma}$ with input $\bar{m}_\sigma$ is ISS with respect to $\widetilde{\mathcal{A}}_\varepsilon$ given in (4.29).*

The proof of this result largely follows the same approach used in the proof of Theorem 4.4.2, namely, a Lyapunov analysis using the function candidate V in (4.36). Since the disturbance is present during flows, we show that the derivative of V can be upper bounded resulting in a bounded disturbance in V when evaluated along a given solution to $\widetilde{\mathcal{H}}_{m_\sigma}$; see [22] for more details.

Proof. Consider the same Lyapunov function candidate from the proof of Theorem 4.2.6 expressed for χ_{m_σ}

$$V(\chi_{m_\sigma}) = V_1(\chi_{m_\sigma}) + V_2(\chi_{m_\sigma}) + V_{\varepsilon r}(\chi_{m_\sigma})$$

The contribution from the perturbation only affects the system during flows. For each $\chi_{m_\sigma} \in \tilde{C}_{m_\sigma}$ the change in V is given by

$$\begin{aligned}\langle \nabla V(\chi_{m_\sigma}), \tilde{f}_{m_\sigma}(\chi_{m_\sigma})\rangle \leq 2\bar{z}_2^\top \exp A_{f_2}^\top \tau P_1 \exp A_{f_2}\tau(B_{f_2}\bar{w}_2 + \bar{m}_{\sigma_2}) \\ + \bar{w}_1^\top (P_1 A_{f_3} + A_{f_3}^\top P_1)\bar{w}_1 \\ + \bar{w}_2^\top (P_2 A_{f_4} + A_{f_4}^\top P_2)\bar{w}_2\end{aligned}$$

From conditions (4.13) and (4.14), let $P_2 A_{f_3} + A_{f_3}^\top P_2 < -\beta_1 I$ and $P_3 A_{f_4} + A_{f_4}^\top P_3 < -\beta_2 I$ then one has

$$\begin{aligned}\langle \nabla V(\chi_{m_\sigma}), \tilde{f}_{m_\sigma}(\chi_{m_\sigma})\rangle \leq \kappa_1 |\bar{z}_2||\bar{w}_2| + \frac{\kappa_1}{|B_{f_2}|}|\bar{z}_2||\bar{m}_{\sigma_2}| \\ - \beta_1|\bar{w}_1|^2 - \beta_2|\bar{w}_2|^2\end{aligned} \tag{4.63}$$

then applying Young's equality to the first and second terms one has

$$\begin{aligned}\langle \nabla V(\chi_{m_\sigma}), \tilde{f}_{m_\sigma}(\chi_{m_\sigma})\rangle &\leq \frac{\kappa_1}{2\epsilon}|\bar{z}_2|^2 + \frac{\kappa_1\epsilon}{2}|\bar{w}_2|^2 + \frac{\kappa_1}{2\rho|B_{f_2}|}|\bar{z}_2|^2 \\ &\quad + \frac{\kappa_1\rho}{2|B_{f_2}|}|\bar{m}_{\sigma_2}|^2 - \beta_1|\bar{w}_1|^2 - \beta_2|\bar{w}_2|^2 \\ &\leq \Big(\frac{\kappa_1}{2\epsilon} + \frac{\kappa_1}{2\rho|B_{f_2}|}\Big)|\bar{z}_2|^2 \\ &\quad + \Big(\frac{\kappa_1\epsilon}{2} - \beta_2\Big)|\bar{w}_2|^2 - \beta_1|\bar{w}_1|^2 \\ &\quad + \frac{\kappa_1\rho}{2|B_{f_2}|}|\bar{m}_{\sigma_2}|^2\end{aligned}$$

Since $|B_{f_2}| = 1$ then

$$\begin{aligned}\langle \nabla V(\chi_{m_\sigma}), \tilde{f}_{m_\sigma}(\chi_{m_\sigma})\rangle &\leq \tilde{\kappa}\big(|\bar{z}_2|^2 + |\bar{w}_1|^2 + |\bar{w}_2|^2\big) \\ &\quad + \frac{\kappa_1\rho}{2}|\bar{m}_{\sigma_2}|^2 \\ &\leq \tilde{\kappa}V(\chi_\varepsilon) + \frac{\kappa_1\rho}{2}|\bar{m}_{\sigma_2}|^2\end{aligned} \tag{4.64}$$

where $\tilde{\kappa} = \max\Big\{\frac{\kappa_1}{2\epsilon} + \frac{\kappa_1}{2\rho}, \Big(\frac{\kappa_1\epsilon}{2} - \beta_2\Big)\Big\}$ and $\epsilon, \rho > 0$. Since the perturbation does not affect the system at jumps then, recall from the proof of Theorem 4.2.6 that, across jumps for each $\chi_{m_\sigma} \in \tilde{D}_{m_\sigma}$ and $g \in \tilde{G}_{m_\sigma}$ one has

$$V(g) - V(\chi_{m_\sigma}) \leq -\bar{\eta}_1^2 + \bar{z}_2^\top \Big(A_{g_2}^\top \exp A_{f_2}^\top v P_1 \exp A_{f_2} v A_{g_2} - P_1\Big)\bar{z}_2$$

leading to the following bound

$$V(g) \leq \Big(1 - \frac{\bar{\kappa}_2}{\alpha_2}\Big)V(\chi_\varepsilon) + \bar{\kappa}_2|\bar{w}|^2$$

from (4.46). Then a general bound for the Lyapunov trajectory is given by

$$V(t,j) \leq \exp\left(\tilde{\kappa}T_2\right)\left(\exp\left(\tilde{\kappa}T_2\right)\left(1-\frac{\bar{\kappa}_2}{\alpha_2}\right)\right)^j V(0,0)$$
$$+ \bar{\kappa}_2 \exp\left(\bar{\kappa}T_2\right)\sup_{(t,j)\in \mathrm{dom}\phi}|\bar{w}(t,j)|^2$$
$$+ \frac{\kappa_1 \rho}{2}\int_0^t \exp\left(\tilde{\kappa}(t-\tau)\right)|\bar{m}_{\sigma_2}|^2$$

□

4.4.4 Noise on the communication and clock rate reference σ^* with aperiodic communication events

Example 4.4.5. *In this example we demonstrate the system $\mathcal{H}$ robustness to noise on the communication channel and the clock rate reference σ^*. Consider the same system presented in the example following Theorem 4.2.6. Figure 4.2 shows ISS for the trajectories of the errors $e_i - e_k$ for the components $i \in \{1,2,3,4,5\}$ of a solution ϕ for the case where the system is subjected to communication noise $m_{e_i}(t,j) \in (0,1)$ and noise on the clock rate reference $m_{\sigma_i^*}(t,j) \in (0.85, 1.15)$ for all $(t,j) \in \mathrm{dom}\phi$, respectively. Moreover, after the respective transient period for each case, the norm of the relative error $|e_i - e_k|$ for each solution converges to an average value of* 0.0229 *when subjected to noise $m_{\sigma_i^*}$ and* 0.0549 *for noise m_{e_i}.*

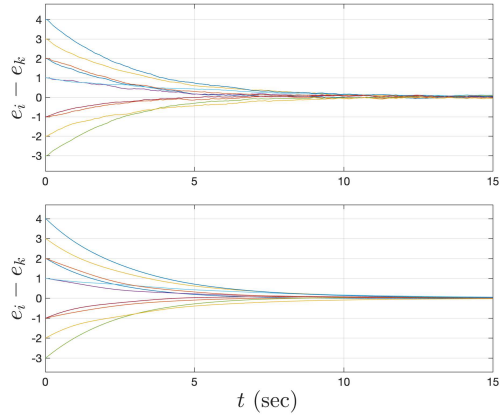

Figure 4.2: (top) The trajectories of the errors $e_i - e_k$ for the components $i \in \{1,2,3,4,5\}$ of a solution ϕ for the case where the system is subjected to communication noise m_{e_i} (top) and noise on the clock rate reference $m_{\sigma_i^*}$ (bottom).

4.5 Comparisons

In this section we compare our algorithm to several contemporary consensus-based clock synchronization algorithms from the literature through a numerical example. In particular, we consider a four agent setting and simulate each algorithm presented in [25] (PI-Consensus), [26] (RandSync), and [1] (Average TimeSync) to our hybrid algorithm HyNTP as in (4.9). We have restricted our comparison to these algorithms due to their shared assumptions on the underlying communication graph being strongly connected. Our first example considers the nominal case of zero noise and a fixed communication event period. The next example also considers the nominal case but with aperiodic communication events. We then present an example where the systems are subjected to communication noise with aperiodic communication. Our final example considers the case of noise on the clock rate while also being subjected to aperiodic communication events.

4.5.1 Nominal case with fixed communication event period

Consider $N = 4$ agents with clock dynamics as in (6.3) and (4.2) over a strongly connected graph with the following adjacency matrix

$$\mathcal{G}_A = \begin{pmatrix} 0 & 1 & 0 & 1 \\ 1 & 0 & 1 & 0 \\ 0 & 1 & 0 & 1 \\ 1 & 0 & 1 & 0 \end{pmatrix} \tag{4.65}$$

and a dwell time between communication events $T = 0.15$. The initial conditions for the clock rates a_i and clock values τ_i for each $i \in \mathcal{V}$ has been randomly chosen within the intervals $(0.5, 1.5)$ and $(0, 200)$, respectively.

For the *HyNTP* algorithm, we let $T_1 = T_2 = T = 0.15$, and $\sigma^* = 1$, then it can be found that the parameters $h = -2$, $\mu = 3$, $\gamma = 0.06$ and $\epsilon = 1.607$ with suitable matrices P_1, P_2, and P_3 satisfy conditions (4.15) and (4.16) in Theorem 4.2.6 with $\bar{\kappa}_1 = 6.86$, $\kappa_1 = 22.98$, $\bar{\kappa}_2 = 1$, and $\alpha_2 = 16.93$.

Figure 4.3 shows the trajectories of $e_i - e_k$, ε_{a_i} for components $i \in \{1, 2, 3, 4, 5\}$ of a solution ϕ for the case where $\sigma = \sigma^*$

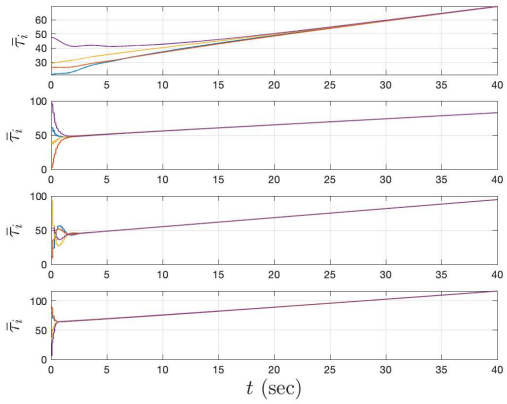

Figure 4.3: The evolution of the trajectories of the adjustable clocks $\bar{\tau}_i$ for each clock synchronization algorithm. From top to bottom, *HyNTP*, *Average TimeSync*, *PI-Consensus*, and *RandSync*.

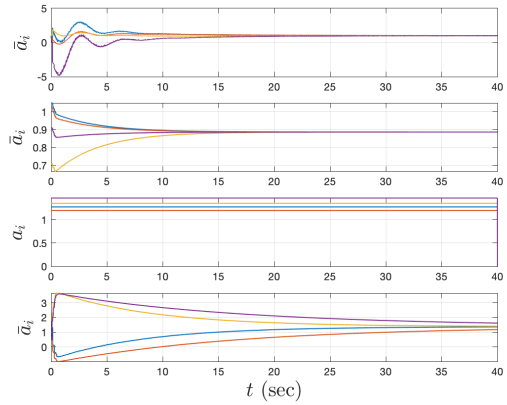

Figure 4.4: The evolution of the trajectories of the adjustable clock rates $\bar{a}_i$ for each clock synchronization algorithm. From top to bottom, *HyNTP*, *Average TimeSync*, *PI-Consensus*, and *RandSync*.

4.5.2 Nominal case with aperiodic communication events

Consider the same $N = 4$ agents with clock dynamics as in (6.3) and (4.2) over a strongly connected graph with the following adjacency matrix

$$\mathcal{G}_A = \begin{pmatrix} 0 & 1 & 0 & 1 \\ 1 & 0 & 1 & 0 \\ 0 & 1 & 0 & 1 \\ 1 & 0 & 1 & 0 \end{pmatrix}$$

and aperiodic communication events such that successive communications events are lower and upper bounded by $T_1 = 0.1$ and $T_2 = 0.5$, respectively. The initial conditions for the clock rates a_i and clock values τ_i for each $i \in \mathcal{V}$ has been randomly chosen within the intervals $(0.5, 1.5)$ and $(0, 200)$, respectively.

For the *HyNTP* algorithm, setting $\sigma^* = 1$, it can be found that the parameters $h = -2$, $\mu = 9$, $\gamma = 0.06$ and $\epsilon = 4.752$ with suitable matrices P_1, P_2, and P_3 satisfy conditions (4.15) and (4.16) in Theorem 4.2.6 with $\bar{\kappa}_1 = 2.02$, $\kappa_1 = 19.22$, $\bar{\kappa}_2 = 1$, and $\alpha_2 = 44.03$.

Figure 4.1 shows the trajectories of $e_i - e_k$, ε_{a_i} for components $i \in \{1, 2, 3, 4, 5\}$ of a solution ϕ for the case where $\sigma = \sigma^*$.

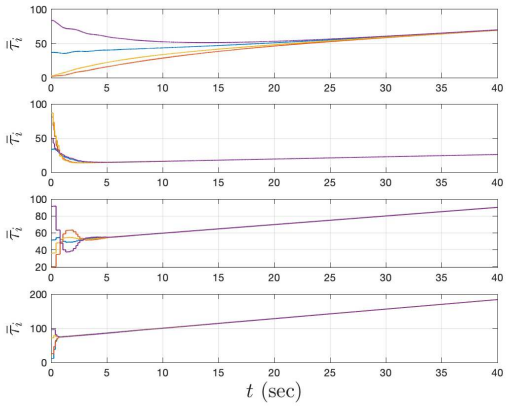

Figure 4.5: The evolution of the trajectories of the adjustable clocks $\bar{\tau}_i$ for each clock synchronization algorithm. From top to bottom, *HyNTP*, *Average TimeSync*, *PI-Consensus*, and *RandSync*.

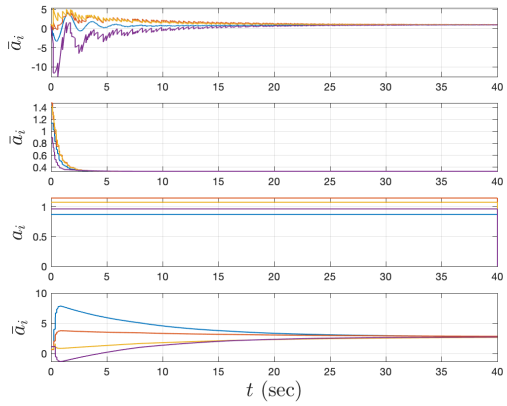

Figure 4.6: The evolution of the trajectories of the adjustable clock rates $\bar{a}_i$ for each clock synchronization algorithm. From top to bottom, *HyNTP*, *Average TimeSync*, *PI-Consensus*, and *RandSync*.

4.5.3 Communication noise with aperiodic communication events

Consider the same $N = 4$ agents with clock dynamics as in (6.3) and (4.2) over a strongly connected graph with the adjacency matrix given in (4.65) and aperiodic communication events such that successive communications events are lower and upper bounded by $T_1 = 0.1$ and $T_2 = 0.5$, respectively. The initial conditions for the clock rates a_i and clock values τ_i for each $i \in \mathcal{V}$ has been randomly chosen within the intervals $(0.5, 1.5)$ and $(0, 200)$, respectively. Moreover, consider the case where the system is subjected to a communication noise $m_{\tau_i}(t, j) \in (0, 1)$ on the clock measurements.

For the *HyNTP* algorithm, setting $\sigma^* = 1$, it can be found that the parameters $h = -2$, $\mu = 9$, $\gamma = 0.06$ and $\epsilon = 4.752$ with suitable matrices P_1, P_2, and P_3 satisfy conditions (4.15) and (4.16) in Theorem 4.2.6 with $\bar{\kappa}_1 = 2.02$, $\kappa_1 = 19.22$, $\bar{\kappa}_2 = 1$, and $\alpha_2 = 44.03$.

4.6 Summary

In this chapter, we modeled a network of clocks with aperiodic communication that utilizes a distributed hybrid controller to achieve synchronization, using the hybrid systems framework. Results were given to guarantee and show synchronization of the timers, exponentially fast. Numerical results validating the exponentially fast convergence of the

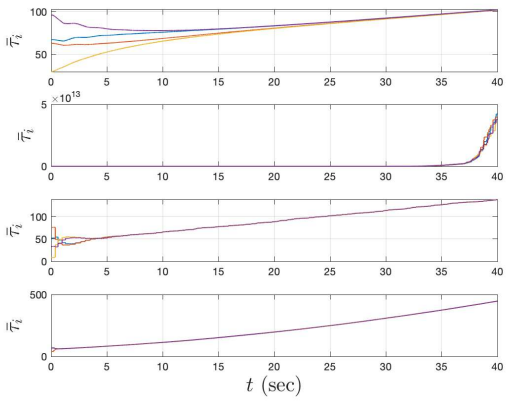

Figure 4.7: The evolution of the trajectories of the adjustable clocks $\bar{\tau}_i$ for each clock synchronization algorithm. From top to bottom, *HyNTP*, *Average TimeSync*, *PI-Consensus*, and *RandSync*.

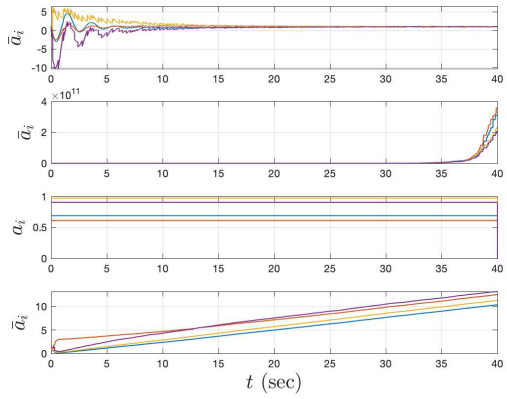

Figure 4.8: The evolution of the trajectories of the adjustable clock rates $\bar{a}_i$ for each clock synchronization algorithm. From top to bottom, *HyNTP*, *Average TimeSync*, *PI-Consensus*, and *RandSync*.

timers were also given. Numerical results were also provided to demonstrate performance against a similar class of clock synchronization algorithms.

Chapter 5

An Adaptive Hybrid Control Algorithm for Sender-Receiver Clock Synchronization

In this chapter, we present a hybrid systems approach to sender-receiver synchronization with an, online, adaptive method to synchronize the clock rates. We show that our algorithm exponentially synchronizes a pair of clocks connected over a network while preserving the messaging protocols and network dynamics of traditional sender-receiver algorithms.

Our proposed solution provides a Lyapunov-based convergence analysis to a set in which the clocks are synchronized with sufficient conditions ensuring their synchronization. In particular, the main contributions include:

- In Section 5.3, a hybrid system model of the sender-receiver synchronization algorithm using the framework proposed in [4] is presented. The proposed model captures the continuous dynamics of the clock states and the hybrid dynamics of the networking protocol by which the timing messages are exchanged for a pair of system nodes to achieve synchronization.

- In Section 5.3.3, we show, through the satisfaction of some basic conditions on the system model, that the algorithm is finite-time attractive to a forward invariant set of interest that represents the correct initialization of the algorithm.

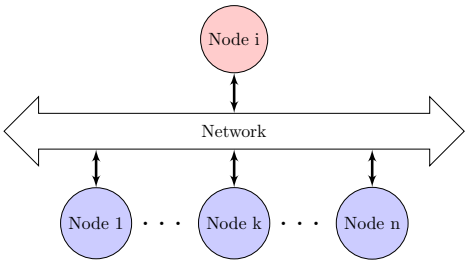

Figure 5.1: General architecture of the system under consideration.

- In Section 5.4, we provide sufficient conditions on the algorithm parameters to show asymptotic attractivity of the hybrid system to a set of interest representing synchronization of the clocks from the initialization set. Furthermore, we characterize the bound for solution trajectories to the systems in terms of parameters that can be used for algorithm design.

- In Section 5.5, we present a multi-agent extension of the proposed model to cover the case of synchronizing the nodes on an n-node network. The feasibility of this multi-agent model is validated with a numerical example of the simulated system.

Unlike the existing algorithms of NTP, PTP, and TPSN, we emphasize to the reader that previous analyses on sender-receiver synchronization have only provided results to their feasibility and that the literature lacks formal results that characterize its performance in a dynamical system setting.

5.1 Motivation for An Adaptive Clock Synchronization Algorithm

5.1.1 Preliminaries on the Sender-Receiver Algorithm

In a network of n nodes, consider nodes i and k in a sender-receiver hierarchy where Node i is a designated reference or parent agent of a synchronizing child agent Node k, see Figure 5.1. Each node has an attached internal clock $\tau_i, \tau_k \in \mathbb{R}$ whose dynamics are given by

$$\begin{aligned} \dot{\tau}_i &= a_i \\ \dot{\tau}_k &= a_k \end{aligned} \tag{5.1}$$

where a_i,$a_k \in \mathbb{R}$ denote the respective clock rates.[1] At times t_j for $j \in \mathbb{N}$ (with $t_0 = 0$), nodes i and k exchange timing measurements with embedded timestamps

$$\begin{aligned} T_j^i &:= \tau_i(t_j) \\ T_j^k &:= \tau_k(t_j) \end{aligned} \tag{5.2}$$

which, integrating (5.1), are equal to

$$\tau_i(t_j) = a_i t_j + \tau_i(0)$$

$$\tau_k(t_j) = a_k t_j + \tau_k(0)$$

respectively. Furthermore, $\tau_i(0)$ and $\tau_k(0)$ represent the clock offset from the initial reference time $t = 0$. The goal is to then synchronize the internal clock of Node k to that of Node i using the exchanged timing measurements given in (5.2).

Before introducing the mechanics of the sender-receiver algorithm, we refer the reader to a visual model of the algorithm in Figure 5.2 as a reference. By assuming the sequence of time instants $\{t_j\}_{j=1}^{\infty}$ is strictly increasing and unbounded, the sender-receiver synchronization algorithm as described in the literature (see [5], [27], and [28]) is given as follows:

(P1) At time t_j, Node i broadcasts a synchronization message with its local time

$$T_j^i = a_i t_j + \tau_i(0)$$

to Node k.

(P2) At time t_{j+1}, Node k receives the synchronization message and records its local time of arrival, T_{j+1}^k, given in local time at

$$T_{j+1}^k = a_k t_{j+1} + \tau_k(0)$$

(P3) At time t_{j+2}, Node k sends a response message with timestamp

$$T_{j+2}^k = a_k t_{j+2} + \tau_k(0)$$

[1] In this paper, we use the term clock rate to explicitly denote the slope of the given linear affine model of a clock. Other terms for this notion include clock drift or clock skew.

(P4) At time t_{j+3}, Node i receives the response message from Node k and records its time of arrival

$$T^i_{j+3} = a_i t_{j+3} + \tau_i(0)$$

(P5) At time t_{j+4}, Node i sends a response receipt message with timestamp

$$T^i_{j+4} = a_i t_{j+4} + \tau_i(0)$$

(P6) At time t_{j+5}, Node k receives the response message from Node i and records its time of arrival

$$T^k_{j+5} = a_k t_{j+5} + \tau_k(0)$$

and then updates its clock to synchronize with the clock of Node i using the collected timestamps T^i_j, T^k_{j+1}, T^k_{j+2}, T^i_{j+3}, and T^i_{j+4}.

Moreover, as done in the literature (see [27] and [29]), it is assumed that the time elapsed between each time instant is governed by

$$t_{j+1} - t_j = \begin{cases} d & \forall j \in \{2i+1 : i \in \mathbb{N}\}, j > 0 \\ c & \forall j \in \{2i : i \in \mathbb{N}\}, j > 0 \end{cases} \tag{5.3}$$

where $0 < c \leq d$. The constant c defines the delay associated with the residence or response time associated with message turnaround while d defines the propagation delay associated with message transmission. Figure 5.2 gives a visual representation of the exchange of timestamps between Nodes i and k against reference time t. Note that the propagation delay from Node i to Node k and vice versa is assumed to symmetric. Moreover, it is also assumed that the delay due to residence time is the same across all nodes.[2]

With the available timestamps, at times t_{j+5}, we can calculate the relative offset $\tilde{o} := \tau_i(0) - \tau_k(0)$ as follows, by first rearranging the terms in the timestamps given in

[2]Most pairwise synchronization protocols such as the Network Time Protocol (NTP), Precision Time Protocol (PTP, IEEE 1588), and the Timing-sync Protocol for Sensor Networks (TPSN) assume that the propagation delay in the message transmission from parent to child and child to parent is symmetric. If the propagation delay between the two nodes is asymmetric it introduces an error to the calculated offset correction that cannot be accounted for, see [13].

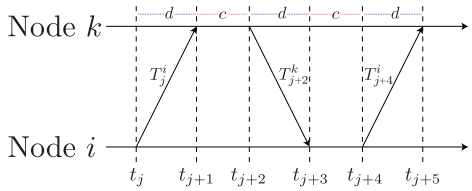

Figure 5.2: Diagram illustrating the message exchange between Nodes i and k for the synchronization algorithm.

(P1)-(P6) one has

$$\begin{aligned}
\tau_i(0) &= T_j^i - a_i t_j \\
\tau_k(0) &= T_{j+1}^k - a_k t_{j+1} \\
\tau_k(0) &= T_{j+2}^k - a_k t_{j+2} \\
\tau_i(0) &= T_{j+3}^i - a_i t_{j+3} \\
\tau_i(0) &= T_{j+4}^i - a_i t_{j+4} \\
\tau_k(0) &= T_{j+5}^k - a_k t_{j+5}
\end{aligned}$$

then we have the following expressions for the offset

$$\begin{aligned}
\tilde{o} &= \tau_i(0) - \tau_k(0) = T_j^i - a_i t_j - T_{j+1}^k + a_k t_{j+1} \\
\tilde{o} &= \tau_i(0) - \tau_k(0) = T_{j+3}^i - a_i t_{j+3} - T_{j+2}^k + a_k t_{j+2} \\
\tilde{o} &= \tau_i(0) - \tau_k(0) = T_{j+4}^i - a_i t_{j+4} - T_{j+5}^k + a_k t_{j+5}
\end{aligned}$$

rearranging terms one has

$$\begin{aligned}
T_j^i - T_{j+1}^k &= a_i t_j - a_k t_{j+1} + \tilde{o} \\
T_{j+3}^i - T_{j+2}^k &= a_i t_{j+3} - a_k t_{j+2} + \tilde{o} \\
T_{j+4}^i - T_{j+5}^k &= a_i t_{j+4} - a_k t_{j+5} + \tilde{o}
\end{aligned} \tag{5.4}$$

Now, if the clock drifts are synchronized, i.e., $a_k = a_i$, we have

$$\begin{aligned}
T_j^i - T_{j+1}^k &= a_i(t_j - t_{j+1}) + \tilde{o} \\
T_{j+3}^i - T_{j+2}^k &= a_i(t_{j+3} - t_{j+2}) + \tilde{o} \\
T_{j+4}^i - T_{j+5}^k &= a_i(t_{j+4} - t_{j+5}) + \tilde{o}
\end{aligned} \tag{5.5}$$

then by noting the bounds on the time elapsed between time instants t_j, as given in (6.5), one has

$$t_{j+1} - t_j = t_{j+3} - t_{j+2} = t_{j+5} - t_{j+4} = d \quad \forall j \in \{2i+1 : i \in \mathbb{N}\}, j > 0 \tag{5.6}$$

then by making the appropriate substitutions in (5.5) we have

$$\begin{aligned} T^i_j - T^k_{j+1} &= -a_i d + \tilde{o} \\ T^i_{j+3} - T^k_{j+2} &= a_i d + \tilde{o} \\ T^i_{j+4} - T^k_{j+5} &= -a_i d + \tilde{o} \end{aligned} \tag{5.7}$$

Since the clock rates $a_i = a_k$ and the quantity of the propagation delay d are currently unknowns to the system, we are left with a linear system of equations to solve for the offset, i.e.,

$$\tilde{o} = \frac{1}{2}\Big((T^i_j - T^k_{j+1}) + (T^i_{j+3} - T^k_{j+2})\Big) \tag{5.8}$$

To demonstrate how this solves the synchronization problem, consider the error between the clocks of nodes i and k at t_{j+5},

$$e_{ik}(t_{j+5}) = \tau_i(t_{j+5}) - \tau_k(t_{j+5})$$

at time t_{j+5} node k applies the offset correction $K_{\tilde{o}} = \tilde{o}$ as follows

$$\begin{aligned} e_{ik}(t_{j+5}) &= \tau_i(t_{j+5}) - (\tau_k(t_{j+5}) - K_{\tilde{o}}) \\ &= \big(a_i t_{j+5} + \tau_i(0)\big) - \big(a_k t_{j+5} + \tau_k(0) - (\tau_i(0) - \tau_k(0))\big) \\ &= a_i t_{j+5} - a_k t_{j+5} \\ &= 0 \end{aligned}$$

Thus, the clocks at nodes i and k synchronize for the case where the clock rates a_i and a_k are already assumed to be synchronized.

5.1.2 The Key Issue: Clock synchronization in the presence of mismatched clock rates.

With the mechanics of the sender-receiver algorithm defined, we will now outline the motivation of this paper by demonstrating the issues that arise with the algorithm and how our proposed solution addresses them.

Now, consider the following system data $a_i = 1$, $a_k = 0.8$ with $c = d = 0.5$ and the given sender-receiver algorithm with only the offset correction $K_{\tilde{o}}$ being applied. Simulating the algorithm, Figure 5.3 shows the plots of the behavior in the error of clocks and the clock rates. As depicted in the figure, the algorithm continually applies the offset correction but due to the mismatch in the clock rates, the error in the clocks fails to converge to zero. This

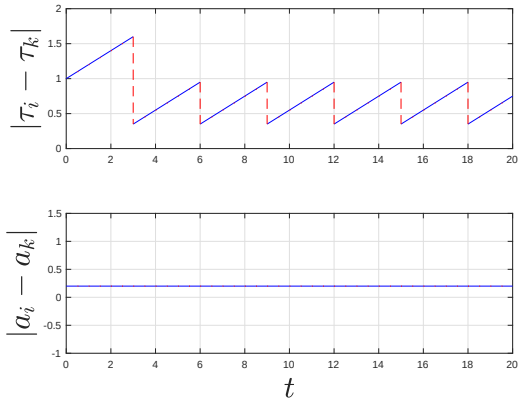

Figure 5.3: The evolution of the error in the clocks and error in the clock rates of Nodes i and k when the algorithm only applies the offset correction $K_{\tilde{o}}$.

is further evidence analytically when noting that if the clock rates are not synchronized in equation (5.4), the formula for the offset calculation in (5.8) will yield an error on the true offset $\tilde{o}$.

To mitigate the effects of the error, protocols such as NTP and IEEE 1588 utilize a variety of bespoke methods to minimize the error in clock rates including but not limited to, control of variable frequency hardware oscillators, pulse addition and deletion of the counted pulses at the hardware oscillator, and an error register to track the deviation of the error, see [11] and [28]. These methods, while suitable for industrial-grade equipment, are often expensive solutions for low-cost applications such as sensor networks. In fact, protocols such as TPSN, designed specifically for low-cost sensor networks, do not provide provisions to correct for the clock rate error, see [10].

5.1.3 Problem Formulation and Proposed Algorithm

The problem to solve consists of synchronizing the internal clock of Node k to that of Node i. More precisely, the goal is to design a hybrid algorithm that is based on exchanging timestamps and guarantees that the clock variable τ_k and the clock rate a_k of Node k are driven to synchronization with τ_i and a_i of the reference Node i, respectively. Moreover, our goal is to provide tractable design conditions that ensure attractivity of a set of interest. This problem is formally stated as follows:

Problem 5.1.1. *Given two nodes in a sender-receiver hierarchy with clocks having dynam-*

ics as in (5.1) with timestamps T_j^i, T_j^k and parameters c and d, design a hybrid algorithm such that each trajectory $t \mapsto (\tau_i(t), \tau_k(t))$ satisfies the clock synchronization property

$$\lim_{t\to\infty} |\tau_i(t) - \tau_k(t)| = 0$$

and the rate synchronization property

$$\lim_{t\to\infty} |\dot{\tau}_i(t) - \dot{\tau}_k(t)| = 0$$

Given the inability of the sender-receiver algorithm to synchronize the clocks, we propose a modification to the algorithm that incorporates an adaptive strategy to synchronize the clock rates. Consider the control law for the synchronization of the clock rate for Node k

$$K_a = \mu(T_{j+4}^i - T_j^i - T_{j+5}^k - T_{j+1}^k) \tag{5.9}$$

with $\mu > 0$ being a controllable parameter. Making the necessary substitutions one has

$$\begin{aligned} K_a &= \mu\Big(\big(a_i t_{j+4} + \tau_i(0)\big) - \big(a_i t_j + \tau_i(0)\big) \\ &\qquad - \big(a_k t_{j+5} + \tau_k(0)\big) - \big(a_k t_{j+1} + \tau_k(0)\big)\Big) \\ &= \mu\big(a_i(2c+2d) - a_k(2c+2d)\big) \\ &= \mu(2c+2d)\big(a_i - a_k\big) \end{aligned} \tag{5.10}$$

The correction K_a can then be applied to the clock dynamics of Node k at times t_{j+5} as follows:

$$a_k^+ = a_k + K_a = a_k + \mu(2c+2d)\big(a_i - a_k\big) \tag{5.11}$$

Observe that this strategy operates under the existing assumptions of the sender-receiver algorithm (symmetric propagation delays and residence times) and does not rely on any additional information that is not already available via the exchanged timing messages. Moreover, since it exploits the integrator dynamics of the system, the computation costs to calculate K_a are minimal. In this next example, we demonstrate the proposed strategy under the same scenario of mismatched skews between Nodes i and k.

To illustrate, the capabilities of the algorithm outlined above, consider the same system data as in Section 5.1, namely, $a_i = 1$, $a_k = 0.8$ with $c = d = 0.5$ and the given sender-receiver algorithm now with both the offset correction $K_{\tilde{o}}$ and clock rate correction K_a being applied. In Figure 5.4, two sets of error plots are presented for two different

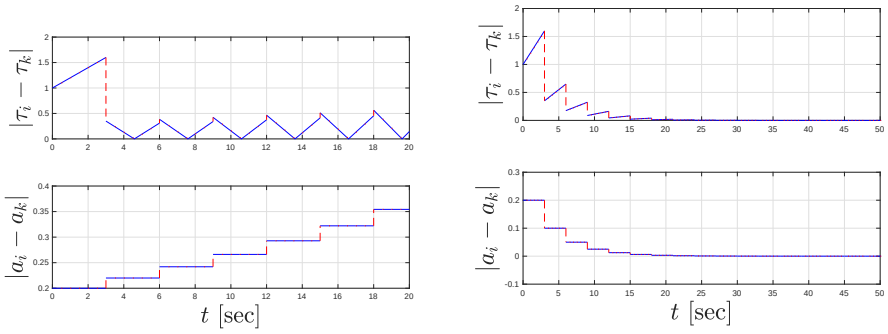

(a) (b)

Figure 5.4: The evolution of the error in the clocks and clock rates of Nodes i and k when the algorithm applies both offset correction $K_{\tilde{o}}$ and clock rate correction K_a. Plot (a) demonstrates the case when μ is chosen arbitrarily while plot (b) depicts the scenario where μ is optimally chosen.

simulations. Figure 5.4(a) gives plots of the errors for the case where the μ is chosen using information on c and d following our forthcoming design conditions while Figure 5.4(b) provide the error plots for the case where μ is chosen arbitrarily. In the case of the ideal μ, the error in the clocks and clock rate converge to zero whereas in the case of the arbitrarily chosen μ, the error fails to converge. This suggests that a sufficient condition to appropriately design μ is necessary to ensure convergence of the error.

5.2 Preliminaries on Hybrid Systems

A hybrid system $\mathcal{H}$ in $\mathbb{R}^n$ is composed by the following *data*: a set $C \subset \mathbb{R}^n$, called the flow set; a set-valued mapping $F : \mathbb{R}^n \rightrightarrows \mathbb{R}^n$ with $C \subset \text{dom } F$, called the flow map; a set $D \subset \mathbb{R}^n$, called the jump set; a set-valued mapping $G : \mathbb{R}^n \rightrightarrows \mathbb{R}^n$ with $D \subset \text{dom } G$, called the jump map. Then, a hybrid system $\mathcal{H} := (C, F, D, G)$ is written in the compact form

$$\mathcal{H} \begin{cases} \dot{x} \in F(x) & x \in C \\ x^+ \in G(x) & x \in D \end{cases} \tag{5.12}$$

where x is the system state. Solutions to hybrid systems are parameterized by (t, j), where $t \in \mathbb{R}_{\geq 0}$ defines ordinary time and $j \in \mathbb{N}$ is a counter that defines the number of jumps. The evolution of ϕ is described by a *hybrid arc* on a *hybrid time domain* [4]. A hybrid time

domain is given by dom $\phi \subset \mathbb{R}_{\geq 0} \times \mathbb{N}$ if, for each $(T, J) \in$ dom ϕ, dom $\phi \cap ([0, T] \times \{0, 1, ..., J\})$ is of the form $\bigcup_{j=0}^{J}([t_j, t_{j+1}] \times \{j\})$, with $0 = t_0 \leq t_1 \leq t_2 \leq t_{J+1}$. A solution ϕ is said to be *maximal* if it cannot be extended by flow or a jump, and *complete* if its domain is unbounded. For a hybrid system that is *well-posed*, the closed set $\mathcal{A} \subset \mathbb{R}^n$ is said to be: *attractive* for $\mathcal{H}$ if there exists $\mu > 0$ such that every solution ϕ to $\mathcal{H}$ with $|\phi(0,0)|_{\mathcal{A}} \leq \mu$ is complete and satisfies $\lim_{t+j \to \infty} |\phi(t, j)|_{\mathcal{A}} = 0$.

5.3 A Hybrid Algorithm for Sender-Receiver Clock Synchronization

In this section we present our hybrid model that captures the network dynamics for the message exchange and our proposed algorithm that ensures synchronization of the clocks. Using the sender-receiver mechanism for exchanging the timing messages, our algorithm combines the offset correction law in (5.8) with the proposed online, adaptive clock rate correction law given in (5.9).

5.3.1 Modeling

Given the mix of continuous and discrete dynamics of the system, i.e., the continuous evolution of the clocks and the discrete events of the computation and network transmission, a hybrid modeling approach is a natural fit to perform the needed analysis and design goals to solve Problem 6.0.1. Thus, with our problem defined formally, we present a hybrid model that captures the proposed algorithm given in Section 5.1.3. To model the hardware and communication dynamics of the system, namely, the residence and transit times elapsed between the timing messages, we consider a global timer $\tau \in [0, d]$ with dynamics

$$\begin{aligned} \dot{\tau} &= -1 \qquad && \tau \in [0, d] \\ \tau^+ &\in \{c, d\} && \tau = 0 \end{aligned} \tag{5.13}$$

In this model, the timer τ is reset to either c or d when $\tau = 0$ in order to preserve the bounds given in (6.5). We remind the reader that the constant c denotes the residence delay and d denotes the transmission or propagation delay. To determine the appropriate choice for the new value of τ, namely, τ^+, we define a discrete variable $q \in \{0, 1\} =: \mathcal{Q}$ to indicate the residence or transmission state of the system, namely, whether the system is

servicing a message at one of the two nodes or whether the system is waiting for the arrival of a message at either of the two nodes, respectively. The state vectors

$$m^i = [m_1^i, m_2^i, m_3^i, m_4^i, m_5^i, m_6^i]^\top \in \mathbb{R}^6$$

and

$$m^k = [m_1^k, m_2^k, m_3^k, m_4^k, m_5^k, m_6^k]^\top \in \mathbb{R}^6$$

represent memory buffers to store the received and transmitted timestamps respectively, for Node i and Node k. In addition, a second discrete variable $p \in \{0, 1, 2, 3, 4, 5\} =: \mathcal{P}$ is used to track at which stage of the message exchange, defined in (P1)-(P6), the algorithm is at. Then, by incorporating the clocks τ_i, τ_k and the clock rates a_i, a_k as state variables to the model as in Section 5.1.1, the state x of the hybrid system model, denoted $\mathcal{H}$, is given by

$$x := (\tau_i, \tau_k, a_i, a_k, \tau, m^i, m^k, p, q) \in \mathcal{X}$$

where

$$\mathcal{X} := \mathbb{R} \times \mathbb{R} \times \mathbb{R} \times \mathbb{R} \times [0, d] \times \mathbb{R}^6 \times \mathbb{R}^6 \times \mathcal{P} \times \mathcal{Q}$$

With the dynamics of the clocks as given in (5.1) and those of the timer τ in (5.13), the flow map is defined as

$$F(x) := (a_i, a_k, 0, 0, -1, 0, 0, 0, 0) \quad \forall x \in C \tag{5.14}$$

the flow set C is defined as

$$C := C_1 \cup C_2 \tag{5.15}$$

where

$$C_1 := \{x \in \mathcal{X} : q = 0, \tau \in [0, c]\}$$

and

$$C_2 := \{x \in \mathcal{X} : q = 1, \tau \in [0, d]\}$$

To model the communication and arrival events of the message exchange and the proposed mechanisms correcting the clock rate and offset, we define the jump map $G : \mathbb{R}^n \to \mathbb{R}^n$ as

$$G(x) := G_i(x) \text{ if } x \in D_i \tag{5.16}$$

where each mapping G_i used to define G corresponds to the message exchange events (P1)-(P6) as follows

- G_1: Node i broadcasts a synchronization message to Node k timestamped with τ_i as in (P1). This event is triggered by the jump set D_1, namely, when the timer $\tau = 0$ and the discrete variable p describing the protocol state is zero. At this event, the timer τ is reset to d, to initiate the message transmission delay. Similarly, the state q is reset to 1 to indicate the message transmission state of the system with p augmented by one to trigger the next protocol state. Finally, m_1^i is set to τ_i to record the time of message broadcast, relative to the clock of Node i. The subsequent memory states $m_2^i, \dots m_6^i$ are reset to $m_1^i, \dots m_5^i$, respectively.

- G_2: Node k receives the synchronization message and timestamps its arrival with τ_k as in (P2). This event is triggered by the jump set D_2, namely, when the timer $\tau = 0$ and the discrete variable p describing the protocol state is one. At this event, the timer τ is reset to c, to initiate the residence delay. Similarly, the state q is reset to 0 to indicate the residence state of the system. Finally, m_1^k is set to τ_k to record the time of message broadcast, relative to the clock of Node i. The subsequent memory states $m_2^k, \dots m_6^k$ are reset to $m_1^i, \dots m_5^i$, respectively.

- G_3: Node k broadcasts a response message timestamped with τ_k as in (P3). This event is triggered by the jump set D_3, namely, when the timer $\tau = 0$ and the discrete variable p describing the protocol state is two. At this event, the timer τ is reset to d, to initiate the message transmission delay. Similarly, the state q is reset to 1 to indicate the message transmission state of the system. Finally, m_1^i is set to τ_i to record the time of message broadcast, relative to the clock of Node i. The subsequent memory states $m_2^i, \dots m_6^i$ are reset to $m_1^i, \dots m_5^i$, respectively.

- G_4: Node i receives the response message and timestamps its arrival with τ_k as in (P4). This event is triggered by the jump set D_4, namely, when the timer $\tau = 0$ and the discrete variable p describing the protocol state is three. At this event, the timer τ is reset to c, to initiate the residence delay. Similarly, the state q is reset to 0 to indicate the residence state of the system. Finally, m_1^k is set to τ_k to record the time of message broadcast, relative to the clock of Node i. The subsequent memory states $m_2^k, \dots m_6^k$ are reset to $m_1^i, \dots m_5^i$, respectively.

- G_5: Node i broadcasts a response receipt message timestamped with τ_i as in (P5). This event is triggered by the jump set D_5, namely, when the timer $\tau = 0$ and the

discrete variable p describing the protocol state is four. At this event, the timer τ is reset to d, to initiate the message transmission delay. Similarly, the state q is reset to 1 to indicate the message transmission state of the system. Finally, m_1^i is set to τ_i to record the time of message broadcast, relative to the clock of Node i. The subsequent memory states $m_2^i, \dots m_6^i$ are reset to $m_1^i, \dots m_5^i$, respectively.

- G_6: Node k uses the timestamped messages to update its clock rate and offset via $K_{\delta}(x)$ in (5.8) and $K_a(x)$ in (5.18), respectively as in (P6). This event is triggered by the jump set D_6, namely, when the timer $\tau = 0$ and the discrete variable p describing the protocol state is five. At this event, the timer τ is reset to c, to initiate the residence delay. Similarly, the state q is reset to 0 to indicate the residence state of the system. Finally, m_1^k is set to τ_k to record the time of message broadcast, relative to the clock of Node i. The subsequent memory states $m_2^k, \dots m_6^k$ are reset to $m_1^i, \dots m_5^i$, respectively.

More precisely, the maps $G_1, G_2, G_3, G_4, G_5, G_6$, updating $x = (\tau_i, \tau_k, a_i, a_k, \tau, m^i, m^k, p, q)$, are defined by[3]

$$
\begin{aligned}
G_1(x) &:= \begin{bmatrix} (\tau_i, \tau_k) \\ (a_i, a_k) \\ d \\ (\tau_i, m_1^i, \dots, m_5^i), m^k) \\ p+1 \\ 1 \end{bmatrix}, \quad G_2(x) := \begin{bmatrix} (\tau_i, \tau_k) \\ (a_i, a_k) \\ c \\ (m^i, \tau_k, m_1^i, \dots, m_5^i) \\ p+1 \\ 0 \end{bmatrix} \\
G_3(x) &:= \begin{bmatrix} (\tau_i, \tau_k) \\ (a_i, a_k) \\ d \\ (m^i, \tau_k, m_1^k, \dots, m_5^k) \\ p+1 \\ 1 \end{bmatrix}, \quad G_4(x) := \begin{bmatrix} (\tau_i, \tau_k) \\ (a_i, a_k) \\ c \\ (\tau_i, m_1^k, \dots, m_5^k, m^k) \\ p+1 \\ 0 \end{bmatrix} \\
G_5(x) &:= \begin{bmatrix} (\tau_i, \tau_k) \\ (a_i, a_k) \\ d \\ (\tau_i, m_1^i, \dots, m_5^i, m^k) \\ p+1 \\ 1 \end{bmatrix}, \quad G_6(x) := \begin{bmatrix} (\tau_i, \tau_k - K_{\tilde{o}}(m^i)) \\ (a_i, a_k + K_a(m^i, \tau_k)) \\ c \\ (m^i, \tau_k, m_1^i, \dots, m_5^i) \\ 0 \\ 0 \end{bmatrix}
\end{aligned} \tag{5.17}
$$

with

$$K_{\tilde{o}}(m^i) = \frac{1}{2}(m_4^i - m_5^i - m_2^i + m_3^i) \tag{5.18}$$

and

$$K_a(m^i, \tau_k) = \mu\big((m_1^i - m_5^i) - (\tau_k - m_4^i)\big) \tag{5.19}$$

with $\mu > 0$. The offset correction implemented by the feedback law $K_{\tilde{o}}$ in (5.18) is an adapted version of the offset correction algorithm given in (5.8) suitable for the hybrid system model where the memory states m^i and m^k contain the stored timestamps T_j^i and T_j^k, respectively. Note that the feedback laws $K_{\tilde{o}}$ and K_a depend on the correct assignment of the timestamps to the memory states. In the forthcoming Lemmas 5.3.3 and 5.3.4, we show finite time attractivity of a set containing the correct assignment of the memory states

[3]Note that $[x^\top, y^\top]^\top = (x, y)$.

for the appropriate feedback. To trigger the jumps corresponding to the particular protocol events (P1)-(P6), we define the jump set as

$$D := D_1 \cup D_2 \cup D_3 \cup D_4 \cup D_5 \cup D_6$$

where

$$\begin{aligned} D_1 &:= \{x \in \mathcal{X} : \tau = 0, p = 0\}, & D_2 &:= \{x \in \mathcal{X} : \tau = 0, p = 1\} \\ D_3 &:= \{x \in \mathcal{X} : \tau = 0, p = 2\}, & D_4 &:= \{x \in \mathcal{X} : \tau = 0, p = 3\} \\ D_5 &:= \{x \in \mathcal{X} : \tau = 0, p = 4\}, & D_6 &:= \{x \in \mathcal{X} : \tau = 0, p = 5\} \end{aligned}$$

With the data defined, we let $\mathcal{H} = (C, F, D, G)$ denote the hybrid system for the pairwise broadcast synchronization algorithm between Node i and Node k.

5.3.2 Error Model

To show that the proposed algorithm solves Problem 6.0.1, we recast the problem as a set stabilization problem. Namely, we show that solutions ϕ to $\mathcal{H}$, with data (C, F, D, G) given in (5.12), converge to a set of interest wherein the clock states τ_i, τ_k and clock rates a_i,a_k, respectively, coincide. To this end, we consider an augmented model of $\mathcal{H}$ in error coordinates to capture such a property. Let $\varepsilon := (\varepsilon_\tau, \varepsilon_a) \in \mathbb{R}^2$, where $\varepsilon_\tau := \tau_i - \tau_k$ defines the clock error and $\varepsilon_a := a_i - a_k$ defines the clock rate error of Nodes i and k. Then, define

$$x_\varepsilon := (\varepsilon, x) \in \mathcal{X}_\varepsilon := \mathbb{R}^2 \times \mathcal{X}$$

which is the state[4] that collects the clock errors, clock rate errors, and the state of the system $\mathcal{H}$. The continuous evolution of x_ε is governed by

$$\dot{x}_\varepsilon = F_\varepsilon(x_\varepsilon) := \big(A_f \varepsilon, F(x)\big) \quad x_\varepsilon \in C_\varepsilon \tag{5.20}$$

where $A_f = \begin{bmatrix} 0 & 1 \\ 0 & 0 \end{bmatrix}$ and f is defined in (5.14). The flow set C_ε is defined as

$$C_\varepsilon := C_{\varepsilon_1} \cup C_{\varepsilon_1} \tag{5.21}$$

where

$$C_{\varepsilon_1} := \{x_\varepsilon \in \mathcal{X}_\varepsilon : q = 0, \tau \in [0, c]\}$$

[4] The full state vector x to $\mathcal{H}$ is retained to facilitate the implementation of the synchronization algorithm for $\mathcal{H}_\varepsilon$.

and

$$C_{\varepsilon_2} := \{x_\varepsilon \in \mathcal{X}_\varepsilon : q = 1, \tau \in [0, d]\}$$

The discrete changes of x_ε are determined by the discrete changes of ε and x, the latter of which is given in (5.16). Through the computation of $\varepsilon^+ = (\varepsilon_\tau^+, \varepsilon_a^+)$ using the jump maps in (5.17), the resulting evolution is modeled by the jump map $G_\varepsilon : \mathcal{X}_\varepsilon \to \mathcal{X}_\varepsilon$ given by

$$G_\varepsilon(x_\varepsilon) := G_{\varepsilon_i}(x_\varepsilon) \quad \text{if } x_\varepsilon \in D_{\varepsilon_i} \tag{5.22}$$

where

$$G_{\varepsilon_1}(x_\varepsilon) := \begin{bmatrix} \varepsilon \\ G_1(x) \end{bmatrix}, \; G_{\varepsilon_2}(x_\varepsilon) := \begin{bmatrix} \varepsilon \\ G_2(x) \end{bmatrix}, \; G_{\varepsilon_3}(x_\varepsilon) := \begin{bmatrix} \varepsilon \\ G_3(x) \end{bmatrix}$$

$$G_{\varepsilon_4}(x_\varepsilon) := \begin{bmatrix} \varepsilon \\ G_4(x) \end{bmatrix}, \; G_{\varepsilon_5}(x_\varepsilon) := \begin{bmatrix} \varepsilon \\ G_5(x) \end{bmatrix}, \; G_{\varepsilon_6}(x_\varepsilon) := \begin{bmatrix} \varepsilon + \begin{bmatrix} K_{\tilde{o}}(m^i) \\ -K_a(m^i, \tau_k) \end{bmatrix} \\ G_6(x) \end{bmatrix}$$

Observe that the feedback laws $K_{\tilde{o}}$ and K_a are employed when ε is updated by G_{ε_6}, similarly to when G_6 is employed $\mathcal{H}$. These discrete dynamics apply when x is in $D_\varepsilon := D_{\varepsilon_1} \cup D_{\varepsilon_2} \cup D_{\varepsilon_3} \cup D_{\varepsilon_4} \cup D_{\varepsilon_5} \cup D_{\varepsilon_6}$, where

$$\begin{aligned} D_{\varepsilon_1} &:= \{x_\varepsilon \in \mathcal{X}_\varepsilon : \tau = 0, p = 0\}, & D_{\varepsilon_2} &:= \{x_\varepsilon \in \mathcal{X}_\varepsilon : \tau = 0, p = 1\} \\ D_{\varepsilon_3} &:= \{x_\varepsilon \in \mathcal{X}_\varepsilon : \tau = 0, p = 2\}, & D_{\varepsilon_4} &:= \{x_\varepsilon \in \mathcal{X}_\varepsilon : \tau = 0, p = 3\} \\ D_{\varepsilon_5} &:= \{x_\varepsilon \in \mathcal{X}_\varepsilon : \tau = 0, p = 4\}, & D_{\varepsilon_6} &:= \{x_\varepsilon \in \mathcal{X}_\varepsilon : \tau = 0, p = 5\} \end{aligned}$$

This hybrid system is denoted

$$\mathcal{H}_\varepsilon = (C_\varepsilon, F_\varepsilon, D_\varepsilon, G_\varepsilon) \tag{5.23}$$

The set to render attractive so as to solve Problem 6.0.1 is given by

$$\mathcal{A}_\varepsilon := \{x_\varepsilon \in \mathcal{X}_\varepsilon : \varepsilon = 0\} \tag{5.24}$$

where $\varepsilon = 0$ implies synchronization of both the clock offset and the clock rate, since, when $\varepsilon_\tau = 0$ and $\varepsilon_a = 0$, then τ_k is synchronized to τ_i.

5.3.3 Basic Properties of $\mathcal{H}_\varepsilon$

Having the hybrid system $\mathcal{H}_\varepsilon$ defined, the next two results establish existence of solutions to $\mathcal{H}_\varepsilon$ and that every maximal solution to $\mathcal{H}_\varepsilon$ is complete. In particular, we show

that, through the satisfaction of some basic conditions on the hybrid system data, which is shown first, the system $\mathcal{H}_\varepsilon$ is well-posed and that each maximal solution to the system is defined for arbitrarily large $t + j$.

Lemma 5.3.1. *The hybrid system $\mathcal{H}_\varepsilon = (C_\varepsilon, F_\varepsilon, D_\varepsilon, G_\varepsilon)$ satisfies the following conditions, defined in [4, Assumption 6.5] as the hybrid basic conditions; namely,*

(A1) C_ε and D_ε are closed subsets of $\mathbb{R}^m$;

(A2) $F_\varepsilon : \mathbb{R}^m \to \mathbb{R}^m$ is continuous;

(A3) $G_\varepsilon : \mathbb{R}^m \rightrightarrows \mathbb{R}^m$ is outer semicontinuous and locally bounded relative to D_ε, and $D_\varepsilon \subset dom\ G_\varepsilon$.

See the appendix for proof.

Lemma 5.3.2. *For every $\xi \in C_\varepsilon \cup D_\varepsilon (= \mathcal{X}_\varepsilon)$, there exists at least one nontrivial solution ϕ to $\mathcal{H}_\varepsilon$ such that $\phi(0, 0) = \xi$. Moreover, every maximal solution to $\mathcal{H}_\varepsilon$ is complete.*

See the appendix for proof.

The effectiveness of the update laws $K_{\tilde{o}}$ and K_a, given in (5.18) and (5.19), in correcting the clock and clock rate of Node k, depend on the assigned values of m^i and m^k at the time $K_{\tilde{o}}$ and K_a, i.e., when jumps according to G_{ε_6} occur. Improper initialization of the memory states may result in updates of the offset and clock rate of Node k that increase the error in the clocks and clock rates relative to Node i. Therefore, to facilitate the analysis of $\mathcal{H}_\varepsilon$ in rendering the set $\mathcal{A}_\varepsilon$ asymptotically attractive, we restrict the values of m^i and m^k to a set smaller than $\mathcal{X}$ where they remain in forward (hybrid) time. More precisely, we restrict the state x_ε to the set

$$\mathcal{M} := \mathcal{M}_1 \cup \mathcal{M}_2 \cup \mathcal{M}_3 \cup \mathcal{M}_4 \cup \mathcal{M}_5 \cup \mathcal{M}_6 \tag{5.25}$$

where

$$\mathcal{M}_1 := \{x_\varepsilon \in \mathcal{X}_\varepsilon : p{=}0, q{=}0\}$$
$$\mathcal{M}_2 := \{x_\varepsilon \in \mathcal{X}_\varepsilon : p{=}1, q{=}1, m_1^i\text{-}\rho_i(x_\varepsilon, 0) = 0\}$$
$$\mathcal{M}_3 := \{x_\varepsilon \in \mathcal{X}_\varepsilon : p{=}2, q{=}0, m_1^k\text{-}\rho_k(x_\varepsilon, 0) = 0, m_2^k\text{-}\rho_i(x_\varepsilon, d) = 0\}$$
$$\mathcal{M}_4 := \{x_\varepsilon \in \mathcal{X}_\varepsilon : p{=}3, q{=}1, m_1^k\text{-}\rho_k(x_\varepsilon, 0) = 0, m_2^k\text{-}\rho_k(x_\varepsilon, c) = 0, m_3^k\text{-}\rho_i(x_\varepsilon, c{+}d) = 0\}$$
$$\mathcal{M}_5 := \{x_\varepsilon \in \mathcal{X}_\varepsilon : p{=}4, q{=}0, m_1^i\text{-}\rho_i(x_\varepsilon, 0) = 0, m_2^i\text{-}\rho_k(x_\varepsilon, d) = 0, m_3^i\text{-}\rho_k(x_\varepsilon, c{+}d) = 0,$$
$$m_4^i\text{-}\rho_i(x_\varepsilon, c{+}2d){=}0\}$$
$$\mathcal{M}_6 := \{x_\varepsilon \in \mathcal{X}_\varepsilon : p{=}5, q{=}1, m_1^i\text{-}\rho_i(x_\varepsilon, 0) = 0, m_2^i\text{-}\rho_i(x_\varepsilon, c) = 0, m_3^i\text{-}\rho_k(x_\varepsilon, c{+}d) = 0,$$
$$m_4^i\text{-}\rho_k(x_\varepsilon, 2c{+}d) = 0, m_5^i\text{-}\rho_i(x_\varepsilon, 2c{+}2d) = 0\}$$

and

$$\begin{aligned} \rho_i(x_\varepsilon, \beta) &:= \tau_i - a_i((1-q)c + qd - \tau) - a_i\beta \\ \rho_k(x_\varepsilon, \beta) &:= \tau_k - a_k((1-q)c + qd - \tau) - a_k\beta \end{aligned} \tag{5.26}$$

for $\beta \geq 0$.

Lemma 5.3.3. *The set $\mathcal{M}$ is forward invariant for the hybrid system $\mathcal{H}_\varepsilon$.*

See the appendix for proof.

Lemma 5.3.4. *Let constants $d \geq c > 0$ be given. For each maximal solution ϕ to $\mathcal{H}_\varepsilon$, there exists $T^* \geq 0$ such that $\phi(t, j) \in \mathcal{M}$ for any $(t, j) \in \text{dom } \phi$ with $t + j \geq T^*$.*

See the appendix for proof.

In our main result, which is presented in the next section, we show asymptotic attractivity of the synchronization set $\mathcal{A}_\varepsilon$ via a Lyapunov analysis on solutions from the initialization set $\mathcal{M}$.

5.4 Main Results

In this section, we present our main result showing asymptotic attractivity of the synchronization set $\mathcal{A}_\varepsilon$ in (5.24) for $\mathcal{H}_\varepsilon$. To show this, we present a Lyapunov analysis along solutions to $\mathcal{H}$ starting from the set $\mathcal{M}$. We remind the reader that $\mathcal{M}$ is the set that denotes valid initialization values of the memory state vectors m^i and m^k for which

the update laws $K_{\tilde{o}}$ and K_a give values to correct the clock rate and offset. To this end, consider the Lyapunov function candidate

$$V(x_\varepsilon) = \varepsilon^\top \exp\big(A_f^\top r(\tau,p,q)\big) P \exp\big(A_f r(\tau,p,q)\big)\varepsilon \tag{5.27}$$

where $P = P^\top \succ 0$, A_f is as given in (5.20), $r(\tau,p,q) := \tau h(q) + d(5-p)$ and $h(q) := 1 + c^{-1}(1-q)(d-c)$ are defined for each $x_\varepsilon \in C_\varepsilon \cup D_\varepsilon$. Note that there exist two positive scalars, α_1 and α_2, such that

$$\alpha_1 |x_\varepsilon|^2_{\mathcal{A}_\varepsilon} \le V(x_\varepsilon) \le \alpha_2 |x_\varepsilon|^2_{\mathcal{A}_\varepsilon} \quad \forall x_\varepsilon \in C_\varepsilon \cup D_\varepsilon \tag{5.28}$$

The function V satisfies the following infinitesimal properties.

Lemma 5.4.1. *Let the hybrid system $\mathcal{H}_\varepsilon$ be given as in (5.23). For each point $x_\varepsilon \in C_\varepsilon$, one has*

$$\langle \nabla V(x_\varepsilon), F_\varepsilon(x_\varepsilon)\rangle \le \begin{cases} 0 & \text{if } x_\varepsilon \in C_{\varepsilon_2} \\ \frac{\gamma}{\alpha_2} V(x_\varepsilon) & \text{if } x_\varepsilon \in C_{\varepsilon_1} \end{cases} \tag{5.29}$$

where

$$\alpha_2 = \max_{\nu\in\mathcal{Q},\sigma\in\mathcal{P}} \Big(\exp\big((\nu h(\nu) + d(5-\sigma))A_f^\top\big) P \exp\big(\big(\nu h(\nu) + d(5-\sigma)\big)A_f\big)\Big) \tag{5.30}$$

$$\gamma = |\alpha| \max\Big\{\frac{p_{11}\epsilon}{2}, \beta + \frac{p_{11}}{2\epsilon}\Big\} \tag{5.31}$$

$\alpha = \frac{2(c-d)}{c}$, $\epsilon > 0$, $\beta = p_{11}6d - p_{12}$, *and* p_{11} *and* p_{12} *come from* $P = \begin{bmatrix} p_{11} & p_{12} \\ p_{21} & p_{22} \end{bmatrix} \succ 0$.

Proof. Before calculating $\langle \nabla V(x_\varepsilon), F_\varepsilon(x_\varepsilon)\rangle$, observe that the full expression of V is given

by

$$
\begin{aligned}
V(x_\varepsilon) &= \begin{bmatrix} \varepsilon_\tau \\ \varepsilon_a \end{bmatrix}^\top \exp\left(A_f^\top r(\tau,p,q)\right) \begin{bmatrix} p_{11} & p_{12} \\ p_{21} & p_{22} \end{bmatrix} \exp\left(A_f r(\tau,p,q)\right) \begin{bmatrix} \varepsilon_\tau \\ \varepsilon_a \end{bmatrix} \\
&= \begin{bmatrix} \varepsilon_\tau \\ \varepsilon_a \end{bmatrix}^\top \begin{bmatrix} 1 & 0 \\ r(\tau,p,q) & 1 \end{bmatrix} \begin{bmatrix} p_{11} & p_{12} \\ p_{21} & p_{22} \end{bmatrix} \begin{bmatrix} 1 & r(\tau,p,q) \\ 0 & 1 \end{bmatrix} \begin{bmatrix} \varepsilon_\tau \\ \varepsilon_a \end{bmatrix} \\
&= \begin{bmatrix} \varepsilon_\tau + \varepsilon_a r(\tau,p,q) \\ \varepsilon_a \end{bmatrix}^\top \begin{bmatrix} p_{11} & p_{12} \\ p_{21} & p_{22} \end{bmatrix} \begin{bmatrix} \varepsilon_\tau + \varepsilon_a r(\tau,p,q) \\ \varepsilon_a \end{bmatrix} \\
&= \begin{bmatrix} \varepsilon_\tau + \varepsilon_a r(\tau,p,q) \\ \varepsilon_a \end{bmatrix}^\top \begin{bmatrix} p_{11}\big(\varepsilon_\tau + \varepsilon_a r(\tau,p,q)\big) + p_{12}\varepsilon_a \\ p_{21}\big(\varepsilon_\tau + \varepsilon_a r(\tau,p,q)\big) + p_{22}\varepsilon_a \end{bmatrix} \\
&= \big(\varepsilon_\tau + \varepsilon_a r(\tau,p,q)\big)\big(p_{11}\big(\varepsilon_\tau + \varepsilon_a r(\tau,p,q)\big) + p_{12}\varepsilon_a\big) + \varepsilon_a\big(p_{21}\big(\varepsilon_\tau + \varepsilon_a r(\tau,p,q)\big) + p_{22}\varepsilon_a\big) \\
&= p_{11}\big(\varepsilon_\tau + \varepsilon_a r(\tau,p,q)\big)^2 + p_{12}\varepsilon_a\big(\varepsilon_\tau + \varepsilon_a r(\tau,p,q)\big) + p_{21}\varepsilon_a\big(\varepsilon_\tau + \varepsilon_a r(\tau,p,q)\big) + p_{22}\varepsilon_a^2
\end{aligned}
\tag{5.32}
$$

then since $p_{12} = p_{21}$

$$
V(x_\varepsilon) = p_{11}\big(\varepsilon_\tau + \varepsilon_a r(\tau,p,q)\big)^2 + 2p_{12}\varepsilon_a\big(\varepsilon_\tau + \varepsilon_a r(\tau,p,q)\big)\big) + p_{22}\varepsilon_a^2 \tag{5.33}
$$

In calculating $\langle \nabla V(x_\varepsilon), F_\varepsilon(x_\varepsilon)\rangle$, one has

$$
\begin{aligned}
\langle \nabla V(x_\varepsilon), F_\varepsilon(x_\varepsilon)\rangle &= \begin{bmatrix} \nabla_{\varepsilon_\tau} V(x_\varepsilon) & \nabla_{\varepsilon_a} V(x_\varepsilon) & \nabla_\tau V(x_\varepsilon) & \nabla_p V(x_\varepsilon) & \nabla_q V(x_\varepsilon) \end{bmatrix} \begin{bmatrix} \varepsilon_a \\ 0 \\ -1 \\ 0 \\ 0 \end{bmatrix} \\
&= \nabla_{\varepsilon_\tau} V(x_\varepsilon)\varepsilon_a - \nabla_\tau V(x_\varepsilon)
\end{aligned}
\tag{5.34}
$$

where

$$
\begin{aligned}
\nabla_{\varepsilon_\tau} V(x_\varepsilon) &= 2p_{11}\big(\varepsilon_\tau + \varepsilon_a r(\tau,p,q)\big) + 2p_{12}\varepsilon_a \\
\nabla_\tau V(x_\varepsilon) &= 2p_{11}\varepsilon_a \nabla_\tau r(\tau,p,q)\big(\varepsilon_\tau + \varepsilon_a r(\tau,p,q)\big) + 2p_{12}\varepsilon_a^2 \nabla_\tau r(\tau,p,q)
\end{aligned}
\tag{5.35}
$$

Substituting (5.35) into (5.34), we obtain

$$\begin{aligned}
\langle \nabla V(x_\varepsilon), F_\varepsilon(x_\varepsilon)\rangle &= \Big(2p_{11}\big(\varepsilon_\tau + \varepsilon_a r(\tau,p,q)\big) + 2p_{12}\varepsilon_a\Big)\varepsilon_a \\
&\qquad - 2p_{11}\varepsilon_a \nabla_\tau r(\tau,p,q)\big(\varepsilon_\tau + \varepsilon_a r(\tau,p,q)\big) - 2p_{12}\varepsilon_a^2 \nabla_\tau r(\tau,p,q) \\
&= 2p_{11}\varepsilon_a\big(\varepsilon_\tau + \varepsilon_a r(\tau,p,q)\big) + 2p_{12}\varepsilon_a^2 \\
&\qquad - 2p_{11}\varepsilon_a \nabla_\tau r(\tau,p,q)\big(\varepsilon_\tau + \varepsilon_a r(\tau,p,q)\big) - 2p_{12}\varepsilon_a^2 \nabla_\tau r(\tau,p,q) \\
&= 2p_{11}\varepsilon_a\big(\varepsilon_\tau + \varepsilon_a r(\tau,p,q)\big)(1 - \nabla_\tau r(\tau,p,q)) + 2p_{12}\varepsilon_a^2(1 - \nabla_\tau r(\tau,p,q)) \\
&= \big(2p_{11}\varepsilon_a\big(\varepsilon_\tau + \varepsilon_a r(\tau,p,q)\big) + 2p_{12}\varepsilon_a^2\big)\big(1 - \nabla_\tau r(\tau,p,q)\big) \\
&= \big(2p_{11}\big(\varepsilon_a\varepsilon_\tau + \varepsilon_a^2 r(\tau,p,q)\big) + 2p_{12}\varepsilon_a^2\big)\big(1 - \nabla_\tau r(\tau,p,q)\big)
\end{aligned}$$

for each $x_\varepsilon \in C_\varepsilon$. Now, with $\nabla_\tau r(\tau,p,q) = \frac{(c-d)(q-1)}{c} + 1$, when $x_\varepsilon \in C_{\varepsilon_2}$ with $q = 1$, $\nabla_\tau r(\tau,p,q) = 1$, thus

$$\langle \nabla V(x_\varepsilon), F_\varepsilon(x_\varepsilon)\rangle = 0$$

When $x_\varepsilon \in C_{\varepsilon_2}$ with $q = 0$, $r(\tau,p,q) = \tau\big(\frac{d-c}{c} + 1\big) + d(5-p)$ and $\nabla_\tau r(\tau,p,q) = \frac{d-c}{c} + 1$ one then has

$$\begin{aligned}
\langle \nabla V(x_\varepsilon), F_\varepsilon(x_\varepsilon)\rangle &= \Big(2p_{11}\varepsilon_a\varepsilon_\tau + 2p_{11}\varepsilon_a^2\Big(\tau\Big(\frac{d-c}{c} + 1\Big) + d(5-p)\Big) + 2p_{12}\varepsilon_a^2\Big)\Big(\frac{c-d}{c}\Big) \\
&= \Big(2p_{11}\varepsilon_a\varepsilon_\tau + 2p_{11}\varepsilon_a^2\Big(\tau\Big(\frac{d-c}{c}\Big) + \tau + d(5-p)\Big) + 2p_{12}\varepsilon_a^2\Big)\Big(\frac{c-d}{c}\Big) \\
&= \Big(\frac{c-d}{c}\Big)2p_{11}\varepsilon_a\varepsilon_\tau + \Big(\frac{c-d}{c}\Big)2p_{11}\varepsilon_a^2\Big(\tau\Big(\frac{d-c}{c}\Big) + \tau + d(5-p)\Big) \\
&\qquad + \Big(\frac{c-d}{c}\Big)2p_{12}\varepsilon_a^2 \\
&= \Big(\frac{2(c-d)}{c}\Big)p_{11}\varepsilon_a\varepsilon_\tau + \Big(\frac{2(c-d)}{c}\Big)p_{11}\varepsilon_a^2\Big(\tau\Big(\frac{d-c}{c}\Big) + \tau + d(5-p)\Big) \\
&\qquad + \Big(\frac{2(c-d)}{c}\Big)p_{12}\varepsilon_a^2
\end{aligned}$$

Let $\alpha = \frac{2(c-d)}{c}$, then since, $0 < c \leq d$ we have that $\alpha \leq 0$

$$\langle \nabla V(x_\varepsilon), F_\varepsilon(x_\varepsilon)\rangle = -|\alpha|p_{11}\varepsilon_a\varepsilon_\tau - |\alpha|p_{11}\varepsilon_a^2\Big(\tau\Big(\frac{d-c}{c}\Big) + \tau + d(5-p)\Big) - |\alpha|p_{12}\varepsilon_a^2$$

Then, recognizing that $\tau \in [0,c]$ when $x_\varepsilon \in C_{\varepsilon_2}$ then we have that $\tau \leq c$, which due to the

fact that $p_{11} > 0$ and $p \in \mathcal{P} = \{0, 1, 2, 3, 4, 5\}$ leading to

$$\begin{aligned}\langle \nabla V(x_\varepsilon), F_\varepsilon(x_\varepsilon)\rangle &\leq -|\alpha| p_{11}\varepsilon_a\varepsilon_\tau + |\alpha| p_{11}\Big(c\Big(\frac{d-c}{c}\Big) + c + d(5-p)\Big)\varepsilon_a^2 - |\alpha| p_{12}\varepsilon_a^2 \\ &\leq -|\alpha| p_{11}\varepsilon_a\varepsilon_\tau + |\alpha| p_{11}\Big((d-c) + c + d(5-p)\Big)\varepsilon_a^2 - |\alpha| p_{12}\varepsilon_a^2 \\ &\leq -|\alpha| p_{11}\varepsilon_a\varepsilon_\tau + |\alpha| p_{11} d(6-p)\varepsilon_a^2 - |\alpha| p_{12}\varepsilon_a^2\end{aligned}$$

for each $x_\varepsilon \in C_{\varepsilon_2}$. We can upper bound the quantity $6 - p$ by noting that $p \in \mathcal{P} = \{0, 1, 2, 3, 4, 5\}$. Thus, we have that $6 - p \leq 6$ for each $p \in \mathcal{P}$, leading to

$$\langle \nabla V(x_\varepsilon), F_\varepsilon(x_\varepsilon)\rangle \leq -|\alpha| p_{11}\varepsilon_a\varepsilon_\tau + |\alpha|\big(p_{11} 6d - p_{12}\big)\varepsilon_a^2$$

Now, with $\beta = p_{11}6d - p_{12}$. Then, we obtain

$$\langle \nabla V(x_\varepsilon), F_\varepsilon(x_\varepsilon)\rangle \leq |\alpha| p_{11}|\varepsilon_a||\varepsilon_\tau| + |\alpha|\beta\varepsilon_a^2 \qquad \forall x_\varepsilon \in C_{\varepsilon_2} \tag{5.36}$$

Then, through an application of Young's inequality one has

$$\begin{aligned}\langle \nabla V(x_\varepsilon), F_\varepsilon(x_\varepsilon)\rangle &\leq |\alpha| p_{11}\Big(\frac{1}{2\epsilon}\varepsilon_a^2 + \frac{\epsilon}{2}\varepsilon_\tau^2\Big) + |\alpha|\beta\varepsilon_a^2 \\ &\leq \frac{|\alpha| p_{11}}{2\epsilon}\varepsilon_a^2 + |\alpha|\beta\varepsilon_a^2 + \frac{|\alpha| p_{11}\epsilon}{2}\varepsilon_\tau^2 \\ &\leq \frac{|\alpha| p_{11}\epsilon}{2}\varepsilon_\tau^2 + |\alpha|\Big(\beta + \frac{p_{11}}{2\epsilon}\Big)\varepsilon_a^2 \\ &\leq \gamma\big(\varepsilon_\tau^2 + \varepsilon_a^2\big) \\ &\leq \gamma\varepsilon^\top\varepsilon\end{aligned}$$

for each $x_\varepsilon \in C_{\varepsilon_2}$. Then, from the definition of V in (5.27)

$$\begin{aligned}\langle \nabla V(x_\varepsilon), F_\varepsilon(x_\varepsilon)\rangle &\leq \gamma|x_\varepsilon|^2 \\ &\leq \frac{\gamma}{\alpha_2} V(x_\varepsilon)\end{aligned}$$

for each $x_\varepsilon \in C_{\varepsilon_2}$ where $\epsilon > 0$, α_2 and γ are positive constants given in (5.30) and (5.31), respectively. □

Lemma 5.4.2. *Let the hybrid system $\mathcal{H}_\varepsilon$ in (5.23) with constants $d \geq c > 0$ be given. If there exist a constant $\mu > 0$ and a positive definite symmetric matrix P such that*

$$A_g^\top \exp\big(6dA_f^\top\big) P \exp\big(6dA_f\big) A_g - P \prec 0 \tag{5.37}$$

where $A_g = \begin{bmatrix} 0 & \gamma_1 \\ 0 & 1\text{–}\mu\gamma_2 \end{bmatrix}$ *and* A_f *is as given in (5.20) with* $\gamma_1 = \frac{1}{2}(3c+4d)$ *and* $\gamma_2 = 2c+2d$ *then, for each* $x_\varepsilon \in \mathcal{M} \cap D_\varepsilon$,

$$V\big(G_\ell(x_\varepsilon)\big) - V\big(x_\varepsilon\big) \leq 0$$

for each $\ell \in \{1,2,3,4,5\}$, *and* [5]

$$V\big(G_6(x_\varepsilon)\big) - V\big(x_\varepsilon\big) \leq -\sigma\varepsilon^\top\varepsilon$$

where

$$\sigma \in \left(0, \text{-}\lambda_{\min}\Big(A_g^\top \exp\big((6d)A_f^\top\big) P \exp\big((6d)A_f\big) A_g - P\Big)\right) \tag{5.38}$$

Proof. For every $g \in G_\varepsilon(x_\varepsilon)$, the state τ is reset to a point in the set $\{c, d\}$. Moreover, for each $x_\varepsilon \in D_\varepsilon$, $\tau = 0$. Hence, when $x_\varepsilon \in D_{\varepsilon_1} \cap \mathcal{M}_1$, we have that $\tau = 0$, $q = 0$, and $p = 0$, leading to

$$\begin{aligned} V(G_{\varepsilon_1}(x_\varepsilon)) - V(x_\varepsilon) &= \varepsilon^\top \exp\big(A_f^\top(d + d(5\text{–}1))\big) P \exp\big(A_f(d + d(5\text{–}1))\big)\varepsilon \\ &\qquad - \varepsilon^\top \exp\big(A_f^\top(0 + d(5-0))\big) P \exp\big(A_f(0 + d(5\text{–}0))\big)\varepsilon \\ &= \varepsilon^\top \exp\big(A_f^\top(5d)\big) P \exp\big(A_f(5d)\big)\varepsilon - \varepsilon^\top \exp\big(A_f^\top(5d)\big) P \exp\big(A_f(5d)\big)\varepsilon \\ &= 0 \end{aligned}$$

When $x_\varepsilon \in D_{\varepsilon_2} \cap \mathcal{M}_2$, we have that $\tau = 0$, $q = 1$, and $p = 1$, leading to

$$\begin{aligned} V(G_{\varepsilon_2}(x_\varepsilon))\text{–}V(x_\varepsilon) &= \varepsilon^\top \exp\big(A_f^\top(c(1 + c^{-1}(d\text{–}c)) + d(5\text{–}2))\big) P \exp\big(A_f(c(1 + c^{-1}(d\text{–}c)) + d(5\text{–}2))\big)\varepsilon \\ &\qquad - \varepsilon^\top \exp\big(A_f^\top(0 + d(5\text{–}1))\big) P \exp\big(A_f(0 + d(5\text{–}1))\big)\varepsilon \\ &= \varepsilon^\top \exp\big(A_f^\top(d + 3d)\big) P \exp\big(A_f(d + 3d)\big)\varepsilon - \varepsilon^\top \exp\big(A_f^\top(4d)\big) P \exp\big(A_f(4d)\big)\varepsilon \\ &= 0 \end{aligned}$$

When $x_\varepsilon \in D_{\varepsilon_3} \cap \mathcal{M}_3$, we have that $\tau = 0$, $q = 0$, and $p = 2$, leading to

$$\begin{aligned} V(G_{\varepsilon_3}(x_\varepsilon)) - V(x_\varepsilon) &= \varepsilon^\top \exp\big(A_f^\top(d + d(5\text{–}3))\big) P \exp\big(A_f(d + d(5\text{–}3))\big)\varepsilon \\ &\qquad - \varepsilon^\top \exp\big(A_f^\top(0 + d(5\text{–}2))\big) P \exp\big(A_f(0 + d(5\text{–}2))\big)\varepsilon \\ &= \varepsilon^\top \exp\big(A_f^\top(3d)\big) P \exp\big(A_f(3d)\big)\varepsilon - \varepsilon^\top \exp\big(A_f^\top(3d)\big) P \exp\big(A_f(3d)\big)\varepsilon \\ &= 0 \end{aligned}$$

[5] Observe that $\varepsilon^+ = A_g\varepsilon$ is the matrix representation of the jump map G_6 for which ε is reset to when $x_\varepsilon \in \mathcal{M}_6 \cap D_\varepsilon$.

When $x_\varepsilon \in D_{\varepsilon_4} \cap \mathcal{M}_4$, we have that $\tau = 0$, $q = 1$, and $p = 3$, leading to

$$\begin{aligned} V(G_{\varepsilon_4}(x_\varepsilon)) - V(x_\varepsilon) &= \varepsilon^\top \exp\big(A_f^\top (c(1 + c^{-1}(d\text{–}c)) + d(5\text{–}4))\big) P \exp\big(A_f(c(1 + c^{-1}(d\text{–}c)) + d(5\text{–}4))\big)\varepsilon \\ &\quad - \varepsilon^\top \exp\big(A_f^\top (0 + d(5\text{–}3))\big) P \exp\big(A_f(0 + d(5\text{–}3))\big)\varepsilon \\ &= \varepsilon^\top \exp\big(A_f^\top (d + d)\big) P \exp\big(A_f(d + d)\big)\varepsilon - \varepsilon^\top \exp\big(A_f^\top (2d)\big) P \exp\big(A_f(2d)\big)\varepsilon \\ &= 0 \end{aligned}$$

When $x_\varepsilon \in D_{\varepsilon_5} \cap \mathcal{M}_5$, we have that $\tau = 0$, $q = 0$, and $p = 4$, leading to

$$\begin{aligned} V(G_{\varepsilon_5}(x_\varepsilon)) - V(x_\varepsilon) &= \varepsilon^\top \exp\big(A_f^\top (d + d(5\text{–}5))\big) P \exp\big(A_f(d + d(5\text{–}5))\big)\varepsilon \\ &\quad - \varepsilon^\top \exp\big(A_f^\top (0 + d(5\text{–}4))\big) P \exp\big(A_f(0 + d(5\text{–}4))\big)\varepsilon \\ &= \varepsilon^\top \exp\big(A_f^\top (d)\big) P \exp\big(A_f(d)\big)\varepsilon - \varepsilon^\top \exp\big(A_f^\top (d)\big) P \exp\big(A_f(d)\big)\varepsilon \\ &= 0 \end{aligned}$$

When $x_\varepsilon \in D_{\varepsilon 6} \cap \mathcal{M}_6$, we have that $\tau = 0$, $q = 1$, and $p = 5$. For resets according to G_{ε_6}, one has

$$\begin{aligned} &V(G_{\varepsilon_6}(x_\varepsilon)) - V(x_\varepsilon) = \\ &\left[\varepsilon + \begin{bmatrix} K_{\tilde{o}}(m^i) \\ -K_a(m^i, \tau_k) \end{bmatrix}\right]^\top \exp\big(A_f^\top (c(1+c^{-1}(d\text{–}c))+d(5\text{–}0))\big) P \exp\big(A_f(c(1+c^{-1}(d\text{–}c))+d(5\text{–}0))\big) \left[\varepsilon + \begin{bmatrix} K_{\tilde{o}}(m^i) \\ -K_a(m^i, \tau_k) \end{bmatrix}\right] \\ &\qquad - \varepsilon^\top \exp\big(A_f^\top (0 + d(0))\big) P \big(A_f^\top (0 + d(0))\big)\varepsilon \\ &\qquad = \left[\varepsilon + \begin{bmatrix} K_{\tilde{o}}(m^i) \\ -K_a(m^i, \tau_k) \end{bmatrix}\right]^\top \exp\big(A_f^\top (6d)\big) P \exp\big(A_f(6d)\big) \left[\varepsilon + \begin{bmatrix} K_{\tilde{o}}(m^i) \\ -K_a(m^i, \tau_k) \end{bmatrix}\right] \\ &\qquad\quad - \varepsilon^\top P \varepsilon \end{aligned}$$

Now, with $x_\varepsilon \in D_{\varepsilon 6} \cap \mathcal{M}_6$, which implies that $p = 5$, $q = 1$, and $\tau = 0$, one has that for jumps with resets according to $G_{\varepsilon_6}(x_\varepsilon)$, the feedback laws $K_{\tilde{o}}$ and K_a applied to τ_k and a_k,

respectively, give

$$\begin{aligned}
K_{\tilde{o}}(m^i) &= \frac{1}{2}(m_4^i - m_5^i - m_2^i + m_3^i) \\
&= \frac{1}{2}\Big(\Big((\tau_k - a_k(2c+2d)) - (\tau_i - a_i(2c+3d))\Big) \\
&\qquad - \Big((\tau_i - a_i(c+d)) - (\tau_k - a_k(c+2d))\Big)\Big) \\
&= \frac{1}{2}\Big(2(\tau_k - \tau_i) + a_i(3c+4d) - a_k(3c+4d)\Big) \\
&= (\tau_k - \tau_i) + \frac{1}{2}(a_i - a_k)(3c+4d) \\
&= -\varepsilon_\tau + \gamma_1 \varepsilon_a \\
K_a(m^i, \tau_k) &= \mu\big((m_1^i - m_5^i) - (\tau_k - m_4^i)\big) \\
&= \mu\big((\tau_i - a_i(d) - (\tau_i - a_i(2c+3d))) \\
&\qquad - (\tau_k - (\tau_k - a_k(2c+2d)))\big) \\
&= \mu\big((a_i(2c+3d) + a_i(d)) - (a_k(2c+2d))\big) \\
&= \mu(a_i - a_k)(2c+2d) \\
&= \mu\gamma_2\varepsilon_a
\end{aligned}$$

where $\gamma_1 = \frac{3c+4d}{2}$ and $\gamma_2 = 2(c+d)$. Using the expressions for $K_{\tilde{o}}(m^i)$ and $K_a(m^i, \tau_k)$, it follows that

$$\begin{aligned}
V(G_{\varepsilon_6}(x_\varepsilon)) - V(x_\varepsilon) &= \left[\varepsilon + \begin{bmatrix} K_{\tilde{o}}(m^i) \\ -K_a(m^i, \tau_k) \end{bmatrix}\right]^\top \exp\big(6dA_f^\top\big) P \exp\big(6dA_f\big) \left[\varepsilon + \begin{bmatrix} K_{\tilde{o}}(m^i) \\ -K_a(m^i, \tau_k) \end{bmatrix}\right] \\
&\qquad - \varepsilon^\top P \varepsilon \\
&= \begin{bmatrix} \varepsilon_\tau - \varepsilon_\tau + \gamma_1\varepsilon_a \\ \varepsilon_a - \mu\gamma_2\varepsilon_a \end{bmatrix}^\top \exp\big(6dA_f^\top\big) P \exp\big(6dA_f\big) \begin{bmatrix} \varepsilon_\tau - \varepsilon_\tau + \gamma_1\varepsilon_a \\ \varepsilon_a - \mu\gamma_2\varepsilon_a \end{bmatrix} - \varepsilon^\top P \varepsilon \\
&= \varepsilon \begin{bmatrix} 0 & \gamma_1 \\ 0 & 1-\mu\gamma_2 \end{bmatrix}^\top \exp\big(6dA_f^\top\big) P \exp\big(6dA_f\big) \begin{bmatrix} 0 & \gamma_1 \\ 0 & 1-\mu\gamma_2 \end{bmatrix} \varepsilon - \varepsilon^\top P \varepsilon \\
&= \varepsilon^\top A_g^\top \exp\big(6dA_f^\top\big) P \exp\big(6dA_f\big) A_g \varepsilon - \varepsilon^\top P \varepsilon \\
&= \varepsilon^\top \Big(A_g^\top \exp\big(6dA_f^\top\big) P \exp\big(6dA_f\big) A_g - P\Big)\varepsilon
\end{aligned}$$

for each $x_\varepsilon \in D_{\varepsilon_6} \cap \mathcal{M}_6$. Then, by continuity of condition (5.37), there exists σ as in (5.38) such that

$$V(G_{\varepsilon_6}) - V(x_\varepsilon) \leq -\sigma\varepsilon^\top\varepsilon$$

for each $x_\varepsilon \in D_{\varepsilon_6} \cap \mathcal{M}_6$. $\square$

Remark 5.4.3. *Observe that condition (5.37) may be difficult to satisfy numerically as it may not be convex in μ and P. The authors in [20] utilize a polytopic embedding strategy to arrive at a linear matrix inequality in which one needs to find some matrices X_i such that the exponential matrix is an element in the convex hull of the X_i matrices. Such an algorithm can be adapted to our setting.*

Theorem 5.4.4. *Let the hybrid system $\mathcal{H}_\varepsilon$ in (5.23) with constants $d \geq c > 0$ be given. If there exist a constant $\mu > 0$ and a positive definite symmetric matrix P such that (5.37) holds with $\gamma_1 = \frac{3c+4d}{2}$ and $\gamma_2 = 2(c+d)$, and σ as in (5.38) such that*

$$\eta^{\frac{1}{6}} \rho < 1 \tag{5.39}$$

with $\eta = \left|1 - \frac{\sigma}{\alpha_2}\right|$ and $\rho = \exp\left(\frac{\gamma c}{2\alpha_2}\right)$ holds, where α_2 and γ are as given in (5.31) and (5.31), respectively, then $\mathcal{A}_\varepsilon$ is globally attractive for $\mathcal{H}_\varepsilon$. Moreover, every maximal solution ϕ_ε to $\mathcal{H}_\varepsilon$ with $\phi(0,0) \in \big(C_\varepsilon \cup D_\varepsilon\big) \cap \mathcal{M}$, satisfies

$$|\phi(t,j)|_{\mathcal{A}_\varepsilon} \leq \sqrt{\frac{\alpha_2}{\alpha_1}\eta^{\frac{j}{6}}\rho^j \exp\Big(\frac{\gamma c}{\alpha_2}\Big)}|\phi(0,0)|_{\mathcal{A}_\varepsilon} \quad \forall (t,j) \in \operatorname{dom} \phi \tag{5.40}$$

where

$$\alpha_1 = \min_{\nu \in \mathcal{Q}, \sigma \in \mathcal{P}} \Big(\exp\big((\nu h(\nu) + d(5-\sigma))A_f^\top\big) P \exp\big(\big(\nu h(\nu) + d(5-\sigma)\big)A_f\big)\Big)$$

and, consequently, $\lim_{t+j\to\infty} |\phi(t,j)|_{\mathcal{A}_\varepsilon} = 0$.

Proof. Pick a maximal solution with initial condition $\phi_\varepsilon(0,0) \in \big(C_\varepsilon \cup D_\varepsilon\big) \cap \mathcal{M}$. Recall the function V in (5.28), from the proof of Lemma 5.4.2 we have that

$$V(G_{\varepsilon_6}(x_\varepsilon)) - V(x_\varepsilon) \leq -\sigma \varepsilon^\top \varepsilon \qquad \forall x_\varepsilon \in D_{\varepsilon_6} \cap \mathcal{M} \tag{5.41}$$

and from the definition of V in (5.28), there exists a positive scalar α_2 as in (5.30) such that

$$V(x_\varepsilon) \leq \alpha_2 |x_\varepsilon|^2_{\mathcal{A}_\varepsilon}$$

rearranging terms one then has

$$-|x_\varepsilon|^2_{\mathcal{A}_\varepsilon} \leq -\frac{1}{\alpha_2} V(x_\varepsilon)$$

Then, by making the appropriate substitutions in (5.41), since $\varepsilon^\top \varepsilon = |x_\varepsilon|^2_{\mathcal{A}_\varepsilon}$ one has

$$V(G_{\varepsilon_6}(x_\varepsilon)) - V(x_\varepsilon) \leq -\frac{\sigma}{\alpha_2} V(x_\varepsilon)$$
$$V(G_{\varepsilon_6}(x_\varepsilon)) \leq \Big|1 - \frac{\sigma}{\alpha_2}\Big| V(x_\varepsilon)$$

From Lemma 5.4.1 we have that for each $x_\varepsilon \in C_\varepsilon$,

$$\langle \nabla V(x_\varepsilon), F_\varepsilon(x_\varepsilon) \rangle \leq \begin{cases} 0 & \text{if } x_\varepsilon \in C_{\varepsilon_2} \\ \frac{\gamma}{\alpha_2} V(x_\varepsilon) & \text{if } x_\varepsilon \in C_{\varepsilon_1} \end{cases} \tag{5.42}$$

and from Lemma 5.4.2 we have that for each $x_\varepsilon \in D_\varepsilon \cap \mathcal{M}$,

$$V(G_{\varepsilon_\ell}(x_\varepsilon)) \leq \begin{cases} V(x_\varepsilon) & \text{if } \ell \in \{1,2,3,4,5\} \\ \Big(1 - \frac{\sigma}{\alpha_2}\Big) V(x_\varepsilon) & \text{if } \ell = 6 \end{cases} \tag{5.43}$$

Pick a solution ϕ to $\mathcal{H}_\varepsilon$ with $\phi_\varepsilon(0,0) \in C_\varepsilon \cap \mathcal{M}_1$. Then for each $(t,j) \in [0,t_1] \times \{0\}$

$$V\big(\phi_\varepsilon(t,0)\big) \leq \exp\Big(\frac{\gamma}{\alpha_2}(t_1 - 0)\Big) V\big(\phi_\varepsilon(0,0)\big)$$

At $(t_1,1)$, following a reset according to G_{ε_1} one has

$$V\big(\phi_\varepsilon(t_1,1)\big) \leq V\big(\phi_\varepsilon(t_1,0)\big)$$

Then, since $\phi_q(t_1,1) = 1$ for each $(t,j) \in [t_1,t_2] \times \{1\}$, we obtain

$$V\big(\phi_\varepsilon(t,1)\big) \leq V\big(\phi_\varepsilon(t_1,1)\big)$$

At $(t_2,2)$, following a reset according to G_{ε_2} one has

$$V\big(\phi_\varepsilon(t_2,2)\big) \leq V\big(\phi_\varepsilon(t_2,1)\big)$$

Then since $\phi_q(t_2,2) = 0$ for each $(t,j) \in [t_2,t_3] \times \{2\}$, we obtain

$$V\big(\phi_\varepsilon(t,2)\big) \leq \exp\Big(\frac{\gamma}{\alpha_2}(t_3 - t_2)\Big) V\big(\phi_\varepsilon(t_2,2)\big)$$

At $(t_3,3)$, following a reset according to G_{ε_3} one has

$$V\big(\phi_\varepsilon(t_3,3)\big) \leq V\big(\phi_\varepsilon(t_3,3)\big)$$

Then since $\phi_q(t_3, 3) = 1$ for each $(t, j) \in [t_3, t_4] \times \{3\}$, we obtain

$$V\big(\phi_\varepsilon(t, 3)\big) \leq V\big(\phi_\varepsilon(t_3, 2)\big)$$

At $(t_4, 4)$ following a reset according to G_{ε_4} one has

$$V\big(\phi_\varepsilon(t_4, 4)\big) \leq V\big(\phi_\varepsilon(t_4, 3)\big)$$

Then since $\phi_q(t_4, 4) = 0$ for each $(t, j) \in [t_4, t_5] \times \{4\}$, we obtain

$$V\big(\phi_\varepsilon(t, 4)\big) \leq \exp\Big(\frac{\gamma}{\alpha_2}(t_5 - t_4)\Big) V\big(\phi_\varepsilon(t_4, 4)\big)$$

At $(t_5, 5)$, following a reset according to G_{ε_5} one has

$$V\big(\phi_\varepsilon(t_5, 5)\big) \leq V\big(\phi_\varepsilon(t_5, 4)\big)$$

then since $\phi_q(t_5, 5) = 1$ for each $(t, j) \in [t_5, t_6] \times \{5\}$, we obtain

$$V\big(\phi_\varepsilon(t, 5)\big) \leq V\big(\phi_\varepsilon(t_5, 5)\big)$$

At $(t_6, 6)$, following a reset according to G_{ε_6} one has

$$V\big(\phi_\varepsilon(t_6, 6)\big) \leq \Big|1 - \frac{\sigma}{\alpha_2}\Big| V\big(\phi_\varepsilon(t_6, 5)\big)$$

Making the appropriate substitutions one has

$$V\big(\phi_\varepsilon(t_6, 6)\big) \leq \Big|1 - \frac{\sigma}{\alpha_2}\Big| \exp\Big(\frac{\gamma}{\alpha_2}(t_5 - t_4)\Big) \exp\Big(\frac{\gamma}{\alpha_2}(t_3 - t_2)\Big) \exp\Big(\frac{\gamma}{\alpha_2}(t_1 - 0)\Big) V\big(\phi_\varepsilon(0, 0)\big)$$

leading to a general bound of the form

$$V\big(\phi_\varepsilon(t, j)\big) \leq \Big|1 - \frac{\sigma}{\alpha_2}\Big|^{\lfloor \frac{j}{6} \rfloor} \Bigg(\prod_{k=0}^{\lfloor \frac{j-1}{2} \rfloor} \exp\Big(\frac{\gamma}{\alpha_2}(t_{2k+1} - t_{2k})\Big)\Bigg) V\big(\phi_\varepsilon(0, 0)\big) \tag{5.44}$$

However, by noting the bounds in (6.5) one has that $t_{j+1} - t_j \leq c(j + 1)$ for each $j \in \{2i : i \in \mathbb{N}\}, j > 0$, then assuming $\gamma > 0$, the bound in (5.44) reduces to

$$V\big(\phi_\varepsilon(t, j)\big) \leq \Big|1 - \frac{\sigma}{\alpha_2}\Big|^{\lfloor \frac{j}{6} \rfloor} \Bigg(\prod_{k=0}^{\lfloor \frac{j-1}{2} \rfloor} \exp\Big(\frac{\gamma}{\alpha_2}(c(2k + 1))\Big)\Bigg) V\big(\phi_\varepsilon(0, 0)\big)$$

$$V\big(\phi_\varepsilon(t, j)\big) \leq \Big|1 - \frac{\sigma}{\alpha_2}\Big|^{\lfloor \frac{j}{6} \rfloor} \Bigg(\exp\Big(\frac{\gamma c}{\alpha_2}\Big)\Bigg)^{\lceil \frac{j}{2} \rceil} V\big(\phi_\varepsilon(0, 0)\big)$$

Using the relation $\lceil \frac{j}{2} \rceil = \frac{j}{2} + 1$ we then have

$$V\big(\phi_\varepsilon(t,j)\big) \leq \Big|1 - \frac{\sigma}{\alpha_2}\Big|^{\lfloor \frac{j}{6} \rfloor} \bigg(\exp\Big(\frac{\gamma c}{\alpha_2}\Big)\bigg)^{\frac{j}{2}} \exp\Big(\frac{\gamma c}{\alpha_2}\Big) V\big(\phi_\varepsilon(0,0)\big)$$

Then noting that $\lfloor \frac{j}{6} \rfloor \leq \frac{j}{6}$

$$V(t,j) \leq \Big|1 - \frac{\sigma}{\alpha_2}\Big|^{\frac{j}{6}} \bigg(\exp\Big(\frac{\gamma c}{2\alpha_2}\Big)\bigg)^{j} \exp\Big(\frac{\gamma c}{\alpha_2}\Big) V(0,0)$$

Then given the definition of V in (5.28) we have that

$$\alpha_1 |x_\varepsilon|^2_{\mathcal{A}_\varepsilon} \leq V\big(\phi_\varepsilon(t,j)\big) \leq \Big|1 - \frac{\sigma}{\alpha_2}\Big|^{\frac{j}{6}} \bigg(\exp\Big(\frac{\gamma c}{2\alpha_2}\Big)\bigg)^{j} \exp\Big(\frac{\gamma c}{\alpha_2}\Big) V\big(\phi_\varepsilon(0,0)\big) \tag{5.45}$$

Finally, by leveraging $V(\phi(0,0)) \leq \alpha_2 |\phi(0,0)|^2_{\mathcal{A}_\varepsilon}$, we arrive at (5.40). □

5.5 About the Multi-Agent Case

In this section, we present an extension to the proposed algorithm model to capture the scenario of synchronizing multiple networked agents. For such a setting, we consider the leader-follower scenario where there exists a single designated reference node to which all the connected nodes synchronize. To this end, let $\tau_R \in \mathbb{R}$ define the clock of the designated reference node and $\tau_S := (\tau_{S_1}, \tau_{S_2}, \ldots, \tau_{S_{n-1}}) \in \mathbb{R}^{n-1}$ define the clocks of the synchronizing child nodes. Moreover, we let $a_R \in \mathbb{R}$ and $a := (a_1, a_2, \ldots, a_{n-1}) \in \mathbb{R}^{n-1}$ define the skews of the reference clock and synchronizing clocks, respectively. Given the leader-follower architecture to synchronize the nodes, the algorithm in $\mathcal{H}$ is modified such that the algorithm modeled by $\mathcal{H}$ is executed for each synchronizing node. In particular, the algorithm executes the synchronization process given by (P1)-(P6) for the reference node τ_R and the i-th child node τ_{S_i}. Upon completion, the algorithm then executes the same synchronization steps (P1)-(P6) for the reference node and the $i+1$-th child node. This procedure is repeated recurrently and cyclically for each pair reference-child node in the network. To enable the modeling of such an algorithm, we define:

- A discrete variable $\ell \in \{1, 2, \ldots, n-1\} =: \mathcal{S}$ that indexes the node to be synchronized. The variable remains constant during flows, namely, $\dot{s} = 0$, and resets to either $s+1$ upon the completion of the synchronization algorithm for $s \in \{1, 2, \ldots, n-2\}$ or is reset to 1 when $s = n-1$.

- For each $\ell \in \mathcal{S}$, a timer variable $\tilde{\tau}_\ell \in [0, 3c + 3d]$ to track the execution of the synchronization algorithm for the respective ℓ-th child node, with dynamics

$$\begin{aligned} \dot{\tilde{\tau}}_\ell &= -1 & \tilde{\tau}_\ell &\in [0, 3c + 3d] \\ \tilde{\tau}_\ell^+ &= 3c + 3d & \tilde{\tau}_\ell &= 0 \end{aligned}$$

  for each $\ell \in \mathcal{S}$. The value $3c+3d$ reflects the duration of the synchronization algorithm executed between the reference and the synchronizing node capturing the total time elapsed during message transmission and residence delay.

The state of this multi-agent system is given by

$$\tilde{x} := (\tau_R, \tau_S, a_R, a, \tau, \tilde{\tau}, m^R, m^S, \ell, p, q) \in \widetilde{\mathcal{X}}$$

where $\tilde{\tau} := (\tilde{\tau}_1, \tilde{\tau}_2, \ldots, \tilde{\tau}_{n-1})$ and

$$\widetilde{\mathcal{X}} := \mathbb{R} \times \mathbb{R}^{n-1} \times \mathbb{R} \times \mathbb{R}^{n-1} \times [0, d] \times [0, 3c + 3d]^{n-1} \times \mathbb{R}^6 \times \mathbb{R}^6 \times \mathcal{S} \times \mathcal{P} \times \mathcal{Q}$$

Then by noting the dynamics of the clocks as given in (5.1) and those of the timer $\tau_{\mathcal{H}}$ above, the continuous dynamics of $\tilde{x}$ is given by the flow map

$$\widetilde{F}(\tilde{x}) = (a_R, a, 0, \mathbf{0}_{n-1\times 1}, -1, -\mathbf{1}_{(n-1)\times 1}, \mathbf{0}_{6\times 1}, \mathbf{0}_{6\times 1}, 0, 0, 0) \quad \forall \tilde{x} \in \widetilde{C} := \widetilde{\mathcal{X}}$$

To model the discrete dynamics of the communication and arrival events of the exchanged timing messages, in addition to the subsequent corrections on the clock rate and offset, we consider the jump map $\widetilde{G}(\tilde{x}) := \{\widetilde{G}^i(\tilde{x}) : \tilde{x} \in \widetilde{D}^i, i \in \mathcal{S}\}$ where

$$\widetilde{G}^i(\tilde{x}) = \widetilde{G}^i_k(\tilde{x}) \quad \text{if } x \in \widetilde{D}^\ell_k$$

and

$$\widetilde{G}_1^i(\tilde{x}) = \begin{bmatrix} \tau_R \\ \tau_S \\ a_R \\ a \\ d \\ \tau_{\mathcal{H}} \\ \left[\left[\tau_R, \quad m_1^R, \quad \cdots, \quad m_5^R\right] \quad m^s\right]^\top \\ \ell \\ p+1 \\ 1 \end{bmatrix}, \quad \widetilde{G}_2^i(\tilde{x}) = \begin{bmatrix} \tau_R \\ \tau \\ a_R \\ a \\ c \\ \tau_{\mathcal{H}} \\ \left[m^R \quad \left[\tau_i, \quad m_1^R, \quad \cdots, \quad m_5^R\right]\right]^\top \\ \ell \\ p+1 \\ 0 \end{bmatrix},$$

$$\widetilde{G}_3^i(\tilde{x}) = \begin{bmatrix} \tau_R \\ \tau_S \\ a_R \\ a \\ d \\ \tau_{\mathcal{H}} \\ \left[m^R \quad \left[\tau_i, \quad m_1^s, \quad \cdots, \quad m_5^s\right]\right]^\top \\ \ell \\ p+1 \\ 1 \end{bmatrix}, \quad \widetilde{G}_4^i(\tilde{x}) = \begin{bmatrix} \tau_R \\ \tau_S \\ a_R \\ a \\ c \\ \tau_{\mathcal{H}} \\ \left[\left[\tau_R, \quad m_1^s, \quad \cdots, \quad m_5^s\right] \quad m^s\right]^\top \\ \ell \\ p+1 \\ 0 \end{bmatrix},$$

$$\widetilde{G}_5^i(\tilde{x}) = \begin{bmatrix} \tau_R \\ \tau_S \\ a_R \\ a \\ d \\ \tau_{\mathcal{H}} \\ \left[\left[\tau_R, \quad m_1^R, \quad \cdots, \quad m_5^R\right] \quad m^s\right]^\top \\ \ell \\ p+1 \\ 1 \end{bmatrix},$$

$$\widetilde{G}_6^i(\tilde{x}) = \begin{bmatrix} \tau_R \\ \tau - \begin{bmatrix} \mathbf{0}_{i-1}, & K_{\tilde{\sigma}}(m^R), & \mathbf{0}_{n-1-i} \end{bmatrix}^\top \\ a_R \\ a + \begin{bmatrix} \mathbf{0}_{i-1}, & K_a(m^R, \tau_{S_i}), & \mathbf{0}_{n-1-i} \end{bmatrix}^\top \\ c \\ \begin{bmatrix} \tau_{\mathcal{H}_1}, & \ldots, & \tau_{\mathcal{H}_i}, & 3c+3d, & \tau_{\mathcal{H}_{i+2}}, & \ldots, & \tau_{\mathcal{H}_{n-1}} \end{bmatrix}^\top \\ \begin{bmatrix} m^R & \begin{bmatrix} \tau_i, & m_1^R, & \cdots, & m_5^R \end{bmatrix} \end{bmatrix}^\top \\ \ell + 1 \\ 0 \\ 0 \end{bmatrix}$$

To handle the condition where $\ell = n-1$ such that the protocol cycles back to synchronizing the first node, we have the following jump map for G_6^{n-1},

$$\widetilde{G}_6^{n-1}(\tilde{x}) = \begin{bmatrix} \tau_R \\ \tau - \begin{bmatrix} \mathbf{0}_{i-1}, & K_{\tilde{\sigma}}(m^R), & \mathbf{0}_{n-1-i} \end{bmatrix}^\top \\ a_R \\ a + \begin{bmatrix} \mathbf{0}_{i-1}, & K_a(m^R, \tau_i), & \mathbf{0}_{n-1-i} \end{bmatrix}^\top \\ c \\ \begin{bmatrix} \tau_{\mathcal{H}_1}, & \ldots, & \tau_{\mathcal{H}_{n-2}}, & 3c+3d \end{bmatrix}^\top \\ \begin{bmatrix} m^R & \begin{bmatrix} \tau_i, & m_1^R, & \cdots, & m_5^R \end{bmatrix} \end{bmatrix}^\top \\ 1 \\ 0 \\ 0 \end{bmatrix}$$

To trigger the jump map corresponding to the particular protocol event, we define the jump set as $\widetilde{D} := \widetilde{D}^1 \cup \widetilde{D}^2 \cup \cdots \cup \widetilde{D}^i \cup \cdots \cup \widetilde{D}^{n-1}$ where $\widetilde{D}^i := \widetilde{D}_1^i \cup \widetilde{D}_2^i \cup \widetilde{D}_3^i \cup \widetilde{D}_4^i \cup \widetilde{D}_5^i \cup \widetilde{D}_6^i$ and

$$\widetilde{D}_1^i := \{\tilde{x} \in \widetilde{\mathcal{X}} : \tau = 0, p = 0, \ell = i\}, \qquad \widetilde{D}_2^i := \{\tilde{x} \in \widetilde{\mathcal{X}} : \tau = 0, p = 1, \ell = i\}$$
$$\widetilde{D}_3^i := \{\tilde{x} \in \widetilde{\mathcal{X}} : \tau = 0, p = 2, \ell = i\}, \qquad \widetilde{D}_4^i := \{\tilde{x} \in \widetilde{\mathcal{X}} : \tau = 0, p = 3, \ell = i\}$$
$$\widetilde{D}_5^i := \{\tilde{x} \in \widetilde{\mathcal{X}} : \tau = 0, p = 4, \ell = i\}, \qquad \widetilde{D}_6^i := \{\tilde{x} \in \widetilde{\mathcal{X}} : \tau = 0, \tau_{\mathcal{H}_i} = 0, p = 5, \ell = i\}$$

This hybrid system is denoted

$$\widetilde{\mathcal{H}} = (\widetilde{C}, \widetilde{F}, \widetilde{D}, \widetilde{G}) \tag{5.46}$$

Error Model

With an abuse of notation, let $\varepsilon := (\varepsilon_1, \ldots, \varepsilon_{n-1}) \in \mathbb{R}^{2(n-1)}$, where $\varepsilon_i = \begin{bmatrix} \tau_R - \tau_i \\ a_R - a_i \end{bmatrix}$ for each $i \in \mathcal{S}$. Then, define

$$\tilde{x}_\varepsilon := (\varepsilon, \tilde{x}) \in \widetilde{\mathcal{X}}_\varepsilon := \mathbb{R}^{2(n-1)} \times \tilde{\mathcal{X}}$$

For each $\tilde{x}_\varepsilon \in \widetilde{C}_\varepsilon := \widetilde{\mathcal{X}}_\varepsilon$, the flow map is given by

$$\widetilde{F}_\varepsilon(\tilde{x}_\varepsilon) = \big(A_F \varepsilon, \widetilde{F}(\tilde{x})\big)$$

where

$$A_F = \begin{bmatrix} A_f & \cdots & 0 \\ \vdots & \ddots & \vdots \\ 0 & \cdots & A_f \end{bmatrix}$$

where $A_f = \begin{bmatrix} 0 & 1 \\ 0 & 0 \end{bmatrix}$.

The discrete dynamics of the protocol are modeled through the jump map $\widetilde{G}_\varepsilon(\tilde{x}) := \{\widetilde{G}^i_\varepsilon(\tilde{x}) : \tilde{x}_\varepsilon \in \widetilde{D}^i_\varepsilon, i \in \mathcal{S}\}$ where

$$\widetilde{G}^i_\varepsilon(\tilde{x}_\varepsilon) = \begin{cases} \widetilde{G}^i_{\varepsilon_1}(\tilde{x}_\varepsilon) \text{ if } \tilde{x}_\varepsilon \in \widetilde{D}^i_{\varepsilon_1} \setminus (\widetilde{D}^i_{\varepsilon_2} \cup \widetilde{D}^i_{\varepsilon_3} \cup \widetilde{D}^i_{\varepsilon_4} \cup \widetilde{D}^i_{\varepsilon_5} \cup \widetilde{D}^i_{\varepsilon_6}) \\ \widetilde{G}^i_{\varepsilon_2}(\tilde{x}_\varepsilon) \text{ if } \tilde{x}_\varepsilon \in \widetilde{D}^i_{\varepsilon_2} \setminus (\widetilde{D}^i_{\varepsilon_1} \cup \widetilde{D}^i_{\varepsilon_3} \cup \widetilde{D}^i_{\varepsilon_4} \cup \widetilde{D}^i_{\varepsilon_5} \cup \widetilde{D}^i_{\varepsilon_6}) \\ \widetilde{G}^i_{\varepsilon_3}(\tilde{x}_\varepsilon) \text{ if } \tilde{x}_\varepsilon \in \widetilde{D}^i_{\varepsilon_3} \setminus (\widetilde{D}^i_{\varepsilon_1} \cup \widetilde{D}^i_{\varepsilon_2} \cup \widetilde{D}^i_{\varepsilon_4} \cup \widetilde{D}^i_{\varepsilon_5} \cup \widetilde{D}^i_{\varepsilon_6}) \\ \widetilde{G}^i_{\varepsilon_4}(\tilde{x}_\varepsilon) \text{ if } \tilde{x}_\varepsilon \in \widetilde{D}^i_{\varepsilon_4} \setminus (\widetilde{D}^i_{\varepsilon_1} \cup \widetilde{D}^i_{\varepsilon_2} \cup \widetilde{D}^i_{\varepsilon_3} \cup \widetilde{D}^i_{\varepsilon_5} \cup \widetilde{D}^i_{\varepsilon_6}) \\ \widetilde{G}^i_{\varepsilon_5}(\tilde{x}_\varepsilon) \text{ if } \tilde{x}_\varepsilon \in \widetilde{D}^i_{\varepsilon_5} \setminus (\widetilde{D}^i_{\varepsilon_1} \cup \widetilde{D}^i_{\varepsilon_2} \cup \widetilde{D}^i_{\varepsilon_3} \cup \widetilde{D}^i_{\varepsilon_4} \cup \widetilde{D}^i_{\varepsilon_6}) \\ \widetilde{G}^i_{\varepsilon_6}(\tilde{x}_\varepsilon) \text{ if } \tilde{x}_\varepsilon \in \widetilde{D}^i_{\varepsilon_6} \setminus (\widetilde{D}^i_{\varepsilon_1} \cup \widetilde{D}^i_{\varepsilon_2} \cup \widetilde{D}^i_{\varepsilon_3} \cup \widetilde{D}^i_{\varepsilon_4} \cup \widetilde{D}^i_{\varepsilon_5}) \end{cases}$$

where

$$\widetilde{G}^i_{\varepsilon_1}(\tilde{x}_\varepsilon) = \begin{bmatrix} \varepsilon \\ \widetilde{G}^i_1(\tilde{x}) \end{bmatrix}, \ \widetilde{G}^i_{\varepsilon_2}(\tilde{x}_\varepsilon) = \begin{bmatrix} \varepsilon \\ \widetilde{G}^i_2(\tilde{x}) \end{bmatrix}, \ \widetilde{G}^i_{\varepsilon_3}(\tilde{x}_\varepsilon) = \begin{bmatrix} \varepsilon \\ \widetilde{G}^i_3(\tilde{x}) \end{bmatrix},$$

$$\widetilde{G}^i_{\varepsilon_4}(\tilde{x}_\varepsilon) = \begin{bmatrix} \varepsilon \\ \widetilde{G}^i_4(\tilde{x}) \end{bmatrix}, \ \widetilde{G}^i_{\varepsilon_5}(\tilde{x}_\varepsilon) = \begin{bmatrix} \varepsilon \\ \widetilde{G}^i_5(\tilde{x}) \end{bmatrix}, \ \widetilde{G}^i_{\varepsilon_6}(\tilde{x}_\varepsilon) = \begin{bmatrix} \big[\varepsilon_1, \ldots, \varepsilon^+_i, \ldots, \varepsilon_{n-1}\big]^\top \\ \widetilde{G}^i_6(\tilde{x}) \end{bmatrix}$$

where

$$\varepsilon^+_i = \begin{bmatrix} \tau_R - \big(\tau_i - K_{\tilde{o}}(\tilde{x})\big) \\ a_R - \big(a_i + K_a(\tilde{x})\big) \end{bmatrix}$$

These discrete dynamics apply for x in $\widetilde{D}_\varepsilon := \widetilde{D}^1_\varepsilon \cup \widetilde{D}^2_\varepsilon \cup \cdots \cup \widetilde{D}^i_\varepsilon \cup \cdots \cup \widetilde{D}^{n-1}_\varepsilon$, where

$\widetilde{D}^i_\varepsilon := \widetilde{D}^i_{\varepsilon_1} \cup \widetilde{D}^i_{\varepsilon_2} \cup \widetilde{D}^i_{\varepsilon_3} \cup \widetilde{D}^i_{\varepsilon_4} \cup \widetilde{D}^i_{\varepsilon_5} \cup \widetilde{D}^i_{\varepsilon_6}$ and

$$\widetilde{D}^i_{\varepsilon_1} := \{\tilde{x}_\varepsilon \in \widetilde{\mathcal{X}}_\varepsilon : \tau = 0, p = 0, \ell = i\}, \qquad \widetilde{D}^i_{\varepsilon_2} := \{\tilde{x}_\varepsilon \in \widetilde{\mathcal{X}}_\varepsilon : \tau = 0, p = 1, \ell = i\}$$
$$\widetilde{D}^i_{\varepsilon_3} := \{\tilde{x}_\varepsilon \in \widetilde{\mathcal{X}}_\varepsilon : \tau = 0, p = 2, \ell = i\}, \qquad \widetilde{D}^i_{\varepsilon_4} := \{\tilde{x}_\varepsilon \in \widetilde{\mathcal{X}}_\varepsilon : \tau = 0, p = 3, \ell = i\}$$
$$\widetilde{D}^i_{\varepsilon_5} := \{\tilde{x}_\varepsilon \in \widetilde{\mathcal{X}}_\varepsilon : \tau = 0, p = 4, \ell = i\}, \qquad \widetilde{D}^i_{\varepsilon_6} := \{\tilde{x}_\varepsilon \in \widetilde{\mathcal{X}}_\varepsilon : \tau = 0, \tau_{\mathcal{H}_i} = 0, p = 5, \ell = i\}$$

This hybrid system is denoted

$$\widetilde{\mathcal{H}}_\varepsilon = (\widetilde{C}_\varepsilon, \widetilde{F}_\varepsilon, \widetilde{D}_\varepsilon, \widetilde{G}_\varepsilon) \tag{5.47}$$

and the set to render attractive for the multi-agent model is given by

$$\widetilde{\mathcal{A}}_\varepsilon := \{\tilde{x}_\varepsilon \in \widetilde{\mathcal{X}}_\varepsilon : \varepsilon_i = 0 \; \forall i \in \mathcal{S}\} \tag{5.48}$$

With the system defined in this manner, one can extend the results of the two-agent model to the multi-agent setting to certify attractivity of $\widetilde{\mathcal{H}}_\varepsilon$ to $\widetilde{\mathcal{A}}_\varepsilon$. To demonstrate the feasibility of the model, a numerical example illustrating the convergence properties of $\widetilde{\mathcal{H}}_\varepsilon$ is included in the following section where a three-agent system is simulated.

5.6 Numerical Results

5.6.1 Two-agent system

Nominal Setting

In this first example, we present a numerical simulation of the two-agent system for the nominal setting that validates our theoretical results, namely we show that with the conditions in (5.37) satisfied, the trajectories of the simulation converge to the desired set.

Example 5.6.1. *Consider Nodes i and k with dynamics as in (5.1) with data $a_i = 1$, $a_k = 1.8$ and $c = 0.1$, $d = 0.2$ to the system $\mathcal{H}$. Setting $\mu = 0.833$, condition (5.37) is satisfied with $P = \begin{bmatrix} 6.2594 & -0.5219 \\ -0.5219 & 11.4302 \end{bmatrix}$. Simulating the system, Figure 6.1 shows the trajectories of the error in the clocks and error in the clock rates of Nodes i and k for a solution ϕ to the system such that $\phi(0,0) \in (C \cup D) \cap \mathcal{M}$. Figure 6.1 also shows the plot of V evaluated along the solution. Notice, that V converges to zero asymptotically following several periodic executions of the algorithm. Observe that the behavior of clock error is more stable than the conventional sender-receiver algorithm simulated in Figure 5.3.* [6]

[6] Code at github.com/HybridSystemsLab/HybridSenRecClockSync

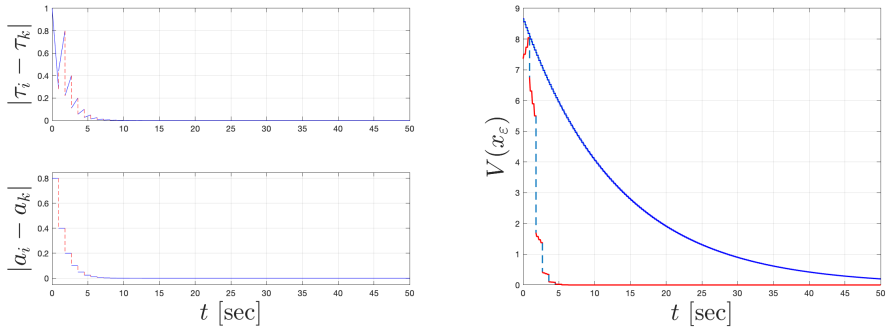

(a) (b)

Figure 5.5: Figure 6.1(a) gives the evolution of the error in the clocks and clock rates of Nodes i and k. Figure 6.1(b) gives V evaluated along the solution.

Variable propagation delay due to communication noise

In the next example, we simulate the case of noise in the communication channel that contributes to a variable propagation delay d. Noise in the communication channel makes the propagation delay between nodes i and k no longer symmetric.

Example 5.6.2. *Consider the same clock dynamics from the previous example, i.e.,* $a_i = 1.1$, $a_k = 0.75$, *with* $\mu = 0.3571$ *and condition (5.37) satisfied for* $c = 0.2$, $d = 0.5$, *and* $P = \begin{bmatrix} 5.435 & 1.041 \\ 1.041 & 16.0982 \end{bmatrix}$. *Now, with* $[d_1, d_2]$ *defining the allowed values of* d *with* $d_1 = 0.49$ *and* $d_2 = 0.51$, *we generate variable propagation delay by replacing the dynamics of* τ *in (5.13) by*

$$\dot{\tau} = -1 \qquad \tau \in [0, d_2]$$
$$\tau^+ \in \cup_{d\in[d_1,d_2]}(1-q)d + qc \quad \tau = 0$$

Figure 5.8 shows a simulation of the trajectories of the error in the clocks and error in the clock rates of Nodes i *and* k. *Observe that absolute error in the clocks converges to zero even in the presence of the perturbation after several periodic executions of the algorithm. The error in clock rates is also able to converge sufficiently close to zero but suffers from some observed variability due to the noise.* [7]

[7] Code at github.com/HybridSystemsLab/HybridSenRecClockSync

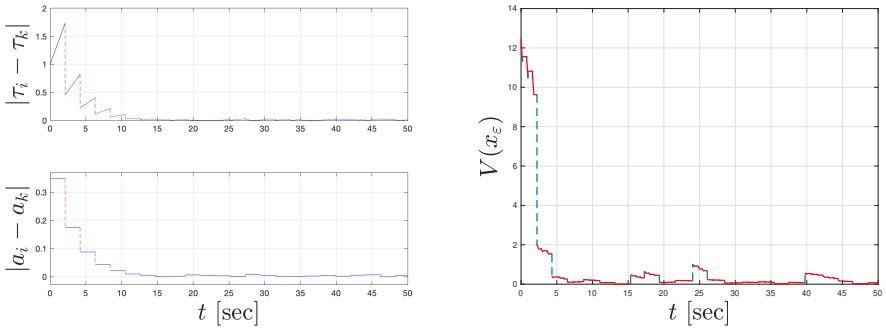

(a) (b)

Figure 5.6: Figure 6.1(a) gives the evolution of the error in the clocks and clock rates of Nodes i and $k$subject to noise on the communication channel. Figure 6.1(b) gives V evaluated along the solution.

Time-varying clock rates

In the next example, we consider the common scenario of time-varying clock skews at both nodes i and k. This noise is injected at the clock dynamics $\dot{\tau}_i$ and $\dot{\tau}_k$. The system is then simulated with the remaining dynamics left unchanged.

Example 5.6.3. *For $c = 0.2$ and $d = 0.5$, consider nodes i and k with clock dynamics*

$$\dot{\tau}_i = a_i + m_a$$
$$\dot{\tau}_k = a_k + m_a$$

where $a_i = 1.1$, $a_k = 0.75$, and $m_a \in (-0.3, 0.3)$ is a Gaussian injected noise on the clock dynamics. Letting $\mu = 0.3571$, condition (5.37) is satisfied with $P = \begin{bmatrix} 5.435 & 1.041 \\ 1.041 & 16.0982 \end{bmatrix}$. Simulating the system, Figure 5.7 shows the trajectories of the error in the clocks and error in the clock rates of Nodes i and k. Again, the system is able to converge after a couple of executions of the algorithm. The error on the clocks observes the most variability due to simulated noise.[8]

5.6.2 Multi-agent model

In this section we present numerical results for the multi-agent model to validate our theoretical results and draw comparisons with other multi-agent clock synchronization models from the literature.

[8]Code at github.com/HybridSystemsLab/HybridSenRecClockSync

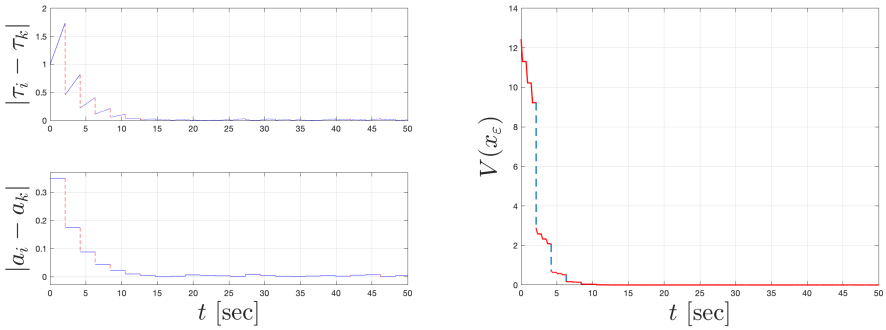

(a) (b)

Figure 5.7: Figure 6.1(a) gives the evolution of the error in the clocks and clock rates of Nodes i and k subject to noise m_a on the clock dynamics. Figure 6.1(b) gives V evaluated along the solution.

Example 5.6.4. *Consider a network of three nodes* $\{R, 1, 2\}$ *where* R *denotes the reference or parent node while nodes* 1,2 *denote the synchronizing child nodes. The data of this system is given by* $a_R, a_1, a_2 \in [0.5, 1.5]$ *and* $c = 0.1$, $d = 0.2$ *with* $\mu = 0.833$. *Simulating the multi-agent system* $\widetilde{\mathcal{H}}$, *Figure 5.7(a) shows the trajectories of the error in the clocks and error in the clock rates of Nodes* 1 *and* 2 *with respect to Node* R. *Note that the errors with respect to each clock converge after several executions of the algorithm on the respective clocks at Nodes* 1 *and* 2. [9]

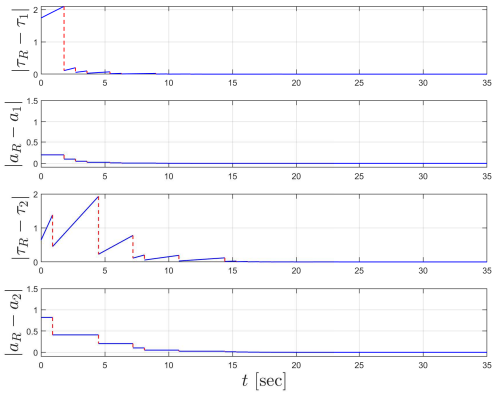

Figure 5.8: The evolution of the error in the clocks and clock rates of Nodes 1 and 2 with respect to Node R.

[9] Code at github.com/HybridSystemsLab/HybridSenRecMultiClockSync

5.7 Summary

In this chapter, we introduced a sender-receiver clock synchronization algorithm with sufficient design conditions ensuring synchronization. Results were given to show asymptotic attractivity of a set of interest reflecting the desired synchronized setting. Numerical results validating the attractivity of the system to the set of interest were also given. An additional model to capture the multi-agent setting was presented with a numerical example to demonstrate its feasibility.

Chapter 6

A General Framework for Hybrid Clock Synchronization

In this section, we motivate a hybrid systems approach to clock synchronization. For many networked control system settings, each agent in the system is fitted with its own internal hardware clock and an instance of a software clock based on the dynamics of the hardware clock. Ideally, the ith agent in the system would have a clock $\tau_i \in \mathbb{R}_{\geq 0}$ such that $\tau_i(t) = t$ where t is the global or real time. Due to the observed variability in oscillator frequency, one generally considers the continuous-time dynamics of the ith hardware clock node given by

$$\dot{\tau}_i = a_i \tag{6.1}$$

where $a_i \in \mathbb{R}$ defines clock drift or skew due to an imperfect oscillator. Solving the differential equation (6.1) gives the following relationship to the ideal clock or real-time reference t:

$$\tau_i(t) = a_i t + \tau_i(0) \quad \forall t \geq 0 \tag{6.2}$$

where the initial condition $\tau_i(0)$ gives the offset from $t = 0$. For a network of n agents, with $\tau = (\tau_1, \tau_2, \ldots, \tau_n)$ the notion of clock synchronization corresponds to the state of the networked system asymptotically satisfying $\tau_i = \tau_j$ for all $i, j \in \{1, 2, \ldots, n\}$, $i \neq j$, i.e.,

$$\lim_{t\to\infty} \tau_i(t) - \tau_j(t) = 0 \qquad \forall i, j \in \{1, 2, \ldots, n\}, i \neq j$$

In an ideal setting with no delay and identical clock skews, synchronization between two agents 1 and 2 can be achieved by the following algorithm: Agent 1 send its time to

Agent 2. Agent 2 calculates its offset relative to 1. Agent 2 applies the offset correction to its clock. For the case of different clock skews, a pair of measurements from Agent 1 would allow Agent 2 to calculate its relative skew $\frac{a_1}{a_2}$ and apply a correction accordingly.

In a realistic setting, however, network communication between agents is often subjected to a variety of delays. Without loss of generality, these delays can be divided into two types: *propagation* time and *residence* time. Propagation time represents the actual time elapsed during message transmission between two nodes when the message is in the network channel. The residence time defines the time elapsed between message reception and egress of its response message. It captures all of the hardware-related delays such as *send* time, *access* time, *transmission* time, *reception* time, and *receive* time, see [5] and [10] for more details. Moreover, depending on the system setting, these observed delays can either be deterministic or stochastic in nature and are the key challenge in networked clock synchronization. In light of this challenge, the goal of clock synchronization is to achieve synchronization while removing or mitigating the effects of delay.

6.0.1 Problem Statement and Proposed Solutions

Consider a group of n agents connected over a network represented by a digraph $\mathcal{G} = (\mathcal{V}, \mathcal{E}, A)$. Two clocks are attached to each node i of $\mathcal{G}$: an (uncontrollable) internal clock $\tau_i \in \mathbb{R}_{\geq 0}$ whose dynamics are given by

$$\dot{\tau}_i = a_i \tag{6.3}$$

and an adjustable (via software) clock $\hat{\tau}_i \in \mathbb{R}_{\geq 0}$ with dynamics given by

$$\dot{\hat{\tau}}_i = f_{\hat{\tau}_i}(a_i, u_i) \tag{6.4}$$

where $a_i \in \mathbb{R}$ is the drift of the internal clock (unknown) and $u_i \in \mathbb{R}$ is a control parameter to control the drift. At times t_j^i for $j \in \mathbb{N}$ (with $t_0^i = 0$), agents exchange information depending on the communication architecture and protocols used. When symmetric communication protocols are used, at each such t_j^i, agent i

- broadcasts a measurement $\hat{\tau}_i$ to its neighbors $\mathcal{N}_i$, and
- receives measurements $\hat{\tau}_k$ from each of its neighbors $k \in \mathcal{N}_i$,

On the other hand, when asymmetric communication protocols are used, at each such t_j^i, agent i

- broadcasts a measurement $\hat{\tau}_i$ to its neighbors $\mathcal{N}_i$.

The resulting sequence of time instants $\{t_j^i\}_{j=1}^{\infty}$ for each node i is assumed to be strictly increasing and unbounded. Moreover, for such a sequence, the time elapsed between each time instant when the clock measurements are exchanged is governed by

$$\begin{aligned} T_1^i \leq t_{j+1}^i - t_j^i \leq T_2^i \quad \forall j \in \mathbb{N} \setminus \{0\} \\ 0 \leq t_1^i \leq T_2^i \end{aligned} \tag{6.5}$$

where $T_2^i \geq T_1^i > 0$ with T_1^i defining the minimum time between consecutive measurements and T_2^i defines the maximum allowable transfer interval (MATI) for each node i.

Remark 6.0.1. *The models for the clocks are based on the hardware and software relationship of the real-time system that implements them. That is, the internal clock τ_i^* is treated as a type of hardware oscillator while the adjustable clock $\hat{\tau}_i$ is treated as a virtual clock, implemented in software (as part of the proposed algorithm), that evolves according to the dynamics of the hardware oscillator. Any virtual clock implemented in node i inherits the drift parameter a_i of the internal clock, which cannot be controlled. More importantly, this drift parameter is not known due to the fact that universal time information is not available to any node. Due to this, $f_{\hat{\tau}_i}$ in (6.4) would involve a_i in defining the rate of change of the software clock $\hat{\tau}_i$.*

Under such a setup, our goal is to design a distributed hybrid controller that drives each clock $\hat{\tau}_i$ to synchronization with every other clock $\hat{\tau}_k$. This problem is formally stated as follows:

Problem 6.0.1. *Given a network of n agents with dynamics as in (6.3) and (6.4) represented by a directed graph $\mathcal{G}$, design a distributed hybrid controller that achieves the following synchronization property:*

i) Clock synchronization: $\lim_{t\to\infty} |\hat{\tau}_i(t) - \hat{\tau}_k(t)| = 0$ *for all* $i, k \in \mathcal{V}$, $i \neq k$

In order to solve Problem 6.0.1, we introduce a hybrid modeling framework that allows for modeling of the network and clock dynamics accompanied by user-defined provisions for a clock synchronization algorithm. In particular, the framework defines sufficient

conditions imposed on the defined algorithm such that asymptotic stability of the system to a synchronization set capturing $\lim_{t\to\infty} |\hat{\tau}_i(t) - \hat{\tau}_k(t)| = 0$ for all $i, k \in \mathcal{V}$, $i \neq k$ is guaranteed.

6.1 Hybrid Modeling Framework

Given a set of n nodes connected over a directed graph $\mathcal{G}$ and the respective models for the internal and virtual clocks given in (6.3) and virtual (6.4), respectively, we consider internal clocks $\tau := (\tau_1, \tau_2, \ldots, \tau_n) \in \mathbb{R}^n_{\geq 0}$, adjustable clocks $\hat{\tau} := (\hat{\tau}_1, \hat{\tau}_2, \ldots, \hat{\tau}_n) \in \mathbb{R}^n_{\geq 0}$, internal clock rates $a := (a_1, a_2, \ldots, a_n) \in \mathbb{R}^n_{\geq 0}$, and clock correction rates $\nu := (\nu_1, \nu_2, \ldots, \nu_n) \in \mathbb{R}^n$.

In order to accommodate the various algorithms, we define an auxiliary state $u := (u_1, u_2, \ldots, u_n) \in \mathbb{R}^n$ with dynamics $\dot{u} = f_u(x)$. Moreover, we include controller states $w := (w_1, w_2, \ldots, w_n) \in \mathbb{R}^m$ whose dimension m is dependent on the dimension of the controller state(s) of the particular algorithm. To this end, we can then define the state of the complete system as follows:

$$x := (\tau, \hat{\tau}, u, \nu, w, \tilde{\tau}) \in \mathbb{R}^n_{\geq 0} \times \mathbb{R}^n_{\geq 0} \times \mathbb{R}^n \times \mathbb{R}^n \times \mathbb{R}^m \times \mathcal{T} =: \mathcal{X}$$

where $\mathcal{T} := [0, T_2^1] \times [0, T_2^2] \times \ldots \times [0, T_2^n]$

To model the network dynamics for the aperiodic communication events between each node i and its set of neighbors, we consider timers $\tilde{\tau} := (\tilde{\tau}_1, \tilde{\tau}_2, \ldots, \tilde{\tau}_n) \in \mathbb{R}^n_{\geq 0}$ such that each timer $\tilde{\tau}_i$ has hybrid dynamics

$$\begin{aligned} \dot{\tilde{\tau}}_i &= -a_i & \tilde{\tau}_i &\in [0, T_2^i] \\ \tilde{\tau}_i^+ &\in [T_1^i, T_2^i] & \tilde{\tau}_i &= 0 \end{aligned} \tag{6.6}$$

This model is such that when $\tilde{\tau}_i = 0$, a communication event between node i and its neighbors is triggered, and $\tilde{\tau}_i$ is reset to a point in $[T_1^i, T_2^i]$ in order to preserve the bound given in (6.5). Note that $\tilde{\tau}$ is treated as an additional software clock that inherits the dynamics of the hardware clock as described in Remark 6.0.1. Then, given the clock dynamics in (6.3), (6.4), and the continuous dynamics in (6.6), the flow dynamics of the symmetric

communication system are given by

$$f_{\mathrm{s}}(x) := \begin{bmatrix} a \\ f_{\hat{\tau}}(a,u) \\ f_u(x,u) \\ h\nu \\ f_w(w) \\ -a \end{bmatrix} \qquad \forall x \in C := \mathcal{X} \tag{6.7}$$

where $f_{\hat{\tau}} := (f_{\hat{\tau}_1}, f_{\hat{\tau}_2}, \ldots, f_{\hat{\tau}_n})$ and $f_{\hat{\tau}_i}$ is modeled as the software clock given in (6.4). The functions $f_u : \mathcal{X} \times \mathbb{R} \to \mathbb{R}$ and $f_w : \mathbb{R}^m \to \mathbb{R}^m$ are to be defined for each algorithm. The choice of $h\nu$ with $h \in \mathbb{R}$ enables additional control of the clock correction during flows as required by certain algorithms such as *HyNTP*. The flow dynamics of the asymmetric communication system are given by

$$f_{\mathrm{a}}(x) := \begin{bmatrix} a \\ f_{\hat{\tau}}(a,u) \\ f_u(x,u) \\ h\nu \\ f_w(w) \\ -a \end{bmatrix} \qquad \forall x \in C := \mathcal{X} \tag{6.8}$$

where $f_{\hat{\tau}} := \mathrm{diag}(a)\mathcal{D}u$ is modeled as the software clock given in (6.4) but whose control parameter u_i depends on the in-degree communication matrix $\mathcal{D}$. In particular, $\mathcal{D} = \mathrm{diag}(I \otimes \mathbf{1}_{d_{in}^1}^\top, \ldots, I \otimes \mathbf{1}_{d_{in}^n}^\top)$ with d_{in}^i being the in-degree of the ith agent. The functions $f_u : \mathcal{X} \times \mathbb{R} \to \mathbb{R}$ and $f_w : \mathbb{R}^m \to \mathbb{R}^m$ are again to be defined for each algorithm. The choice of $h\nu$ with $h \in \mathbb{R}$ again enables additional control of the clock correction during flows as required by certain algorithms. The discrete dynamics take the following general form for both the symmetric and asymmetric algorithms:

$$G(x) := \{G_i(x) : x \in D_i, i \in \mathcal{V}\} \tag{6.9}$$

where

$$G_i(x) := \begin{bmatrix} \tau \\ g_{\hat{\tau}}(x) \\ g_u(x) \\ g_\nu(x) \\ g_w(x) \\ (\tilde{\tau}_1, \ldots, \tilde{\tau}_{i-1}, [T_1^i, T_2^i], \tilde{\tau}_{i+1}, \ldots, \tilde{\tau}_n) \end{bmatrix} \tag{6.10}$$

is allowed at each $x \in D := \bigcup_{i \in \mathcal{V}} D_i$ with $D_i := \{x \in \mathcal{X} : \tilde{\tau}_i = 0\}$ where $g_{\hat{\tau}} : \mathcal{X} \to \mathbb{R}^n_{\geq 0}$, $g_u : \mathcal{X} \to \mathbb{R}^n$, $g_\nu : \mathcal{X} \to \mathbb{R}^n$, $g_w : \mathcal{X} \to \mathbb{R}^m$ are functions to be defined depending on the particular algorithm to be modeled. With the data defined, we let

$$\mathcal{H}_s = (C, f_{\mathrm{s}}, D, G) \tag{6.11}$$

denote the hybrid system for the modeling framework under symmetric communication protocols and

$$\mathcal{H}_a = (C, f_{\mathrm{a}}, D, G) \tag{6.12}$$

denote the hybrid system for the modeling framework under asymmetric communication protocols.

Given that the functional maps f_s, f_a, and G are comprised of functions that are to be defined by the dynamics of the respective algorithms, we impose continuity and boundedness assumptions on f_u, f_w, $g_{\hat{\tau}}$, g_u, g_ν, and g_w in order to satisfy continuity and boundedness conditions on the system data for $\mathcal{H}_s$ and $\mathcal{H}_a$.

Assumption 6.1.1. *The functions $f_u : \mathcal{X} \times \mathbb{R}^n \to \mathcal{X}$ and $f_w : \mathbb{R}^m \to \mathbb{R}^m$ are continuous and locally bounded relative to C.*

Assumption 6.1.2. *The functions $g_{\hat{\tau}} : \mathcal{X} \to \mathbb{R}^n_{\geq 0}$, $g_u : \mathcal{X} \to \mathbb{R}^n$, $g_\nu : \mathcal{X} \to \mathbb{R}^n$, $g_w : \mathcal{X} \to \mathbb{R}^m$ are outer continuous and bounded relative to D.*

Lemma 6.1.3. *Suppose Assumption 6.1.1 and Assumption 6.1.2. Then, hybrid systems $\mathcal{H}_s$ and $\mathcal{H}_a$ satisfy the following conditions, defined in [4, Assumption 6.5] as the hybrid basic conditions.*

(A1) C and D are closed sets of $\mathbb{R}^m$.

(A2) $f_a : \mathbb{R}^m \to \mathbb{R}^m$ *and* $f_s : \mathbb{R}^m \to \mathbb{R}^m$ *are continuous and, hence, locally bounded relative to* C *and* $C \subset$ *dom* f*.*

(A3) $G : \mathbb{R}^m \rightrightarrows \mathbb{R}^m$ *is outer semicontinuous and locally bounded relative to* D*, and* $D \subset$ *dom* G*.*

Proof. By inspection of the hybrid system data defining $\mathcal{H}_s$ given in (5.12), the following is observed:

- The set C is a closed subset of $\mathbb{R}^m$ since, $C = \mathcal{X}$ and $\mathcal{X}$ is the Cartesian product of closed sets. Similar arguments show that D is closed since it can be written as

$$\begin{aligned} D = &\mathbb{R}^n_{\geq 0} \times \mathbb{R}^n_{\geq 0} \times \mathbb{R}^n \times \mathbb{R}^n \times \mathbb{R}^m \times \{0\} \times [0, T_2^2] \times \ldots \times [0, T_2^n] \\ &\cup \mathbb{R}^n_{\geq 0} \times \mathbb{R}^n_{\geq 0} \times \mathbb{R}^n \times \mathbb{R}^n \times \mathbb{R}^m \times [0, T_2^1] \times \{0\} \times \ldots \times [0, T_2^n] \\ &\vdots \\ &\cup \mathbb{R}^n_{\geq 0} \times \mathbb{R}^n_{\geq 0} \times \mathbb{R}^n \times \mathbb{R}^n \times \mathbb{R}^m \times [0, T_2^1] \times [0, T_2^2] \times \ldots \times \{0\} \end{aligned}$$

  Thus, (A1) holds.

- Given Assumption 6.1.1, we have that $f_a : \mathcal{X} \to \mathcal{X}$ and $f_s : \mathcal{X} \to \mathcal{X}$ are continuous on C. Moreover, since dom $f_a = \mathcal{X} = C$ and dom $f_s = \mathcal{X} = C$, $C \subset$ dom f_a and $C \subset$ dom f_s hold. Thus, (A2) holds.

- To show that the set-valued map G defined in (6.9) satisfies (A3), note that the graph of G is given by

$$\begin{aligned} \text{gph}(G) &= \{(x, y) : x \in D, y \in G(x)\} \\ &= D \times \left(\mathbb{R}^n_{\geq 0} \times \mathbb{R}^n_{\geq 0} \times \mathbb{R}^n \times \mathbb{R}^n \times \mathbb{R}^m \times \mathcal{T}\right) \end{aligned}$$

  is closed. Thus, via [4, Lemma 5.10], G is outer semicontinuous and locally bounded at each $x \in D$. Moreover, by definition, we have that dom $G = D$. Hence, (A3) holds.

Observe that similar arguments can be made on the data of $\mathcal{H}_a$ such that (A1), (A2), and (A3) hold. □

With the defined model, we consider the following set and provide conditions guaranteeing that it is rendered stable for $\mathcal{H}_s$ and $\mathcal{H}_a$ solving Problem 6.0.1:

$$\mathcal{A} := \{x \in \mathcal{X} : \hat{\tau}_i = \hat{\tau}_k \quad \forall i, k \in \mathcal{V}\} \tag{6.13}$$

for which synchronization of the clocks is implied. In the following section, we outline a procedure to facilitate the set stabilization analysis. We show that through a change of coordinates, a Lyapunov-based set stabilization analysis can be performed that shows the system $\mathcal{H}$ solves Problem 6.0.1.

In the next section, we introduce several clock synchronization protocols that rely on bidirectional communication of connected nodes at communication events. We refer to such synchronization algorithms as symmetric due to this observed bidirectional flow of information.

6.1.1 Symmetric Communication Protocols

RandSync

The *RandSync* protocol proposed by the authors in [26] is a randomized consensus protocol that drives the error in the clocks $\hat{\tau}_i \in \mathbb{R}_{\geq 0}$ for each $i \in \mathcal{V}$ to synchronization using a second-order controller variable $\nu_i \in \mathbb{R}$ for each $i \in \mathcal{V}$. The algorithm is described as follows, at times $\{t_j^i\}_{j=1}^{\infty}$,

1. Agent k sends its time reading to neighboring agents $k \in \mathcal{N}(i)$;
2. Agent k receives time readings from the neighboring agents $k \in \mathcal{N}(i)$;
3. Agent k uses the received time readings $\hat{\tau}_i(t_j^i)$ by updating their clock $\hat{\tau}_k$ and control parameter ν_k as follows

$$\begin{cases} \hat{\tau}_i(t_{j+1}^k) = \hat{\tau}_i(t_j^k) + \sum_{k\in\mathcal{N}(i)} a_{ik}(t_j^k)\big(\hat{\tau}_k(t_j^k) - \hat{\tau}_i(t_j^k)\big) \\ \nu_i(t_{j+1}^k) = \nu_i(t_j^k) + \alpha \sum_{k\in\mathcal{N}(i)} a_{ik}(t_j^k)\big(\hat{\tau}_k(t_j^k) - \hat{\tau}_i(t_j^k)\big) \end{cases} \quad \forall k \in \mathcal{N}(i) \qquad (6.14)$$

where $\alpha > 0$ is a gain parameter and $a_{ik}(t_j^i) \geq 0$ are the elements of a weighted adjacency matrix A such that $\sum_{k\neq i} a_{ik}(t_j^i) < 1$. The given updates of $\hat{\tau}_i$ and ν_i, respectively, drive the clock state and the clock rate of each agent to their respective average values.

Composing the protocol as a hybrid system, we have

$$\left.\begin{aligned}\dot{\hat{\tau}}_i &= a_i u_i \\ \dot{u}_i &= h_i u_i \\ \dot{\nu}_i &= h_i \nu_i\end{aligned}\right\} \qquad \tilde{\tau}_i \in [0, T_2]$$

$$\left.\begin{aligned}\hat{\tau}_i^+ &= \hat{\tau}_i + \sum_{k\in\mathcal{N}(i)} (\hat{\tau}_i - \hat{\tau}_k) \\ u_i^+ &= \nu_i + \alpha \sum_{k\in\mathcal{N}(i)} (\hat{\tau}_i - \hat{\tau}_k) \\ \nu_i^+ &= \nu_i + \alpha \sum_{k\in\mathcal{N}(i)} (\hat{\tau}_i - \hat{\tau}_k)\end{aligned}\right\} \quad \tilde{\tau}_i = 0 \tag{6.15}$$

where the resets $\hat{\tau}_i^+$ and ν_i^+ follow from (6.18). However, since $\dot{\hat{\tau}}_i = a_i u_i$, u_i assumes the role of adjusting the clock rate thus, ν_i becomes an auxiliary control parameter.

To adequately capture the hybrid dynamics of the RandSync protocol into the framework defined by $\mathcal{H}_s$, the functions f_u and f_w contained in the flow map f_s are defined as follows:

$$\begin{aligned} f_u(u) &= hu \\ f_w(x) &= 0 \end{aligned} \tag{6.16}$$

The functions $g_{\hat{\tau}}$, g_u, g_ν, and g_w employed in the jump map G are defined as follows:

$$\begin{aligned} g_{\hat{\tau}}(\hat{\tau}) &= \hat{\tau} + \mathcal{L}\hat{\tau} \\ g_u(\nu, \hat{\tau}) &= \nu + \alpha\mathcal{L}\hat{\tau} \\ g_\nu(\nu, \hat{\tau}) &= \nu + \alpha\mathcal{L}\hat{\tau} \\ g_w(w) &= w \end{aligned} \tag{6.17}$$

where $\mathcal{L}$ is the graph Laplacian given by $\mathcal{L} = \mathcal{D} - A$ with entries

$$\ell_{ij} = \begin{cases} \sum_{k=1,k\neq i}^{n} a_{ik} & \text{if } i = j \\ -a_{ik} & \text{if } i \neq j \end{cases} \qquad \forall i \in \mathcal{V}$$

Note that w is unused for this protocol and its evolution is kept constant.

PI-Consensus

Similarly, the authors in [25], propose a discrete proportional integral controller to achieve clock synchronization. At times t_j^i, each node i exchanges timing measurements

$\hat{\tau}_i \in \mathbb{R}_{\geq 0}$ with its neighbors $\mathcal{N}(i)$. Using the exchanged measurements, node i updates its clock $\hat{\tau}_i$ and controller parameter $\nu_i \in \ reals$ as follows

$$\begin{cases} \hat{\tau}_i(t^i_{j+1}) = \hat{\tau}_i(t^i_j) + \nu_i(t^i_j) - \sum_{k\in\mathcal{N}(i)} a_{ij}(\hat{\tau}_k(t^i_j) - \hat{\tau}_i(t^i_j)) \\ \nu_i(t^i_{j+1}) = \nu_i(t^i_j) + \alpha \sum_{k\in\mathcal{N}(i)} a_{ij}(\hat{\tau}_k(t^i_j) - \hat{\tau}_i(t^i_j))) \end{cases} \quad \forall k \in \mathcal{N}(i) \tag{6.18}$$

where $\alpha \in (0,1)$ and $a_{ik} \neq 0$ are the elements of an adjacency matrix A.

Composing the protocol as a hybrid system with sporadic communication via the time $\tilde{\tau}$ in (6.6), we have

$$\left.\begin{aligned} \dot{\hat{\tau}}_i &= a_i u_i \\ \dot{u}_i &= h_i u_i \\ \dot{\nu}_i &= h_i \nu_i \end{aligned}\right\} \qquad \tilde{\tau}_i \in [0, T_2]$$

$$\left.\begin{aligned} \hat{\tau}_i^+ &= \hat{\tau}_i + \nu_i - \sum_{k\in\mathcal{N}(i)} (\hat{\tau}_i - \hat{\tau}_k) \\ u_i^+ &= \nu_i + \alpha \sum_{k\in\mathcal{N}(i)} (\hat{\tau}_i - \hat{\tau}_k) \\ \nu_i^+ &= \nu_i + \alpha \sum_{k\in\mathcal{N}(i)} (\hat{\tau}_i - \hat{\tau}_k) \end{aligned}\right\} \quad \tilde{\tau}_i = 0 \tag{6.19}$$

where the resets $\hat{\tau}_i^+$ and ν_i^+ follow from (6.18). However, since $\dot{\hat{\tau}}_i = a_i u_i$, u_i assumes the role of adjusting the clock rate thus, ν_i becomes an auxiliary control parameter.

To adequately capture the hybrid dynamics of the PI-Consensus protocol into the framework defined by $\mathcal{H}_s$, the functions f_u and f_w contained in the flow map f_s are defined as follows:

$$\begin{aligned} f_u(u) &= hu \\ f_w(x) &= 0 \end{aligned} \tag{6.20}$$

The functions $g_{\hat{\tau}}$, g_u, g_ν, and g_w employed in the jump map G are defined as follows:

$$\begin{aligned} g_{\hat{\tau}}(\hat{\tau}) &= \hat{\tau} + (\nu - \mathcal{L}\hat{\tau}) \\ g_u(\nu, \hat{\tau}) &= \nu + \alpha\mathcal{L}\hat{\tau} \\ g_\nu(\nu, \hat{\tau}) &= \nu + \alpha\mathcal{L}\hat{\tau} \\ g_w(w) &= w \end{aligned} \tag{6.21}$$

where, again, $\mathcal{L}$ is the graph Laplacian given by $\mathcal{L} = \mathcal{D} - A$ with entries

$$\ell_{ij} = \begin{cases} \sum_{k=1,k\neq i}^{n} a_{ik} & \text{if } i = j \\ -a_{ik} & \text{if } i \neq j \end{cases} \quad \forall i \in \mathcal{V}$$

Note that w is unused for this protocol and its evolution is kept constant across both flows and jumps.

6.1.2 HyNTP

An additional algorithm that makes use of symmetric communication is our distributed algorithm first proposed in [30] but modified for the decentralized scenario and adapted to the clock dynamics proposed in (6.3) and (6.4). This hybrid algorithm combines a distributed discrete controller with a local continuous estimator to estimate the clock skews. At times t_j^i, each node i exchanges timing measurements with its neighbors $\mathcal{N}(i)$. Then, using the exchanged measurements and local estimate of the clock skew the controller applies a control input as follows:

$$\left.\begin{aligned} \dot{\tilde{\tau}}_i &= a_i u_i \\ \dot{u}_i &= h_i \nu_i - \mu_i(\bar{\tau}_i - \tau_i) \\ \dot{\nu}_i &= h_i \nu_i \\ \dot{\hat{a}}_i &= -\mu(\bar{\tau}_i - \tau_i) \\ \dot{\bar{\tau}}_i &= \hat{a}_i - (\bar{\tau}_i - \tau_i) \end{aligned}\right\} \quad \tilde{\tau}_i \in [0, T_2]$$

$$\left.\begin{aligned} \hat{\tau}_i^+ &= \hat{\tau}_i \\ u_i^+ &= -\gamma \sum_{k\in\mathcal{N}(i)} (\hat{\tau}_i - \hat{\tau}_k) - \hat{a}_i + \sigma^* \\ \nu_i^+ &= -\gamma \sum_{k\in\mathcal{N}(i)} (\hat{\tau}_i - \hat{\tau}_k) \\ \hat{a}_i^+ &= \hat{a}_i \\ \bar{\tau}_i^+ &= \bar{\tau}_i \end{aligned}\right\} \quad \tilde{\tau}_i = 0 \tag{6.22}$$

where $h, \sigma^* \in \mathbb{R}$ and $\mu, \gamma > 0$ are controller parameters. The parameter σ^*, in particular, is a controllable clock rate that is injected with the control input. Note that ν_i is treated

as an auxiliary state of the controller. Moreover, the state u_i is kept constant in between events and is reset to the new value of $\nu_i - a_i + \sigma^*$ at jumps. Furthermore, note that the distributed controller only uses local and communicated information from the neighboring nodes at communication event times t_j.

To accommodate the HyNTP protocol, we define additional states $\bar{\tau} := (\bar{\tau}_1, \bar{\tau}_2, \ldots, \bar{\tau}_n) \in \mathbb{R}^n$ and $\hat{a} := (\hat{a}_1, \hat{a}_2, \ldots, \hat{a}_n) \in \mathbb{R}^n$ that respectively represent the estimator clock and clock rate. Then we define error coordinates $\varepsilon_\tau := \bar{\tau} - \tau$ and $\varepsilon_a := a - \hat{a}$ such that the auxiliary variable is defined as

$$w = (\varepsilon_a, \varepsilon_\tau) \in \mathbb{R}^n \times \mathbb{R}^n$$

and define the dynamics of w as follows:

$$\begin{aligned} \dot{\varepsilon}_a &= -\mu\varepsilon_\tau \\ \dot{\varepsilon}_\tau &= -\varepsilon_\tau + \varepsilon_a \end{aligned} \tag{6.23}$$

Then, to compose the HyNTP protocol in the framework given by $\mathcal{H}_s$, the functions f_u and f_w employed in the flow map f_s are defined as follows:

$$\begin{aligned} f_u(\nu, u, \varepsilon_\tau) &= h\nu - \mu\varepsilon_\tau \\ f_w(w, \tau) &= \begin{bmatrix} -\mu\varepsilon_\tau \\ -\varepsilon_\tau + \varepsilon_a \end{bmatrix} \end{aligned} \tag{6.24}$$

The functions $g_{\hat{\tau}}$, g_u, g_ν, and g_w employed in the jump map G are defined as follows:

$$\begin{aligned} g_{\hat{\tau}}(\hat{\tau}) &= \hat{\tau} \\ g_u(a, \hat{\tau}, \varepsilon_a) &= \big(\mathrm{diag}(a)\big)^{-1}\big(-\gamma\mathcal{L}\hat{\tau} + \varepsilon_a + \sigma^*\mathbf{1}_n\big) \\ g_\nu(\hat{\tau}) &= -\gamma\mathcal{L}\hat{\tau} \\ g_w(w) &= w \end{aligned} \tag{6.25}$$

In the next section, we introduce several clock synchronization protocols that utilize on one-way communication protocols between connected nodes at communication events. We refer to such synchronization algorithms as asymmetric due to the observed single directional flow of information.

6.1.3 Asymmetric Communication Protocols

RandSync-Broadcast Algorithm

The *RandSync* protocol proposed by the authors in [26] is a randomized consensus protocol that drives the error in the clocks $\hat{\tau}_i \in \mathbb{R}_{\geq 0}$ for each $i \in \mathcal{V}$ to synchronization using a second-order controller variable $\nu_i \in \mathbb{R}$ for each $i \in \mathcal{V}$. The algorithm is described as follows: at times $\{t_j^i\}_{j=1}^{\infty}$,

1. Agent i sends its time reading $\hat{\tau}_i(t_j^i)$ to neighboring agents $k \in \mathcal{N}(i)$;
2. Agent k receives the time readings from Agent i;
3. Agent k uses the received time readings $\hat{\tau}_i(t_j^i)$ by updating their clock $\hat{\tau}_k$ and control parameter ν_k as follows

$$\begin{cases} \hat{\tau}_k(t_{j+1}^k) = \hat{\tau}_k(t_j^k) + a_{ik}(t_j^k)\big(\hat{\tau}_k(t_j^k) - \hat{\tau}_i(t_j^k)\big) \\ \nu_k(t_{j+1}^k) = \nu_k(t_j^k) + \alpha a_{ik}(t_j^k)\big(\hat{\tau}_k(t_j^k) - \hat{\tau}_i(t_j^k)\big) \end{cases} \quad \forall k \in \mathcal{N}(i)^{out} \tag{6.26}$$

   where $\alpha > 0$ is a gain parameter and $a_{ik}(t_j^k) = a_{ik}(t_j^k) \in (0,1)$ for $k \in \mathcal{N}(i)^{out}$ and zero otherwise.

Composing the protocol as a hybrid system, we have

$$\left.\begin{aligned} \dot{\hat{\tau}}_i &= a_i u_i \\ \dot{u}_i &= h_i u_i \\ \dot{\nu}_i &= h_i \nu_i \end{aligned}\right\} \qquad \tilde{\tau}_i \in [0, T_2]$$

$$\left.\begin{aligned} \hat{\tau}_{ki}^+ &= \hat{\tau}_k + a_{ki}(\hat{\tau}_i - \hat{\tau}_k) \\ u_{ki}^+ &= a_k(\nu_k + a_{ki} q(\hat{\tau}_i - \hat{\tau}_k)) \\ \nu_{ki}^+ &= \nu_k + a_{ki} q(\hat{\tau}_i - \hat{\tau}_k) \end{aligned}\right\} \quad \tilde{\tau}_i = 0 \tag{6.27}$$

Then, to compose the RandSync-Broadcast protocol in the framework given by $\mathcal{H}_a$, the functions f_u and f_w employed in the flow map f_a are defined as follows:

$$\begin{aligned} f_u(u) &= hu \\ f_w(w, \tau) &= 0 \end{aligned} \tag{6.28}$$

the functions $g_{\hat{\tau}}$, g_u, g_ν, and g_w employed in the jump map G are defined as follows:

$$\begin{aligned} g_{\hat{\tau}}(\hat{\tau}) &= (I + q\Gamma_i)\hat{\tau} \\ g_u(a, \hat{\tau}, \varepsilon_a) &= \operatorname{diag}(a)\big(I + q\Gamma_i\big)\nu \\ g_\nu(\hat{\tau}) &= \big(I + q\Gamma_i\big)\nu \\ g_w(x) &= w \end{aligned} \tag{6.29}$$

where $\Gamma_i = \mathbf{1}_n v_i^\top - I$ gives the adjacency matrix at $\tilde{\tau}_i = 0$ and v_i is the ith canonical vector. Note that w is unused for this protocol and its evolution is kept constant across both flows and jumps.

Average TimeSync

The authors in [1] propose the *Average TimeSync* protocol that utilizes consensus-based controllers to individually synchronize both the clock drifts and clock offsets. The mechanics of the algorithm are given as follows. At times t_j^i, node i broadcasts its time $\hat{\tau}_i(t_j^i)$ to its neighbors $\mathcal{N}(i)$. Upon receipt of the timestamp by nodes $k \in \mathcal{N}(i)$, each node updates its clocks and clock rates as follows:

$$\begin{cases} \hat{\tau}_k(t_{j+1}^i) = \nu_k(t_j^i)\tau_k(t_j^i) + \hat{o}_k(t_j^i) \\ \nu_k(t_{j+1}^i) = \rho_v \nu_k(t_j^i) + (1 - \rho_v)\eta_{ik}\nu_k \\ \eta_{ki}(t_{j+1}^i) = \rho_\eta \eta_{ki}(t_j^i) + (1 - \rho_\eta)\frac{\tau_i(t_j^i) - \tau_i(t_{j-1}^i)}{\tau_k(t_j^i) - \tau_k(t_{j-1}^i)} \\ \hat{o}_k(t_{j+1}^i) = \hat{o}_k(t_j^i) + (1 - \rho_o)\big(\hat{\tau}_i(t_{j+1}^i) - \hat{\tau}_k(t_{j+1}^i)\big) \end{cases} \qquad \forall k \in \mathcal{N}(i) \tag{6.30}$$

where $\rho_v \in (0,1)$, $\rho_\eta \in (0,1)$, and $\rho_o \in (0,1)$. Composing the protocol as a hybrid system, we have

$$\left.\begin{aligned} \dot{\hat{\tau}}_i &= a_i u_i \\ \dot{u}_i &= h_i u_i \\ \dot{\nu}_i &= h_i \nu_i \\ \dot{\eta}_{ki} &= 0 \\ \dot{\hat{o}}_{ki} &= 0 \end{aligned}\right\} \qquad \tilde{\tau}_i \in [0, T_2]$$

$$\left.\begin{aligned} \hat{\tau}_k(t^i_{j+1}) &= \nu_k(t^i_j)\tau_k(t^i_j) + \hat{o}_k(t^i_j) \\ u_k(t^i_{j+1}) &= \rho_v \nu_k(t^i_j) + (1-\rho_v)\eta_{ik}\nu_k \\ \nu_k(t^i_{j+1}) &= \rho_v \nu_k(t^i_j) + (1-\rho_v)\eta_{ik}\nu_k \\ \eta_{ki}(t^i_{j+1}) &= \rho_\eta \eta_{ki}(t^i_j) + (1-\rho_\eta)\frac{\tau_i(t^i_j) - \tau_i(t^i_{j-1})}{\tau_k(t^i_j) - \tau_k(t^i_{j-1})} \\ \hat{o}_k(t^i_{j+1}) &= \hat{o}_k(t^i_j) + (1-\rho_o)\big(\hat{\tau}_i(t^i_{j+1}) - \hat{\tau}_k(t^i_{j+1})\big) \end{aligned}\right\} \quad \tilde{\tau}_i = 0 \tag{6.31}$$

Then, composing the Average TimeSync protocol into the hybrid framework $\mathcal{H}$, we define controller sub-states $\hat{o} := (\hat{o}_1, \hat{o}_2, \ldots, \hat{o}_n) \in \mathbb{R}^n$, $\eta := (\bar{\eta}_1, \bar{\eta}_2, \ldots, \bar{\eta}_n) \in \mathbb{R}^{n^2}$, $\ell := (\bar{\ell}_1, \bar{\ell}_2, \ldots, \bar{\ell}_n) \in \mathbb{R}^{n^2}$, $m := (\bar{m}_1, \bar{m}_2, \ldots, \bar{m}_n) \in \mathbb{R}^{n^2}$ where $\bar{\eta}_i = (\eta_{i1}, \eta_{i2}, \ldots, \eta_{in}) \in \mathbb{R}^n$, $\bar{\ell}_i := (\ell^i_1, \ell^i_2, \ldots, \ell^i_n) \in \mathbb{R}^n$ and $\bar{m}_i := (m^i_1, m^i_2, \ldots, m^i_n) \in \mathbb{R}^n$ then we let

$$w = (\hat{o}, \eta, \ell, m) \in \mathbb{R}^n \times \mathbb{R}^{n^2} \times \mathbb{R}^{n^2} \times \mathbb{R}^{n^2}$$

$$\begin{aligned} f_u(u) &= 0 \\ f_w(w, \tau) &= 0 \end{aligned} \tag{6.32}$$

and

$$\begin{aligned} g_{\hat{\tau}}(\hat{\tau}) &= \Gamma_i \mathrm{diag}\big(g_\nu(\eta,\nu)\big)\tau + \Gamma_i\big(\hat{\tau} + \hat{o} + (1-\rho_o)\Gamma_i\hat{\tau}\big) \\ g_u(a, \hat{\tau}, \varepsilon_a) &= 0 \\ g_\nu(\hat{\tau}) &= \big(I + (1-\rho_v)\Gamma_k\big)\mathrm{diag}(\eta_k)\nu_k \\ g_w(x) &= \begin{bmatrix} \hat{o} + (1-\rho_o)\Gamma_i\hat{\tau} \\ \Gamma_i\Big(\rho_\eta\eta + (1-\rho_\eta)\big(\mathrm{diag}(\tau - m)\big)^{-1}\mathrm{diag}(\tau - \ell)\Big) \\ [\ell^1_1, \ldots, \ell^1_{i-1}, \tau_i, \ell^1_{i+1}, \ldots \ell^1_n, \ldots, \ell^n_1, \ldots, \ell^n_{i-1}, \tau_i, \ell^n_{i+1}, \ldots \ell^n_n]^\top \\ [m^1_1, \ldots, m^1_n, \ldots, m^i_1, \ldots, m^i_{i-1}, \tau_i, m^i_{i+1}, \ldots m^i_n \ldots m^1_n, \ldots, m^n_n]^\top \end{bmatrix} \end{aligned} \tag{6.33}$$

where $\Gamma_i = \mathbf{1}_n v_i^\top - I$ gives the adjacency matrix at $\tilde{\tau}_i = 0$ and v_i is the ith canonical vector. Note that w is unused for this protocol and its evolution is kept constant across both flows and jumps.

6.2 Numerical Results

In this section, we present numerical results to simulate our modeling framework and validate its feasibility for both symmetric and asymmetric communication scenarios.

6.2.1 Symmetric Communication: HyNTP Case Study

To validate the model $\mathcal{H}_s$ for symmetric communication, consider five agents with dynamics as in (6.3) and (6.4) over a strongly connected digraph with the following adjacency matrix

$$\mathcal{G}_A = \begin{pmatrix} 0 & 1 & 1 & 0 & 1 \\ 1 & 0 & 1 & 0 & 0 \\ 1 & 0 & 0 & 1 & 0 \\ 0 & 0 & 1 & 0 & 1 \\ 1 & 0 & 1 & 1 & 0 \end{pmatrix}$$

Given $T_1 = 0.01$, $T_2 = 0.1$, and $\sigma^* = 1$, then it can be found that the parameters $h = -0.4$, $\mu = 1$, $\gamma = 3.5$, $\rho = 1.3$ synchronize the clocks. Figure 6.1(a) shows the trajectories of $\hat{\tau}_i$ for components $i \in \{1, 2, 3, 4, 5\}$ of a solution ϕ for the case where $\sigma^* = 1$ with initial conditions $\phi_{\hat{\tau}}(0, 0) = (1, -1, 2, -2, 0)$ and clock rates a_i in the range $(0.85, 1.15)$. The plot in Figure 6.1(b) depicts a trajectory for a Lyapunov function candidate V evaluated along the solution ϕ projected onto the regular time domain.

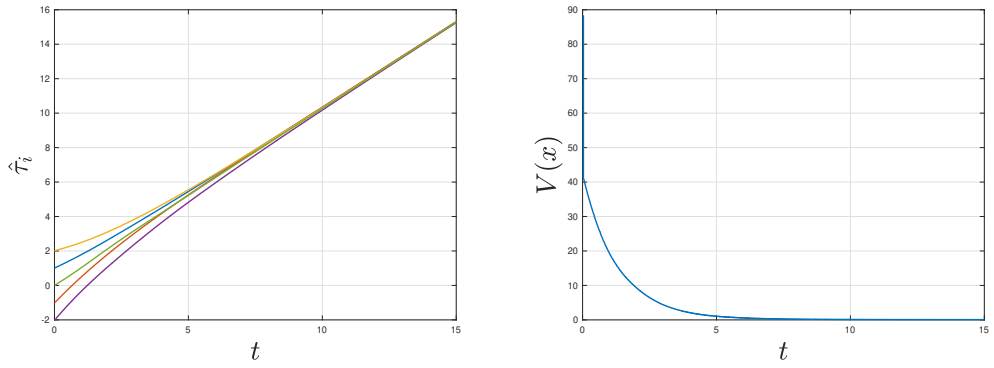

(a) (b)

Figure 6.1: Figure 6.1(a) gives the evolution of the error in the clocks and clock rates of Nodes i and k. Figure 6.1(b) gives $V(x)$ evaluated along the solution.

6.2.2 Asymmetric Communication: RandSync Case Study

In this section, we present numerical results to simulate our modeling framework $\mathcal{H}_a$ for asymmetric communication protocols using the RandSync algorithm system. Consider five agents with dynamics as in (6.3) and (6.4) over a strongly connected digraph with the following adjacency matrix

$$\mathcal{G}_A = \begin{pmatrix} 0 & 1 & 1 & 0 & 1 \\ 1 & 0 & 1 & 0 & 0 \\ 1 & 0 & 0 & 1 & 0 \\ 0 & 0 & 1 & 0 & 1 \\ 1 & 0 & 1 & 1 & 0 \end{pmatrix}$$

Given $T_1 = 0.01$, $T_2 = 0.1$ then it can be found that the parameters $h = 0$, $\alpha = 0.1$, $q = 0.9$ synchronize the clocks.

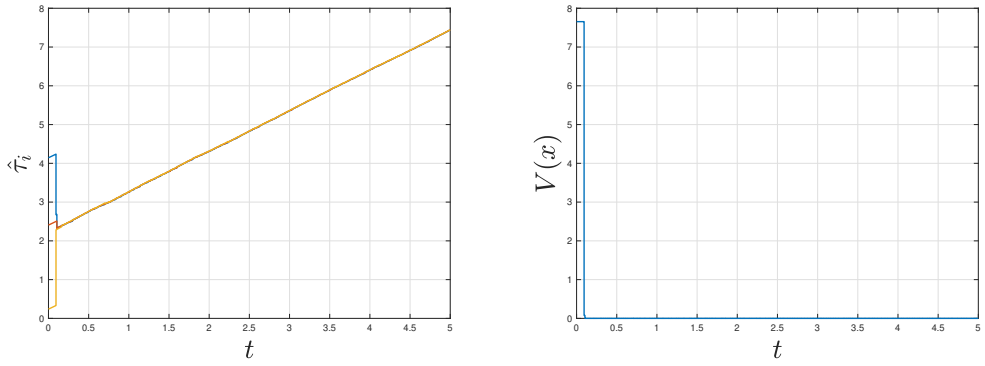

(a) (b)

Figure 6.2: Figure 6.1(a) gives the evolution of the error in the clocks and clock rates of Nodes i and k. Figure 6.1(b) gives $V(x)$ evaluated along the solution.

Chapter 7

Conclusion

In this thesis, several clock synchronization schemes utilizing a hybrid systems approach were presented. These algorithms gave performance guarantees on the convergence of the clocks and the clock rates via an analysis using the hybrid systems framework. The need for clock synchronization schemes with performance guarantees was demonstrated through the problem of a networked observer, with accompanying clock synchronization subsystem, that estimates the state of a plant via sporadic measurement broadcasts. The result of the problem gave sufficient conditions on the performance required by the accompanying clock synchronization subsystem. In particular, the sufficient condition on the convergence rate of the plant and observer clocks formulated the clock synchronization problem that concerns this research.

The problem was solved through the presentation of several hybrid-based clock synchronization algorithms that included the introduction of *HyNTP*, a distributed hybrid algorithm that synchronizes the time and rate of a set of clocks connected over a network. Results were given to guarantee and show synchronization of the timers, exponentially fast. Numerical results validating the exponentially fast convergence of the timers were also given. Numerical results were also provided to demonstrate performance against a similar class of clock synchronization algorithms.

A sender-receiver clock synchronization algorithm with sufficient design conditions ensuring synchronization was also presented to address the problem. For this algorithm, results were given to show asymptotic attractivity of a set of interest reflecting the desired synchronized setting. Numerical results validating the attractivity of the system to the set of interest were also given. An additional model to capture the multi-agent setting was

also presented with a numerical example to demonstrate its feasibility. Future work will consider stability of the system and robustness properties to specific perturbations.

Finally, a general framework to study the clock synchronization problem using a hybrid systems approach was introduced. In particular, the data for a hybrid system model that captures the dynamics of hardware and software timers, the communication network, and the controller dynamics to synchronize the clocks and clock rates was defined. The flexibility of the model was demonstrated against a class of clock synchronization algorithms from the literature and numerical simulated to demonstrate its feasibility. Future work will consider stability of the framework model to a synchronization set of interest with sufficient conditions on the system parameters.

Appendix A

Appendix A - Proofs of Lemmas for Hybrid Observer

A.1 Proof of Lemma 3.1.3

Proof. The following hold:

- (A1) in [8, Assumption 6.5] holds since C_a and D_a are closed sets.
- (A2) in [8, Assumption 6.5] holds since F_a is outer semicontinuous and bounded relative to C_a.
- (A3) in [8, Assumption 6.5] holds since $G_a\big|_{D_b=\emptyset}$ is an outer semicontinuous construction using continuous functions G_1 and G_2. In fact, the set of points where the mappings G_1 and G_2 are applied are mutually exclusive due to $D_{a_1} \cap D_{a_2} = \emptyset$. Then, $G_a\big|_{D_b=\emptyset} : \mathcal{X}_a \rightrightarrows \mathcal{X}_a$ is outer semicontinuous and locally bounded relative to D_a and $D_a \subset \text{dom } G_a$.

Thus, $\mathcal{H}_a$ with $D_b = \emptyset$ satisfies the hybrid basic conditions. □

A.2 Proof of Lemma 3.1.4

Proof. To prove item 1), pick $x \in D_a$

- If $x \in D_{a_1}$, since $D_b = \emptyset$ $G_a(x_a, \tau_P, \tau_O) = G_1(x_a, \tau_P) \subset D_{a_2} \subset C_{a_2}$
- If $x \in D_{a_2}$, since $D_b = \emptyset$ $G_a(x_a, \tau_P, \tau_O) = G_2(x_a, \tau_O) \subset D_{a_1} \subset C_{a_1}$

Therefore, item 1) holds.

To prove item 2), pick $x \in C_a \setminus D_a$. The tangent cone $T_{C_a}(x_a)$ is given by

$$T_{C_a}(x_a) = \begin{cases} \mathbb{R}^n \times \mathbb{R}^n \times \mathbb{R}_{\geq 0} \times \mathbb{R}_{\geq 0} \times \{0\} \times \mathbb{R}^m \times \mathbb{R}_{\geq 0} & \text{if } x_a \in \mathcal{X}_a^1 \\ \mathbb{R}^n \times \mathbb{R}^n \times \mathbb{R} \times \mathbb{R}_{\geq 0} \times \{0\} \times \mathbb{R}^m \times \mathbb{R}_{\geq 0} & \text{if } x_a \in \mathcal{X}_a^2 \\ \mathbb{R}^n \times \mathbb{R}^n \times \mathbb{R}_{\geq 0} \times \mathbb{R}_{\geq 0} \times \{0\} \times \mathbb{R}^m \times \mathbb{R}_{\geq 0} & \text{if } x_a \in \mathcal{X}_a^3 \\ \mathbb{R}^n \times \mathbb{R}^n \times \mathbb{R}_{\geq 0} \times \mathbb{R}_{\geq 0} \times \{1\} \times \mathbb{R}^m \times \mathbb{R}_{\geq 0} & \text{if } x_a \in \mathcal{X}_a^4 \\ \mathbb{R}^n \times \mathbb{R}^n \times \mathbb{R}_{\geq 0} \times \mathbb{R}_{\geq 0} \times \{1\} \times \mathbb{R}^m \times \mathbb{R}_{\geq 0} & \text{if } x_a \in \mathcal{X}_a^5 \\ \mathbb{R}^n \times \mathbb{R}^n \times \mathbb{R}_{\geq 0} \times \mathbb{R} \times \{1\} \times \mathbb{R}^m \times \mathbb{R}_{\geq 0} & \text{if } x_a \in \mathcal{X}_a^6 \end{cases}$$

where

$$\begin{aligned} \mathcal{X}_a^1 &:= \{x_a \in \mathcal{X}_a : q = 0, \tau_N = 0, \tau_\delta = -1\} \\ \mathcal{X}_a^2 &:= \{x_a \in \mathcal{X}_a : q = 0, \tau_N = (0, T_2^N), \tau_\delta = -1\} \\ \mathcal{X}_a^3 &:= \{x_a \in \mathcal{X}_a : q = 0, \tau_N = T_2^N, \tau_\delta = -1\} \\ \mathcal{X}_a^4 &:= \{x_a \in \mathcal{X}_a : q = 1, \tau_\delta = 0\} \\ \mathcal{X}_a^5 &:= \{x_a \in \mathcal{X}_a : q = 1, \tau_\delta = T^d\} \\ \mathcal{X}_a^6 &:= \{x_a \in \mathcal{X}_a : q = 1, \tau_\delta = (0, T^d)\} \end{aligned}$$

By inspection $F_a(x_a) \subset T_{C_a}(x_a)$. Therefore item 2) holds. □

A.3 Proof of Lemma 3.1.5

Proof. To prove completeness of solutions we consider the extension of [8, Proposition 6.10] for the case of Hybrid Systems with inputs as presented in [33]. Given that $\mathcal{H}_a$ satisfies the hybrid basic conditions, consider an arbitrary $x_a \in C_a \cup D_a$ and recall the tangent cone $T_{C_a}(x_a)$ from the result of Lemma 3.1.5. Since F_a is independent of the inputs, by inspection, $F_a(x_a) \cap T_{C_a}(x_a) \neq \emptyset$ holds for every (x_a, τ_P, τ_O) such that $x \in C_a \setminus D_a$. Then, case (c) in [8, Proposition 6.10] can be ruled out since by item 1) Lemma 3.1.4 with $D_b = \emptyset$, $G_a(D_a) \subset C_a \cup D_a$. Case (b) in [8, Proposition 6.10] can be excluded since by inspection F_a is Lipschitz continuous on C_a. Thus, each ϕ to $\mathcal{H}_a$ with $D_b = \emptyset$ and inputs (τ_P, τ_O) such that $\{t : (t, j) \in \text{dom } \phi\}$ is unbounded must satisfy case (a) in [8, Proposition 6.10]. Observe that the notions in [8, Proposition 6.10] □

Appendix B

Appendix B - Proofs of Lemmas and select Propositions for Hybrid Consensus Clock Synchronization

B.1 Proof of Lemma 4.2.2

Proof. By inspection of the hybrid system data defining $\mathcal{H}$ given in (4.9) and below it, the following is observed:

- The set C is a closed subset of $\mathbb{R}^m$ since, $C = \mathcal{X}$ and $\mathcal{X}$ is the Cartesian product of closed sets. Similar arguments show that D is closed since it can be written as

$$D = \mathbb{R}^n \times \mathbb{R}^n \times \mathbb{R}^n \times \mathbb{R}^n_{\geq 0} \times \mathbb{R}^n \times \mathbb{R}^n_{\geq 0} \times \{0\}$$

  Thus, (A1) holds.

- $f : \mathcal{X} \to \mathcal{X}$ is linear affine in the state and thus continuous on C. Moreover, since dom $f = \mathcal{X} = C$, $C \subset$ dom f holds. Thus, (A2) holds.

- To show that the set-valued map G defined in (4.9) satisfies (A3), note that the graph of G is given by

$$\begin{aligned} \text{gph}(G) &= \{(x, y) : x \in D, y \in G(x)\} \\ &= D \times \left(\mathbb{R}^n \times \mathbb{R}^n \times \mathbb{R}^n \times \mathbb{R}^n_{\geq 0} \times \mathbb{R}^n \times \mathbb{R}^n_{\geq 0} \times [T_1, T_2]\right) \end{aligned}$$

is closed. Thus, via [4, Lemma 5.10], G is outer semicontinuous and locally bounded at each $x \in D$. Moreover, by definition, we have that dom $G = D$. Hence, (A3) holds.

□

B.2 Proof of Lemma 4.2.3

Proof. For each $\xi \in C$, the tangent cone $T_C(\xi)$, as defined in [4, Definition 5.12], is given by

$$T_C(\xi) = \begin{cases} \mathbb{R}^n \times \mathbb{R}^n \times \mathbb{R}^n \times \mathbb{R}^n_{\geq 0} \times \mathbb{R}^n \times \mathbb{R}^n_{\geq 0} \times \mathbb{R}_{\geq 0} & \text{if } \xi \in \mathcal{X}^1 \\ \mathbb{R}^n \times \mathbb{R}^n \times \mathbb{R}^n \times \mathbb{R}^n_{\geq 0} \times \mathbb{R}^n \times \mathbb{R}^n_{\geq 0} \times \mathbb{R} & \text{if } \xi \in \mathcal{X}^2 \\ \mathbb{R}^n \times \mathbb{R}^n \times \mathbb{R}^n \times \mathbb{R}^n_{\geq 0} \times \mathbb{R}^n \times \mathbb{R}^n_{\geq 0} \times \mathbb{R}_{\leq 0} & \text{if } \xi \in \mathcal{X}^3 \end{cases}$$

where $\mathcal{X}^1 := \{x \in \mathcal{X} : \tau = 0\}$, $\mathcal{X}^2 := \{x \in \mathcal{X} : \tau \in (0, T_2)\}$, and $\mathcal{X}^3 := \{x \in \mathcal{X} : \tau = T_2\}$. By inspection, from the definition of f in (4.9, $f(x) \cap T_C(x) \neq \emptyset$ holds for every $x \in C \backslash D$. Then, since $\mathcal{H}$ satisfies the hybrid basic conditions, as shown in Lemma 4.2.2, by [4, Proposition 6.10] there exists a nontrivial solution ϕ to $\mathcal{H}$ with $\phi(0,0) = \xi$. Moreover, every $\phi \in \mathcal{S}_{\mathcal{H}}$ satisfies one of the following conditions:

a) ϕ is complete;

b) dom ϕ is bounded and the interval I^J, where $J = \sup_j \text{dom } \phi$, has nonempty interior and $t \mapsto \phi(t, J)$ is a maximal solution to $\dot{x} \in F(x)$, in fact $\lim_{t \to T} |\phi(t, J)| = \infty$, where $T = \sup_t \text{dom } \phi$;

c) $\phi(T, J) \notin C \cup D$, where $(T, J) = \sup \text{ dom } \phi$.

Now, since $G(D) \subset C \cup D = \mathcal{X}$ due to the definition of G, case c) does not occur. Additionally, one can eliminate case b) since f is globally Lipschitz continuous on C due to being linear affine in the state. Hence, only a) holds. □

B.3 Proof of Lemma 4.2.5

Proof. Pick an initial condition $\xi \in \mathcal{A}$. Let ϕ be a maximal solution to $\mathcal{H}$ with $\phi(0,0) = \xi$.[1]

[1] Note that for a given solution $\phi(t, j)$ to $\mathcal{H}$, the solution components are given by $\phi(t, j) = \big(\phi_e(t, j), \phi_u(t, j), \phi_\eta(t, j), \phi_{\tau^*}(t, j), \phi_{\hat{a}}(t, j), \phi_{\hat{\tau}}(t, j), \phi_\tau(t, j)\big)$

- Consider the case where $\phi(0,0) \in \mathcal{A} \setminus D$. The initial conditions of the components of ϕ satisfy $\phi_{e_i}(0,0) = \phi_{\eta_i}(0,0) = 0$ for the clock errors e_i, $\phi_{\hat{\tau}_i}(0,0) = \phi_{\tau_i^*}(0,0)$ for the estimated clocks $\hat{\tau}_i$, $\phi_{\hat{a}_i}(0,0) = \phi_{a_i}(0,0)$ for the clock rates $\hat{a}_i$ and $\phi_{u_i}(0,0) = \phi_{\eta_i}(0,0) - \phi_{\hat{a}_i}(0,0) + \sigma^*$ for the control input for each $i \in \mathcal{V}$. With f being linear affine and, thus, globally Lipschitz continuous on C, the constrained differential equation $\dot{x} = f(x)\ x \in C$ has unique solutions. Let $[0, t_1] \times \{0\} \subset \text{dom } \phi$ with $t_1 > 0$, which exists since $\phi(0,0) \in \mathcal{A} \setminus D$. Observe that, from the definition of f, the solution components of the states u, η, and e during this interval remain constant. This is evident since $\dot{\phi}_u = h\phi_\eta(0,0) - \mu\big(\phi_{\hat{\tau}}(0,0) - \phi_{\tau^*}(0,0)\big) = 0$ with $\phi_\eta(0,0) = 0$, $\dot{\phi}_\eta = h\phi_\eta(0,0) = 0$, and $\phi_{\hat{\tau}}(0,0) = \phi_{\tau^*}(0,0)$; hence, $\dot{\phi}_e = \phi_a(0,0) + \phi_u(0,0) - \sigma^* \mathbf{1}_n = 0$. From the definition of f in (4.9) we have that the components of the solution ϕ satisfy $\phi_{e_i}(t,j) = \phi_{e_k}(t,j)$, $\phi_\eta(t,j) = 0$, $\phi_{\hat{a}_i}(t,j) = \phi_{a_i}(t,j)$, $\phi_{\hat{\tau}_i}(t,j) = \phi_{\tau_i^*}(t,j)$, and $\phi_{u_i}(t,j) = \phi_{\eta_i}(t,j) - \phi_{\hat{a}_i}(t,j) + \sigma^*$ for each $(t,j) \in [0,t_1] \times \{0\}$. Therefore, the solution ϕ does not leave the set $\mathcal{A}$ during the interval $[0,t_1] \times \{0\}$ when $\phi(0,0) \in \mathcal{A} \setminus D$.

- Consider the case where $\phi(0,0) \in \mathcal{A} \cap D$. Since flow is not possible from $\phi(0,0)$ as $\phi_\tau(0,0) = 0$, $(\{0\} \times \{0\}) \cup (\{0\} \times \{1\}) \subset \text{dom } \phi$ as the solution ϕ jumps initially. By inspection, the jump map G in (4.9) only affects the states η, u, and τ, whereas the value of the other state components remains unchanged. Since the quantity $-\gamma \mathcal{L} e$ in the jump map is zero at $\phi(0,0)$, we have that $\phi_\eta(0,1) = -\gamma \mathcal{L} \phi_e(0,0) = 0$. Moreover, since $\hat{a}$ is constant across jumps, $\phi_{\hat{a}}(0,1) = \phi_{\hat{a}}(0,0)$, then,

$$\begin{aligned} \phi_u(0,1) &= -\gamma \mathcal{L} \phi_e(0,0) - \phi_{\hat{a}}(0,0) + \sigma^* \mathbf{1}_n \\ &= \phi_\eta(0,1) - \phi_{\hat{a}}(0,1) + \sigma^* \mathbf{1}_n \end{aligned}$$

  Lastly, we have that the timer τ resets to a point in the interval $[T_1, T_2]$, namely, $\phi_\tau(0,1) \in [T_1, T_2]$. Then, the full solution ϕ at $(0,1)$ satisfies

$$\phi(0,1) \in \begin{bmatrix} \phi_e(0,1) \\ \phi_\eta(0,1) - \phi_{\hat{a}}(0,1) + \sigma^* \mathbf{1}_n \\ \phi_\eta(0,1) \\ \phi_{\tau^*}(0,1) \\ \phi_{\hat{a}}(0,1) \\ \phi_{\hat{\tau}}(0,1) \\ [T_1, T_2] \end{bmatrix}$$

Hence, from the definition of $\mathcal{A}$, $\phi(0,1) \in \mathcal{A}$.

Since this property holds for each $\xi \in \mathcal{A}$, we have that solutions from $\mathcal{A}$ cannot flow out of $\mathcal{A}$ and cannot jump out of $\mathcal{A}$ since $G(\mathcal{A} \cap D) \subset \mathcal{A}$. Hence, $\mathcal{A}$ is forward invariant for $\mathcal{H}$. $\square$

B.4 Proof of Lemma 4.3.2

Proof. For each $x \in \mathcal{X}$, the distance from x to the set $\mathcal{A}$ is given as

$$|x|_{\mathcal{A}} = \inf_{y \in \mathcal{A}} |x - y| \tag{B.1}$$

Evaluating the distance directly, one has

$$\begin{aligned}
|x|_{\mathcal{A}} &= \inf_{y \in \mathcal{A}} |x - y| \\
&= \inf_{e^* \in E, \alpha_{\tau^*} \in \mathbb{R}^n_{\geq 0}, \alpha_\tau \in [0, T_2]} |(e, u, \eta, \tau^*, \hat{a}, \hat{\tau}, \tau) \\
&\qquad\qquad - (e^*, \eta - \hat{a} + \sigma^* \mathbf{1}_n, 0, \alpha_{\tau^*}, a, \tau^*, \alpha_\tau)| \\
&= \inf_{e^* \in E, \alpha_{\tau^*} \in \mathbb{R}^n_{\geq 0}, \alpha_\tau \in [0, T_2]} |(e - e^*, u - \eta + \hat{a} - \sigma^* \mathbf{1}_n, \eta, \\
&\qquad\qquad \tau^* - \alpha_{\tau^*}, \hat{a} - a, \hat{\tau} - \tau^*, \tau - \alpha_\tau)| \\
&= \inf_{e^* \in E} |(e - e^*, u - \eta + \hat{a} - \sigma^* \mathbf{1}_n, \eta, 0, \hat{a} - a, \hat{\tau} - \tau^*, 0)| \\
&= \inf_{e^* \in E} \operatorname{sqrt}\Big((e - e^*)^\top (e - e^*) \\
&\qquad + (u - \eta + \hat{a} - \sigma^* \mathbf{1}_n)^\top (u - \eta + \hat{a} - \sigma^* \mathbf{1}_n) \\
&\qquad + \eta^\top \eta + (\hat{a} - a)^\top (\hat{a} - a) + (\hat{\tau} - \tau^*)^\top (\hat{\tau} - \tau^*) \Big)
\end{aligned}$$

where $E := \{e^* \in \mathbb{R}^n : e^*_i = e^*_k \ \forall i, k \in \mathcal{V}\}$. When $u = \eta - \hat{a} + \sigma^* \mathbf{1}_n$ we have

$$\begin{aligned}
|x|_{\mathcal{A}} = \inf_{e^* \in E} \operatorname{sqrt}\Big(&(e - e^*)^\top (e - e^*) + \eta^\top \eta \\
&+ (\hat{a} - a)^\top (\hat{a} - a) + (\hat{\tau} - \tau^*)^\top (\hat{\tau} - \tau^*) \Big)
\end{aligned}$$

For each $x_\varepsilon \in \mathcal{X}_\varepsilon$, the distance from x_ε to the set $\mathcal{A}_\varepsilon$ is given as

$$|x_\varepsilon|_{\mathcal{A}_\varepsilon} = \inf_{y \in \mathcal{A}_\varepsilon} |x_\varepsilon - y| \tag{B.2}$$

Evaluating the distance directly, one has

$$\begin{aligned}
|x_\varepsilon|_{\mathcal{A}_\varepsilon} &= \inf_{y\in\mathcal{A}_\varepsilon} |x_\varepsilon - y| \\
&= \inf_{e^*\in E,\alpha_{\tau^*}\in\mathbb{R}^n_{\geq 0},\alpha_\tau\in[0,T_2]} |(e,\eta,\varepsilon_a,\varepsilon_\tau,\tau) \\
&\qquad\qquad - (e^*,0,0,0,\alpha_\tau)| \\
&= \inf_{e^*\in E,\alpha_{\tau^*}\in\mathbb{R}^n_{\geq 0},\alpha_\tau\in[0,T_2]} |(e-e^*,\eta,\varepsilon_a,\varepsilon_\tau,\tau-\alpha_\tau)| \\
&= \inf_{e^*\in E} |(e-e^*,\eta,\varepsilon_a,\varepsilon_\tau,0)| \\
&= \inf_{e^*\in E} \sqrt{(e-e^*)^\top(e-e^*)+\eta^\top\eta+\varepsilon_a^\top\varepsilon_a+\varepsilon_\tau^\top\varepsilon_\tau}
\end{aligned}$$

Making the appropriate substitutions for ε_τ and ε_a, we get

$$\begin{aligned}
|x_\varepsilon|_{\mathcal{A}_\varepsilon} = \inf_{e^*\in E} \mathrm{sqrt}\Big((e-e^*)^\top(e-e^*)+\eta^\top\eta+(\hat{a}-a)^\top(\hat{a}-a) \\
+(\hat{\tau}-\tau^*)^\top(\hat{\tau}-\tau^*)\Big)
\end{aligned}$$

Now, for each $(x_\varepsilon,\hat{\tau},\tau^*)\in\mathcal{X}$, the distance from the point $\widetilde{M}(x_\varepsilon,\hat{\tau},\tau^*)$ to the set $\mathcal{A}$ is given by

$$|\widetilde{M}(x_\varepsilon,\hat{\tau},\tau^*)|_{\mathcal{A}} = \inf_{y\in\mathcal{A}} |\widetilde{M}(x_\varepsilon,\hat{\tau},\tau^*)-y| \tag{B.3}$$

Computing this distance, one has

$$\begin{aligned}
|\widetilde{M}(x_\varepsilon,\hat{\tau},\tau^*)|_{\mathcal{A}} &= \inf_{y\in\mathcal{A}} |\widetilde{M}(x_\varepsilon,\hat{\tau},\tau^*)-y| \\
&= \inf_{e^*\in E,\alpha_{\tau^*}\in\mathbb{R}^n_{\geq 0},\alpha_\tau\in[0,T_2]} |(e,\eta-(a-\varepsilon_a)+\sigma^*\mathbf{1}_n,\eta, \\
&\qquad\qquad \hat{\tau}-\varepsilon_\tau, a-\varepsilon_a, \varepsilon_\tau+\tau^*,\tau) \\
&\qquad - (e^*,\eta-\hat{a}+\sigma^*\mathbf{1}_n,0,\alpha_{\tau^*},a,\tau^*,\alpha_\tau)|
\end{aligned}$$

Making the appropriate substitutions for ε_τ and ε_a, we get

$$\begin{aligned}
&|\widetilde{M}(x_\varepsilon, \hat{\tau}, \tau^*)|_{\mathcal{A}} \\
&\quad = \inf_{e^* \in E, \alpha_{\tau^*} \in \mathbb{R}^n_{\geq 0}, \alpha_\tau \in [0, T_2]} |(e, \eta - \hat{a} + \sigma^* \mathbf{1}_n, \eta, \tau^*, \hat{a}, \hat{\tau}, \tau) \\
&\qquad\qquad - (e^*, \eta - \hat{a} + \sigma^* \mathbf{1}_n, 0, \alpha_{\tau^*}, a, \tau^*, \alpha_\tau)| \\
&\quad = \inf_{e^* \in E, \alpha_{\tau^*} \in \mathbb{R}^n_{\geq 0}, \alpha_\tau \in [0, T_2]} |(e - e^*, \eta - \hat{a} + \sigma^* \mathbf{1}_n - \eta + \hat{a} - \sigma^* \mathbf{1}_n, \\
&\qquad\qquad \eta - 0, \tau^* - \alpha_{\tau^*}, \hat{a} - a, \hat{\tau} - \tau^*, \tau - \alpha_\tau)| \\
&\quad = \inf_{e^* \in E} |(e - e^*, 0, \eta, 0, \hat{a} - a, \hat{\tau} - \tau^*, 0)| \\
&\quad = \inf_{e^* \in E} \operatorname{sqrt}\Big((e - e^*)^\top (e - e^*) + \eta^\top \eta + (\hat{a} - a)^\top (\hat{a} - a) \\
&\qquad\qquad + (\hat{\tau} - \tau^*)^\top (\hat{\tau} - \tau^*) \Big)
\end{aligned}$$

Thus, we have that

$$|\widetilde{M}(x_\varepsilon, \hat{\tau}, \tau^*)|_{\mathcal{A}} = |x|_{\mathcal{A}} = |x_\varepsilon|_{\mathcal{A}_\varepsilon}$$

□

B.5 Proof of Lemma 4.3.3

Proof. Suppose the set $\mathcal{A}_\varepsilon$ is GES for $\mathcal{H}_\varepsilon$. By Definition 2.2.1 there exist $\kappa, \alpha > 0$ such that each maximal solution ϕ^ε to $\mathcal{H}_\varepsilon$ satisfies

$$|\phi^\varepsilon(t, j)|_{\mathcal{A}_\varepsilon} \leq \kappa \exp(-\alpha(t + j)) |\phi^\varepsilon(0, 0)|_{\mathcal{A}_\varepsilon} \tag{B.4}$$

for each $(t, j) \in \operatorname{dom} \phi^\varepsilon$. Now, pick any maximal solution ϕ to $\mathcal{H}$. Through an application of Lemma 4.3.1, there exists a corresponding solution ϕ^ε to $\mathcal{H}_\varepsilon$ such that

$$\phi(t, j) = \widetilde{M}\big(\phi^\varepsilon(t, j), \phi_{\hat{\tau}}(t, j), \phi_{\tau^*}(t, j)\big)$$

for each $(t, j) \in \operatorname{dom} \phi$. Given that ϕ^ε satisfies (B.4), using relationship (4.24) between distances in Lemma 4.3.2 we have that ϕ satisfies

$$|\phi(t, j)|_{\mathcal{A}} \leq \kappa \exp(-\alpha(t + j)) |\phi(0, 0)|_{\mathcal{A}} \tag{B.5}$$

Then, the set $\mathcal{A}$ is GES for $\mathcal{H}$. □

B.6 Proof of Lemma 4.3.4

Proof. Pick a solution $\tilde{\phi} \in \mathcal{S}_{\tilde{\mathcal{H}}_\varepsilon}$ with $\tilde{\phi} = (\tilde{\phi}_{\bar{z}_1}, \tilde{\phi}_{\bar{z}_2}, \tilde{\phi}_{\bar{w}_1}, \tilde{\phi}_{\bar{w}_2}, \tau)$, however, recall that $\bar{z}_1 := (\bar{e}_1, \bar{\eta}_1)$, $\bar{z}_2 := (\bar{e}_2, \ldots, \bar{e}_N, \bar{\eta}_2, \ldots, \bar{\eta}_N)$, $\bar{w}_1 = (\bar{\varepsilon}_{a_1}, \bar{\varepsilon}_{\tau_1})$, and $\bar{w}_2 = (\bar{\varepsilon}_{a_2}, \ldots, \bar{\varepsilon}_{a_n}, \bar{\varepsilon}_{\tau_2}, \ldots, \bar{\varepsilon}_{\tau_n})$. Thus, through a reordering of the solution trajectories, one has that with some of the above notation, $\tilde{\phi}$ can be rewritten as $\tilde{\phi} = (\tilde{\phi}_{\bar{e}}, \tilde{\phi}_{\bar{\eta}}, \tilde{\phi}_{\bar{\varepsilon}_a}, \tilde{\phi}_{\bar{\varepsilon}_\tau}, \tau)$. Then, recall the change of coordinates $\bar{e} = \mathcal{T}^{-1}e$, $\bar{\eta} = \mathcal{T}^{-1}\eta$, $\bar{\varepsilon}_a = \mathcal{T}^{-1}\varepsilon_a$, and $\bar{\varepsilon}_\tau = \mathcal{T}^{-1}\varepsilon_\tau$. Since $\mathcal{T}^{-1}$ is an invertible time-invariant linear operator, applying its inverse $\mathcal{T}$ to the components of $\tilde{\phi}$, one has $\big(\mathcal{T}\tilde{\phi}_{\bar{e}}(t,j), \mathcal{T}\tilde{\phi}_{\bar{\eta}}(t,j), \mathcal{T}\tilde{\phi}_{\bar{\varepsilon}_a}(t,j), \mathcal{T}\tilde{\phi}_{\bar{\varepsilon}_\tau}(t,j)\big) = \big(\phi_e(t,j), \phi_\eta(t,j), \phi_{\varepsilon_a}(t,j), \phi_{\varepsilon_\tau}(t,j)\big)$ for each $(t,j) \in \operatorname{dom} \tilde{\phi}$. Note that the dynamics of the variable τ, responsible for governing the flows and the jumps of both $\mathcal{H}_\varepsilon$ and $\widetilde{\mathcal{H}}_\varepsilon$, is identical for the two systems. Thus, the set of solutions for the component τ is the same between the two system. Therefore, it follows that $\tilde{\phi}(t,j) = \Gamma^{-1}\phi(t,j)$ for each $(t,j) \in \operatorname{dom} \tilde{\phi}$.

Conversely, we can pick a solution $\phi \in \mathcal{S}_{\mathcal{H}_\varepsilon}$, let $\phi = (\phi_e, \phi_\eta, \phi_{\varepsilon_a}, \phi_{\varepsilon_\tau}, \tau)$ and recall the change of coordinates $\bar{e} = \mathcal{T}^{-1}e$, $\bar{\eta} = \mathcal{T}^{-1}\eta$, $\bar{\varepsilon}_a = \mathcal{T}^{-1}\varepsilon_a$, and $\bar{\varepsilon}_\tau = \mathcal{T}^{-1}\varepsilon_\tau$. Since $\mathcal{T}^{-1}$ is a time-invariant linear operator, applying it to the components of ϕ, one has $\big(\mathcal{T}^{-1}\phi_e(t,j), \mathcal{T}^{-1}\phi_\eta(t,j), \mathcal{T}^{-1}\phi_{\varepsilon_a}(t,j), \mathcal{T}^{-1}\phi_{\varepsilon_\tau}(t,j)\big) = \big(\tilde{\phi}_{\bar{e}}(t,j), \tilde{\phi}_{\bar{\eta}}(t,j), \tilde{\phi}_{\bar{\varepsilon}_a}(t,j), \tilde{\phi}_{\bar{\varepsilon}_\tau}(t,j)\big)$ for each $(t,j) \in \operatorname{dom} \phi$. Thus, it follows that $\phi(t,j) = \Gamma\tilde{\phi}(t,j)$ for each $(t,j) \in \operatorname{dom} \phi$. □

B.7 Proof of Lemma 4.3.5

Proof. Pick a point $\tilde{z}' = (\bar{e}'_1, \bar{\eta}'_1, \bar{e}'_2, \ldots, \bar{e}'_N, \bar{\eta}'_2, \ldots, \bar{\eta}'_N, \bar{\varepsilon}'_{a_1}, \bar{\varepsilon}'_{\tau_1}, \bar{\varepsilon}'_{a_2}, \ldots, \bar{\varepsilon}'_{a_n}, \bar{\varepsilon}'_{\tau_2}, \ldots, \bar{\varepsilon}'_{\tau_n}) \in \mathbb{R}^{4N}$ such that $(\tilde{z}', \tau') \in \tilde{\mathcal{A}}_\varepsilon$ for some $\tau' \in [0, T_2]$, i.e., $\tilde{z}' = (e_1^*, 0, \mathbf{0}_{N-1}, \mathbf{0}_{N-1}, 0, 0, \mathbf{0}_{N-1}, \mathbf{0}_{N-1})$ with $e_1^* \in \mathbb{R}$. Given that the digraph $\mathcal{G}$ is strongly connected, there exists a nonsingular matrix $\mathcal{T}$ as in (4.26) that allows for the following coordinate change: $\bar{e} = \mathcal{T}^{-1}e$, $\bar{\eta} = \mathcal{T}^{-1}\eta$, $\bar{\varepsilon}_a = \mathcal{T}^{-1}\varepsilon_a$, and $\bar{\varepsilon}_\tau = \mathcal{T}^{-1}\varepsilon_\tau$. Now, by left

multiplying $(\tilde{z}', \tau')$ by Γ one has

$$\begin{aligned}
e=&\mathcal{T}\begin{bmatrix}\bar{e}_1' & \bar{e}_2' & \dots & \bar{e}_N'\end{bmatrix}^\top = \begin{bmatrix}v_1 & \mathcal{T}_1\end{bmatrix}\begin{bmatrix}e_1^* & \mathbf{0}_{N-1}^\top\end{bmatrix}^\top = e_1^*\mathbf{1}_N \\
\eta =& \mathcal{T}\begin{bmatrix}\bar{\eta}_1' & \bar{\eta}_2' & \dots & \bar{\eta}_N'\end{bmatrix}^\top = \begin{bmatrix}v_1 & \mathcal{T}_1\end{bmatrix}\begin{bmatrix}0 & \mathbf{0}_{N-1}^\top\end{bmatrix}^\top = \mathbf{0}_N \\
\varepsilon_a =& \mathcal{T}\begin{bmatrix}\bar{\varepsilon}_{a_1}' & \bar{\varepsilon}_{a_2}' & \dots & \bar{\varepsilon}_{a_n}'\end{bmatrix}^\top = \begin{bmatrix}v_1 & \mathcal{T}_1\end{bmatrix}\begin{bmatrix}0 & \mathbf{0}_{N-1}^\top\end{bmatrix}^\top = \mathbf{0}_N \\
\varepsilon_\tau =& \mathcal{T}\begin{bmatrix}\bar{\varepsilon}_{\tau_1}' & \bar{\varepsilon}_{\tau_2}' & \dots & \bar{\varepsilon}_{\tau_n}'\end{bmatrix}^\top = \begin{bmatrix}v_1 & \mathcal{T}_1\end{bmatrix}\begin{bmatrix}0 & \mathbf{0}_{N-1}^\top\end{bmatrix}^\top = \mathbf{0}_N \\
\tau =& 1\tau' = \tau'
\end{aligned} \tag{B.6}$$

Then, since $e = e_1^*\mathbf{1}_N$ we have that $e_i = e_k$ for each $i, k \in \mathcal{V}$. Since τ' was not subject to a coordinate change, then the point $(e, \eta, \varepsilon_a, \varepsilon_\tau, \tau) = (e_1^*\mathbf{1}_N, \mathbf{0}_N, \mathbf{0}_N, \mathbf{0}_N, \tau')$ is an element of $\mathcal{A}_\varepsilon$.

Now, pick a point $z' = (e, \eta, \varepsilon_a, \varepsilon_\tau) \in \mathbb{R}^{4N}$ such that $z' \in \mathcal{A}_\varepsilon$. This requires that $e_i = e_k$, $\eta_i = 0$, $\varepsilon_{a_i} = 0$, and $\varepsilon_{\tau_i} = 0$ for each $i, k \in \mathcal{V}$; thus, $z' = (e^*, \mathbf{0}_N, \mathbf{0}_N, \mathbf{0}_N)$, where $e^* \in E := \{e^* \in \mathbb{R}^n : e_i^* = e_k^* \ \forall i, k \in \mathcal{V}\}$. Then, by left multiplying (z', τ') by Γ^{-1}, one has

$$\begin{aligned}
\bar{e} &= \mathcal{T}^{-1}[e^*] = \begin{bmatrix}e_1^* & \mathbf{0}_{N-1}^\top\end{bmatrix}^\top \\
\bar{\eta} &= \mathcal{T}^{-1}\mathbf{0}_N = \begin{bmatrix}0 & \mathbf{0}_{N-1}^\top\end{bmatrix}^\top \\
\bar{\varepsilon}_a &= \mathcal{T}^{-1}\mathbf{0}_N = \begin{bmatrix}0 & \mathbf{0}_{N-1}^\top\end{bmatrix}^\top \\
\bar{\varepsilon}_\tau &= \mathcal{T}^{-1}\mathbf{0}_N = \begin{bmatrix}0 & \mathbf{0}_{N-1}^\top\end{bmatrix}^\top \\
\tau &= 1\tau = \tau
\end{aligned} \tag{B.7}$$

giving the point $(\bar{e}, \bar{\eta}, \bar{\varepsilon}_a, \bar{\varepsilon}_\tau, \tau) = (e_1^*, \mathbf{0}_{N-1}, \mathbf{0}_N, \mathbf{0}_N, \mathbf{0}_N)$. Rearranging the components into the form $(\bar{z}_1, \bar{z}_2, \bar{w}_1, \bar{w}_2, \tau)$ where $\bar{z}_1 = (\bar{e}_1, \bar{\eta}_1)$, $\bar{z}_2 = (\bar{e}_2, \dots, \bar{e}_N, \bar{\eta}_2, \dots, \bar{\eta}_N)$, $\bar{w}_1 = (\bar{\varepsilon}_{a_1}, \bar{\varepsilon}_{\tau_1})$, and $\bar{w}_2 = (\bar{\varepsilon}_{a_2}, \dots, \bar{\varepsilon}_{a_n}, \bar{\varepsilon}_{\tau_2}, \dots, \bar{\varepsilon}_{\tau_n})$ one has $(e_1^*, 0, \mathbf{0}_{N-1}, \mathbf{0}_{N-1}, 0, 0, \mathbf{0}_{N-1}, \mathbf{0}_{N-1})$ which is an element of $\tilde{\mathcal{A}}_\varepsilon$.

To relate the set distances between $|x_\varepsilon|_{\mathcal{A}_\varepsilon}$ and $|\chi_\varepsilon|_{\tilde{\mathcal{A}}_\varepsilon}$ for every $x_\varepsilon \in \mathcal{X}_\varepsilon$ and $\chi_\varepsilon \in \mathcal{X}_\varepsilon$, note that by definition, one has $|x_\varepsilon|_{\mathcal{A}_\varepsilon} = \inf_{y \in \mathcal{A}_\varepsilon}|x_\varepsilon - y|$ and $|\chi_\varepsilon|_{\tilde{\mathcal{A}}_\varepsilon} = \inf_{y \in \tilde{\mathcal{A}}_\varepsilon}|\chi_\varepsilon - y|$, respectively. Recall that $\chi_\varepsilon = \Gamma^{-1}x_\varepsilon$ and $x_\varepsilon = \Gamma\chi_\varepsilon$. Computing the distance $|\chi_\varepsilon|_{\tilde{\mathcal{A}}_\varepsilon}$, one has

$$\begin{aligned}
|\chi_\varepsilon|_{\tilde{\mathcal{A}}_\varepsilon} = |\Gamma^{-1}x_\varepsilon|_{\tilde{\mathcal{A}}_\varepsilon} &= \inf_{y \in \tilde{\mathcal{A}}_\varepsilon}|\Gamma^{-1}x_\varepsilon - y| \\
&= \inf_{e^* \in \mathbb{R}}|\Gamma^{-1}x_\varepsilon \\
&\quad - (e^*, 0, \mathbf{0}_{N-1}, \mathbf{0}_{N-1}, 0, 0, \mathbf{0}_{N-1}, \mathbf{0}_{N-1})|
\end{aligned}$$

Then, by using the relation $(e^*, 0, \mathbf{0}_{N-1}, \mathbf{0}_{N-1}, 0, 0, \mathbf{0}_{N-1}, \mathbf{0}_{N-1}) = \Gamma^{-1}(e^*\mathbf{1}_N, \mathbf{0}_N, \mathbf{0}_N, \mathbf{0}_N)$ one has

$$\begin{aligned}
|\Gamma^{-1}x_\varepsilon|_{\tilde{\mathcal{A}}_\varepsilon} &= \inf_{e^*\in\mathbb{R}}|\Gamma^{-1}x_\varepsilon - \Gamma^{-1}(e^*\mathbf{1}_N, \mathbf{0}_N, \mathbf{0}_N, \mathbf{0}_N)| \\
&= \inf_{e^*\in\mathbb{R}}\big|\Gamma^{-1}\big(x_\varepsilon - (e^*\mathbf{1}_N, \mathbf{0}_N, \mathbf{0}_N, \mathbf{0}_N)\big)\big| \\
&\leq |\Gamma^{-1}|\Big(\inf_{e^*\in\mathbb{R}}|x_\varepsilon - (e^*\mathbf{1}_N, \mathbf{0}_N, \mathbf{0}_N, \mathbf{0}_N)|\Big) \\
&\leq |\Gamma^{-1}|\Big(\inf_{y\in\mathcal{A}_\varepsilon}|x_\varepsilon - y|\Big) \\
&\leq |\Gamma^{-1}||x_\varepsilon|_{\mathcal{A}_\varepsilon}
\end{aligned}$$

Conversely, computing the distance $|x_\varepsilon|_{\mathcal{A}_\varepsilon}$, one has

$$\begin{aligned}
|x_\varepsilon|_{\mathcal{A}_\varepsilon} = |\Gamma\chi_\varepsilon|_{\mathcal{A}_\varepsilon} &= \inf_{y\in\mathcal{A}_\varepsilon}|\Gamma\chi_\varepsilon - y| \\
&= \inf_{e^*\in\mathbb{R}}|\Gamma\chi_\varepsilon - (e^*\mathbf{1}_N, \mathbf{0}_N, \mathbf{0}_N, \mathbf{0}_N)|
\end{aligned}$$

Then by using the relation $(e^*\mathbf{1}_N, \mathbf{0}_N, \mathbf{0}_N, \mathbf{0}_N) = \Gamma(e^*, 0, \mathbf{0}_{N-1}, \mathbf{0}_{N-1}, 0, 0, \mathbf{0}_{N-1}, \mathbf{0}_{N-1})$, one has

$$\begin{aligned}
|\Gamma\chi_\varepsilon|_{\mathcal{A}_\varepsilon} &= \inf_{e^*\in\mathbb{R}}|\Gamma\chi_\varepsilon - \Gamma(e^*, 0, \mathbf{0}_{N-1}, \mathbf{0}_{N-1}, 0, 0, \mathbf{0}_{N-1}, \mathbf{0}_{N-1})| \\
&= \inf_{e^*\in\mathbb{R}}\big|\Gamma\big(\chi_\varepsilon - (e^*, 0, \mathbf{0}_{N-1}, \mathbf{0}_{N-1}, 0, 0, \mathbf{0}_{N-1}, \mathbf{0}_{N-1})\big)\big| \\
&\leq |\Gamma|\Big(\inf_{e^*\in\mathbb{R}}|\chi_\varepsilon - (e^*, 0, \mathbf{0}_{N-1}, \mathbf{0}_{N-1}, 0, 0, \mathbf{0}_{N-1}, \mathbf{0}_{N-1})|\Big) \\
&\leq |\Gamma|\Big(\inf_{y\in\tilde{\mathcal{A}}_\varepsilon}|\chi_\varepsilon - y|\Big) \\
&\leq |\Gamma||\chi_\varepsilon|_{\tilde{\mathcal{A}}_\varepsilon}
\end{aligned}$$

□

B.8 Proof of Proposition 4.3.6

Proof. First, we prove that GES of $\tilde{\mathcal{A}}_\varepsilon$ for $\widetilde{\mathcal{H}}_\varepsilon$ implies GES of $\mathcal{A}_\varepsilon$ for $\mathcal{H}_\varepsilon$. Suppose the set $\tilde{\mathcal{A}}_\varepsilon$ is GES for $\widetilde{\mathcal{H}}_\varepsilon$. By Definition 2.2.1, there exist $\kappa, \alpha > 0$ such that

$$|\tilde{\phi}(t,j)|_{\tilde{\mathcal{A}}_\varepsilon} \leq \kappa\exp(-\alpha(t+j))|\tilde{\phi}(0,0)|_{\tilde{\mathcal{A}}_\varepsilon} \quad \forall (t,j) \in \text{dom } \tilde{\phi} \tag{B.8}$$

holds for every solution $\tilde{\phi}$ to $\widetilde{\mathcal{H}}_\varepsilon$. Pick a (maximal) solution $\tilde{\phi} \in \mathcal{S}_{\widetilde{\mathcal{H}}_\varepsilon}$ with initial condition $\tilde{\phi}(0,0) \in \widetilde{C}_\varepsilon \cup \widetilde{D}_\varepsilon$. According to Lemma 4.3.4, there exists a maximal solution ϕ to $\mathcal{H}_\varepsilon$ such that

$$\tilde{\phi}(t,j) = \Gamma^{-1}\phi(t,j) \tag{B.9}$$

for each $(t,j) \in \text{dom } \tilde{\phi}$, where $\Gamma^{-1} = \text{diag}(\mathcal{T}^{-1}, \mathcal{T}^{-1}, \mathcal{T}^{-1}, \mathcal{T}^{-1}, 1)$. Given that $\tilde{\phi}$ satisfies (B.8), applying (B.9) and the relationship between distances in Lemma 4.3.5 given in (4.30) to the right-hand side of (B.8), we have that

$$\begin{aligned} |\tilde{\phi}(t,j)|_{\tilde{\mathcal{A}}_\varepsilon} &\leq \kappa \exp(-\alpha(t+j))|\tilde{\phi}(0,0)|_{\tilde{\mathcal{A}}_\varepsilon} = \kappa \exp(-\alpha(t+j))|\Gamma^{-1}\phi(0,0)|_{\tilde{\mathcal{A}}_\varepsilon} \\ &\leq \kappa \exp(-\alpha(t+j))|\Gamma^{-1}||\phi(0,0)|_{\mathcal{A}_\varepsilon} \end{aligned} \tag{B.10}$$

By rearranging the relationship given in (4.31), we obtain

$$\frac{1}{|\Gamma|}|x_\varepsilon|_{\mathcal{A}_\varepsilon} = \frac{1}{|\Gamma|}|\Gamma\chi_\varepsilon|_{\mathcal{A}_\varepsilon} \leq |\chi_\varepsilon|_{\tilde{\mathcal{A}}_\varepsilon} \tag{B.11}$$

Applying it to the left-hand side of (B.10), we have

$$\frac{1}{|\Gamma|}|\phi(t,j)|_{\mathcal{A}_\varepsilon} \leq |\tilde{\phi}(t,j)|_{\tilde{\mathcal{A}}_\varepsilon} \leq \kappa \exp(-\alpha(t+j))|\Gamma^{-1}||\phi(0,0)|_{\mathcal{A}_\varepsilon}$$

Thus, we have that ϕ satisfies

$$|\phi(t,j)|_{\mathcal{A}_\varepsilon} \leq \tilde{\kappa} \exp(-\alpha(t+j))|\phi(0,0)|_{\mathcal{A}_\varepsilon} \quad \forall (t,j) \in \text{dom } \phi \tag{B.12}$$

where $\tilde{\kappa} = \kappa|\Gamma||\Gamma^{-1}|$. Then, the set $\mathcal{A}_\varepsilon$ is GES for $\mathcal{H}_\varepsilon$.

Conversely, suppose the set $\mathcal{A}_\varepsilon$ is GES for $\mathcal{H}_\varepsilon$. By Definition 2.2.1, there exist $\kappa, \alpha > 0$ such that

$$|\phi(t,j)|_{\mathcal{A}_\varepsilon} \leq \kappa \exp(-\alpha(t+j))|\phi(0,0)|_{\mathcal{A}_\varepsilon} \quad \forall (t,j) \in \text{dom } \phi \tag{B.13}$$

holds for every maximal solution ϕ to $\mathcal{H}_\varepsilon$. Pick a maximal solution $\phi \in \mathcal{S}_{\mathcal{H}_\varepsilon}$ with initial condition $\phi(0,0) \in C_\varepsilon \cup D_\varepsilon$. According to Lemma 4.3.4, there exists a solution $\tilde{\phi}$ to $\widetilde{\mathcal{H}}_\varepsilon$ such that

$$\phi(t,j) = \Gamma\tilde{\phi}(t,j) \tag{B.14}$$

for each $(t,j) \in \text{dom } \phi$, where $\Gamma = \text{diag}(\mathcal{T}, \mathcal{T}, \mathcal{T}, \mathcal{T}, 1)$. Given that ϕ satisfies (B.13), applying (B.14) and the relationship between distances in Lemma 4.3.5 to the right-hand side of (B.8), we have that

$$\begin{aligned} |\phi(t,j)|_{\mathcal{A}_\varepsilon} &\leq \kappa \exp(-\alpha(t+j))|\phi(0,0)|_{\mathcal{A}_\varepsilon} = \kappa \exp(-\alpha(t+j))|\Gamma\tilde{\phi}(0,0)|_{\mathcal{A}_\varepsilon} \\ &\leq \kappa \exp(-\alpha(t+j))|\Gamma||\tilde{\phi}(0,0)|_{\tilde{\mathcal{A}}_\varepsilon} \end{aligned} \tag{B.15}$$

By rearranging the relationship given in (4.30), we obtain

$$\frac{1}{|\Gamma^{-1}|}|\chi_\varepsilon|_{\tilde{\mathcal{A}}_\varepsilon} = \frac{1}{|\Gamma^{-1}|}|\Gamma^{-1}x_\varepsilon|_{\tilde{\mathcal{A}}_\varepsilon} \leq |x_\varepsilon|_{\mathcal{A}_\varepsilon} \tag{B.16}$$

Applying it to the left-hand side of (B.15), we have

$$\frac{1}{|\Gamma^{-1}|}|\tilde{\phi}(t,j)|_{\mathcal{A}_\varepsilon} \leq |\phi(t,j)|_{\mathcal{A}_\varepsilon} \leq \kappa \exp(-\alpha(t+j))|\Gamma||\tilde{\phi}(0,0)|_{\mathcal{A}_\varepsilon}$$

Thus, we have that $\tilde{\phi}$ satisfies

$$|\tilde{\phi}(t,j)|_{\tilde{\mathcal{A}}_\varepsilon} \leq \kappa' \exp(-\alpha(t+j))|\tilde{\phi}(0,0)|_{\tilde{\mathcal{A}}_\varepsilon} \quad \forall (t,j) \in \text{dom } \tilde{\phi} \tag{B.17}$$

where $\kappa' = \kappa|\Gamma^{-1}||\Gamma|$. Then, the set $\tilde{\mathcal{A}}_\varepsilon$ is GES for $\widetilde{\mathcal{H}}_\varepsilon$. □

B.9 Proof of Proposition 4.3.7

Proof.

$$V_{\varepsilon_r}(\chi_{\varepsilon_r}) = \bar{w}_1^\top P_2 \bar{w}_1 + \bar{w}_2^\top P_3 \bar{w}_2 \tag{B.18}$$

It satisfies

$$\alpha_{\bar{\omega}_1}|\chi_{\varepsilon_r}|^2_{\tilde{\mathcal{A}}_{\varepsilon_r}} \leq V(\chi_{\varepsilon_r}) \leq \alpha_{\bar{\omega}_2}|\chi_{\varepsilon_r}|^2_{\tilde{\mathcal{A}}_{\varepsilon_r}} \quad \forall \chi_{\varepsilon_r} \in \tilde{C}_{\varepsilon_r} \cup \tilde{D}_{\varepsilon_r} \tag{B.19}$$

with $\alpha_1 = \min\{\lambda_{min}(P_2), \lambda_{min}(P_3)\}$ and $\alpha_2 = \max\{\lambda_{max}(P_2), \lambda_{max}(P_3)\}$. For each $\chi_{\varepsilon_r} \in \tilde{C}_{\varepsilon_r}$

$$\begin{aligned}\langle \nabla V_{\varepsilon_r}(\chi_{\varepsilon_r}), \tilde{f}(\chi_{\varepsilon_r})\rangle \leq\ & \bar{w}_1^\top (P_2 A_{f_3} + A_{f_3}^\top P_2)\bar{w}_1 \\ & + \bar{w}_2^\top (P_3 A_{f_4} + A_{f_4}^\top P_3)\bar{w}_2\end{aligned} \tag{B.20}$$

The conditions in (4.13) imply the existence of positive numbers β_1 and β_2 such that

$$P_2 A_{f_3} + A_{f_3}^\top P_2 \leq -\beta_1 I$$

$$P_3 A_{f_4} + A_{f_4}^\top P_3 \leq -\beta_2 I$$

Then

$$\begin{aligned}\langle \nabla V_{\varepsilon_r}(\chi_{\varepsilon_r}), \tilde{f}_{\varepsilon_r}(\chi_{\varepsilon_r})\rangle &\leq -\beta_1|\bar{w}_1|^2 - \beta_2|\bar{w}_2|^2 \\ &\leq -\tilde{\beta}\big(|\bar{w}_1|^2 + |\bar{w}_2|^2\big) \\ &\leq -\tilde{\beta}\big(|\chi_{\varepsilon_r}|^2_{\tilde{\mathcal{A}}_{\varepsilon_r}}\big) \\ &\leq -\frac{\tilde{\beta}}{\alpha_{\bar{\omega}_2}} V_{\varepsilon_r}(\chi_{\varepsilon_r})\end{aligned} \tag{B.21}$$

where $\tilde{\beta} = \min\{\beta_1, \beta_2\} > 0$. For all $\chi_{\varepsilon_r} \in \tilde{D}_{\varepsilon_r}$ and $g \in \tilde{G}_{\varepsilon_r}(\chi_{\varepsilon_r})$

$$V_{\varepsilon_r}(g) - V_{\varepsilon_r}(\chi_{\varepsilon_r}) = 0 \tag{B.22}$$

Now, pick a solution $\tilde{\phi}$ to $\widetilde{\mathcal{H}}_{\varepsilon_r}$ with initial condition $\tilde{\phi}(0,0) \in \widetilde{C}_{\varepsilon_r} \cup \widetilde{D}_{\varepsilon_r}$. As a result of (B.21) and (B.22), direct integration of $(t,j) \mapsto V_{\varepsilon_r}(\tilde{\phi}(t,j))$ over dom $\tilde{\phi}$ gives

$$V_{\varepsilon_r}(\tilde{\phi}(t,j)) \leq \exp\Big(-\frac{\tilde{\beta}}{\alpha_{\bar{\omega}_2}}t\Big)V_{\varepsilon_r}(\tilde{\phi}(0,0)) \quad \forall (t,j) \in \text{dom } \tilde{\phi} \tag{B.23}$$

Now, given the relation established in (4.12), for any solution $\tilde{\phi}$ to $\widetilde{\mathcal{H}}_{\varepsilon_r}$, we have $jT_2 \leq t \Rightarrow -t \leq -jT_2$. Then, for any $\gamma \in (0,1)$ we have $-\gamma t \leq -\gamma T_2 j$. Moreover,

$$\begin{aligned} -t = -(1-\gamma)t - \gamma t &\leq -(1-\gamma)t - \gamma T_2 j \\ &\leq -\min\{1-\gamma, \gamma T_2\}(t+j) \end{aligned} \tag{B.24}$$

leading to

$$V_{\varepsilon_r}(\tilde{\phi}(t,j)) \leq \exp\Big(-\frac{\bar{\gamma}\tilde{\beta}}{\alpha_{\bar{\omega}_2}}(t+j)\Big)V_{\varepsilon_r}(\tilde{\phi}(0,0)) \tag{B.25}$$

for each $(t,j) \in \text{dom } \tilde{\phi}$ where $\bar{\gamma} = \min\{1-\gamma, \gamma T_2\}$. Then, by combining this inequality with (B.19), one has

$$\alpha_{\bar{\omega}_1}|\chi_{\varepsilon_r}|^2_{\tilde{\mathcal{A}}_{\varepsilon_r}} \leq V_{\varepsilon_r}(\tilde{\phi}(t,j)) \leq \exp\Big(-\frac{\bar{\gamma}\tilde{\beta}}{\alpha_{\bar{\omega}_2}}(t+j)\Big)V_{\varepsilon_r}(\tilde{\phi}(0,0)) \tag{B.26}$$

then leveraging $V_{\varepsilon_r}(\tilde{\phi}(0,0)) \leq \alpha_{\bar{\omega}_2}|\tilde{\phi}(0,0)|^2_{\tilde{\mathcal{A}}_{\varepsilon_r}}$ we have

$$|\tilde{\phi}(t,j)|^2_{\tilde{\mathcal{A}}_{\varepsilon_r}} \leq \frac{\alpha_{\bar{\omega}_2}}{\alpha_{\bar{\omega}_1}} \exp\Big(-\frac{\bar{\gamma}\tilde{\beta}}{\alpha_{\bar{\omega}_2}}(t+j)\Big)|\tilde{\phi}(0,0)|^2_{\tilde{\mathcal{A}}_{\varepsilon_r}} \tag{B.27}$$

then

$$|\tilde{\phi}(t,j)|_{\tilde{\mathcal{A}}_{\varepsilon_r}} \leq \sqrt{\frac{\alpha_{\bar{\omega}_2}}{\alpha_{\bar{\omega}_1}}} \exp\Big(-\frac{\bar{\gamma}\tilde{\beta}}{2\alpha_{\bar{\omega}_2}}(t+j)\Big)|\tilde{\phi}(0,0)|_{\tilde{\mathcal{A}}_{\varepsilon_r}} \tag{B.28}$$

Observe that this bound holds for each solution $\tilde{\phi}$ to $\widetilde{\mathcal{H}}_{\varepsilon_r}$. Maximal solutions to $\widetilde{\mathcal{H}}_{\varepsilon_r}$ are complete due to the reduction property established in Lemmas 4.3.4, 4.3.1, and 4.2.5. In particular, Lemma 4.3.4 establishes the relation between $\widetilde{\mathcal{H}}_{\varepsilon}$ and $\mathcal{H}_{\varepsilon}$, Lemma 4.3.1 establishes the reduction from $\mathcal{H}$ to $\mathcal{H}_{\varepsilon}$, the former for which we have established completeness of solutions in Lemma 4.2.5. Therefore, the set $\tilde{\mathcal{A}}_{\varepsilon_r}$ is globally exponentially stable for $\widetilde{\mathcal{H}}_{\varepsilon_r}$. □

B.10 Proof of Proposition 4.4.2

:

Proof. Consider the same Lyapunov function candidate $V(\chi_m) = V_1(\chi_m) + V_2(\chi_m) + V_{\varepsilon_r}(\chi_m)$ from the proof of Theorem 4.2.6 in Section 4.3.4. During flows, there is no contribution from the perturbation thus the derivative of V is unchanged from the proof of Theorem 4.2.6. Thus, one has that (**??**) holds with $\widetilde{f}_\varepsilon(\chi_\varepsilon)$ replaced by $\widetilde{f}_m(\chi_m)$, namely,

$$\begin{aligned}\langle \nabla V(\chi_m), \tilde{f}(\chi_m)\rangle \leq\ & 2\bar{z}_2^\top \big(\exp(A_{f_2}^\top \tau) P \exp(A_{f_2}\tau)\big) B_{f_2}\bar{w}_2 \\ & + \bar{w}_1^\top (P_1 A_{f_3} + A_{f_3}^\top P_1)\bar{w}_1 \\ & + \bar{w}_2^\top (P_2 A_{f_4} + A_{f_4}^\top P_2)\bar{w}_2\end{aligned}$$

then by following the same notions of the proof in Theorem 4.2.6, one has $\langle \nabla V(\chi_m), \widetilde{f}(\chi_m)\rangle \leq \frac{\bar{\kappa}_1}{\alpha_2} V(\chi_m)$ where $\bar{\kappa}_1 = \max\Big\{\frac{\kappa_1}{2\epsilon}, \Big(\frac{\kappa_1 \epsilon}{2} - \beta_2\Big)\Big\}$ and $\varepsilon > 0$. At jumps, triggered when $\tau = 0$, one has, for each $\chi_m \in \widetilde{D}_m \setminus \widetilde{\mathcal{A}}_\varepsilon$ and $g \in \widetilde{G}_m(\chi_m)$

$$\begin{aligned}V(g)\text{-}V(\chi_m) \leq & \\ & - \bar{\eta}_1^2 + (A_{g_2}\bar{z}_2)^\top \exp(A_{f_2}^\top \tau) P_1 \exp(A_{f_2}\tau)(A_{g_2}\bar{z}_2) \\ & -2(B_g \bar{m}_{\bar{z}_2})^\top \exp(A_{f_2}^\top \tau) P_1 \exp(A_{f_2}\tau)(A_{g_2}\bar{z}_2) \\ & + (B_g \bar{m}_{\bar{z}_2})^\top \exp(A_{f_2}^\top \tau) P_1 \exp(A_{f_2}\tau)(B_g \bar{m}_{\bar{z}_2}) \\ & -\bar{z}_2^\top P_1 \bar{z}_2\end{aligned} \tag{B.29}$$

From (4.15) and the proof in Theorem 4.2.6, there exists a scalar κ_2 such that $\bar{z}_2^\top (A_{g_2}^\top \exp(A_{f_2}^\top v) P_1 \exp(A_{f_2} v) A_{g_2} - P_1)\bar{z}_2 \leq -\kappa_2 \bar{z}_2^\top \bar{z}_2$ leading to

$$\begin{aligned}V(g)\text{-}V(\chi_m) \leq & -\bar{\eta}_1^2 - \kappa_2 \bar{z}_2^\top \bar{z}_2 \\ & - 2(B_g \bar{m}_{\bar{z}_2})^\top \exp(A_{f_2}^\top \tau) P_1 \exp(A_{f_2}\tau)(A_{g_2}\bar{z}_2) \\ & + (B_g \bar{m}_{\bar{z}_2})^\top \exp(A_{f_2}^\top \tau) P_1 \exp(A_{f_2}\tau)(B_g \bar{m}_{\bar{z}_2})\end{aligned} \tag{B.30}$$

Let $Q = \exp(A_{f_2}^\top \tau) P_1 \exp(A_{f_2}\tau)$, then applying Young's inequality on the third term such that

$$\bar{m}_{\bar{z}_2}^\top B_g^\top Q A_{g_2} \bar{z}_2 \leq \frac{\big|(B_g^\top Q A_{g_2})(B_g^\top Q A_{g_2})^\top\big|}{2\epsilon_2} \bar{m}_{\bar{z}_2}^\top \bar{m}_{\bar{z}_2} + \frac{\epsilon_2}{2} \bar{z}_2^\top \bar{z}_2$$

where $\epsilon_2 > 0$. Then, we have

$$\begin{aligned}V(g)\text{-}V(\chi_m) \leq & -\bar{\eta}_1^2 - \big(\kappa_2 + \frac{\epsilon_2}{2}\big)\bar{z}_2^\top \bar{z}_2 + \big(|B_g^\top Q B_g| \\ & - \frac{1}{2\epsilon_2} |(B_g^\top Q A_{g_2})(B_g^\top Q A_{g_2})^\top|\big) \bar{m}_{\bar{z}_2}^\top \bar{m}_{\bar{z}_2}\end{aligned} \tag{B.31}$$

By noting $|A_{g_2}|, |B_g| \leq \gamma \lambda_{max}(\bar{\mathcal{L}})$ let $\kappa_{\bar{m}_2} = \big(\lambda_{max}(\bar{\mathcal{L}})\big)^2 \max\limits_{v \in [0, T_2]} \Big\{\lambda_{max}\big(\exp(A_{f_2}^\top v) P_1 \exp(A_{f_2} v)\big)\Big\}$, we let $\epsilon_2 = \kappa_2$ and obtain

$$V(g)\text{-}V(\chi_m) \leq -\bar{\eta}_1^2 - \frac{3\kappa_2}{2} \bar{z}_2^\top \bar{z}_2 + \big(\gamma^2 \kappa_{\bar{m}_2} - \frac{\gamma^4 \kappa_{\bar{m}_2}^2}{2\kappa_2}\big) \bar{m}_{\bar{z}_2}^\top \bar{m}_{\bar{z}_2}$$

Now, let $\tilde{\kappa}_{\bar{m}_2} = \gamma^2 \kappa_{\bar{m}_2} - \frac{1}{2\kappa_2}\gamma^4 \kappa_{\bar{m}_2}^2$ then at jumps one has

$$V(g) - V(\chi_m) \leq -\bar{\kappa}_2(|\bar{\eta}_1|^2 + |\bar{z}_2|^2) + \tilde{\kappa}_{\bar{m}_2}|\bar{m}_{\bar{z}_2}|^2 \tag{B.32}$$

where $\bar{\kappa}_2 = \max\{1, \frac{3\kappa_2}{2}\}$. Now, recall from (4.45) in the proof of Theorem 4.2.6 that

$$-(|\bar{\eta}_1|^2 + |\bar{z}_2|^2) \leq -\frac{1}{\alpha_2} V(\chi_\varepsilon) + |\bar{w}|^2 \tag{B.33}$$

Then, plugging (4.45) into (B.32) one has

$$V(g) \leq \Big(1 - \frac{3\kappa_2}{2\alpha_2}\Big) V(\chi_m) + \frac{3\kappa_2}{2}|\bar{w}|^2 + \tilde{\kappa}_{\bar{m}_2}|\bar{m}_{\bar{z}_2}|^2$$

Noting $\langle \nabla V(\chi_\varepsilon), \widetilde{f}(\chi_\varepsilon)\rangle \leq \frac{\bar{\kappa}_1}{\alpha_2} V(\chi_\varepsilon)$, one can then pick a solution with initial conditions $\tilde{\phi}(0,0) \in \widetilde{C}_m \cup \widetilde{D}_m$ and find that the trajectory of $V(\tilde{\phi}(t,j))$ is bounded as follows:

$$\begin{aligned} V(\tilde{\phi}(t,j)) \leq & \\ & \exp\big(\frac{\bar{\kappa}_1}{\alpha_2} T_2\big)\Big(\exp\big(\frac{\bar{\kappa}_1}{\alpha_2} T_2\big)\Big(1 - \frac{3\kappa_2}{2\alpha_2}\Big)\Big)^j V(\tilde{\phi}(0,0)) \\ & + \frac{3\kappa_2}{2}\exp\big(\bar{\kappa} T_2\big)\sup_{(t,j)\in \mathrm{dom}\phi}|\bar{w}(t,j)|^2 \\ & + \tilde{\kappa}_{\bar{m}_2}\exp\Big(\frac{\kappa}{2\epsilon_2} T_2\Big)\sup_{(t,j)\in \mathrm{dom}\phi}|\bar{m}_{\bar{z}_2}|^2 \end{aligned}$$

The result follows from an analysis of $V(\tilde{\phi}(t,j))$ over dom $\tilde{\phi}$ utilizing the same approach as in the proof of Theorem 4.2.6. □

Appendix C

Appendix C - Proofs of Lemmas for Hybrid Consensus Clock Synchronization

C.1 Proof of Lemma 5.3.1

Proof. By inspection of the hybrid system data $(C_\varepsilon, F_\varepsilon, D_\varepsilon, G_\varepsilon)$ defining $\mathcal{H}_\varepsilon$ given in (5.23), the following is observed:

- The set C_ε is a closed subset of $\mathbb{R}^m$ since C_ε is the union of the sets C_{ε_1} and C_{ε_2}, both of which are the Cartesian product of closed sets. Similar arguments show that D_ε is closed since it can be written as the finite union of closed sets, that is,

$$D_\varepsilon = \bigcup_{p \in \mathcal{P}} \left(\mathbb{R}^2 \times \mathbb{R} \times \mathbb{R} \times \mathbb{R} \times \mathbb{R} \times \{0\} \times \mathbb{R}^6 \times \mathbb{R}^6 \times \{p\} \times \mathcal{Q} \right)$$

  Thus, (A1) holds.

- The function $F_\varepsilon : \mathcal{X}_\varepsilon \to \mathcal{X}_\varepsilon$ is linear affine in the state and thus continuous on C_ε. Thus, (A2) holds.

- To show that the set-valued map G_ε defined in (5.22) satisfies (A3), observe that by inspection, for each $i \in \{1, 2, 3, 4, 5, 6\}$ G_{ε_i} is a continuous map. Moreover, for each

$i \in \{1,2,3,4,5,6\}$ D_{ε_i} is closed and

$$D_{\varepsilon_i} \cap D_{\varepsilon_k} = \emptyset \qquad \forall i,k \in \{1,2,3,4,5,6\}, i \neq k$$

which implies that there is a (uniform) finite separation between these sets. This is due to the fact that these sets are defined for different values of the logic variables. Hence, (A3) holds as G_ε is a piecewise function with each piece being continuous.

□

C.2 Proof of Lemma 5.3.2

Proof. Consider an arbitrary $\xi \in C_\varepsilon \cup D_\varepsilon$. The tangent cone $T_{C_\varepsilon}(\xi)$, as defined in [4, Definition 5.12], given by

$$T_{C_\varepsilon}(\xi) = \begin{cases} \mathbb{R}^2 \times \mathbb{R} \times \mathbb{R} \times \mathbb{R} \times \mathbb{R} \times \mathbb{R}_{\geq 0} \times \mathbb{R}^6 \times \mathbb{R}^6 \times \mathcal{P} \times \mathcal{Q} & \text{if } \xi \in \mathcal{X}_\varepsilon^1 \\ \mathbb{R}^2 \times \mathbb{R} \times \mathbb{R} \times \mathbb{R} \times \mathbb{R} \times \mathbb{R} \times \mathbb{R}^6 \times \mathbb{R}^6 \times \mathcal{P} \times \mathcal{Q} & \text{if } \xi \in \mathcal{X}_\varepsilon^2 \\ \mathbb{R}^2 \times \mathbb{R} \times \mathbb{R} \times \mathbb{R} \times \mathbb{R} \times \mathbb{R}_{\leq 0} \times \mathbb{R}^6 \times \mathbb{R}^6 \times \mathcal{P} \times \mathcal{Q} & \text{if } \xi \in \mathcal{X}_\varepsilon^3 \end{cases}$$

where $\mathcal{X}_\varepsilon^1 := \{x_\varepsilon \in \mathcal{X}_\varepsilon : \tau = 0\}$, $\mathcal{X}_\varepsilon^2 := \{x_\varepsilon \in \mathcal{X}_\varepsilon : \tau \in (0,d)\}$, and $\mathcal{X}_\varepsilon^3 := \{x_\varepsilon \in \mathcal{X}_\varepsilon : \tau = d\}$. By inspection, $F_\varepsilon(x_\varepsilon) \cap T_{C_\varepsilon}(x_\varepsilon) \neq \emptyset$ holds for every $x_\varepsilon \in C_\varepsilon \setminus D$. Then, by [4, Proposition 6.10], there exists a nontrivial solution ϕ to $\mathcal{H}_\varepsilon$ with $\phi(0,0) = \xi$. Moreover, by the same result, every $\phi \in \mathcal{S}_{\mathcal{H}_\varepsilon}$ satisfies one of the following conditions:

a) ϕ is complete;

b) dom ϕ is bounded and the interval I^J, where $J = \sup_j \text{dom } \phi$, has nonempty interior and $t \mapsto \phi(t,J)$ is a maximal solution to $\dot{x} \in F(x)$, in fact $\lim_{t \to T} |\phi(t,J)| = \infty$, where $T = \sup_t \text{dom } \phi$;

c) $\phi(T,J) \notin C \cup D$, where $(T,J) = \sup \text{ dom } \phi$.

Now, since $G_\varepsilon(D_\varepsilon) \subset C_\varepsilon \cup D_\varepsilon$ case (c) does not occur. Additionally, one can eliminate case (b) since, by inspection, F_ε is Lipschitz continuous on C_ε. □

C.3 Proof of Lemma 5.3.3

Proof. Pick an initial condition $\phi(0,0) \in \mathcal{M}$.

- If $\phi(0,0) \in \mathcal{M} \cap (C_\varepsilon \setminus D_\varepsilon)$, then the solution initially flows according to $\dot{x}_\varepsilon = F_\varepsilon(x)$. Observe that the trajectories of m^i, m^k, p, and q remain constant since F_ε is defined so that $\dot{m}^i = \dot{m}^k = \dot{p} = \dot{q} = 0$. Moreover, note that the gradient of ρ_i and ρ_k with respect to $x_\varepsilon = (\varepsilon, \tau_i, \tau_k, a_i, a_k, \tau, m^i, m^k, p, q)$ satisfy

$$\nabla_{x_\varepsilon}\rho_i(x_\varepsilon,\beta) = \begin{bmatrix} \mathbf{0}_{2\times 1} \\ 1 \\ 0 \\ \tau - \beta - dq + c(q-1) \\ 0 \\ a_i \\ \mathbf{0}_{6\times 1} \\ \mathbf{0}_{6\times 1} \\ 0 \\ a_i(c-d) \end{bmatrix}, \quad \nabla_{x_\varepsilon}\rho_k(x_\varepsilon,\beta) = \begin{bmatrix} \mathbf{0}_{2\times 1} \\ 0 \\ 1 \\ 0 \\ \tau - \beta - dq + c(q-1) \\ a_k \\ \mathbf{0}_{6\times 1} \\ \mathbf{0}_{6\times 1} \\ 0 \\ a_k(c-d) \end{bmatrix} \tag{C.1}$$

  Then one has $\dot{\rho}_i(x_\varepsilon,\beta) = \langle \nabla\rho_i(x_\varepsilon,\beta), F_\varepsilon(x_\varepsilon)\rangle = 1a_i + a_i(-1) = 0$ and $\dot{\rho}_k(x_\varepsilon,\beta) = \langle \nabla\rho_k(x_\varepsilon,\beta), F_\varepsilon(x_\varepsilon)\rangle = 1a_k + a_k(-1) = 0$. Therefore, when ϕ initially flows from a point in $\mathcal{M}$, it remains in $\mathcal{M}$ over the interval of flow. This property holds for every solution over any of its intervals of flows that starts at a point in $\mathcal{M}$.

- If $\phi(0,0) \in \mathcal{M} \cap D_\varepsilon$, then the solution initially jumps according to $x_\varepsilon^+ = G_\varepsilon(x_\varepsilon)$. In particular,

  - if $\phi(0,0) \in \mathcal{M}_1 \cap D_{\varepsilon_1}$, the solution jumps according to $x_\varepsilon^+ = G_{\varepsilon_1}(x_\varepsilon)$. The timer τ resets according to $\tau^+ = d$ while $q^+ = 1$ and $p^+ = 1$. Moreover, $(m_1^i)^+$ is assigned to the value of τ_i, evaluating $\rho_i(x_\varepsilon^+, 0)$, we have that for each $x_\varepsilon \in D_{\varepsilon_1}$

$$\begin{aligned} \rho_i(x_\varepsilon^+,0) &= \tau_i - a_i((1-q^+)c + q^+d - \tau^+) - a_i 0 \\ &= \tau_i - a_i((1-1)c + d - d) \\ &= \tau_i \end{aligned}$$

    Thus, by recalling the definition of $\mathcal{M}_2 = \{x_\varepsilon \in \mathcal{X}_\varepsilon : p{=}1, q{=}1, m_1^i\text{-}\rho_i(x_\varepsilon,0) = 0\}$, we have that $G_{\varepsilon_1}(\mathcal{M}_1 \cap D_\varepsilon) \subset \mathcal{M}_2$ holds for each $x_\varepsilon \in D_{\varepsilon_1}$.

  - if $\phi(0,0) \in \mathcal{M}_2 \cap D_\varepsilon$, the solution jumps according to $x_\varepsilon^+ = G_{\varepsilon_2}(x_\varepsilon)$. The timer τ resets according to $\tau^+ = c$ while $q^+ = 0$ and $p^+ = 2$. Then, by definition of

G_{ε_2}, for each $x_\varepsilon \in D_{\varepsilon_2}$, one has

$$\begin{aligned}\rho_k(x_\varepsilon^+, 0) &= \tau_k - a_k((1-q^+)c + q^+d - \tau^+) - a_k 0 \\ &= \tau_k - a_k((1-0)c - c) \\ &= \tau_k\end{aligned}$$

which is equal to $(m_1^k)^+$ and

$$\begin{aligned}\rho_i(x_\varepsilon^+, d) &= \tau_i - a_i((1-q^+)c + q^+d - \tau^+) - a_i d \\ &= \tau_i - a_i((1-0)c - c) - a_i d \\ &= \tau_i - a_i d\end{aligned}$$

which is equal to $(m_2^k)^+ = m_1^i$. Therefore, by recalling the definition $\mathcal{M}_3 = \{x_\varepsilon \in \mathcal{X}_\varepsilon : p{=}2, q{=}0, m_1^k\text{-}\rho_k(x_\varepsilon, 0) = 0, m_2^k\text{-}\rho_i(x_\varepsilon, d) = 0\}$, we have $G_{\varepsilon_2}(\mathcal{M}_2 \cap D_\varepsilon) \subset \mathcal{M}_3$ for each $x_\varepsilon \in D_{\varepsilon_2}$.

– if $\phi(0,0) \in \mathcal{M}_3 \cap D_\varepsilon$, the solution jumps according to $x_\varepsilon^+ = G_{\varepsilon_3}(x_\varepsilon)$. The timer τ resets according to $\tau^+ = d$ while $q^+ = 1$ and $p^+ = 3$. Then, by definition of G_{ε_3}, for each $x_\varepsilon \in D_{\varepsilon_3}$, one has

$$\begin{aligned}\rho_k(x_\varepsilon^+, 0) &= \tau_k - a_k((1-q^+)c + qd - \tau^+) - a_k 0 \\ &= \tau_k - a_k((1-1)c + d - d) \\ &= \tau_k\end{aligned}$$

which is equal to $(m_1^k)^+$,

$$\begin{aligned}\rho_k(x_\varepsilon^+, c) &= \tau_k - a_k((1-q^+)c + qd - \tau^+) - a_k c \\ &= \tau_k - a_k((1-1)c + d - d) - a_k c \\ &= \tau_k - a_k c\end{aligned}$$

which is equal to $(m_2^k)^+ = m_1^k$, and

$$\begin{aligned}\rho_i(x_\varepsilon^+, c+d) &= \tau_i - a_i((1-q^+)c + qd - \tau^+) - a_i(c+d) \\ &= \tau_i - a_i((1-1)c + d - d) - a_i(c+d) \\ &= \tau_i - a_i(c+d)\end{aligned}$$

which is equal to $(m_3^k)^+ = m_2^k$. Therefore, by recalling the definition $\mathcal{M}_4 = \{x_\varepsilon \in \mathcal{X}_\varepsilon : p{=}3, q{=}1, m_1^k\text{-}\rho_k(x_\varepsilon, 0) = 0, m_2^k\text{-}\rho_k(x_\varepsilon, c) = 0, m_3^k\text{-}\rho_i(x_\varepsilon, c{+}d) = 0\}$, we have $G_{\varepsilon_3}(\mathcal{M}_3 \cap D_\varepsilon) \subset \mathcal{M}_4$ for each $x_\varepsilon \in D_{\varepsilon_3}$.

– if $\phi(0,0) \in \mathcal{M}_4 \cap D_\varepsilon$, the solution jumps according to $x_\varepsilon^+ = G_{\varepsilon_4}(x_\varepsilon)$. The timer τ resets according to $\tau^+ = c$ while $q^+ = 0$ and $p^+ = 4$. Then, by definition of G_{ε_4}, for each $x_\varepsilon \in D_{\varepsilon_4}$, one has

$$\begin{aligned}\rho_i(x_\varepsilon^+, 0) &= \tau_i - a_i((1-q^+)c + qd - \tau^+) - a_i\beta \\ &= \tau_i - a_i((1-0)c - c) \\ &= \tau_i\end{aligned}$$

which is equal to $(m_1^k)^+$,

$$\begin{aligned}\rho_k(x_\varepsilon^+, d) &= \tau_k - a_k((1-q^+)c + qd - \tau^+) - a_k d \\ &= \tau_k - a_k((1-0)c - c) - a_k d \\ &= \tau_k - a_k d\end{aligned}$$

which is equal to $(m_2^i)^+ = m_1^k$,

$$\begin{aligned}\rho_k(x_\varepsilon^+, c+d) &= \tau_k - a_k((1-q^+)c + qd - \tau^+) - a_k(c+d) \\ &= \tau_k - a_k((1-0)c - c) - a_k(c+d) \\ &= \tau_k - a_k(c+d)\end{aligned}$$

which is equal to $(m_3^i)^+ = m_2^k$,

$$\begin{aligned}(m_4^i)^+ = m_3^k &= \rho_i(x_\varepsilon^+, c+2d) \\ &= \tau_i - a_i((1-q^+)c + qd - \tau^+) - a_i(c+2d) \\ &= \tau_i - a_i((1-0)c - c) - a_i(c+2d) \\ &= \tau_i - a_i(c+2d)\end{aligned}$$

which is equal to $(m_4^i)^+ = m_3^k$. Therefore, by recalling the definition $\mathcal{M}_5 = \{x_\varepsilon \in \mathcal{X}_\varepsilon : p{=}4, q{=}0, m_1^i\text{-}\rho_i(x_\varepsilon, 0) = 0, m_2^i\text{-}\rho_k(x_\varepsilon, d) = 0, m_3^i\text{-}\rho_k(x_\varepsilon, c{+}d) = 0, m_4^i\text{-}\rho_i(x_\varepsilon, c{+}2d){=}0\}$, we have $G_{\varepsilon_4}(\mathcal{M}_4 \cap D_\varepsilon) \subset \mathcal{M}_5$ for each $x_\varepsilon \in D_{\varepsilon_4}$.

– if $\phi(0,0) \in \mathcal{M}_5 \cap D_\varepsilon$, the solution jumps according to $x_\varepsilon^+ = G_{\varepsilon_5}(x_\varepsilon)$. The timer τ resets according to $\tau^+ = d$ while $q^+ = 1$ and $p^+ = 5$. Then, by definition of G_{ε_5}, for each $x_\varepsilon \in D_{\varepsilon_5}$, one has

$$\begin{aligned}\rho_i(x_\varepsilon^+, 0) &= \tau_i - a_i((1-q^+)c + qd - \tau^+) - a_i 0 \\ &= \tau_i - a_i((1-1)c + d - d) \\ &= \tau_i\end{aligned}$$

which is equal to $(m_1^k)^+$,

$$\begin{aligned}\rho_i(x_\varepsilon^+, c) &= \tau_k - a_k((1-q^+)c + qd - \tau^+) - a_k 0 \\ &= \tau_k - a_k((1-1)c + d - d) - a_k c \\ &= \tau_k - a_k c\end{aligned}$$

which is equal to $(m_2^i)^+ = m_1^i$,

$$\begin{aligned}\rho_k(x_\varepsilon^+, c+d) &= \tau_k - a_k((1-q^+)c + qd - \tau^+) - a_k(c+d) \\ &= \tau_k - a_k((1-1)c + d - d) - a_k(c+d) \\ &= \tau_k - a_k(c+d)\end{aligned}$$

which is equal to $(m_3^i)^+ = m_2^i$,

$$\begin{aligned}\rho_k(x_\varepsilon^+, 2c+d) &= \tau_k - a_k((1-q^+)c + qd - \tau^+) - a_k(2c+d) \\ &= \tau_k - a_k((1-1)c + d - d) - a_k(2c+d) \\ &= \tau_k - a_k(2c+d)\end{aligned}$$

which is equal to $(m_4^i)^+ = m_3^i$,

$$\begin{aligned}\rho_i(x_\varepsilon^+, 2c+2d) &= \tau_i - a_i((1-q^+)c + qd - \tau^+) - a_i(2c+2d) \\ &= \tau_i - a_i((1-1)c + d - d) - a_i(2c+2d) \\ &= \tau_i - a_i(2c+2d)\end{aligned}$$

which is equal to $(m_5^i)^+ = m_4^i$. Therefore, by recalling the definition $\mathcal{M}_6 = \{x_\varepsilon \in \mathcal{X}_\varepsilon : p{=}5, q{=}1, m_1^i\text{-}\rho_i(x_\varepsilon, 0) = 0, m_2^i\text{-}\rho_i(x_\varepsilon, c) = 0, m_3^i\text{-}\rho_k(x_\varepsilon, c{+}d) = 0, m_4^i\text{-}\rho_k(x_\varepsilon, 2c{+}d) = 0, m_5^i\text{-}\rho_i(x_\varepsilon, 2c{+}2d) = 0\}$, we have $G_{\varepsilon_5}(\mathcal{M}_5 \cap D_\varepsilon) \subset \mathcal{M}_6$ for each $x_\varepsilon \in D_{\varepsilon_5}$.

– if $\phi(0,0) \in \mathcal{M}_6 \cap D_\varepsilon$, the solution jumps according to $x_\varepsilon^+ = G_{\varepsilon_6}(x_\varepsilon)$. The timer τ resets according to $\tau^+ = c$ while $q^+ = 0$ and $p^+ = 0$. Therefore, by recalling the definition $\mathcal{M}_1 = \{x_\varepsilon \in \mathcal{X}_\varepsilon : p{=}0, q{=}0\}$, we have $G_{\varepsilon_5}(\mathcal{M}_6 \cap D_\varepsilon) \subset \mathcal{M}_1$ for each $x_\varepsilon \in D_{\varepsilon_6}$.

□

C.4 Proof of Lemma 5.3.4

Proof. Pick a solution $\phi \in \mathcal{S}_{\mathcal{H}_\varepsilon}$ with initial condition $\phi(0,0) \in C_\varepsilon \cup D_\varepsilon$. Since, the flow map F_ε enforces $\dot{p} = 0$, the p component of ϕ remains constant during flows. At jumps, namely, when $\phi(t,j) \in D_\varepsilon$, since for each $\ell \in \{1,2,3,4,5\}$, G_{ε_ℓ} enforces that $p^+ = p + 1$, the evolution of p is monotonically increasing in $\{0,1,2,3,4,5\}$ until $p = 5$, from where G_6 resets p to 0. In fact, when the solution ϕ jumps according to G_{ε_6}, we have that $p^+ = 0$ and $q^+ = 0$ resulting in a value for x_ε after the jump that is in $\mathcal{M}_1$. Now, due to the monotonic behavior of p and the completeness of solutions to $\mathcal{H}_\varepsilon$ given by Lemma 5.3.2, there exists $(t,j) \in \text{dom } \phi$ such that $\phi(t,j) = G_{\varepsilon_6}(\phi(t,j))$. Given such (t,j), let $T^* = t + j$. Then, given that $G_{\varepsilon_6}(\phi(t,j)) \subset \mathcal{M}_1$ and the forward invariance of $\mathcal{M}$ given by Lemma 5.3.3, we have that $\phi(t,j) \in \mathcal{M}$ for each $(t,j) \in \text{dom } \phi$ such that $t + j \geq T^*$. □

Bibliography

[1] Y. Li and R. G. Sanfelice, "A robust finite-time convergent hybrid observer for linear systems," in *52nd IEEE Conference on Decision and Control*, pp. 3349–3354, Dec 2013.

[2] S. Graham and P. R. Kumar, "Time in general-purpose control systems: the control time protocol and an experimental evaluation," in *2004 43rd IEEE Conference on Decision and Control (CDC) (IEEE Cat. No.04CH37601)*, vol. 4, pp. 4004–4009 Vol.4, Dec 2004.

[3] J. P. Hespanha, P. Naghshtabrizi, and Y. Xu, "A survey of recent results in networked control systems," vol. 95, pp. 138–162, Jan 2007.

[4] W. Zhang, M. S. Branicky, and S. M. Phillips, "Stability of networked control systems," vol. 21, pp. 84–99, Feb 2001.

[5] Y.-C. Wu, Q. Chaudhari, and E. Serpedin, "Clock synchronization of wireless sensor networks," *IEEE Signal Processing Magazine*, vol. 28, no. 1, pp. 124–138, 2010.

[6] B. Sundararaman, U. Buy, and A. D. Kshemkalyani, "Clock synchronization for wireless sensor networks: a survey," *Ad hoc networks*, vol. 3, no. 3, pp. 281–323, 2005.

[7] F. Ferrante, F. Gouaisbaut, R. G. Sanfelice, and S. Tarbouriech, "State estimation of linear systems in the presence of sporadic measurements," *Automatica*, vol. 73, pp. 101 – 109, 2016.

[8] R. Goebel, R. G. Sanfelice, and A. R. Teel, *Hybrid Dynamical Systems: Modeling, Stability, and Robustness*. Princeton University Press, 2012.

[9] J. R. Vig, "Introduction to quartz frequency standards," tech. rep., ARMY LAB COM-

MAND FORT MONMOUTH NJ ELECTRONICS TECHNOLOGY AND DEVICES LAB, 1992.

[10] S. Ganeriwal, R. Kumar, and M. B. Srivastava, "Timing-sync protocol for sensor networks," in *Proceedings of the 1st international conference on Embedded networked sensor systems*, pp. 138–149, ACM, 2003.

[11] D. L. Mills, "Internet time synchronization: the network time protocol," *IEEE Transactions on communications*, vol. 39, no. 10, pp. 1482–1493, 1991.

[12] IEEE, "IEEE standard for a precision clock synchronization protocol for networked measurement and control systems," *IEEE Std 1588-2008 (Revision of IEEE Std 1588-2002)*, pp. 1–300, July 2008.

[13] N. M. Freris, S. R. Graham, and P. Kumar, "Fundamental limits on synchronizing clocks over networks," *IEEE Transactions on Automatic Control*, vol. 56, no. 6, pp. 1352–1364, 2010.

[14] Y. Nakamura, K. Hirata, and K. Sugimoto, "Synchronization of multiple plants over networks via switching observer with time-stamp information," in *2008 SICE Annual Conference*, pp. 2859–2864, IEEE, 2008.

[15] M. Maróti, B. Kusy, G. Simon, and Á. Lédeczi, "The flooding time synchronization protocol," in *Proceedings of the 2nd international conference on Embedded networked sensor systems*, pp. 39–49, ACM, 2004.

[16] J. Elson, L. Girod, and D. Estrin, "Fine-grained network time synchronization using reference broadcasts," *ACM SIGOPS Operating Systems Review*, vol. 36, no. SI, pp. 147–163, 2002.

[17] A. Seuret and K. H. Johansson, "Networked control under time-synchronization errors," in *Time Delay Systems: Methods, Applications and New Trends*, pp. 369–381, Springer, 2012.

[18] Y. Li and R. G. Sanfelice, "Finite time stability of sets for hybrid dynamical systems," *Automatica*, vol. 100, pp. 200–211, 02/2019 2019.

[19] M. Guarro, F. Ferrante, and R. G. Sanfelice, "A hybrid observer for linear systems under delayed sproadic measurements," *Technical Report*, 2019.

[20] F. Ferrante, F. Gouaisbaut, R. G. Sanfelice, and S. Tarbouriech, "State estimation of linear systems in the presence of sporadic measurements," *Automatica*, vol. 73, pp. 101 – 109, 2016.

[21] L. Hetel, C. Fiter, H. Omran, A. Seuret, E. Fridman, J.-P. Richard, and S. I. Niculescu, "Recent developments on the stability of systems with aperiodic sampling: An overview," *Automatica*, vol. 76, pp. 309 – 335, 2017.

[22] P. Naghshtabrizi and J. P. Hespanha, *Implementation Considerations For Wireless Networked Control Systems*, pp. 1–27. New York, NY: Springer New York, 2011.

[23] J. A. Fax and R. M. Murray, "Information flow and cooperative control of vehicle formations," *IEEE Transactions on Automatic Control*, vol. 49, pp. 1465–1476, Sep. 2004.

[24] D. Luenberger, "An introduction to observers," vol. 16, pp. 596–602, Dec 1971.

[25] R. Carli, A. Chiuso, L. Schenato, and S. Zampieri, "A pi consensus controller for networked clocks synchronization," *IFAC Proceedings Volumes*, vol. 41, no. 2, pp. 10289–10294, 2008.

[26] S. Bolognani, R. Carli, E. Lovisari, and S. Zampieri, "A randomized linear algorithm for clock synchronization in multi-agent systems," *IEEE Transactions on Automatic Control*, vol. 61, no. 7, pp. 1711–1726, 2015.

[27] N. M. Freris, V. S. Borkar, and P. Kumar, "A model-based approach to clock synchronization," in *Proceedings of the 48h IEEE Conference on Decision and Control (CDC) held jointly with 2009 28th Chinese Control Conference*, pp. 5744–5749, IEEE, 2009.

[28] J. C. Eidson, *Measurement, control, and communication using IEEE 1588*. Springer Science & Business Media, 2006.

[29] O. Simeone, U. Spagnolini, Y. Bar-Ness, and S. H. Strogatz, "Distributed synchronization in wireless networks," *IEEE Signal Processing Magazine*, vol. 25, no. 5, pp. 81–97, 2008.

[30] M. Guarro and R. G. Sanfelice, "HyNTP: An Adaptive Hybrid Network Time Protocol for Clock Synchronization in Heterogeneous Distributed Systems," in *American Control Conference*, (Denver, United States), pp. 1482–1493, IEEE, 2020.

[31] Q.-L. H. Dong Yue and C. Peng, "State feedback controller design of networked control systems," *IEEE Transactions on Circuits and Systems II: Express Briefs*, vol. 51, pp. 640–644, Nov 2004.

[32] Y. Li, S. Phillips, and R. G. Sanfelice, "Robust distributed estimation for linear systems under intermittent information," *IEEE Transactions on Automatic Control*, vol. 63, pp. 973–988, April 2018.

[33] J. Chai and R. G. Sanfelice, "Forward invariance of sets for hybrid dynamical systems (Part I)," *To appear in IEEE Transactions on Automatic Control*, 2019.

[34] D. Nesic and A. R. Teel, "Input-output stability properties of networked control systems," vol. 49, pp. 1650–1667, Oct 2004.

[35] L. A. Montestruque and P. J. Antsaklis, "On the model-based control of networked systems," vol. 39, pp. 1837 – 1843, 2003.

[36] P. Seiler and R. Sengupta, "Analysis of communication losses in vehicle control problems," in *Proceedings of the 2001 American Control Conference. (Cat. No.01CH37148)*, vol. 2, pp. 1491–1496 vol.2, 2001.

[37] M. Cloosterman, N. van de Wouw, M. Heemels, and H. Nijmeijer, "Robust stability of networked control systems with time-varying network-induced delays," in *Proceedings of the 45th IEEE Conference on Decision and Control*, pp. 4980–4985, Dec 2006.

[38] R. M. Jungers, A. Kundu, and W. Heemels, "Observability and controllability analysis of linear systems subject to data losses," IEEE, 2017.

[39] D. Bernstein, *Matrix Mathematics: Theory, Facts, and Formulas - Second Edition.* Princeton University Press, 2009.

[40] T. C. Mei Yu, Long Wang and F. Hao, "An lmi approach to networked control systems with data packet dropout and transmission delays," in *2004 43rd IEEE Conference on Decision and Control (CDC) (IEEE Cat. No.04CH37601)*, vol. 4, pp. 3545–3550 Vol.4, Dec 2004.

[41] A. R. Teel, "Connections between razumikhin-type theorems and the iss nonlinear small gain theorem," *IEEE Transactions on Automatic Control*, vol. 43, pp. 960–964, July 1998.

[42] W. Zhang and M. S. Branicky, "Stability of networked control systems with time-varying transmission period.," in *In 39th Annual Allerton Conference on Communication Control and Computing*, vol. 39, p. 1205–1214 Vol.39, 2001.

[43] L. Hetel, J. Daafouz, J. Richard, and M. Jungers, "Delay-dependent sampled-data control based on delay estimates," *Systems and Control Letters*, vol. 60, no. 2, pp. 146 – 150, 2011.

[44] D. Nesic, A. R. Teel, and D. Carnevale, "Explicit computation of the sampling period in emulation of controllers for nonlinear sampled-data systems," *IEEE Transactions on Automatic Control*, vol. 54, pp. 619–624, March 2009.

[45] K. Y. Guisheng Zhai, Bo Hu and A. N. Michel, "Qualitative analysis of discrete-time switched systems," in *Proceedings of the 2002 American Control Conference (IEEE Cat. No.CH37301)*, vol. 3, pp. 1880–1885 vol.3, May 2002.

[46] A. S. Matveev and A. V. Savkin, "The problem of state estimation via asynchronous communication channels with irregular transmission times," *IEEE Transactions on Automatic Control*, vol. 48, pp. 670–676, April 2003.

[47] T. Ahmed-Ali, R. Postoyan, and F. Lamnabhi-Lagarrigue, "Continuous–discrete adaptive observers for state affine systems," *Automatica*, vol. 45, no. 12, pp. 2986 – 2990, 2009.

[48] D. Dačić and D. Nešić, "Observer design for wired linear networked control systems using matrix inequalities," *Automatica*, vol. 44, no. 11, pp. 2840 – 2848, 2008.

[49] W. P. M. H. Heemels, A. R. Teel, N. van de Wouw, and D. Nesic, "Networked control systems with communication constraints: Tradeoffs between transmission intervals, delays and performance," *IEEE Transactions on Automatic Control*, vol. 55, pp. 1781–1796, Aug 2010.

[50] S. Bolognani, R. Carli, and S. Zampieri, "A pi consensus controller with gossip communication for clock synchronization in wireless sensors networks," *IFAC Proceedings Volumes*, vol. 42, no. 20, pp. 78–83, 2009.

[51] R. Carli, F. Fagnani, A. Speranzon, and S. Zampieri, "Communication constraints in the average consensus problem," *Automatica*, vol. 44, no. 3, pp. 671–684, 2008.

[52] Y. Kikuya, S. M. Dibaji, and H. Ishii, "Fault tolerant clock synchronization over unreliable channels in wireless sensor networks," *IEEE Transactions on Control of Network Systems*, pp. 1–1, 2018.

[53] S. Phillips, Y. Li, and R. G. Sanfelice, "A hybrid consensus protocol for pointwise exponential stability with intermittent information," *IFAC-PapersOnLine*, vol. 49, no. 18, pp. 146–151, 2016.

[54] R. Olfati-Saber and R. M. Murray, "Consensus problems in networks of agents with switching topology and time-delays," *IEEE Transactions on Automatic Control*, vol. 49, pp. 1520–1533, Sept 2004.

[55] C. D. Godsil and G. F. Royle, *Algebraic Graph Theory*. 2001.

[56] L. Schenato and F. Fiorentin, "Average timesynch: A consensus-based protocol for clock synchronization in wireless sensor networks," *Automatica*, vol. 47, no. 9, pp. 1878–1886, 2011.

[57] J. He, P. Cheng, L. Shi, and J. Chen, "Time synchronization in wsns: A maximum value based consensus approach," in *2011 50th IEEE Conference on Decision and Control and European Control Conference*, pp. 7882–7887, Dec 2011.

[58] K. Narendra and A. Annaswamy, "A new adaptive law for robust adaptation without persistent excitation," *IEEE Transactions on Automatic Control*, vol. 32, pp. 134–145, February 1987.

[59] R. Leidenfrost and W. Elmenreich, "Firefly clock synchronization in an 802.15. 4 wireless network," *EURASIP Journal on Embedded Systems*, vol. 2009, no. 1, p. 186406, 2009.